Investigations on Design Transformation of Microstrip Antennas and Its Applications in Energy Harvesting

Ph. D. Thesis

Submitted by

MONIKA MATHUR
(College ID: - 2012REC9047)

Under Supervision of

Dr. GHANSHYAM SINGH
Associate Professor, Department of ECE, MNIT Jaipur
And
Dr. S. K. BHATNAGAR
Director (Research) and HOD, Department of ECE, SKIT Jaipur

Submitted as a partial fulfillment of the degree of Doctor of Philosophy

In

DEPARTMENT OF ELECTRONICS AND COMMUNICATION ENGINEERING

MALAVIYA NATIONAL INSTITUTE OF TECHNOLOGY JAIPUR
(AUGUST, 2017)

DECLARATION OF AUTHORSHIP

I, Monika Mathur, declare that this thesis titled, 'Investigations on Design Transformation of Microstrip Antennas and Its Applications in Energy Harvesting' and the work presented in it are my own. I confirm that:

This work was done wholly or mainly while in candidature for a Ph.D. degree at MNIT.

Where any part of this thesis has previously been submitted for a degree or any other qualification at MNIT Jaipur or any other institution, this has been clearly stated.

Where I have consulted the published work of others, this is always clearly attributed.

Where I have quoted from the work of others, the source is always given. With the exception of such quotations, this thesis is entirely my own work.

I have acknowledged all main sources of help.

Where the thesis is based on work done by myself jointly with others, I have made clear exactly what was done by others and what I have contributed myself.

Signed: _____

Date: _____

ACKNOWLEDGEMENTS

The satisfaction and euphoria that accompany the successful completion of any work, will be incomplete unless a profound thanks is conveyed to all those whose kind encouragement and valuable guidance made this work a grand success.

I express my sincere gratitude to Dr. Ghanshyam Singh, Associate Professor, Department of Electronics & Communication Engineering, and Dr. S. K. Bhatnagar Director (Research) and HOD, Department of Electronics and Communication Engineering, SKIT Jaipur, for their valuable supervision, support and inspiration during my study at MNIT, Jaipur. Their constantly energetic attitude, optimism and result oriented outlook have been helpful to me during the work and in the writing of the thesis. Without his continuous and strong support, my Ph.D. would not have started and finished smoothly.

I am very grateful to Prof. K. K. Sharma, Head, Dept. of ECE, my respected DREC committee members Dr. Vijay Janyani, Dr. Ritu Sharma, and Dr. Ravi Maddila for their valuable suggestions during my research work and presentations at the end of each semester. I am also thankful to The Head DPGC, Dr. D. Boolchandani for their moral support as a convener DPGC.

I extend my sincere thanks to my parents Mr. P. L. Mathur and Mrs. Sarla Mathur for their continuous support. Without their support, persistence, initial motivation and love I would not be where I am today. I also owe special thanks to my husband Mr. Deepak Mathur, for encouraging me at every step of research process and always provide me the mental and physical support where I need. A very special thanks to my son Master Pallav Mathur and my nephew Mr. Vinav Mathur they always believed in me and they were always ready to help me in any possible ways. A big thanks to all my family members for their blessing and motivations.

Finally, I would like to add few heartfelt words for my colleague Mr. Ankit Agrawal, My faculty members of Electronics and communication department, SKIT and my fellow research scholars who gave me unending support right from the beginning.

(MONIKA MATHUR)

ABSTRACT

For several decades there has been a very large requirement for microstrip antennas. This demanded design formulae. These were evolved by analysis of data followed by numerical data fitting. It was generally observed that the electrical length of the microstrip antenna was greater than its physical length due to fringing fields. The Empirical formula for this extension in physical length (ΔL) gives a very good approximation, but is not directly related to the physical length. Bhatnagar's postulate was evolved to correlate this extension of physical length (ΔL) with an electrical length (L_e) and to put the things on a firm footing. Millions of designs are available for microstrip antenna but there is no relation between them. Consequently, the entire design, simulation, fabrication and testing cycle has to be repeated freshly for every new design. This cycle has to be iterated several times to reach the goal. Bhatnagar's postulate gave a new insight in the design cycle. "Equivalent design concept" and "transformation of design" approach were evolved. I have investigated these issues deeply and widely. Originally the postulate was for rectangular microstrip antenna. I have investigated several shapes and feed lines and have developed formulae for these. The results have been successfully applied to harvesting ambient microwave energy.

There are many methods to design and fabricate these antennas. Generally, classical formulae are used for designing the structure of the antenna. Whenever a new structure is to be designed the entire calculation and simulation work has to be repeated with the new design data. Also, when anyone fabricates the simulated design and if measured result does not shows the desired value of frequency, then they have to repeat all the steps with re-calculations, re-design, and re-fabricate. With these problems in mind , we planned to do the work for antenna designing formulae in easy form or at least try to overcome the step of recalculation with complex formulae. Two types of formulae are presented in this thesis. One formula is for multilayered designed microstrip antenna specially designed for LTCC techniques.

This is for retuning the resonance frequency of the multilayered fabricated antenna on its desired designed value simply by cutting the material from the one or two layers of the multilayered substrate. According to this formula, the area of cutting the material is inversely proportional to the ratio of desired resonance frequency to

the frequency which has to be re-tuned.

In this light of finding the new formulae equivalence of the design concept is presented by S. K. Bhatnagar. They give the Bhatnagar postulate and from that theory, they presented a set of formulae for the patch dimensions by the equivalence of design concept. These sets of formulae are very easy to learn. To complete that set of formulae this thesis adds on the set of formulae for the feed line dimensions by using the same equivalence of design concept. The second formula of this thesis says that if designed frequency of resonance is same for two structures then we can easily transform one good design of antenna having one type of substrate into another type of substrate.

The RF energy harvesting field is the most demanding area nowadays. A RF energy harvesting module contains three main blocks - microstrip antenna, matching circuit and RF to DC converter circuit. Most of the work in this field presented the RF module having single, double or triple band microstrip antenna. This thesis presented the novel design of a monopole antenna for a wide range of operation, especially for RF energy harvesting purpose. A coplanar waveguide (CPW) fed monopole antenna is presented for covering almost all useful band ranges from 900MHz-9.9 GHz (Radio, GSM, ISM, UWB bands). It provides the band reject characteristics for the range 3.1GHz-5.6GHz (HIPERLAN, C-Band, and W-LAN) due to avoiding interference of this range for this application. For cover Ultra Wide Band (UWB) range optimization by modification on the coplanar waveguide (CPW) ground structure has applied. Other useful ranges (Radio, GSM, and ISM) have also optimized by controlling the gap between the patch and CPW ground. Also, considering the CPW ground as open terminal transmission line model and applying the principles of discontinuities bandwidth enhancement and impedance matching for UWB range has gained. For particular band rejection, a parasitic patch above the patch has optimized. The structure is compact of size $50 \times 40 \times 1.6$ mm^3. The gain of the antenna is varying for 2dBi -7dBi for different frequencies.

One of the important need of RF energy harvesting circuit is that the antenna of this module should be capable of capturing the maximum energy from the spectrum so that RF-DC converter circuit of this module have got maximum RF input power accordingly the increase in DC output value. To fulfill this essential need the arrangement of the 2×1 and 2×2 array of the designed structure has been

presented. The captured RF power of these two and four antennas has combined with the help of Wilkinson power combiner. The advantage of using this combiner is that for matching the impedances we can use the resistors with this combiner easily.

Further a novel seven stage RF-DC converter circuit has been presented in this thesis. At the end , a novel single substrate module of RF energy harvesting with 2×2 array arrangement has been presented. The novelty of this module is that it uses a different approach for matching in between the antenna and converter circuit . The idea is that the input impedance of RF-DC converter circuit has measured on the resonance frequencies the SMD components of that impedance is soldered at the wilkinson power combiner of the antenna section. This arrangement should be able to provide the maximal energy to the device. No connectors are there in the module so no need to match the impedance for particular value 50 ohms. The measured results satisfied the conditions. This module provides the DC voltage of the value 1.823V with the +40dBm RF input power for the load resistance of 20Kohms. This voltage is sufficient to amplify and may be used for powering low power devices.

TABLE OF CONTENTS

CERTIFICATE III
DECLARATION OF AUTHORSHIP IV
ACKNOWLEDGEMENTS V
ABSTRACT VI
TABLE OF CONTENTS IX
LIST OF FIGURES XIV
LIST OF TABLES XX
ABBRIVIATIONS XXI
CHAPTER-1: INTRODUCTION 1
1.1Advances in Technology 1
1.2 Motivation of the Research 1
1.3 Research Contribution 2
1.4 Thesis Organization 3
1.5 Historical Background of Microstrip Antenna 5
1.5.1 Microstrip Antenna 5
1.5.2 Feeding Techniques 8
1.5.2.1 Microstrip line 8
1.5.2.2 Coaxial probe feed 10
1.5.2.3 Aperture coupling 11
1.5.2.4 Proximity-coupled feed 12
1.5.2.5 Comparison amongst feeding techniques 13
1.5.3 Types of Microstrip Antennas 14
1.5.3.1 Microstrip patch antenna 15
1.5.4 Methods of Analysis 16
1.5.4.1 Transmission-line model 18
1.5.5 Performance Parameters of Microstrip Antenna 27
1.5.5.1 Input impedance 27

1.5.5.2 Resonance frequency 28

1.5.5.3 VSWR 28

1.5.5.4 Radiation pattern 28

1.5.5.5 Gain 28

1.5.5.6 Current distribution 29

1.6 Bhatnagar Postulates And It's Implication 29

1.6.1 Transformation of One Design into Another 30

1.6.2 Generalization of Laws of Transformation [60] 31

1.7 RF Energy Harvesting 33

CHAPTER 2: INVESTIGATIONS CONCERNING DIELECTRIC CONSTANT ENGINEERING 35

2.1 Introduction 35

2.2 Literature Review 36

2.3 Design of the Rectangular Patch Antenna 38

2.3.1 Design Calculation 38

2.3.2 Antenna Design Procedure 40

2.3.3 The Effects on Percentage Frequency Ratio by the Area Ratio for Air-Cavity in One Layer of Dielectric (Aircavity-1) 45

2.3.4 The Effects of Percentage Frequency Ratio by the Area Ratio for Air-Cavity in Two Layers of Dielectric (Aircavity-2) 49

2.3.5 Discussions 52

2.4 Analytical Model 52

2.5 Measured Result 56

2.6 Conclusion 58

CHAPTER 3:NOVEL TECHNIQUE FOR ESTIMATING FEED LINE DIMENSIONS OF RECTANGULAR AND TRIANGULAR MICROSTRIP ANTENNA 60

3.1 Introduction 60

3.2 Literature Review 61
3.3 Mathematical Expression of Feedline of MS Antenna for Transformation of Designs 63
3.4 Modification in the Width Formula of Transformation of Designs Formulae Set 71
3.5 Validation of Transformation Formulae for Feed Line and the Width of Patch for Rectangular Shape Patch 72
3.5.1 Case I 72
3.5.2 Case II 74
3.5.3 Measured Result of Rectangular Patch Antenna with Line Feed Designed by Transformation of Designs Formulae 78
3.6 Transformation Design Formulae for Equilateral Triangular Shape Patch and Its Feed Line Design of MS Antenna 79
3.7 Validation of Transformation Formulae for Feed Line for Equilateral Triangle Shape Patch 80
3.8 Conclusion 84
CHAPTER 4: INVESTIGATIONS OF COPLANAR MONOPOLE WIDEBAND ANTENNA AND IT'S ARRAY ARRANGMENTS 87
4.1 Introduction 87
4.2 Literature Review 87
4.3 A New Coplanar Monopole Antenna Design 89
4.4 Parametric Analysis 93
4.4.1 Effect of the Gap Between the Patch and CPW Ground (S1, S2) 93
4.4.2 Effect of Chamfering of the Corners of Ground (Lcl And Lcr) As Well As the Gap Between the Parasitic Patch and Resonant Patch 94
4.4.3 Effect of Cutting Slots in the CPW Ground 95
4.4.4 Effect of Stubs in the Feedline for Impedance Matching 96
4.5 Experimental Verification 98
4.5.1 Measurement of Return Loss 98
4.5.2 Measured Radiation Patterns (E-plane & H-plane) 100

4.5.3 Current Distribution 101

4.5.4 Gain and Radiation Efficiency 102

4.6 Some Possible Array Arrangements of the Proposed Coplanar Monopole Antenna 102

4.6.1 An Array Structure of 2×1 (Vertically Connected) Compact Coplanar Monopole Antenna with Wilkinson Power Combiner 103

4.6.2 An Array Structure of 2×1 (Horizontally Connected) Compact Coplanar Monopole Antenna with Wilkinson Power Combiner 108

4.6.3 An Array Structure of 2×2 Compact Coplanar Monopole Antenna with Wilkinson Power Combiner 113

4.6.4 The Stacking of Two Single Structure (Back To Back) of Compact Coplanar Monopole Antenna 118

4.7 State of Art of the Designed Antenna (Single Coplanar Monopole Antenna) 127

4.8 Conclusion 128

CHAPTER-5 : DEVELOPMENT OF A NOVEL RF ENERGY HARVESTING MODULE 129

5.1 Introduction 129

5.2 Literature Review 130

5.3 Design of RF Energy Harvesting Module 132

5.3.1 Receiving Antenna 132

5.3.2 Matching Network 132

5.3.3 RF- DC Converter (Energy Conversion) Circuit 136

5.3.4 Lab Measurement of Different Array Structures As Receiving Antenna for Energy Harvesting Module 140

5.4 A Novel RF Energy Harvesting Module With 2×2 Antenna Array of Coplanar Structure on a Single Substrate 144

5.5 Conclusion 149

CHAPTER 6 : CONCLUSION AND FUTURE ASPECTS 150

6.1 Future Aspects 154

PUBLICATION DETAILS 171
APPENDIX-A 172
BRIEF CV 175

LIST OF FIGURES

Fig. 1.1. Microstrip rectangular patch antenna with microstrip feed line 6

Fig. 1.2. The Microstrip feed line at the radiating edge 9

Fig. 1.3. Equivalent circuit of the microstrip feed line 9

Fig. 1.4. An antenna with a quarter-wavelength matching section 9

Fig. 1.5. Coaxial probe feeding at the radiating patch 11

Fig. 1.6 . Equivalent circuit of coaxial feedline ……10

Fig. 1.7. Aperture-coupled feed 12

Fig. 1.8. Equivalent circuit of aperture-coupled feed 12

Fig. 1.9. Proximity-coupled feed 13

Fig. 1.10. Equivalent circuit of proximity-coupled feed 13

Fig. 1.11. Rectangular microstrip patch antenna with radiating slots 15

Fig. 1.12. Different shapes of microstrip patch elements 16

Fig. 1.13. Microstrip line 18

Fig. 1.14. Electric field lines 18

Fig. 1.15. Effective dielectric constant 19

Fig. 1.16. Physical and effective length of a rectangular microstrip patch 20

Fig. 1.18. Variation of normalized input resistance 25

Fig. 1.19. Block diagram of RF energy harvesting module 33

Fig. 2.1. Design structure of four layer dielectric on simulator. 41

Fig. 2.2. Frequency- return loss curve of four layer dielectric structure with optimization of feed for 50 Ω. 41

Fig. 2.3. Top view of structure of antenna with change in dimensions of air-cavity-142

Fig. 2.4. Top veiw of structure of antenna with air-cavity2 42

Fig. 2.5. Variation of resonance frequency ratio (f/f_0) with the ratio of width of the cavity to patch width (W_c/W_p). The ratio of cavity length to patch length (R_L) is the parameter..... 43

Fig. 2.6. Variation of resonance frequency ratio (f/f_0) with the ratio of length of the cavity to length of patch (L_c/L_p). The ratio (R_W) of cavity width to patch width is the parameter..... 44

Fig. 2.7. Graph between percentage frequency ratio and area ratio having ε_r = 4.4, f_0=2.4 GHz, d = h/4 mm. 46

Fig. 2.8. Graph between percentage frequency ratio and area ratio having ε_r=4.4, f_0=1.8 GHz, d=h/4 mm. 46

Fig. 2.9. Graph between percentage frequency and area ratio having ε_r=4.4, f_0=1.6 GHz, d=h/4 mm. 47

Fig. 2.10. Graph between percentage frequency ratio and area ratio having ε_r=2.2, f_0 =2.4 GHz, d= h/4 mm. 47

Fig. 2.11. Graph between percentage frequency ratio and area ratio having ε_r=3, f_o =2.4 GHz, d=h/4mm. 48

Fig. 2.12. Collective graph of percentage frequency ratio and area ratio having ε_r=4.4, 2.2, 3 f_o =2.4, 1.8, 1.6 GHz and d=h/4 mm. 48

Fig. 2.13. Graph between percentage frequency ratio and area ratio having ε_r=4.4, f_o=2.4 GHz, d=h/2mm. 49

Fig. 2.14. Graph between percentage frequency ratio and area ratio having ε_r=4.4, f_o=1.8 GHz, d=h/2 mm. 49

Fig. 2.15. Graph between percentage frequency ratio and area ratio having ε_r= 4.4, f_o=1.6 GHz, d=h/2 mm. 50

Fig. 2.16. Graph between percentage frequency ratio and area ratio having ε_r=2.2, f_o=2.4 GHz, d=h/2 mm. 50

Fig. 2.17. Graph between percentage frequency ratio and area ratio having ε_r=3, f_o=2.4 GHz, d = h/2 mm. 51

Fig. 2.18. Collective graph of percentage frequency ratio and area ratio having = 4.4, 2.2, 3 f_0 =2.4, 1.8, 1.6 GHz and d = h/2 mm 51

Fig. 2.19. Analytical model for MS antenna 53

Fig. 2.20. Equivalent capacitance of above analytical model of MS antenna. 53

Fig. 2.21(a) Four layered fabricated antenna on substrate FR4 Epoxy ($\boldsymbol{\varepsilon_r = 4.4}$) (b) second layer of substrate after removing the material 57

Fig. 2.22 Measur. result of four layered fabrica. antenna without and with cavity .. 58

Fig. 3.1. Graphical representation of dielectric constant of substrate (ε_r) with Wo/h when Wo/h ≤ 1 65

Fig. 3.2. Graphical representation of dielectric constant of substrate (ε_r) withWo/h when Wo/h>1 68

Fig. 3.3. (a) Good design structure for ε_r = 9.2 from the simulator (b) Simulated return loss versus frequency plot for ε_r = 9.2 73

Fig. 3.4 . Simulated return loss versus frequency plot for ε_{r2} = 10.2 74

Fig. 3.5. Simulated return loss versus frequency plot for ε_r = 2.2 75

Fig. 3.6. Simulated return loss versus frequency plot for ε_{r2} = 4.4. 76

Fig. 3.7. (a) Fabricated antenna on substrate Rogers RO3210 (ε_{r2} = 10.2) (b) Fabricated antenna on substrate Rogers FR4 Epoxy (ε_{r2} = 4.4) 78

Fig. 3.8. Measured return loss curve for the case-I and II 79

Fig. 3.9. Structural diagram of equilateral triangular shape patch antenna from the simulator 81

Fig. 3.10. Simulated return loss plot of the equilateral triangular patch on substrate FR4 Epoxy (ε_r = 4.4) for designing frequency f_r = 2 GHz 82

Fig. 3.11. Simulated return loss plot of structure having an equilateral triangular patch on substrate Rogers/ Duroid5880 (tm) (ε_r = 2.2) for designing frequency f_r = 2.01 GHz 82

Fig. 3.12 . Simulated return loss plot of the structure having an equilateral triangular patch on substrate Rogers RO 3003 (ε_r = 3) for designing frequency f_r = 2.01 GHz .. 83

Fig. 3.13. Simulated return loss plot for structure having an equilateral triangular patch on substrate Rogers TMM10i (ε_r = 9.8) for design frequency f_r = 2.01 GHz 83

Fig. 4.1. Proposed coplanar waveguide fed monopole antenna structure..... 90

Fig. 4.2. Simulated return loss curves of basic structure with conventional ground and effect of applying CPW ground. 92

Fig. 4.3. Optimized simulated return loss curve for the CPW ground structure after chamfering and adding optimized parasitic patch structure. 94

Fig. 4.4. Simulated return loss curve for optimized results by introducing slots in the CPW ground for enhancing the range of UWB 96

Fig. 4.5. Simulated return loss curve for the optimized result of connecting the stubs in the feed line..... 96

Fig. 4.6. (a) Simulation result for S_{11} of the new design (b) Simulation result of VSWR for the new design. 97

Fig. 4.7. Photograph of fabricated antenna. 98

Fig. 4.8. (a) Measured results of S_{11} parameter of the proposed design. (b) Measured results of VSWR parameter of the proposed design 99

Fig. 4.9. Measured radiation pattern (H-plane & E plane) at Φ= 90o 101

Fig. 4.10. Simulation result of new design for current distribution at one of the resonant frequency 2.4GHz 102

Fig. 4.11. Simulated structure of 2×1 array of design (vertically connected)..... 104

Fig. 4.12. Simulated return loss (S11) curve for 2×1 array of design (vertically connected) 104

Fig. 4.13. (a) Fabricated design (b) Measured return loss (S_{11}) curve for 2×1 array of design (vertically connected) 105

Fig. 4.14. Simulated VSWR curve of 2×1 array of design (vertically connected) ..106

Fig. 4.15 Simulated Gain of the structure of 2×1 array of design (vertically connected) 106

Fig. 4.16. (a) Simulated realized peak gain and (b) radiation efficiency of the structure of 2×1 array of design (vertically connected) 107

Fig. 4.17. Field patterns of the structure of 2×1 array of design (vertically connected) (a) H- field (b) E- field..... 107

Fig. 4.18. Current distribution of the structure of 2×1 array of design (vertically connected) 108

Fig. 4.19. Simulated structure of 2×1 array of design (Horizontally connected)..... 109

Fig. 4.20. Simulated result of return loss of the structure of 2×1 array of design (Horizontally connected) 109

Fig. 4.21. Measured result of return loss of the structure of 2×1 array of design (Horizontally connected) 110

Fig. 4.22. VSWR curve of the structure of 2×1 array of design (Horizontally connected) 110

Fig. 4.23. Gain- frequency curve of the structure of 2×1 array of design (Horizontally connected) 111

Fig. 4.24. (a) Peak Realized gain and (b) Radiation efficiency of the structure of 2×1 array of design (Horizontally connected) 111

Fig. 4.25. (a) H- field and (b) E-field pattern of tthe structure of 2×1 array of design (Horizontally connected) 112

Fig. 4.26. Current Distribution of the structure of the 2×1 array of design (Horizontally connected). 112

Fig. 4.27. Structure of 2×2 array of the design of the coplanar monopole antenna from the Simulator..... 113

Fig. 4.28. Simulation result of the 2×2 array of the design of the coplanar monopole antenna. 114

Fig. 4.29. (a) Fabicated design and (b) measured result of the 2×2 array of the design of the coplanar monopole antenna. 115

Fig. 4.30. VSWR curve of the 2×2 array of the design of the coplanar monopole antenna 116

Fig. 4.31. Gain – frequency curve of the 2×2 array of the design of the coplanar monopole antenna. 116

Fig. 4.32 (a) Peak Realized gain and (b) Radiation efficiency of the 2×2 array of the design of the coplanar monopole antenna..... 117

Fig. 4.33. (a) H- Field Pattern (b) E- field pattern of the **2** ×2 array of the design of the coplanar monopole antenna 117

Fig. 4.34. Current distribution of the 2×2 array of the design of the coplanar monopole antenna. 118

Fig. 4.35. Simul. structure of two back to back stacked coplanar monopole ante..... 119

Fig. 4.36. Simulated return loss (S_{11}) result of two back to back stacked coplanar monopole antenna. 119

Fig. 4.37. Simulated return loss (S_{22}) result of two stacked coplanar monopole antenna. 120

Fig. 4.38. Simulated return loss (S_{12}) result of two back to back stacked coplanar monopole antenna 120

Fig. 4.39. Simula. return loss (S_{21}) of two stacked coplanar monopole antenna 121

Fig. 4.40. Fabricated structure of two back to back stacked coplanar monopole antenna 121

Fig. 4.41. Measured return loss (a)(S_{11}) (b) S_{22} (c) S_{21} and (d) S_{12} results of two back to back stacked coplanar monopole antenna 123

Fig. 4.42. Gain-frequency curve of two back to back stacked coplanar monopole antenna 124

Fig. 4.43. (a) Peak realized gain (b) radiation efficiency of two back to back stacked coplanar monopole antenna 125

Fig. 4.44. (a) H- field Pattern (b) E-field pattern of two back to back stacked coplanar monopole antenna 125

Fig. 5.1 General block diagram for the energy harvesting system. 132

Fig. 5.2 Wilkinson power divider/combiner 133

Fig. 5.3. Measured real and imaginary impedance at the input port of RF-DC converter circuit of the module. 135

Fig. 5.4. Seven stage RF-DC converter circuit on the RF designer circuit 137

Fig. 5.5. DC voltage at the first stage 138

Fig. 5.6. Simulated DC output voltage 138

Fig. 5.7. Simulated power input verses - DC output voltage curve for the frequency 900 MHz-10 GHz. 139

Fig. 5.8. Fabricated structure of the seven stage RF-DC converter circuit. 139

Fig. 5.9. Fabricated structure of the seven stage RF-DC converter circuit connected to the microwave source 140

Fig. 5.10. RF-DC converter circuit with single coplanar monopole antenna 142

Fig. 5.11. RF-DC converter circuit with 2×1 array coplanar monopole antenna..... 143

Fig. 5.12. RF-DC converter circuit with 2× **2** array coplanar monopole antenna 143

Fig. 5.13. Fabricated RF energy harvesting module 144

Fig. 5.14. Experimental horn transmitting antenna set up for RF energy harvesting module..... 145

Fig. 5.15. Input RF power versus DC output graph for the five resonance frequencies of the antenna of the RF energy module 147

Fig. 5.16. Inp. power versus effici. curve for f_0 = 9.4GHz and R = 20K ohms. 148

Fig. 5.17. Load resis. versus efficie. cur. for f_0 = 9.4GHz at inp. power = 10 dBm. . 148

LIST OF TABLES

Table 1.1 Comparison Amongst Feeding Techniques 14

Table 3.1 Design Parameters of a Microstrip Antenna for ε_r = 9.2 and h= 1.524 mm 72

Table 3.2 Design Parameters of a Microstrip Antenna for ε_r = 2.2, h = 1.575 mm 75

Table 3.3 Comparison of Simulation Results of Different Rectangular Microstrip Antenna Designed on Different Substrates 77

Table 3.4 A Summary Table of Return Loss Results on the Simulator By Applying the Law of Transformation of Design for Equilateral Triangle Shape Patch for MS Antenna 84

Table 4.1 Comparative Results for Different Possible Array Arrangements of the Coplanar Monopole Antenna 126

Table 4.2 State of Art of the Designed Antenna 127

Table 5.1 Spice Model of Schottkey Diode 136

Table 5.2 Measurement of Received Power at the Port for Coplanar Monopole Antenna Structures with the Microwave Power Source of 10 MHz-14 GHz with + 10 dBm Power 141

Table 5.3 Measurement of DC Output Voltage with The Microwave Power Source of 10 dBm 142

Table 5.4 Measurement of DC Output Voltage of RF Energy Harvesting Module with the Transmitting Horn Antenna Set Up 146

ABBRIVIATIONS

CPW	Coplanar Waveguide
DCE	Dielectric Constant Engineering
DC	Direct Current
HFSS	High Frequency Structure Simulator
LTCC	Low Temperature Co-Fired Ceramic
MSPA	Microstrip Patch Antenna
RF	Radio Frequency
SMA	Sub Miniturized Version A
VSWR	Voltage Standing Ratio
WLAN	Wireless Local Area Network
UWB	Ultra- Wideband

Chapter-1: INTRODUCTION

1.1Advances in Technology

Microstrip antenna is the heart of wireless communication systems. Miniaturization of microstrip antenna structure and its designing are the main challenges for the researchers of this field. There are many designing formulae available for designing the structure of microstrip antenna for the given specifications and for the various shapes of patch. The people work for the change in the designing formulae as per their requirement and usefulness. For the designing of the microstrip antenna, always considered the working range of frequencies and it is demanded that the structure should be degined as compact as possible with wide band operation. For the integrated technologies, these antennas are likely to be designed with the whole circuit on a single substrate. Array designing of the structure is also the trying for enhancing the characteristics of the antenna.

At the present time, finding the different design formulae are also opted for making the process of designing more easy. The Equivalent design concept is one of the example of it.

Also the RF energy harvesting is the latest field of work. From last 2-3 years the antenna and its array for this module of RF energy harvesting is greatly presented for some specific applications. They show the work of designing the antenna structure, RF-DC Converter circuit and impedance matching in between these antenna and converter circuit for the particular application. So that the module will automatically capture the microwave energy from the atmosphere and convert it in to the suitable DC voltage to charge the low powering devices without any wired arrangement. It eliminates the need of the charger.

1.2 Motivation of the Research

Lots of research work has been done on Microstrip antennas as these are in large demand. Antenna parameters depend on the dielectric constant and thickness of the substrate material as well as on the resonance frequency. Shape and size of the resonating patch should be accurately calculated. The resonating length is typically equal to half wavelength in the material of substrate. However, fringing fields exist at the periphery of the patch. Therefore effective dimensions of the patch are slightly larger than its physical dimensions. Fringing fields are not confined in one material. Effective dielectric constant is therefore estimated and

used. Large number of formula has been introduced by curve fitting of experimental data. Iterative methods have been used in solving this formula. In this formula the extension in physical dimension is neither related with resonance frequency nor with the physical dimension itself. A separate formula is required for every shape. These is no correlation is any two designs.

Bhatnagar's postulate, equivalence of design concept and transformation of design approach opened a new method for solving design issues for the rectangular patch MSA. Extension in physical dimension has been directly related with the resonant frequency, dielectric constant and thickness of the substrate and the physical dimension itself. A relation has been established between two designs that resonate at the same frequency.

Feed line dimensions are also very important in any MSA design. My investigations have filled this gap and extended Bhatnagar's work to triangular MSA. Very interesting and important results of my research work is that the formulae derived for rectangular patch hold good for triangular patch also. These formulae do not depend on curve fitting and empirical values.

Every manufacturing process has got same tolerance or probable error associated with it. If tighter tolerances are required than same pieces may have to be rejected. No method was available for fine tuning of the resonant frequency during the process of fabrication. I have invented a method for this fine tuning during the fabrication process. My method is based on dielectric constant engineering. It is suitable for LTCC process where several layers of dielectric material are employed in MSA fabrication.

In addition to above said studies, RF energy harvesting module has also investigated by me. Many RF energy harvesting modules have been presented in the literature. The impedance matching between the antenna and converter circuit is the main issue for this. For matching purpose different methods have been presented in the literature. The connector less and multi frequency operated RF energy module was needed in this concern. This novelty has been presented by this work.

1.3 Research Contribution

This thesis contributes the easiest technique for fine tuning the resonant frequency which may be altered due to the fabrication error. It will be helpful in the mass production of

antenna or in the LTCC multilayered fabrication in which fabrication error tolerance could be considered before; for tuning the resonant frequency on the desired value.

This thesis also suggested an adds-on formulae of transformation of design for feedline dimensions using an equivalent design concept. The addition of these formulae makes complete set for the transformation of design. It proposes an easy designing technique for transform a good design on one type of substrate onto another substrate if both the designs have the same resonant frequency is same .

A coplanar monopole antenna has also been presented for RF energy harvesting purpose. This antenna works for wideband ranges from 900 MHz- 3.1 GHz and 5.6 GHz-9.9 GHz with the band rejection from3.1 GHz-5.6 GHz. Different array arrangement is presented which improves the characteristics of this antenna.

A novel RF energy harvesting module has been presented. The module has a novel antenna array structure and RF-DC converter circuit with different novel idea of impedance matching.This module is able to produce 1.823 V DC with respect to + 40 dBm input power. Which is a sufficient amount of DC voltage for powering the low power devices.

1.4 Thesis Organization

Chapter 1 INTRODUCTION

This chapter includes the motivation, contribution of the research and thesis organization. Also, this chapter thrashes out backround of microstrip antenna. The research work presented in this thesis is to concerned new formulae for designing of microstrip antenna. Therefore, this chapter includes all the basic knowledge about microstrip antenna performance parameters as well as the classical design formulae.The base of our investigations is the equivalent design formulae. So this chapter also includes brief theory about the equivalent design formulae by using Bhatnagar's postulate. This chpapter also includes the basics of RF energy harvesting modules and its need and applications.

In this thesis the research work carried out by me has been embodied in chapters 2, 3, 4, and 5. Every chapter embodies its own review of the corresponding work , its problem statement and also the methodology adopted to do that particular work.

Chapter 2 INVESTIGATIONS CONCERNING DIELECTRIC CONSTANT ENGINEERING

It represents the formula developed by me for multilayered microstrip antenna for fine tuning the resonance frequency of fabricated antenna. This tuning is achieved by cutting the material from one or two layer of the multilayered substrate. The area of cutting the material is calculated from this formula. Detail investigation is discussed in this chapter.

Chapter 3 NOVEL TECHNIQUE FOR ESTIMATING THE FEED LINE DIMENSIONS OF RECTANGULAR AND TRIANGULAR MICROSTRIP ANTENNA

The transformation of design formula for feed line by using Bhatnagar's constant for micro strip antenna for different shapes of patch i.e. rectangular, triangular has been discussed. It includes the derivation of formula and its validation from simulated and measured results.

Chapter 4 INVESTIGATIONS OF COPLANAR MONOPOLE WIDEBAND ANTENNA AND IT'S ARRAY ARRANGEMENTS

An antenna covering the wide bands from 900 MHz-10 GHz has been designed especially for RF energy harvesting purpose. It also rejects the band of WLAN & HIPER LAN (3.1 GHz-5.6 GHz) for the same purpose. This chapter includes simulated & measured results of the designed structure. Different array arrangements of the designed structure for enhancing the gain and increase the received power on the designed antenna i.e. 2×1 array, 2×2 array on the single substrate and combining their powers by using a power coupler, stacking of two single structure back to back has been discussed in this chapter. This chapter includes simulated & measured results of different array arrangement and their comparative statement.

Chapter 5 DEVELOPMENT OF A NOVEL RF ENERGY HARVESTING MODULE

A seven stage Converter circuit for harvester module has been presented with its simulated & measured results along with the single structure of the antenna. In addition to that, a novel idea of matching of antenna and converter circuit of RF energy harvesting module on a single substrate is demonstrated. Measured result of DC output of the designed harvester circuit on a single substrate with the 2×2 array of design is also presented.

Chapter 6 CONCLUSION AND FUTURE ASPECTS

The conclusion of the whole work , as well as the future aspects of this field is presented in this chapter.

1.5 Historical Background of Microstrip Antenna

Wireless communication has became the most promising and fastest growing system of communication industry. Antenna plays an important role in wireless communication [1]. The antenna is a transmitter or receiver part of the communication system that is used to capture or to radiate the EM waves.The wave radiate from the guided wave to the free space wave. If the distance between the transmission line is several times of the wavelengths, then the wave is emmited to the space and can be called free space wave. The antenna is the region between guided wave and free space wave [2].

Due to the advancement in technology, antennas have to be versatile in terms of efficiency, cost, size, weight, ease of installation etc. . The microstrip antenna can be used to fulfill these requirements. The concept of microstrip antenna was given by Deschamps [3] in 1950s. Later on, practical antennas were made by Munson [4] and Howell [5] in 1970s. They are inexpensive, easily fabricated using printed circuit technology and compatible with MMIC designs. The resonant frequency, radiation pattern, polarization, impedance are some of the parameters which can be easily controlled by changing the patch shape [6]. Before explain the work, it is necessary to understand the basics of microstrip antenna.

1.5.1 Microstrip Antenna

The antenna geometry is designed on the top layer of substrate having the dielectric constant ε_r and a ground plane below the substrate [7]. Fig 1.1 shows the structure of a microstrip antenna with microstrip feed line.

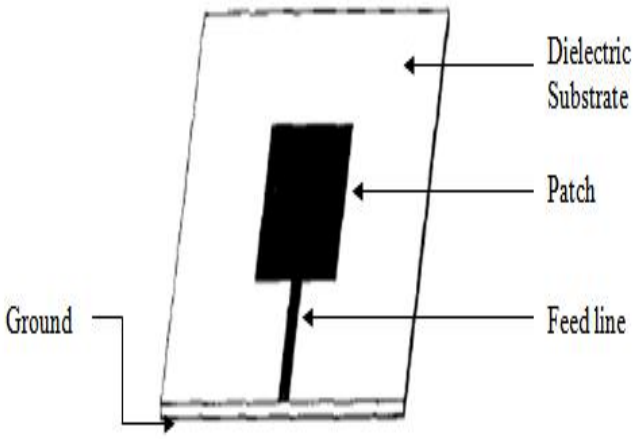

Fig. 1.1. Microstrip rectangular patch antenna with microstrip feed line [7]

Microstrip antenna has some advantages and disadvantages [8], [9] which are summarized below:

Advantages

- Low profile with the planar arrangement having light weight and small volume
- Low manufacture cost due to ease of using it on printed circuit board
- Can be easily integrated with other MICs on the same substrate
- Allow both type of polarizations i.e. linear and cross.
- Can be made in small size for mobile communication.
- Can be used to operate on multi frequencies.

Disadvantages

- The ohmic loss is increases due to the feeding arrangement for antenna arrays.
- The power handling capacity is lower.
- Extraneous radiation from feeds and junctions.
- The surface waves are also excited.

- Polarization is difficult to attain.

Applications [10]-[13]: Microstrip antenna can be used in-

- Direct broadcast service in Satellite communication
- Satellite navigation receivers
- Radio altimeters
- Command and control systems
- Doppler and other radars
- Missiles and telemetry
- Biomedical radiators and intruder alarms
- Integrated antennas
- Feed element in complex antennas
- Mobile radio
- Remote sensing and environmental instrumentation

Limitations of Microstrip Antenna

The microstrip antenna's narrow bandwidth and low gain are the limitations. Due to the requirement of the microstrip antenna to be low volume and low profile, these factors further decline the above two limitations. It is due to the fact that the size, bandwidth and efficiency of an antenna are interlinked to each other. As the size of the antenna decreases, the operating bandwidth or the antenna efficiency may decrease. Generally, the size of the antenna is related to gain i.e. lower the size of an antenna, lower will be the gain. Researchers have been using various techniques to reduce the size of an antenna with the gain and bandwidth enhancement. Some of the techniques are using high dielectric substrate material, slotted patch antenna and stacked configuration [14], [15]. Substrate loading methods can be used to increase the radiation efficiency. Use of two patches i.e. parasitic and the driven patch [16] may also enhance the gain and bandwidth of an antenna.

1.5.2 Feeding Techniques

There are different feeding configurations for the microstrip antenna. The four most popular feeding methods are

- Microstrip line,
- coaxial probe,
- Aperture coupling
- and Proximity coupling.

These feeding methods can be categorized into two groups – contacting and non-contacting. In the contacting method, the conducting element in the form of microstrip line is directly feed the RF power to the radiating patch. In the non-contacting method, the RF power is transferred by electromagnetic field coupling of the microstrip line to the radiating patch. The two types of feed technique used as contacting schemes are linefeed and coaxial-probe feed and the remaining two feeding techniques used as non-contacting schemes are aperture coupling and proximity coupling. A brief description of these feeding configurations is given below:

1.5.2.1 Microstrip line

The microstrip feed line is simple to model and fabricate. The conducting line is directly connected to the patch. The width of conducting line is much less than the patch. The matching with the patch can be easily done by varying the feed position. The etching is done on the same substrate as with the patch. So this provides a planar structure [10]. But if the thickness of the substrate increases,the bandwidth will be limited (2-5%). Because an increase in thickness will increases the surface waves and counterfeit radiation. The solution of this problem can be overcome by modifying or cutting a slot in the ground plane [17]. A microstrip antenna with microstrip feed line is widely used as harmonic transponders at 10.6 GHz [18]. It can also be used for dual frequency operation which extends its use towards microwave circuitry and antenna arrays [19]. The microstrip feed line diagram and equivalent circuit are shown in Fig. 1.2 and 1.3 respectively.

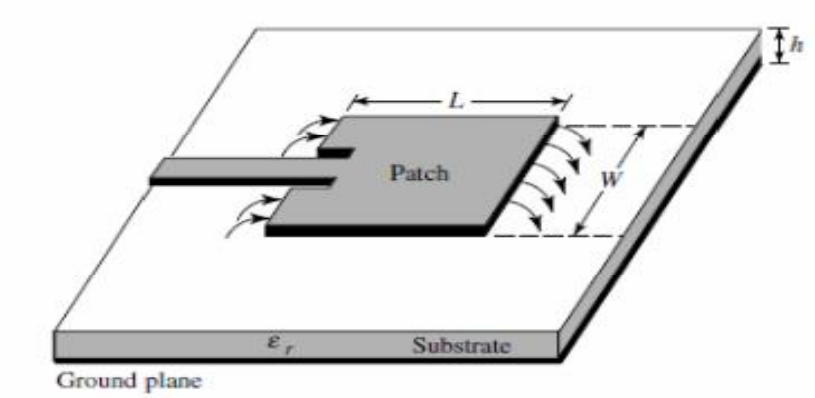

Fig. 1.2. The Microstrip feed line at the radiating edge [10]

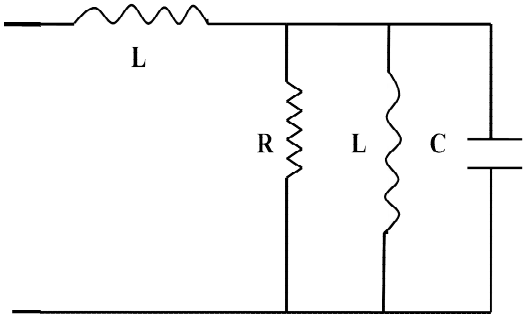

Fig. 1.3. Equivalent circuit of the microstrip feed line [10]

Quarter-wavelength transmission line can also be used for impedance matching between the microstrip antenna and a transmission line as shown in Fig. 1.4.

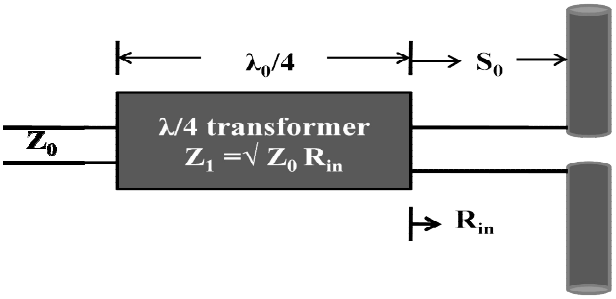

Fig. 1.4. An antenna with a quarter-wavelength matching section [10]

Let quarter-wavelength transmission line has characteristic impedance Z_1 and that of transmission line has Z_0. The transformer is placed at a distance of s_0 from the antenna. The matching is to be done between the input impedance (Z_{in}) and the characteristic impedance (Z_0). The impedance of the microstrip antenna is taken as Z_L, and then the input impedance

(Z_{in}) from the beginning of the quarter-wavelength transmission line will be [10] as shown in eq. (1.1)

$$Z_{in} = Z_0 = \frac{Z_1^2}{Z_L} \tag{1.1}$$

On rearranging,

$$Z_1 = \sqrt{Z_0 Z_L} \tag{1.2}$$

So if values of impedance are known for the transmission line and the antenna, then the value of characteristic impedance of the quarter wavelength transformer to be connected is equal to the square root of their product [10]. The value of input impedance Z_{in} can be changed by suitable selection of Z_1, so that $Z_{in} = Z_0$ and the matching is done. The impedance Z_1 depends on the width of the quarter-wavelength transmission line. So, the parameter Z_0 will have a lower value for a wide strip of quarter-wavelength transmission line [20].

1.5.2.2 Coaxial probe feed

The coaxial probe feed line is simple to fabricate but difficult to model. The inner conductor is connected to the radiating patch and outer is attached to the ground. The impedance matching is much easier than a microstrip feed line at the position of the probe can be easily adjusted as per requirement [8]. It has low spurious radiation and narrow bandwidth (2-5%). The analysis of the input impedance of a probe feed can be done using transmission line or cavity model. The input impedance of the antenna depends on the feed location and its dimensions [21]. Generally the probe inductive reactance in series with antenna impedance is considered for calculating total input impedance, but results will be better if the capacitive reactance between the patch and the ground plane is also taken into account with the inductive reactance of the probe [22]. The coaxial probe feed in single or multilayered microstrip antenna can be used for WLAN (2.4-2.48, 5.15-5.825 GHz) band applications [23]. Experimental works [24], [25] shows that the input resistance of the probe-fed structure shows cosine squared behaviour. The coaxial probe feed diagram and equivalent circuit are shown in Fig. 1.5 and 1.6 respectively.

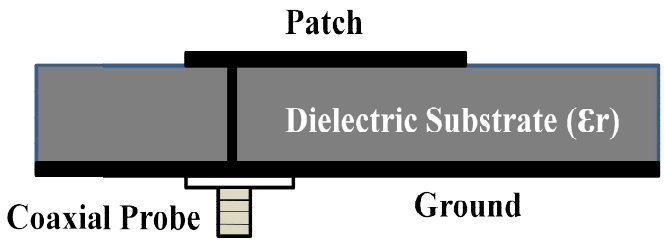

Fig. 1.5. Coaxial probe feeding at the radiating patch [10]

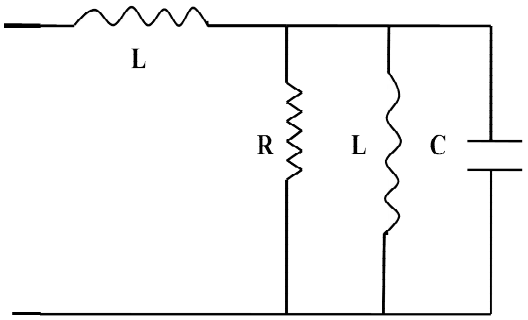

Fig. 1.6. Equivalent circuit of coaxial probe feed line [10]

1.5.2.3 Aperture coupling

Aperture-coupled feed is used to overcome the problem with the microstrip feed line and coaxial probe feed as they possess asymmetries which produce higher order modes which give cross polarized radiation [7]. In this feeding technique, two dielectric substrates are used which are separated by ground plane. The radiating patch is at the top of the upper substrate and the microstrip feed line at the bottom of the lower substrate [8]. The energy of the microstrip feed line is coupled to the radiating patch through a slot/aperture in the ground plane. Generally, a high dielectric substrate is used at the bottom and low dielectric substrate at the top. It has low spurious radiations. The matching is done by controlling the width of the feed and length of the slot [8]. The bandwidth of an antenna can be enhanced by adding a shunt stub and shorting pins to the feed line [26] or by varying the aperture position, width and size [27]. Also, the dual frequency antenna with large bandwidth can be made with the help of this feed line [28]. The aperture-coupled feed diagram and equivalent circuit are shown in Fig. 1.7 and 1.8 respectively.

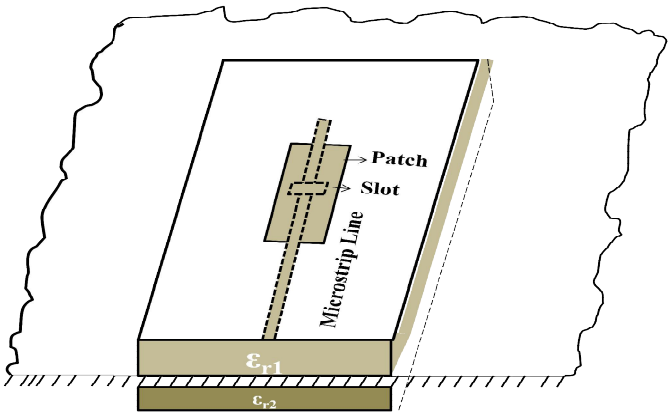

Fig. 1.7. Aperture-coupled feed [10]

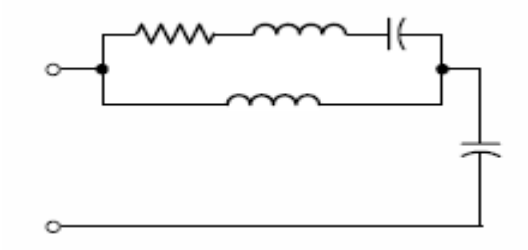

Fig. 1.8. Equivalent circuit of aperture-coupled feed [10]

1.5.2.4 Proximity-coupled feed

Proximity-coupled feed is also known as an electromagnetic coupled microstrip line. It requires multilayered fabrication. In this, two dielectric substrates are used. The radiating patch is at the top of the upper substrate and feed line is between two dielectric substrates. It produces less spurious radiation than microstrip feed line [9]. The nature of the coupling between radiating patch and the feed line is capacitive. The coupling tunes the bandwidth and matches the impedance. It also requires right alignment of the feed line with the radiating patch otherwise mismatching will occur [29]. With this feeding technique, 13% bandwidth can be achieved. Broadband impedance matching can be done using narrow cavity backed configuration [29] which can increase bandwidth up to 40 % and provide critical coupling.

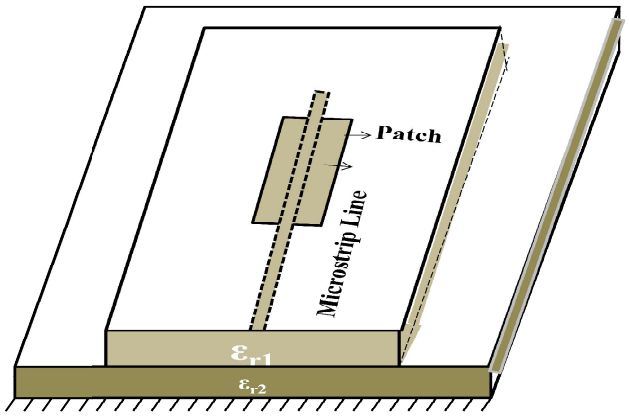

Fig. 1.9. Proximity-coupled feed [10]

With proximity-coupled feed line, the antenna can be work simultaneously on Bluetooth (2.4-2.485 GHz), WiMAX (3.3–3.7 GHz), and WLAN (5.15–5.35 and 5.725–5.85 GHz) bands using a stepped-impedance resonating structure [30]. The applications above mentioned can be increased by using a corner-truncated rectangular patch with a rectangular slot, meandered microstrip feed, and defected ground plane in an antenna so that it can also operate in LTE2300 (2300–2400 MHz) and UMTS (1920–2170 MHz) band [31]. The proximity-coupled feed diagram and equivalent circuit are shown in Fig. 1.9 and 1.10 respectively.

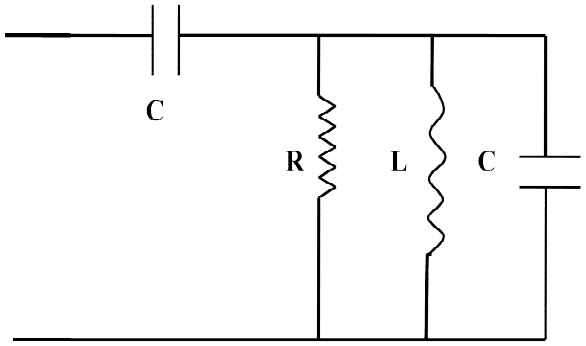

Fig. 1.10. Equivalent circuit of proximity-coupled feed [10]

1.5.2.5 Comparison amongst feeding techniques

The different types of feeding for a microstrip patch antenna are explained above. To understand them quickly the Table 1.1 shows the comparisons between the feeding techniques in terms of their characteristics [32].

Table 1.1 Comparison Amongst the Feeding Techniques

Characteristic	Microstrip feed	Coaxial feed	Aperture feed	Proximity feed
Return loss	Less	More	Less	More
Resonant frequency	More	Less	Least	Highest
Impedance matching	Easy	Easy	Easy	Easy
VSWR	Lower than 1.5	Between1.4 to 1.8	Approx equal to 2	Less than 1.23
Reliability	Better	Poor due soldering	Good	Good
Spurious feed radiation	More	More	More	More
Polarization purity	Poor	Poor	Excellent	Poor
Ease of fabrication	Simple	Soldering and drilling needed	Alignment required	Alignment required
Bandwidth	2 - 5 %	2 – 5 %	21 %	13 %

1.5.3 Types of Microstrip Antennas

There are different types of microstrip antenna configuration. They are characterized by a large number of physical parameters. They have different geometric shapes and dimensions [8], [33]. The microstrip antenna can be divided into four categories which are [8]

- Microstrip patch antenna
- Microstrip or printed dipole antenna

- Printed slot antenna
- Microstrip traveling-wave antenna

All antennas cannot be discussed here as the work is only based on the microstrip patch antenna. So an overview of microstrip patch antenna is given below.

1.5.3.1 Microstrip patch antenna

A microstrip patch antenna has a radiating patch on one side of a dielectric substrate and ground plane on the other side. The radiating patch is of copper or gold and can have any shape, but regular shapes are used to simply for analysis and results [34]. The simplest microstrip patch antenna is shown in Fig. 1.11.

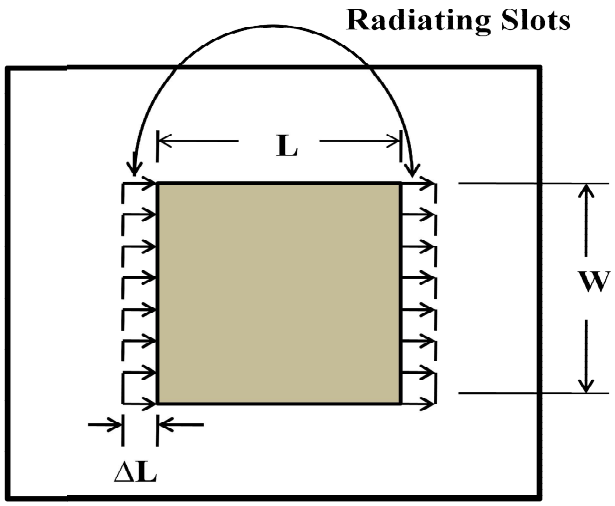

Fig. 1.11. Rectangular microstrip patch antenna with radiating slots [7]

The rectangular microstrip patch antenna has some performance predictions. The length of the patch (L) is usually $0.3333\ \lambda_0 < L < 0.5\ \lambda_0$, where λ_0 is the free-space wavelength. The patch on the substrate material is taken to be very thin such that $t << \lambda_0$ (where t is the patch thickness). The thickness (h) of the dielectric substrate material is usually $0.003\ \lambda_0 \leq h \leq 0.05\ \lambda_0$. The choice of dielectric constant (ε_r) of the substrate material is typically in the range $2.2 \leq \varepsilon_r \leq 12$. The radiation from the Microstrip patch antennas is primarily due to the fringing fields between the patch edge and the ground plane. The antenna gives good performance if a thick dielectric substrate material having a low dielectric

constant is chosen. With this, it also provides better radiation, larger bandwidth and better efficiency. But, the size of the antenna becomes larger if these constraints are taken. So, if a compact antenna has to be designed then a thin dielectric substrate material having a high dielectric constant is required. It may cause the antenna to become less efficient and result in narrower bandwidth. Therefore a balance is required between the antenna dimensions and the antenna performance.

Most commonly used patch conductors are rectangular and circular in shape and may have more than one feed point. The antennas discussed here have inset feed, but multi feed point antennas can be constructed for use at frequencies up to Ku band [6], [8]. The Fig. 1.12 shows different shapes of microstrip patch elements.

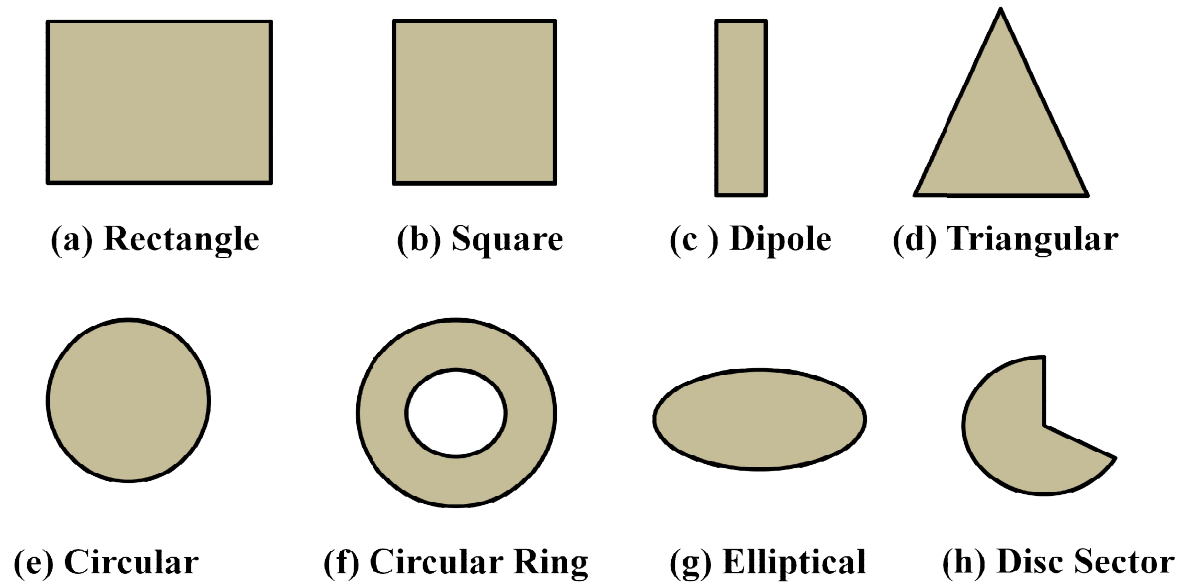

Fig. 1.12. Different shapes of microstrip patch elements [10]

1.5.4 Methods of Analysis

The MSA mainly consists of a two-dimensional radiating patch over a thin dielectric substrate. Therefore, for analysis point of view, it can classify as a two dimensional planar component. The methods of analysis for MSAs can be separated into two groups.

The first group consists of the methods which are established on the ground of equivalent magnetic current distribution around the patch edges as similar to slot antennas.

The three analytical techniques are given below

- The transmission line model [35], [36]: It is the simplest method of analysis, but less accurate and widely used for rectangular patches.
- The cavity model [37], [38]: It is more complicated than the transmission line model, but also has some advantage over transmission line model like it gives good physical insight, more versatile and more accurate.
- The multiport network model [39], [40]: This model consists of many circuit networks that are connected to each other and each one of them shows one attribute of the MPA.

The second group consists of the methods which are established on the ground of equivalent electric current distribution on the patch conductor and the ground plane as similar to dipole antennas.

The numerical methods for analyzing microstrip patch antennas are as follows:

- The finite-difference time domain method (FDTD) [41]: It's a technique of numerical analysis and is widely used for computational electrodynamics. This method is complicated and computationally slow. It is more versatile than other methods [42].
- The finite-element method (FEM) [43]: It is also a numerical technique for boundary value problems to find an approximate solution. It is widely used for the antenna array [44].
- The method of moments (MOM) [45]: It is usually used for rectangular and non-rectangular shapes of microstrip antenna. The model for the microstrip patch and dielectric slab are surface currents and polarization currents respectively [46].
- The spectral domain technique (SDT) [47]: It is another numerical technique for making models of microstrip antenna. It is difficult and the most sophisticated for the model. It is very efficient in terms of time saving and accuracy [48].

The analysis of rectangular microstrip patch antenna can be done using transmission-line, cavity model and full wave as explained above. Here, only transmission line model analysis is discussed below.

1.5.4.1 Transmission-line model

The transmission-line model is easy, but less accurate than other methods. In this, the microstrip patch antenna consists of two radiating slot of width W and thickness h separated by a distance L with a low impedance Z_c. The microstrip line is shown in Fig. 1.13.

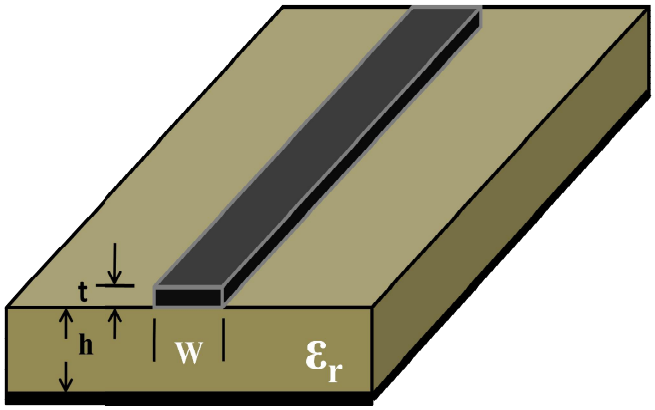

Fig. 1.13. Microstrip line [10]

The transmission line model for calculating the mutual coupling between two rectangular microstrip antennas can be easily done by making the following assumptions [49]

- The mutual coupling is due to the concurrent effect of
  - Interaction through free space radiation
  - Interaction through surface waves
- The rectangular microstrip antenna can be represented by two narrow slots

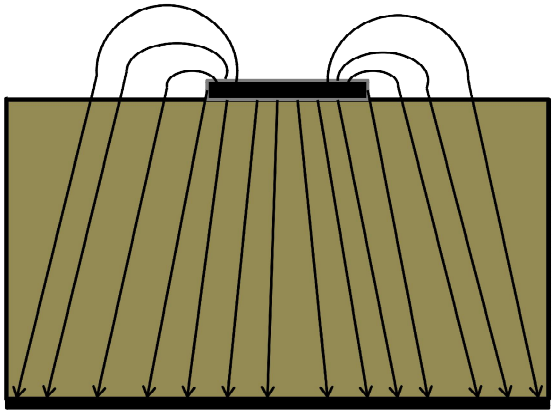

Fig. 1.14. Electric field lines [10]

The fields at the edges of the patch undergo fringing as the dimensions of the patch are finite. The fringing is dependent on the dimensions of the patch and thickness of the substrate. The electric field lines for a microstrip feed line are shown in Fig. 1.14. Most of the electric lines stayed within the substrate and some are in the air. As $W/h \gg 1$ and $\varepsilon_r \gg 1$, fringing causes the microstrip feed line to look like wider electrically resemble to its physical dimensions [8], [10].

Accommodated to that fringing, an effective dielectric constant ε_{reff} is introduced which is shown in Fig. 1.15. The range of the effective dielectric constant is $1 < \varepsilon_{reff} < \varepsilon_r$. For $\varepsilon_r \gg 1$, the value of ε_{reff} is almost equal to the actual value of the dielectric constant ε_r of the substrate. The value of ε_{reff} very much depends on frequency. For a low frequency, its value is constant and as the frequency increases to higher value, the value of ε_{reff} also increases and nearly closes to the value of dielectric constant ε_r of substrate [10].

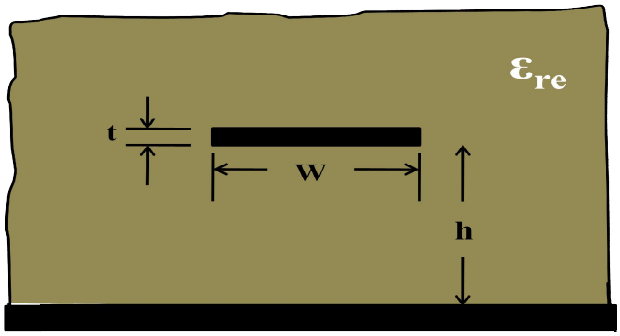

Fig. 1.15. Effective dielectric constant [10]

For higher-order mode, cavity model is generally used instead of the transmission line model [10]. The transmission line model has disadvantages, but can be made more accurate by considering the mutual radiative coupling between the equivalent slots and the effect of the side slots on the radiation conductance. The new model generated from this is implemented to antennas having a single microstrip transmission line [50]. Input characteristic of the rectangular microstrip antenna for the wide band of frquencies can be shown by the transmission line model. It uses a series combination of transmission lines for each transverse magnetic (TM) mode. The results are good when three transmission lines are used for the range of frequency at which the TM_{02} mode is excited [51].

The expression of the effective dielectric constant can be given as in eq. (1.3) [10]

For $W/h > 1$

$$\varepsilon_{reff} = \frac{\varepsilon_r + 1}{2} + \frac{\varepsilon_r - 1}{2}\left(1 + 12\frac{h}{W}\right)^{-½} \quad (1.3)$$

where, ε_{reff} = Effective dielectric constant of substrate material

ε_r = Dielectric constant of substrate material

h = Thickness of dielectric substrate material

W = Width of the patch

Another expression of the effective dielectric constant is given as [9] in eq. (1.4)

$$\varepsilon_{reff} = \frac{\varepsilon_r + 1}{2} + \frac{\varepsilon_r - 1}{2}\left(1 + 10\frac{h}{W}\right)^{-½} \quad (1.4)$$

The fringing effect [52] also causes to electrically increase the dimensions of the patch as compared to its physical dimensions. The effect is shown in Fig. 1.16, where the length of the patch is increased at both ends by ΔL. The increase in length ΔL is a function of effective dielectric constant (ε_{reff}) and width to thickness ratio (W/h).

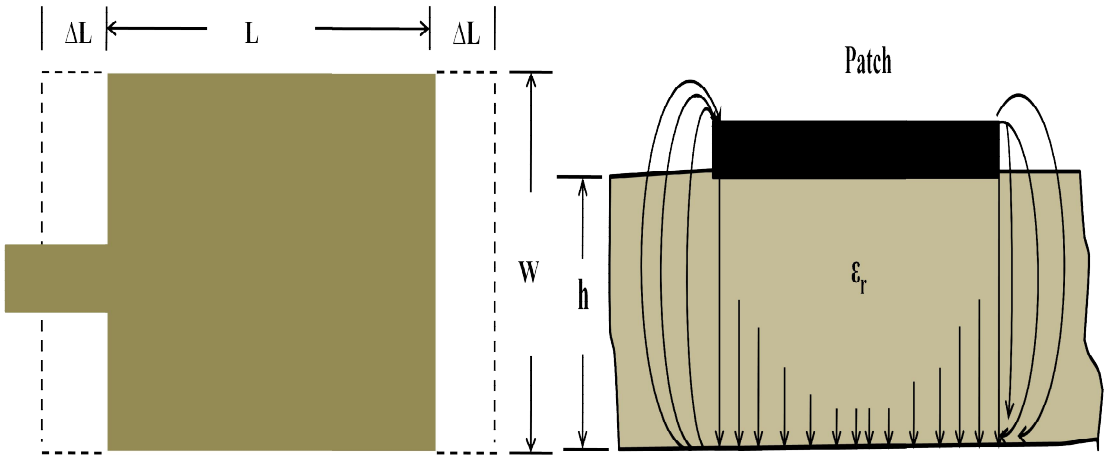

(a) Top view (b) Side view

Fig. 1.16. Physical and effective length of a rectangular microstrip patch [10]

The Normalized extension in the length is given by [10]

$$\frac{\Delta L}{h} = 0.412 \frac{(\varepsilon_{reff} + 0.3)\left(\frac{W}{h} + 0.264\right)}{(\varepsilon_{reff} - 0.258)\left(\frac{W}{h} + 0.8\right)} \tag{1.5}$$

Some researchers have used a dfferent formula for extension in length (Δ L) [9]. It is

$$\Delta L = \frac{h}{\sqrt{\varepsilon_r}} \tag{1.6}$$

Yet other expression of extension of the length (Δ L) in use is [9][53]

$$\Delta L = h\, \xi_1\, \xi_2\, \xi_5 / \xi_4\, \xi_3 \tag{1.7}$$

where

$$\xi_1 = 0.434907 \frac{\varepsilon_{reff}^{0.81} + 0.26}{\varepsilon_{reff}^{0.81} - 0.189} \frac{(W/h)^{0.8544} + 0.236}{(W/h)^{0.8544} + 0.87} \tag{1.8}$$

$$\xi_2 = 1 + \frac{(W/h)^{0.371}}{2.358\varepsilon_r + 1} \tag{1.9}$$

$$\xi_3 = 1 + \frac{0.5274 \arctan\left[0.084\, (W/h)^{1.9413/\xi_2}\right]}{\varepsilon_{reff}^{0.9236}} \tag{1.10}$$

$$\xi_4 = 1 + 0.0377 \arctan[0.067\, (W/h)^{1.456}]\{6 - 5 \exp[0.036(1 - \varepsilon_r)]\} \tag{1.11}$$

$$\xi_5 = 1 - 0.218 \exp(-7.5\, W/h) \tag{1.12}$$

where, ε_{reff} is effective dielectric constant of substrate material and other parameters have the usual meaning. ξ_1 , ξ_2 , ξ_3 , ξ_4 and ξ_5 are the parameters to calculate the value of extension in the length (ΔL)

The electrical length of the patch is given by the eq. (1.13) [10]

$$L_{eff} = L + 2\, \Delta\, L \tag{1.13}$$

where, L_{eff} = Effective length of the patch

and L = Physical length of the patch

The effective length of patch is given by the eq. (1.14) [10]

$$L_{eff} = \frac{\lambda_g}{2} \tag{1.14}$$

Where λ_g is guided wavelength in dielectric medium and is given by the eq. (1.15)

$$\lambda_g = \frac{\lambda_0}{\sqrt{\varepsilon_{reff}}} \tag{1.15}$$

$$\lambda_0 = \frac{c}{f} \tag{1.16}$$

where, λ_0 = free space wavelength

c = velocity of light in free space, 3×10^8 m/s and f = resonant frequency

The width of the patch is given by the eq. (1.17) [10]

$$W = \frac{c}{2f}\sqrt{\frac{2}{\varepsilon_r + 1}} \tag{1.17}$$

Another expression is used for width of patch W which is given by [54] the eq. (1.18)

$$W = \frac{\lambda_0}{2\sqrt{\varepsilon_r}} \tag{1.18}$$

The resonant input resistance can be varied with the help of inset feed by recessing a distance y_0 to form a slot as shown in Fig. 1.17. The matching of impedance of the microstrip feed line with radiating patch can be done by using this technique [55].

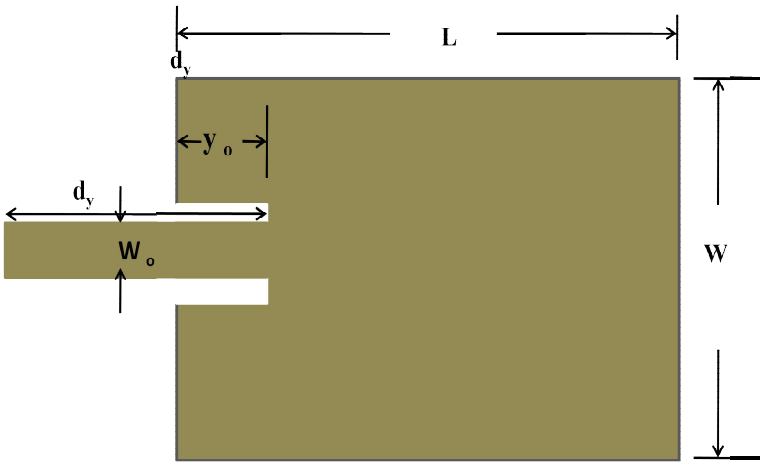

Fig. 1.17. Microstrip feed line [10]

The input resistance of the inset feed is given by the eq. (1.19) [10]

$$R_{in}(y = y_0) = \frac{1}{2(G_1 \pm G_{12})}\left[\cos^2\left(\frac{\pi}{L}y_0\right) + \frac{G_1^2 + B_1^2}{Y_c^2}\sin^2\left(\frac{\pi}{L}y_0\right) - \frac{B_1}{Y_c}\sin\left(\frac{2\pi}{L}y_0\right)\right] \quad (1.19)$$

where $Y_c = 1/Z_c$ and generally for most microstrips $G_1/Y_c << 1$ and $B_1/Y_c << 1$, then above equation reduces to

$$R_{in}(y = y_0) = \frac{1}{2(G_1 \pm G_{12})}\cos^2\left(\frac{\pi}{L}y_0\right) \quad (1.20)$$

$$R_{in}(y = y_0) = R_{in}(y = 0)\cos^2\left(\frac{\pi}{L}y_0\right) \quad (1.21)$$

where, R_{in} ($y = y_0$) = Input resistance at a distance y_0

R_{in} ($y = 0$) = Input resistance at the edge of the patch

L= Length of the patch

Y_c = Admittance of the line

G_1= Conductance of the line

G_{12}= Mutual Conductance of the line

B_1= Suseptance of the line

The distance y_0 can be easily determined by the eq. (1.21).

The values of G_1 and G_{12} mentioned in the eq. (1.19) are given by

$$G_1 = \frac{I_1}{120\,\pi^2} \tag{1.22}$$

where

$$I_1 = \int_0^{\pi} \left[\frac{\sin\left(\frac{k_0 W}{2}\cos\theta\right)}{\cos\theta}\right]^2 \sin^3\theta\, d\theta \tag{1.23}$$

$$= -2 + \cos(X) + XS_i(X) + \frac{\sin(X)}{X} \tag{1.24}$$

$$X = k_0 W \tag{1.25}$$

Asymptotic values of equations (1.23) and (1.24) are

$$G_1 = \begin{cases} \frac{1}{90}\left(\frac{W}{\lambda_0}\right)^2 & W \ll \lambda_0 \\ \frac{1}{120}\left(\frac{W}{\lambda_0}\right) & W \gg \lambda_0 \end{cases} \tag{1.26}$$

and

$$G_{12} = \frac{1}{120\pi^2}\int_0^{\pi} \left[\frac{\sin\left(\frac{k_0 W}{2}\cos\theta\right)}{\cos\theta}\right]^2 J_0(k_0 L\sin\theta)\sin^3\theta\, d\theta \tag{1.27}$$

where J_o is the Bessel function of the first kind of order zero.

The eq. (1.21) works well for the inset-feed patch antenna [56]. The graph in Fig. 1.18 is calculated by using eq. (1.21). The graph shows that as the inset feed reaches to the centre of the patch from the edge, the input impedance changes very rapidly and closes to zero [34]. At the centre of the patch, input resistance also changes very rapidly.

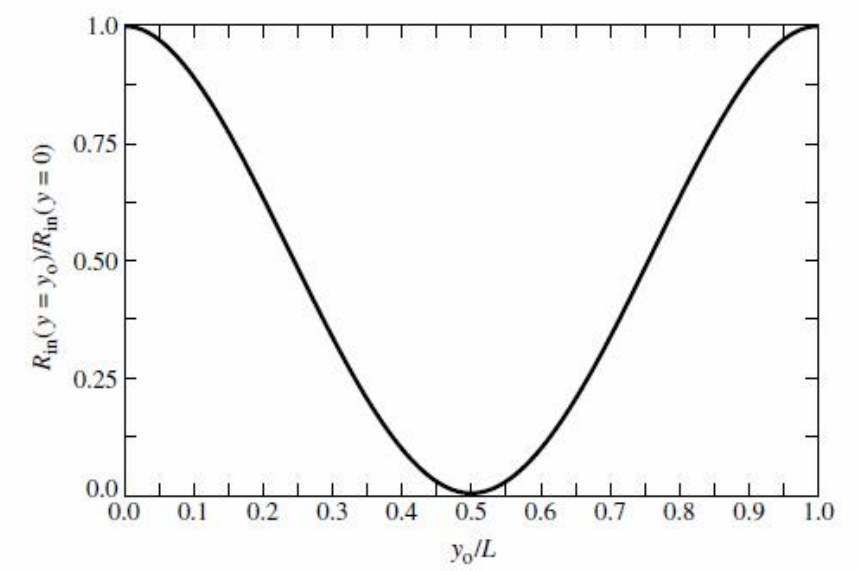

Fig. 1.18. Variation of normalized input resistance [10]

The characteristic impedance Z_c of a Microstrip line is given by the eq. (1.28) and (1.29) [10]

For $\frac{W_0}{h} \leq 1$

$$Z_C = \frac{60}{\sqrt{\varepsilon_{reff}}}\left[\ln\left(\frac{8h}{Wo} + \frac{Wo}{4h}\right)\right] \tag{1.28}$$

For $\frac{W_0}{h} > 1$

$$Z_C = \frac{120\pi}{\sqrt{\varepsilon_{reff}}\left[\frac{W_0}{h} + 1.393 + 0.667\ln\left(\frac{W_0}{h} + 1.444\right)\right]} \tag{1.29}$$

where, W_0 = Width of the microstrip line and h= substrate height

The characteristic impedance of a microstrip line can also be given as [8] assuming the thickness of the strip line negligible

$$Z_0 = \frac{\eta_0}{2\pi\sqrt{\varepsilon_{re}}}\ln\left\{F_1/u + \sqrt{1 + 4/u^2}\right\} \tag{1.30}$$

where,

$$F_1 = 6 + (2\pi - 6) \times \exp\{-(30.666/u)^{0.7528}\} \tag{1.31}$$

$$\eta_0 = 120\pi \tag{1.32}$$

$$u = W/h \tag{1.33}$$

and

$$\varepsilon_{re} = \frac{\varepsilon_r + 1}{2} + \frac{\varepsilon_r - 1}{2}\left(1 + \frac{10}{u}\right)^{-ab} \tag{1.34}$$

in which

$$a = 1 + \frac{1}{49}\ln\left\{\frac{u^4 + (u/52)^2}{u^4 + 0.432}\right\} + \frac{1}{18.7}\ln\left\{1 + \left(\frac{u}{18.1}\right)^3\right\} \tag{1.35}$$

$$b = 0.564\left(\frac{\varepsilon_r - 0.9}{\varepsilon_r + 0.3}\right)^{0.053} \tag{1.36}$$

Another expression for characteristic impedance of a microstrip line can be given as [57] in eq. (1.37)

$$Z_0 = \frac{\eta_0}{2\sqrt{2}\pi\sqrt{\varepsilon_r + 1}}\ln\left\{1 + \frac{4h}{w'}\left[\frac{14 + 8/\varepsilon_r}{11}\frac{4h}{w'} + \sqrt{\left(\frac{14 + 8/\varepsilon_r}{11}\right)^2\left(\frac{4h}{w'}\right)^2 + \frac{1 + 1/\varepsilon_r}{2}\pi^2}\right]\right\} \tag{1.37}$$

where w’ is an equivalent strip width that takes the thickness t of the strip into account and is given by

$$w' = W + \Delta w' \tag{1.38}$$

where

$$\Delta w' = \Delta w\left(\frac{1 + 1/\varepsilon_r}{2}\right) \tag{1.39}$$

$$\frac{\Delta w}{t} = \frac{1}{\pi}\ln\left[\frac{4e}{\sqrt{\left(\frac{t}{h}\right)^2 + \left(\frac{\frac{1}{\pi}}{\frac{W}{t} + 1.1}\right)^2}}\right] \tag{1.40}$$

All the formule are called classical formule for antenna designing. These formulae are frequently used for designing the rectangular patch antenna . But these formulae are not easy to learn . Every time complex calculations have to be done .

1.5.5 Performance Parameters of Microstrip Antenna

The design parameters are already described above. All the parameters which are used to describe the nature of microstrip antenna are called performance parameters of that microstrip antenna. In other word performance parameters are important specifications used to show characteristics of any microstrip antenna.. There are many such parameters for microstrip antenna but for sake of convenienece only those parameters are described below which are mentioned in this work.

1.5.5.1 Input impedance

Iinput impedance for microstrip antenna is defined as the impedance measured at the outer terminals of antenna. In other word we can say that it is the ratio of magnetic field component to electric field component[58]. The formulae for calculating the input impedance of antenna are already discussed above.The input impedance of designed antenna is important to find because the impedance matching is the major design issue. Standared connectors available in the market have impedance of 50 and 75 ohms, so the impedance of line feed should be matched to this impedance for maximum transfer of power and minimum losses. The input impedance is estimated from the graph of input impedance with respect to operational range of frequency.

1.5.5.2 Resonance frequency

Resonance frequency for microstrip antenna is defined as the frequency at which the antenna shows zero reactance. But In fact for thicker substrate antenna the zero value of reactance can not be achieved. So the resonance frequency can be redefined as the frequency at which the resistance shows maximum value [59]. To design any structure of antenna it is the nessasary to define the resonance frequency of structure . All the design parameters are calculated for this paramter. The resonant frequency is checked with the help of return loss (S_{11}) in dB vs frequency (f_o) in GHz graph.

1.5.5.3 VSWR

VSWR is the voltage standing wave ratio and it is the maximum to minimum ratio of voltages of the antenna. It can be measured by the reflection coefficient (Γ). Reflection coefficient is the ratio of incident wave amplitude and the refelected wave amplitude. The formula for calculating VSWR is as shown below by eq. (1.41)

$$\text{VSWR} = \left(\frac{|\Gamma| + 1}{|\Gamma| - 1}\right) \tag{1.41}$$

The value of VSWR should be in between 1 to 2 at the resonance frequency.

1.5.5.4 Radiation pattern

Radiation patten is the 2 or 3 dimension graph or pattern of E-Field and H- field intensity in the particular direction or in the particular angles . Intensity is measured in $\mu w/m^2$ and angles are defined in solid angle (degrees). This E- Fild pattern graph shows that where antenna radiates maximum (by main lobe) and where the radiation is minimum (by side lobes) . It also indicates whether the design antenna is omni directional or not. The H-field graph is used to show the current density of antenna in the particular angles or directions.

1.5.5.5 Gain

Gain is the multiplication of antenna efficiency and directivity**.**

$$\text{Gain (G)} = (\text{efficiency } (\eta) \times \text{directivity (D)}) \tag{1.42}$$

Directivity is the ratio of radiated power by the antenna to the radiated power by an istotropic antenna. Efficiency represents the losses of the antenna . It includes the ohmic , conductor, dielectric loss. The gain is measured in dBi or in dB. The unit dBi means the gain with respect to the isotropic antenna gain.

1.5.5.6 Current distribution

Current distribution shows the current path of the antenna.

1.6 Bhatnagar Postulates And It's Implication

The designing of microstrip patch antenna requires different formulae to calculate its parameters. Some are simple and some are quite complex. There is no uniformity in formulae. Also, if one set of formulae are considered for designing of an antenna, then they have to be calculated again and again for each design for the new structure of the antenna. So there is no relation between any two antenna designs despite of the same formulae used. To sort out this problem, transformation of rectangular microstrip patch antenna was given by using Bhatnagar's Postulate and Equivalent Design Concept which gives a relation between any two antenna designs.

The Bhatnagar's Postulate [60-61] for a rectangular antenna gives the direct relationship for extension in the physical length of the patch (d), patch width (W_p), dielectric substrate thickness (h) and electrical length of the patch (L_e) as shown in eq. (1.43)

$$d = \beta \frac{h \times L_e}{W_p} \tag{1.43}$$

where $d = 2\ \Delta L$ and β = constant of proportionality (Bhatnagar constant) and it does not depend on resonant frequency (f_0), dielectric constant (ε_r) and thickness (h) of the substrate material. Its value is unity for a rectangular patch.

From the above equation, a new parameter "H" is obtained which is called as the normalized thickness of the dielectric substrate and is given by eq. (1.44)

$$H = \frac{h}{\lambda_g} \tag{1.44}$$

Where

$$\lambda_g = \frac{\lambda_0}{\sqrt{\varepsilon_r}}$$

And

$$\lambda_0 = \frac{c}{f_0}$$

Therefore

$$H = \frac{1}{c} \times h \times \sqrt{\varepsilon_r} \times f_0 \tag{1.45}$$

Where c is the velocity of light.

The formula says that any variation in resonant frequency (f_0), substrate height (h) or dielectric constant (ε_r) will change the value of H. The uniqueness of H is that any change in the above three parameters can be offset by a suitable change in the other parameter to put H constant. This makes the H as a new superior parameter in the microstrip antenna designing.

1.6.1 Transformation of One Design into Another

Two designs of a patch antenna are said to be equivalent if their resonant frequencies are equal [60]. Let "H" be a constant among two designs of an antenna then it gives the relation as in eq. (1.46)

$$h_2 = \Psi h_1 \tag{1.46}$$

where

$$\Psi = \sqrt{\frac{\varepsilon_{r1}}{\varepsilon_{r2}}} \tag{1.47}$$

Ψ = Scaling factor.

ε_{r1} = Dielectric constant of substrate material for design 1

ε_{r2} = Dielectric constant of substrate material for design 2

h_2 = Thickness of substrate material for design 1

h_1 = Thickness of substrate material for design 2

Bhatnagar's postulate and the equivalent design conceptestablish relation between the two designs . This relation is given by the set of equations from (1.48) to (1.51)as follows [60], [61]

$$W_{p2} = \Psi W_{p1} \tag{1.48}$$

$$L_{e2} = \Psi L_{e1} \tag{1.49}$$

$$\Delta L_2 = \Psi \Delta L_1 \tag{1.50}$$

$$L_{p2} = \Psi L_{p1} \tag{1.51}$$

where, W_{p1}, W_{p2} = Width of the patch of design 1 and design 2 respectively

L_{e1}, L_{e2} = Electrical length of the patch of design 1 and design 2 respectively

ΔL_1, ΔL_2 = Extension length of the patch of design 1 and design 2 respectively

L_{p1}, L_{p2} = Physical length of the patch of design 1 and design 2 respectively

1.6.2 Generalization of Laws of Transformation [60]

The Laws of transformation are based on constant H values and for this the resonance frequency f_0 is constant between two designs. When transforming one design into another, the equation (1.46) restricts the value of thickness (h_2) as Ψh_1 so that H remains constant. But each dielectric sheet has some specific standard thickness. Therefore, the value of h_2 should be chosen from standard thickness given by manufacturer unless the material is specially produced for desired value of h_2. So, transformation laws should be generalized to meet this condition. The equations (1.48) to (1.51) will be changed accordingly and we get

$$H_2 = \frac{H_1}{\Psi \phi} \tag{1.52}$$

$$W_{p2} = \frac{W_{p1}}{\phi} \tag{1.53}$$

$$L_{e2} = \Psi L_{e1} \tag{1.54}$$

$$\Delta L_2 = \frac{\Delta L_1}{\phi} \tag{1.55}$$

$$L_{p2} = \Psi L_{p1} + \frac{\Psi h_1 - h_2}{\varepsilon_{r2}} \tag{1.56}$$

where,

$$\phi = \frac{h_1}{h_2} \tag{1.57}$$

The literature mentioned above is necessary to understand the concept and designing of a microstrip antenna. These concepts are used throughout this work . The designs have been validated by simulation in HFSS software [62].

The new concept of normalized thickness 'H' of the dielectric substrate is now fundamental parameter that governs the microstrip antenna. The properties of microstrip antenna not depend on the parameter resonant frequency (f_0), dielectric constant (ε_r) and thickness (h) of the substrate material independently. This new parameter embodies the whole effect of these three parameters. Scaling factor Ψ is another important parameter. It gives the link between any two designs.according to this individual values of ε_{r1} and ε_{r2} do not matter now . The important relation is the square root of the ratio of these two dielectric constants. All the new transformed dimensions are directly proportional to a known good design.

As it is known, for rectangular microstrip patch antenna both patch and feed line are important for designing. The above work is validated for patch design transformation only. So this thesis works to fill this gap by finding new simplified formulae for the feed line dimension of the rectangular microstrip patch antenna also. So that design may be transformed in a full manner.

1.7 RF Energy Harvesting

Energy harvesting from RF field have also the same potential as in water, solar, wind field. The application of this energy harvesting is in charging the low power devices which is used in mobile, biomedical, satellite etc . In atmosphere a lot of energy is available and may be captured on a suitable receiving antenna with sufficient magnitude. The idea of the RF energy harvesting is that this suitably rceived energy or power with suitably designed antenna is converted in to DC voltage with the help of RF-DC converter/multiplier circuit.The proper matching in between antenna and converter circuit is needed so that maximum energy of ambient enegy is converted into DC output. RF energy harvesting modules comprises of three sections as shown in Fig.1.19.

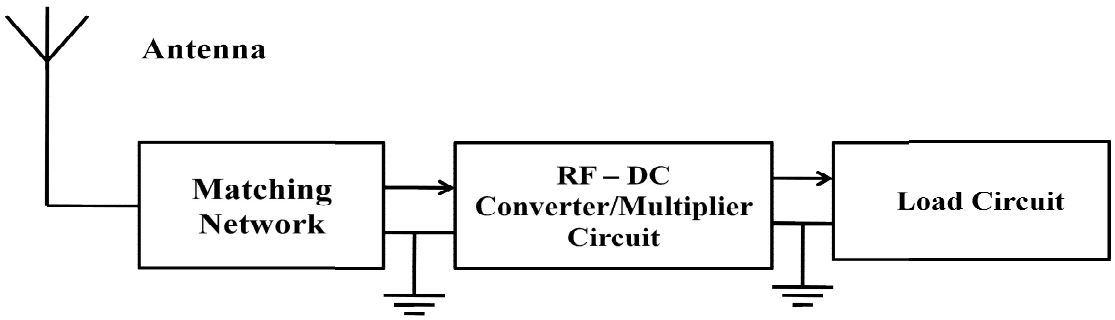

Fig. 1.19. Block diagram of RF energy harvesting module [58]

Low power devices are compact in size so they need miniaturized structure of harvester circuit. The antenna of this module should therefore be of microstrip / monople /PFA planar design . To design a harvesting module one has to design first his own antenna for the particular application/problem with desired performance, then design its RF- DC converter circuit and if needed also design its multiplier circuit to increase the DC output [63-66].

The performance of the module is checked by mainly two characteristics graphs, first is the graph between the DC power ouput in volts versus input power in dB m or power density in $\mu w/m^2$ and the second graph is between the Conversion efficiency in (%) versus input power in dB m or power density in $\mu w/m^2$.

The module is first designed with the help of licensed software high frequency structure simulator(HFSS version 16) and simulated structure is fabricated on a substrate. For measurement purpose the module is placed in front of the different horn antennas of the range

900 MHz-10 GHz and the respective DC output from the output of themodule is measured on the digital multimeter . The power is measured on power meter.

The conversion efficiency is calculated by the formula given below [67] in eq. (1.58)

$$\eta_{\text{RF to DC}} = \frac{P_{\text{out-DC}}}{P_{\text{in-AC}}\, A_{\text{eff}}} = \left(\frac{V^2{}_{\text{out-DC}}}{R_{\text{Load}}}\right) \frac{1}{P_{\text{in-AC}}\, A_{\text{eff}}} \tag{1.58}$$

$$\text{here} \quad A_{\text{eff}} = \left(\frac{\lambda_0{}^2}{4\pi}\right) G \tag{1.59}$$

Where $P_{\text{in-AC}}$ is the power density incident on the antenna in $\mu w/m^2$, $V_{\text{out-DC}}$ is the DC output voltage and R_{load} is the load resistive in nature. A_{eff} is the effective area of the antenna and G is the gain of the antenna.The comparison of simulated and measured results will prove the design of RF energy harvesting module.

Chapter 2: INVESTIGATIONS CONCERNING DIELECTRIC CONSTANT ENGINEERING

2.1 Introduction

Microwave integrated circuit technology has developed very rapidly due to its numerous unique and attractive features. For good design of microwave integrated circuits, accurate value of dielectric constant of substrate material should be known. For Integrated circuits, especially in LTCC technology, antenna structure may be composed of several substrates. The frequency of operation is dependent on the composite dielectric constant of the multilayered substrate.

Due to multilayer dielectric structure and for dielectric constant engineering a term effective composite dielectric constant has been used. Here the effective dielectric constant refers to the value of dielectric constant that a hypothetical material should have such that the microwave properties of the structure are not changed if the materials of the structure are replaced by the hypothetical material. One of the objectives of this dissertation is to find out a simple method of calculating that effective dielectric constant (ε_{reff}) of the multilayerd substrate.

When the MS antenna has more than two layers, the patch is on the first layer and ground is on the last layer for that structures sometimes the physical dimensions change due to fabrication errors occurs and that will alters the resonance frequency. That frequency can be retuned to the designed frequency without affecting patch dimensions. This thesis presents a new formula to cut dielectric material of known dimension (the area is calculated by the proposed formula) from that middle layers of the composite substrate which are beneath the layer of the substrate having the patch structure. The process is suitable only for the multilayered substrate. This method is very useful for the bulk fabrication of patch antennas in integrated circuit technologies. The results are simulated and analyzed using FDTD based optimizing licensed tool ANSYS_HFSS version16.

In this work three different dielectric materials are investigated for three different resonant frequencies. A graph between the Area Ratio (R) and the ratio of resonant frequency with cavity and without the cavity (f/f_0) has been plotted to generalize the findings. Here the area ratio is the ratio of the area of the cavity to the area of the patch.

This work has used the well-known relation of dielectric constant (ε_0) and resonance frequency (f_0) as in eq. (2.1) [68]

$$f_0 = \frac{c}{2(L + \Delta L)}\sqrt{\frac{1}{\varepsilon_0}} \tag{2.1}$$

During antenna fabrication it is possible that the physical length (L) of the patch may become different from it's designed value. The value of f_0 will then become different from it's designed value . The central idea of these investigations is that any variation in f_0 (from its designed value) may be offset by suitably varying the value of ε_0 . Modifications in the physical structure of the substrate for manuplating the value of ε_{reff} has been termed as "Dielectric Constant Engineering". I have done this for the case of multilayer substrate. The innovation is to cut a predetermined cavity in one or more layers of the substrates. I have located the cavity centrally below the radiating patch.

To analyze the mathematical relation of variation in resonant frequency with the cavity dimensions, the sandwhich comprising of the patch conductor, substrate layer(s) and cavity has been modeled as a capacitor.This relation has a significant role in the proposed concept of DCE.

2.2 Literature Review

The Dielectric Constant Engineering (DCE) has emerged as a new tool for manipulating the characteristics of microstrip antenna (MSPA). This approach is especially suited for Low -Temperature Co-fired Ceramic (LTCC) kind of substrates where the antenna substrate is a multilayer structure. Multilayer substrate is preferred due to ease of modification in the physical structure of the material. In this work DCE can be achieved by

(i) Modifying the physical structure of the material and,

(ii) Incorporating a second material in the original material.

In former one, a small cavity is cut from the dielectric substrate beneath the patch, which will be assumed as air filled in that cavity by putting $\varepsilon_0 = 1$ and in the later one another material of some other dielectric constant can be inserted into that cavity of the specified cavity size.

For finding an easy method to calculate the effective dielectric constant the literature related to multilayered dielectric structure and methods of calculating composite dielectric constant have been studied.

This thesis is concerned with the dielectric constant engineering for improvement in performance parameter of MS antenna. The resonant frequency has been considered as a performance parameter in this work. So from the literature, different methods of measuring/calculating dielectric constant of the multilayered substrate and its effect on resonant frequency due to fabrication errors were deeply studied.

Different methods are available for measurement of dielectric constant of material at microwave frequencies. One very common technique is the use of waveguide cavities which are partially or completely filled with the dielectric material to be measured. Another technique was described by the strip line method in which dielectric material was used as dielectric filling material in the tri plate-type strip lines [69]. A new method of calculating the dielectric constant was reported in which parallel plate resonator was used to find the characteristic of resonance frequency by using dielectric material [70].The method was very good but very complex to solve. In some literature, the dielectric constant and other properties of the substrate are measured by slab type materials [71]. In this method the slab under test is placed in the cavity of slab type microstrip antenna. This method is applicable for only cavity type structure. In fact, it is not applicable to all type of structures.

An iteration method to compute the dielectric constant of the substrate from the knowledge of resonant frequency and the input impedance of rectangular patch antenna was also presented [72] however this method is very lengthy and complex . A simple nondestructive method for the measurement of dielectric constant of slab type materials was also studied [73] . The experimental procedure of this paper was very simple and consists of measuring only the resonant frequency of microstrip patch radiator of any shape. It also tells about the uncertainty of the dielectric constant value. But this paper does not suggest any formula to calculate the dielectric constant of multilayer dielectric structure. It did not considered the effect of the change in the value of resonance frequency due to fabrication error. This paper only considered the single layered structure and the formula for effective dielectric constant. It did not consider any performance parameters.

In literature, the analytical formula for ε_{eff} is complicated [74, 75]. However, [76] showed a spectral domain technique for calculating $\varepsilon_{eff..}$ The results implied that consideration of any thin material on a substrate must be taken into account for evaluation of the effective dielectric constant. Quasi-TEM assumption has been used in these calculations [77]. Furthermore, superposition of partial capacitance has also been applied to the analysis for co-planar waveguide experimentally [78]. A new simple and accurate formula for effective dielectric constant based on the quasi-TEM assumption and superposition of partial capacitance was derived [79]. That is shown as in eq. (2.2)

$$\varepsilon_{eq} = \frac{d_1 + d_2}{\frac{d_1}{\varepsilon_{r_1}} + \frac{d_2}{\varepsilon_{r_2}}} \tag{2.2}$$

Where ε_{r1} and ε_{r2} are the relative dielectric constant of the two layers. And d_1 and d_2 are the distances between the boundaries. But this paper does not specify what will be the effect on resonance frequency if there is any change in multilayer dielectric material. Of course, this paper had no need of it. But our work/investigation needed that; so this paper is also not so useful for us. All the briefly literature cited above, just helps us to understand the behavior of multilayered dielectric structure and some methods for calculating effective dielectric constant. Although these papers have provided the knowledge for understanding the different methods of finding the composite dielectric constant of the multilayerd substrate and its effect on resonance frequency but no formula or method is directly applicable in this chapter of our thesis. This thesis has reported a new method for calculating the resonance frequency by modifying dielectric material by inserting the air-cavity in multilayered dielectric structure.

Problem statement

This part of the work is devoted to finding a new technique for fine tuning the resonance frequency of multilayered microstrip antenna which considered the fabrication error tolerance. It minimizes the error due to the fabrication and save time by eliminating the repeatative process of designing,simulation and fabrication, if error occurs. .

Methodology adopted

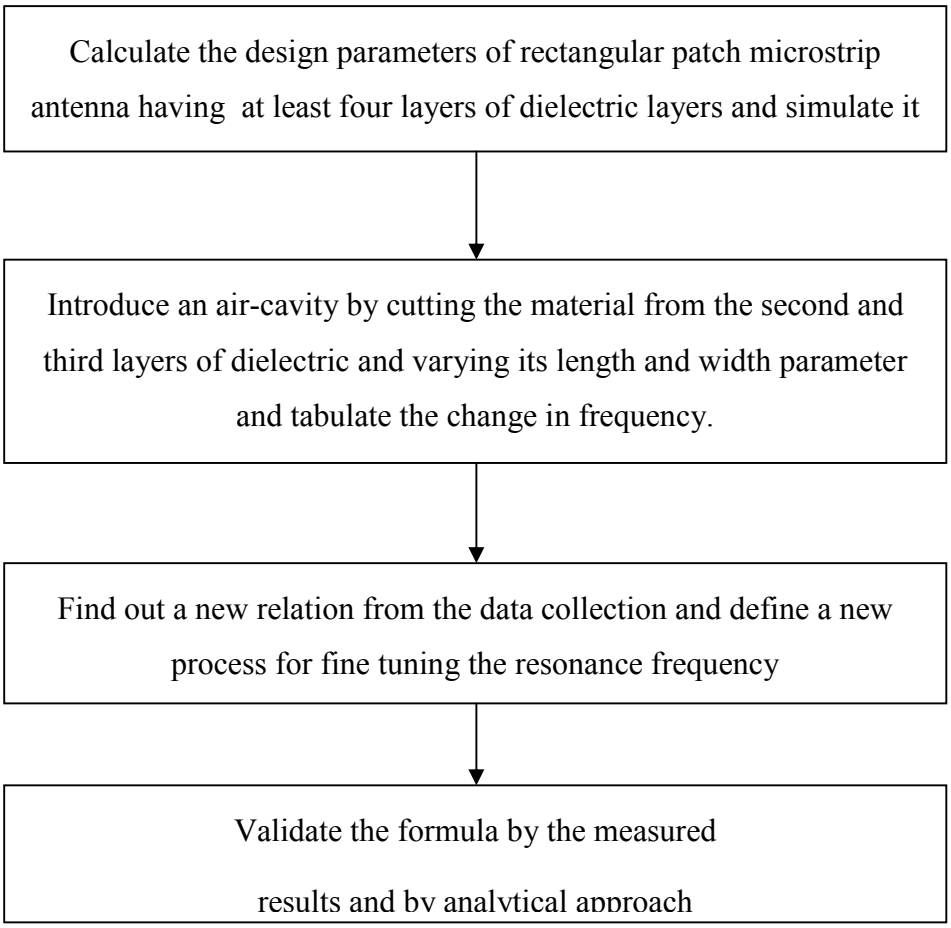

2.3 Design of the Rectangular Patch Antenna

2.3.1 Design Calculation:-

Throughout this work, some parameters have been given specific values (unless otherwise stated).These are:

Dielectric Constant of the Substrate (ε_r):

The dielectric material used for the microstrip patch antenna is FR4 epoxy with ε_r = 4.4, as this is the most popular material used due to low cost.

Frequency of Operation (f_0):

In this design, the frequency of operation for the Patch antenna has been selected as 2.4 GHz.

Thickness of the dielectric substrate (h): 1.6 *4 = 6.4 mm

The antenna is being excited with a line feed located at distance d_y from the center of the patch towards the y- direction as shown in Fig. 1.17. For impedance matching an inset has been cut in the patch. Size of the inset has been optimized by HFSS. Microstrip feed line has been extended into the inset by an amount equal to the length of the inset. At the end of the inset the feed line is joined with the patch.

1) Calculation of Width (**W)**:

By the formula:

$$W = \frac{c}{2f}\sqrt{\frac{2}{\varepsilon_r + 1}} \tag{2.3}$$

Width (W) = 0.038036 m = 38 mm

2) Calculation of Effective dielectric constant (ε_{reff}**)**:

From the equation

$$\varepsilon_{reff} = \frac{\varepsilon_r + 1}{2} + \frac{\varepsilon_r - 1}{2}\left[1 + 12\,\frac{h}{W}\right]^{-\left(\frac{1}{2}\right)} \tag{2.4}$$

Effective Dielectric Constant (ε_{reff}*)* = 3.687

3) Calculation of effective length:

From the equation

$$L_{eff} = \frac{C}{2f}\frac{1}{\sqrt{\varepsilon_{reff}}} \tag{2.5}$$

L_{eff}**= 0.03258 m = 32.58 mm**

4) Calculation of the length extension (***ΔL***) :

From the equation

$$\Delta L = \frac{0.412h(\varepsilon_{reff} + 0.3)\left(\frac{W}{h} + 0.264\right)}{(\varepsilon_{reff} - 0.258)\left(\frac{W}{h} + 0.8\right)} \quad (2.6)$$

***ΔL*= 2.8215 mm = 2.8 mm**

5) Calculation of the physical length of the patch (***L*):**

$$L = L_{eff} - 2\Delta L \quad (2.7)$$

By the equation

$$L = \frac{C}{2f}\frac{1}{\sqrt{\varepsilon_{reff}}} - 2\frac{0.412h(\varepsilon_{reff} + 0.3)\left(\frac{W}{h} + .264\right)}{(\varepsilon_{reff} - 0.258)\left(\frac{W}{h} + 0.8\right)} \quad (2.8)$$

L =29.4 mm

6) The feed place determination:

The feed line has been designed to have a characteristic impedance of 50 ohm. For impedance matching an inset has to be cut in the patch and the feed line has to be joined with the patch at the end of this inset. Length of this inset has been optimized by using parametric analysis tool of HFSS.

2.3.2 Antenna Design Procedure

The physical dimensions for the micro-strip antennas structure have been calculated above. The physical structure has been simulated by using the 3D electromagnetic simulator HFSS . Fig. 2.1 shows geometry of the patch antenna with directly coupled feed. In this work multilayered microstrip antenna having four dielectric layers of the same dielectric constant (4.4) with height of 1.6 mm individually have been considered. So the total height of structure is (4× 1.6 mm) 6.4 mm with inset feed in which a 50 Ω micro-strip line is used to feed the antenna. For impedance matching, inset dimensions have been optimized with the help of HFSS simulations.

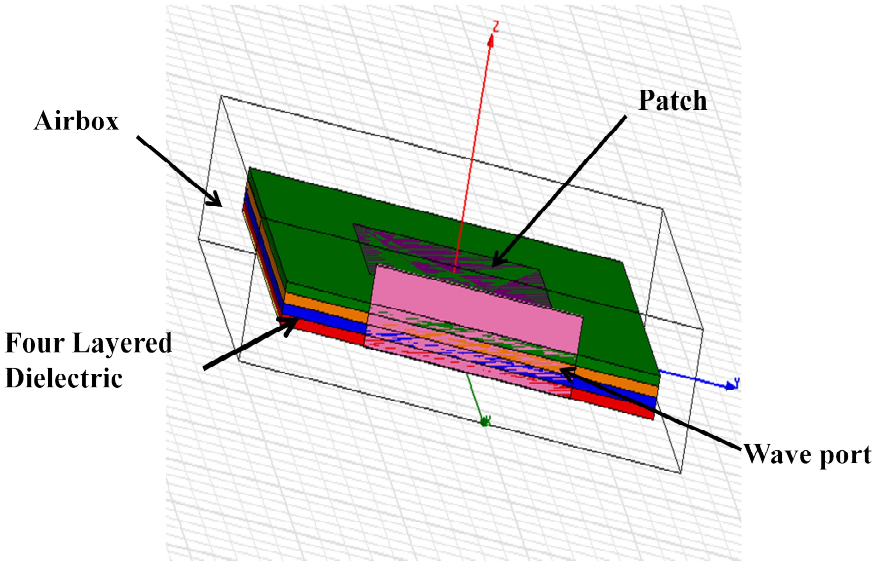

Fig. 2.1. Design structure of four layer dielectric (all the 4 layers having same dielectric Constant) on simulator.

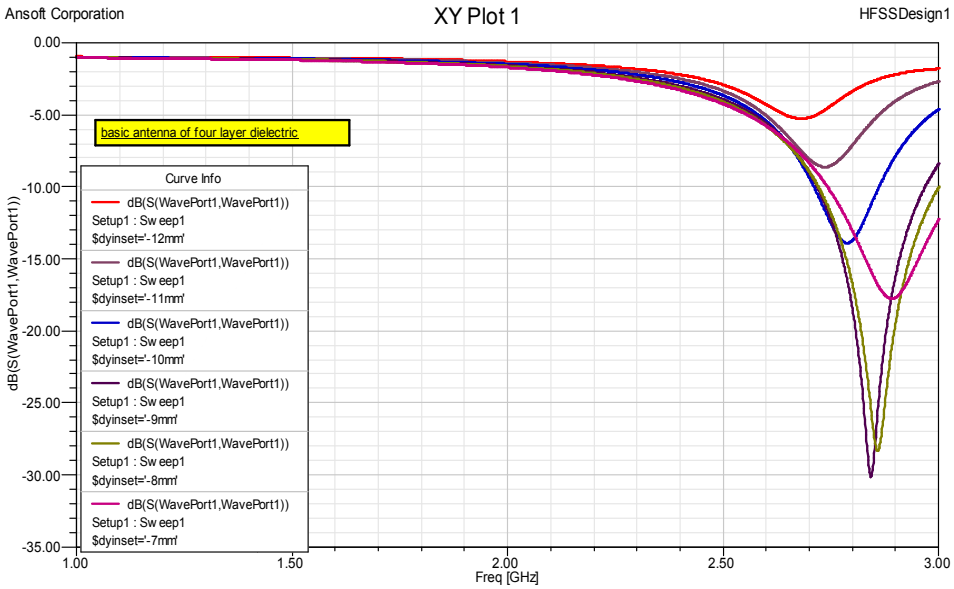

Fig. 2.2. Frequency- return loss curve of four layer dielectric structure with optimization of feed for 50Ω.

Here as shown in graph the structure was designed for 2.4 GHz resonance frequency . In this design the simulated resonance frequency (-30.5 dB) is marked on 2.85 GHz. This resonance frequency is related to the composite dielectric constant of structure. The investigations on the effect on resonance frequency by cutting the rectangular dimensions material from the second layer (next to top) of dielectric were performed first. And then the same effects were investigated for cutting the material from two layers (second and third).

The cutting of the material from the dielectric is abbreviated as 'air-cavity1' and 'air-cavity 2' respectively.Because removing the material results in filling air as dielectric in that space. The simulated structure with air-cavity1 and air-cavity2 are shown in Fig. 2.3 and 2.4 respectively.

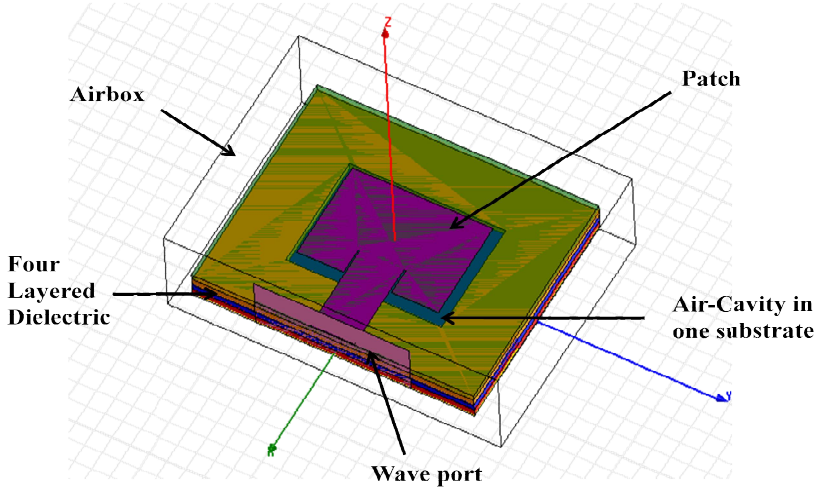

Fig. 2.3. Top view of structure of antenna with change in dimensions of air-cavity-1

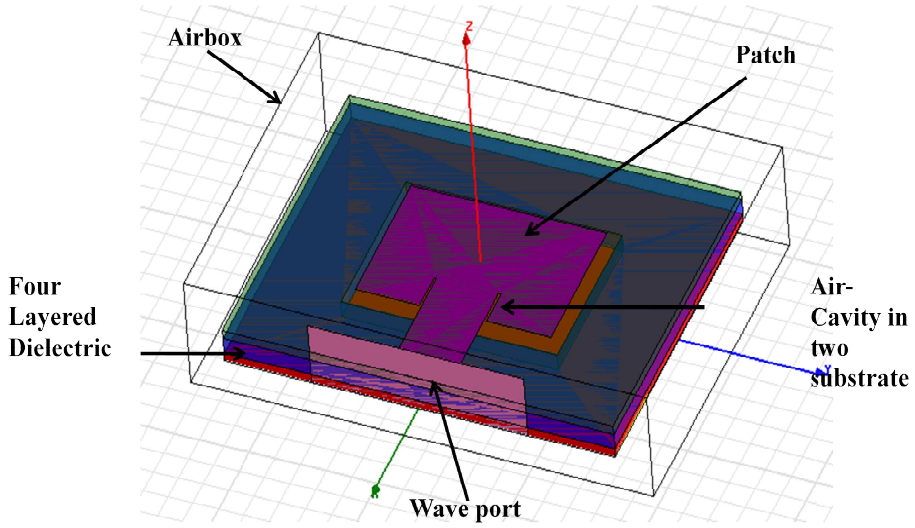

Fig.2.4. Top veiw of structure of antenna with air-cavity2

The investigations have more than 150 simulation results, because the changes in resonance frequency have been observed by changing every dimension- length, width and

area of air-cavity very finely (Keeping one dimension of air-cavity constant, increasing another dimension from 0 to 1.5 times of patch dimension, at every 2 mm difference). For the sake of convenience of the reader all simulated results are not shown in this thesis . Fig. 2.5 and Fig. 2.6 of this chapter collectively show the overall effect on resonance frequency with change in dimensions (length and width) of the cavity. In these graphs the ratio of the simulated resonance frequency (f) with the cavity and designed resonance frequency (f_0 =2.4GHz) without cavity has been considered because we have to find out the process of retuning of resonance frequency so it is necessary to know the relation of dielectric constant to this ratio.

If L_c is the cavity length , L_p is the patch length ,W_c is the cavity width and W_p is the patch width then Fig. 2.5 shows the dependence of f/f_o on W_c/W_p with L_c as the parameter. f increases as W_c increases. Fig. 2.6 shows the dependence of f/f_o on L_c/L_p with W_c as a parameter. Again f increases with L_c. The depth of the cavity seems to have little or no effect on the shift in the resonance frequency. Analysis of the results reported here indicate that when a cavity is made (in the antenna dielectric) just below the patch, the resonance frequency (f) of the structure increases.

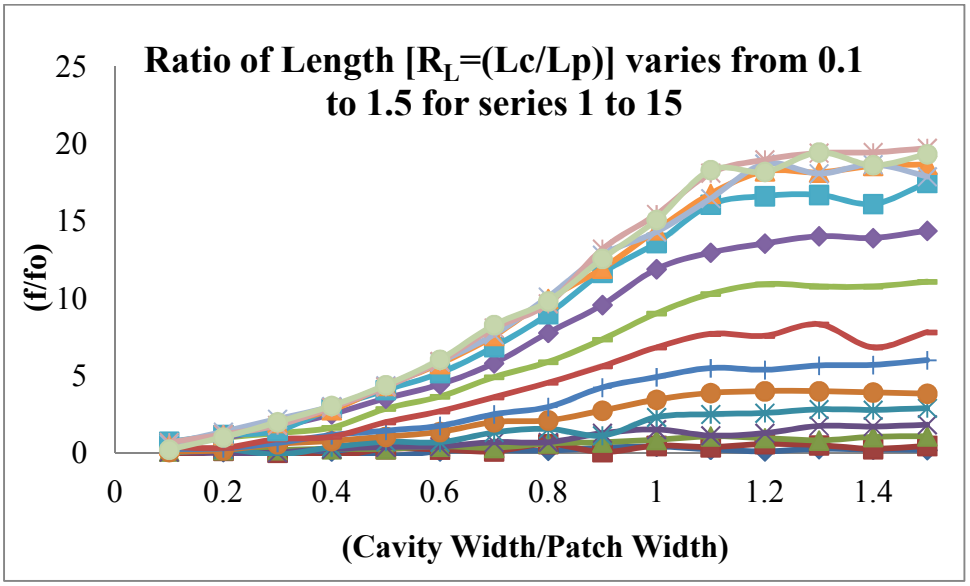

Fig. 2.5. Variation of resonance frequency ratio (f/f_0) with the ratio of the width of the cavity to patch width (Wc/Wp). The ratio of cavity length to patch length (R_L) is the parameter.

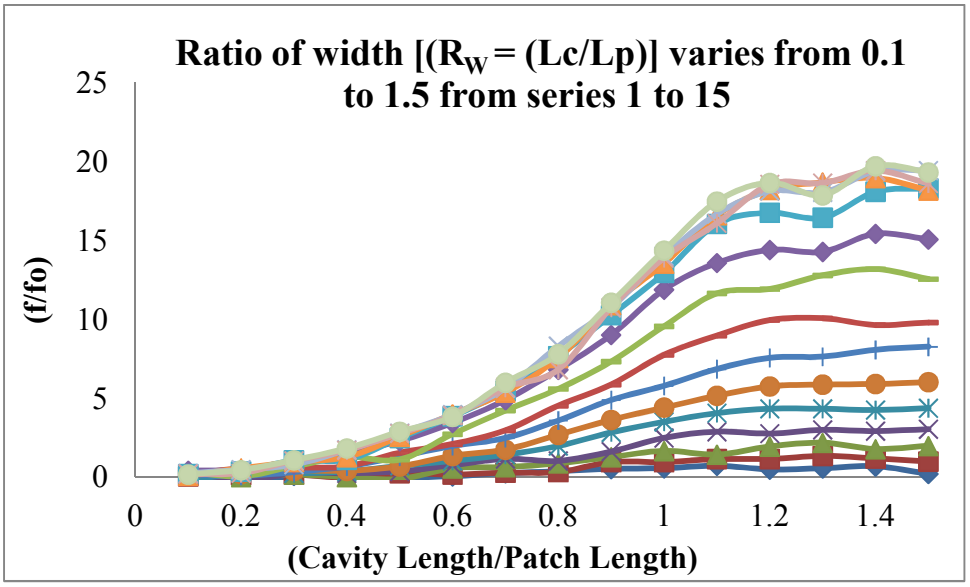

Fig. 2.6. Variation of resonance frequency ratio (f/f_0) with the ratio of length of the cavity to length of patch (L_c/L_p). The ratio (R_W) of cavity width to patch width is the parameter.

From Fig. 2.5 and Fig. 2.6 it can be inferred that the effect on the resonance frequency by the change in length and width have approximately the same value. Perhaps it is the area of the cavity that matters.Therefore, further investigations have been concentrated on the effect of air cavity area on resonance frequency.

The area ratio (area of cavity /area of the patch) and frequency ratio (Resonance frequency with cavity/resonance frequency without cavity) have been selected as parameters.

Results have been analyzed by taking three types of observations

(a) By varying frequency of resonance (f_o) of same dielectric constant (ε_r)

(b) By varying dielectric constant (ε_r) with same resonance frequency(f_o)

(c) By varying thickness of dielectric (h).[The results of observations have also been verified for cutting the cavity in both single layer and double layer of substrate. This may be call as varying the thickness of composite/effective dielectric height (h)]. This may be called as change in height of the cavity (d) .

This has been done for various values of the resonance frequency (f_o), dielectric constant (ε_r) and thickness (h) of the substrate material. Simulation results have been taken for three values of f_o -1.6, 1.8 and 2.4 GHz. For each value of f_o, three values of ε_r - 2.2, 3 and 4.4 and value of h- 6.4 mm have been considered. A cavity has been made in the antenna

dielectric just below the patch. Two values, d_1= h/2, and d_2= h/4, have been considered for the depth (d_c) of the cavity. For each combination of f_o, ε_r, W, h and d_c, 256 values of cavity area have been considered. HFSS simulations yielded the resonance frequency (f) of the structure. Results of > 2560 simulations have been analyzed.

Another important result of present investigations is that the increase in f can be controlled by suitably selecting the cavity dimensions. Thus the resonance frequency of the antenna can be tuned during its fabrication. Thus the result of fabrication tolerances can be offset by following this method (creating an air cavity).

As the size of the cavity increases, the composite dielectric constant of the antenna substrate will decrease. This will result in an increase in f. This will continue to happen till the area of the cavity approximately equals the effective area of the patch (accounting for the fringing field effect). Further increase in the cavity area would have little or no effect on f. This thesis proposes the following empirical relation between change in frequency and area of the cavity.

$$P(f) = \alpha R^2 + \beta R + \Upsilon \quad ; \quad \text{for } R \leq 1.27 \tag{2.9}$$

$$P(f) = m R + n \quad ; \quad \text{for } R > 1.27 \tag{2.10}$$

$$\text{Where} \quad P(f) = \left(\frac{f - f_o}{f_o}\right) * 100 \tag{2.11}$$

$$\text{And} \quad R = A_c/A_p \tag{2.12}$$

α, β , Υ, m and n are constants.

P (f) is the percentage change in the resonance frequency f_o when a cavity of cross-sectional area A_c is made under the patch. R is the ratio of the area of cavity (A_c) and the area of the patch (A_p) and α is a constant. For the cases analyzed here α = 11.2.

2.3.3 The Effects on Percentage Frequency Ratio by the Area Ratio for Air-Cavity in One Layer of Dielectric (Aircavity-1):

1) The graph for resonance frequency 2.4 GHz and Dielectric constant 4.4 with height of air-cavity h/4 is as shown below in Fig. 2.7

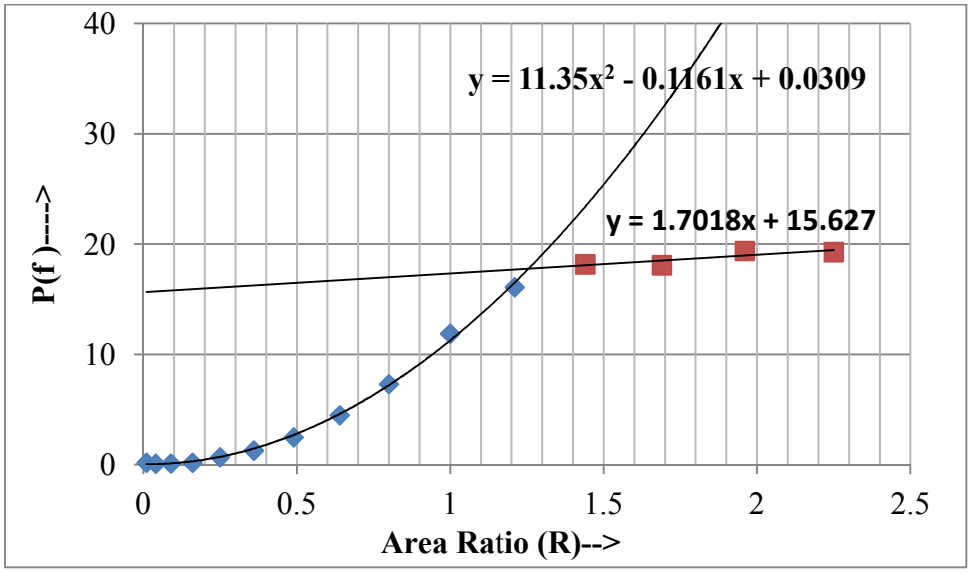

Fig. 2.7. Graph between percentage frequency ratio and the area ratio having εr=4.4, f_0=2.4 GHz, d=h/4 mm.

2) The graph for resonance frequency 1.8 GHz with dielectric constant 4.4 and height of air-cavity h/4 is as shown in Fig. 2.8.

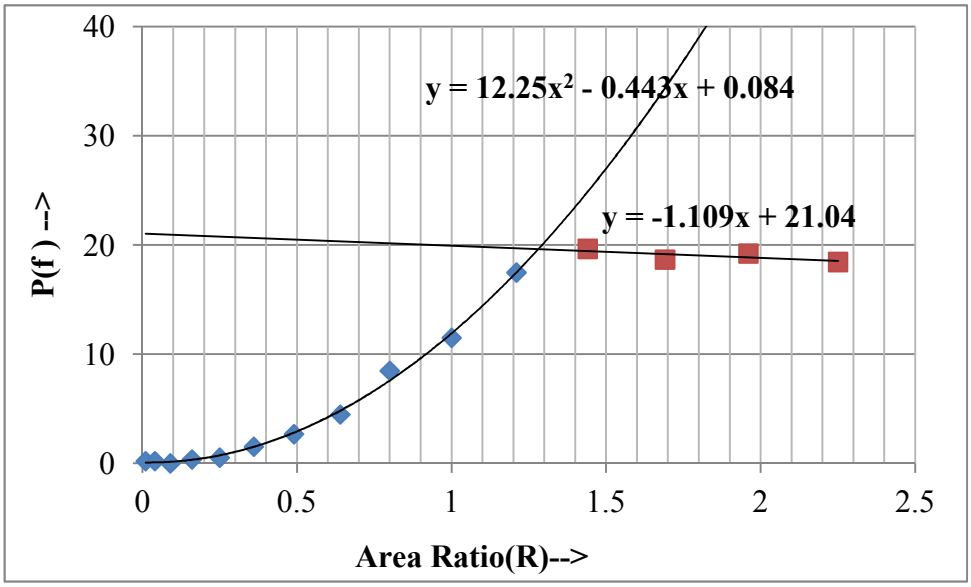

Fig. 2.8. Graph between percentage frequency ratio and the area ratio having ε_r=4.4, f_o=1.8 GHz, d=h/4 mm.

3) The graph for resonance frequency 1.6 GHz with same dielectric constant and height as taken in above is as in Fig. 2.9

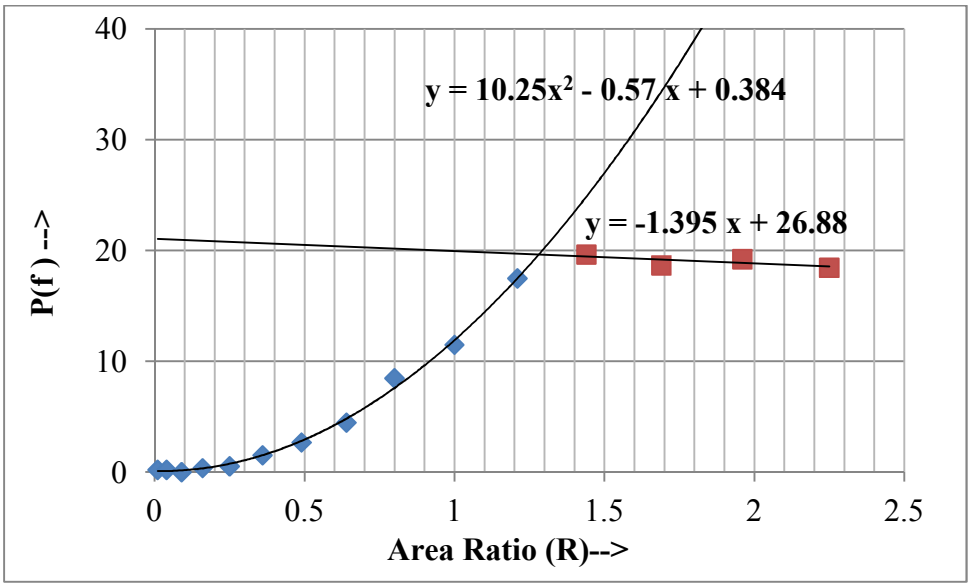

Fig. 2.9. Graph between percentage frequency and the area ratio having ε_r=4.4, f_o=1.6 GHz, d=h/4 mm.

4) The graph for resonance frequency 2.4 GHz but having a value of 2.2 of dielectric constant with same height as taken above is as shown in Fig. 2.10

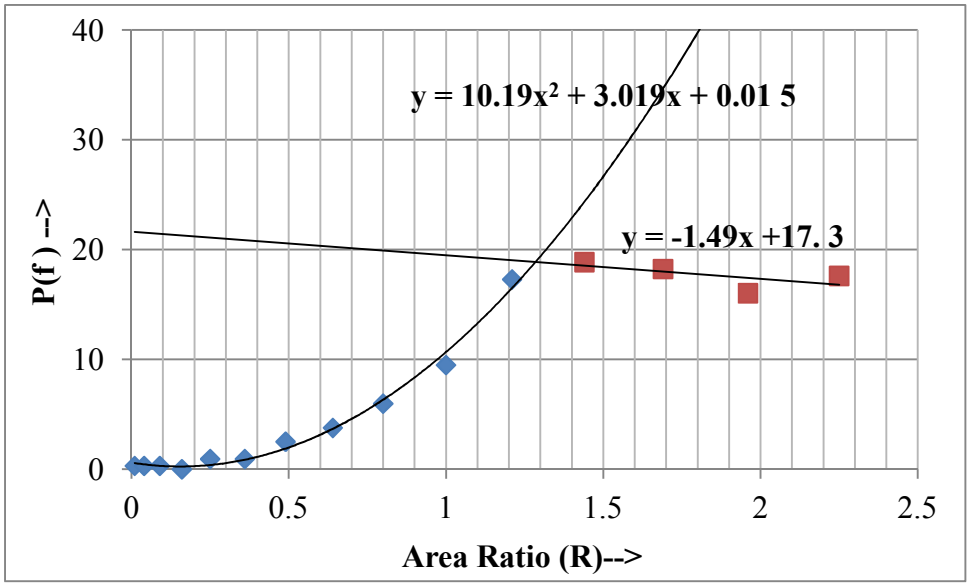

Fig. 2.10. Graph between percentage frequency ratio and the area ratio having ε_r=2.2, f_o =2.4 GHz, d= h/4 mm.

5) The graph of resonance frequency 2.4 GHz but dielectric constant of value 3 with same height as taken above is as shown in Fig. 2.11.

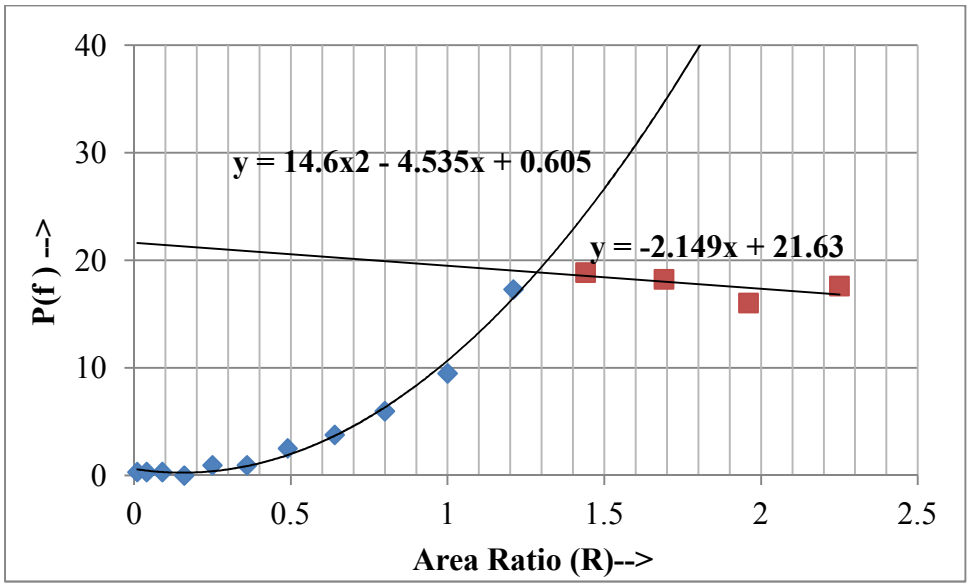

Fig. 2.11. Graph between percentage frequency ratio and the area ratio having ε_r=3, f_o =2.4 GHz, d=h/4mm.

To compare the values, a collective graph of all above observations has been drawn as shown below in Fig. 2.12. The mathematical relation between the terms is found by the curve fitting formula.

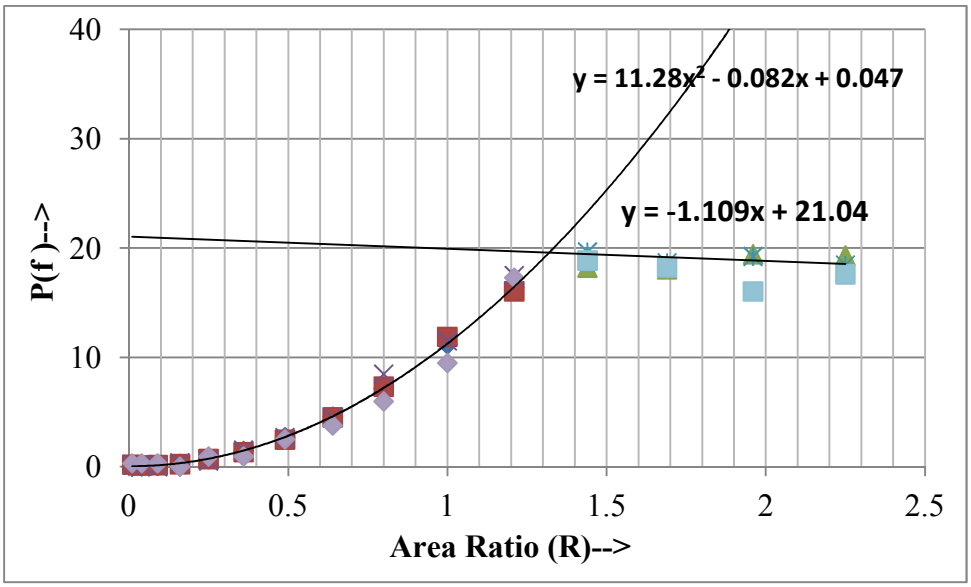

Fig. 2.12. Collective graph of the percentage frequency ratio and the area ratio having ε_r=4.4, 2.2, 3 f_o =2.4, 1.8, 1.6 GHz and d=h/4 mm.

2.3.4 The Effects of Percentage Frequency Ratio by the Area Ratio for Air-Cavity in Two Layers of Dielectric (Aircavity-2):

1) The graph for resonance frequency 2.4 GHz and Dielectric constant 4.4 with the air-cavity height h/2 is as shown in Fig. 2.13

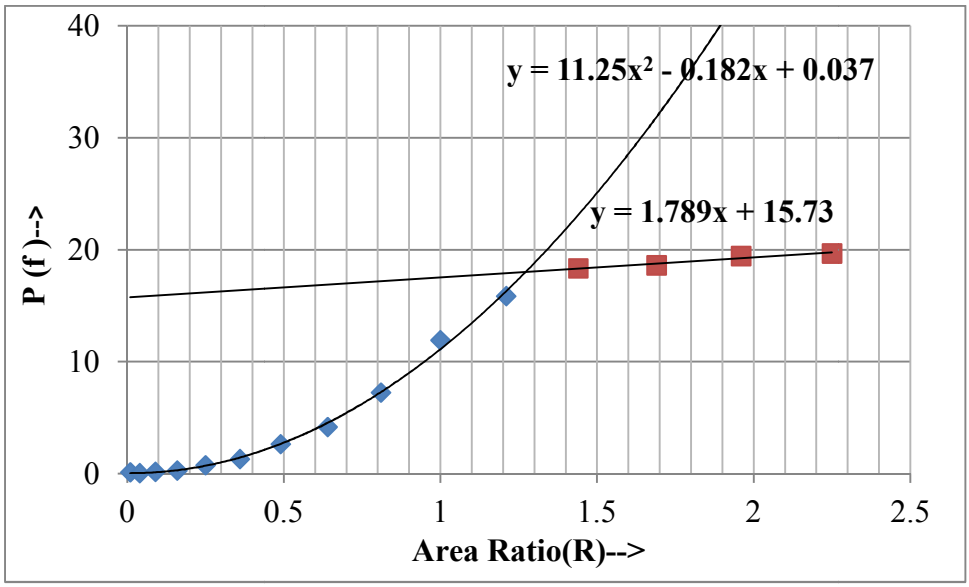

Fig. 2.13. Graph between percentage frequency ratio and the area ratio having ε_r=4.4, f_o=2.4 GHz, d=h/2mm.

2) The graph of the resonance frequency 1.8GHz with same dielectric constant & height as taken in above graph is as shown in Fig. 2.14

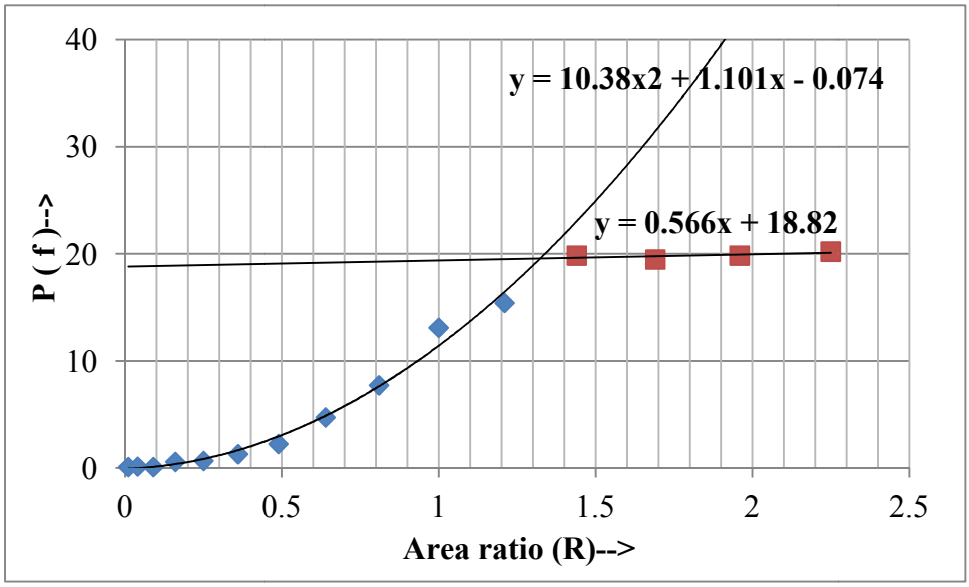

Fig. 2.14. Graph between percentage frequency ratio and area ratio having ε_r=4.4, f_o=1.8 GHz, d=h/2 mm.

3) The graph for resonance frequency 1.6GHz with same dielectric constant & height as taken in the graph as shown in Fig. 2.15

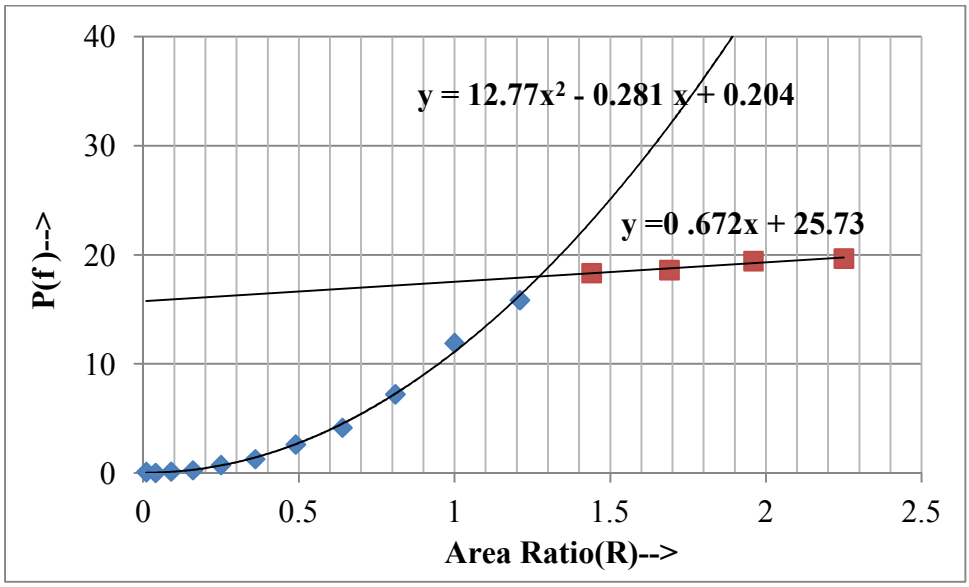

Fig. 2.15. Graph between percentage frequency ratio and the area ratio having ε_r= 4.4, f_o=1.6 GHz, d=h/2 mm.

4) The graph of resonance frequency 2.4 GHz but having value of 2.2 of dielectric constant with height as taken above is as shown in Fig. 2.16

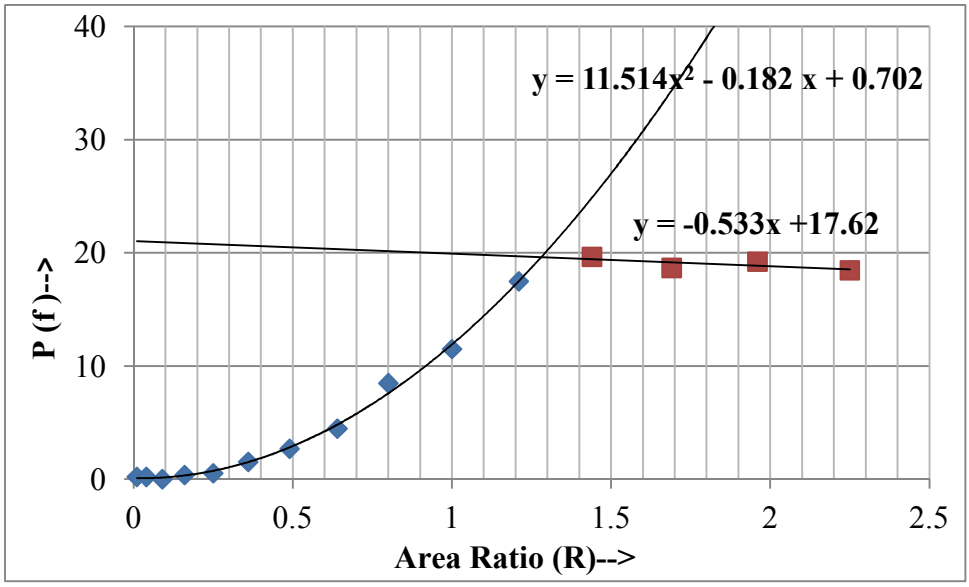

Fig. 2.16. Graph between percentage frequency ratio and area ratio having ε_r=2.2, f_o=2.4 GHz, d=h/2 mm.

5) The graph for resonance frequency 2.4GHz but dielectric constant of value 3 with height as taken above is as shown in Fig. 2.17

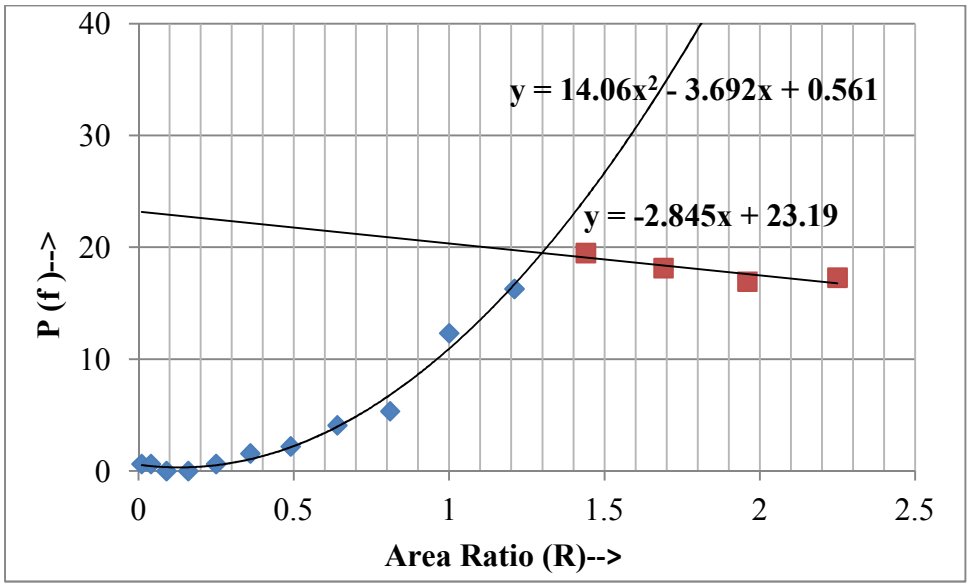

Fig. 2.17. Graph between percentage frequency ratio and the area ratio having ε_r=3, f_o=2.4 GHz, d=h/2mm.

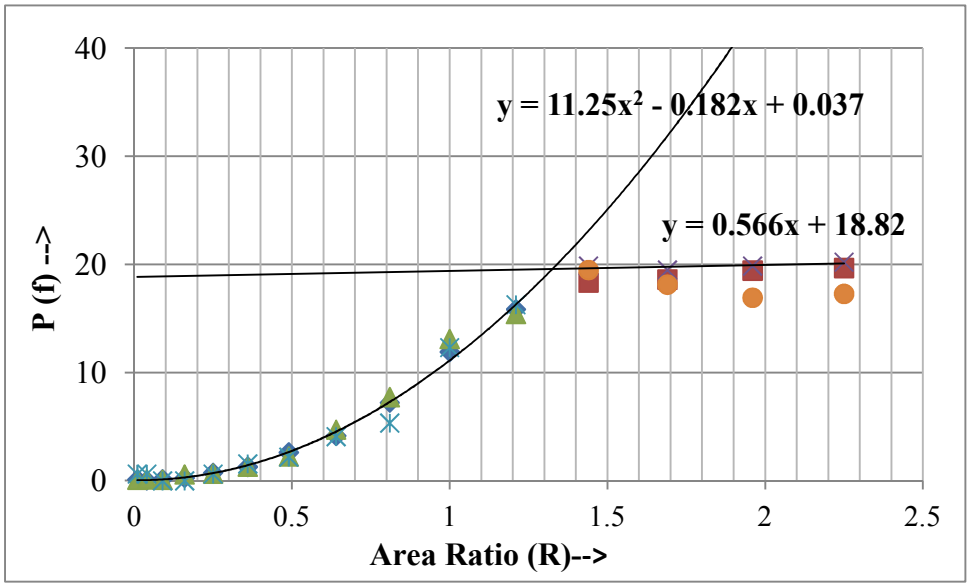

Fig. 2.18. Collective graph of percentage frequency ratio and the area ratio having εr= 4.4, 2.2, 3 f_0 =2.4, 1.8, 1.6 GHz and d = h/2 mm

To compare the values of all above graphs, a collective values graph in one graph has been drawn as shown in above Fig. 2.18. So that a relation in between frequency ratios and area ratios could be found out by the curve fitting .

2.3.5 Discussions

The results by inserting air-cavities in two layers are different from the case when air-cavity is inserted in one layer only because there is a change in thickness of the air-cavity.

From above graphs (Fig. 2.12 and Fig. 2.18) it has been observed that

(a) For R =0 there is no cavity so f =f_o and f/f_o=1. This is indicated by the polynomial formula also. But practically the simulated resonance frequency f is not equal to designed resonance frequency . In this work as shown in Fig. 2.1 f = 2.85 GHz and f_0 is taken 2.4 GHz so f/f_o=1.18. That's why in the graphs of Fig. 2.12 and 2.18 f/f_0 are not on the origin.

(b) The polynomial shows that f/f_o increases with R. This is expected because the dielectric constant decreases as the cavity size increase as in eq. (2.9).

(c) For R > 1.2 the cavity becomes larger than the patch (beyond the fringing field). Further increase in cavity size has no effect on f. Therefore f/f_0 becomes constant represented by a linear formula as in eq. (2.10).

2.4 Analytical Model

A relation between resonance frequency ratio and dimensions of air-cavity has been obtained from simulation results. In this part of the work the dependence of resonance frequency on air cavity would be derived by considering the MS antenna as a parallel plate capacitor. Initially, the ratio of dielectric constant, with cavity and without cavity, is calculated from the physical structure of the antenna from the array of capacitors in series and parallel combination. The structure can be considered as three capacitors in parallel. The analysis is applied to mid capacitor in which the patch and air-cavity lies, another first and last capacitor could be ignored to avoid complexity in the calculation. Further, the composite dielectric constant has been calculated by considering capacitors in series from top to bottom layer. After calculating composite dielectric constant it is converted into the dimension of the cavity to the dimension of patch ratio {area ratio of the cavity to patch (A_c/A_p)}. This value of the equivalent composite dielectric constant value in terms of area ratios gives some relation to the resonance frequency. For finding that relation considers the Fig. 2.19 of MS antenna and its equivalent circuit diagram as in Fig. 2.20. In this diagram for the sake of convenience the air cavity is shown in front of dielectric, actually, it is in the middle of that dielectric layer below the patch.

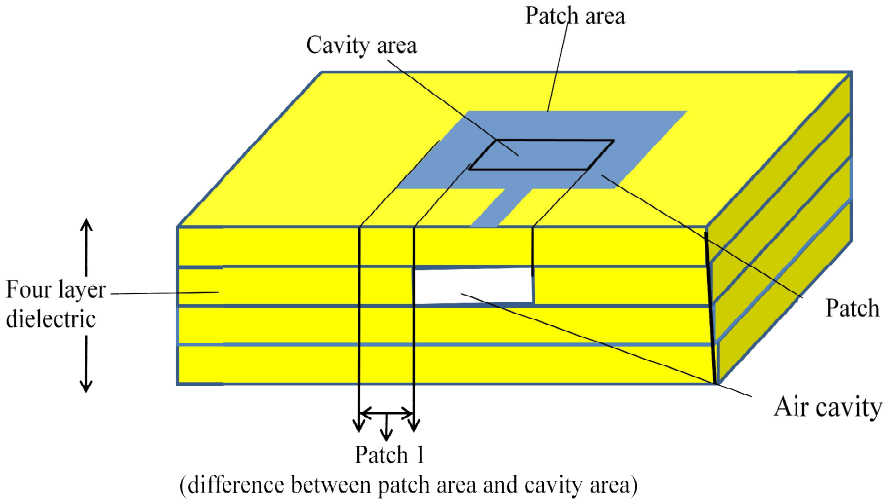

Fig. 2.19. Analytical model for MS antenna

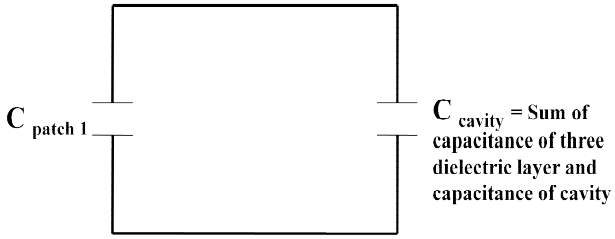

Fig. 2.20. Equivalent capacitance of above analytical model of MS antenna.

For calculating capacitance of patch1, the area of patch1 will be remaining area that is the difference area of patch area and the cavity area. In above diagram the patch1 is shown only at one side actually it is the rectangular area. Cavity area is also rectangular area and patch area is also rectangular and the difference of these two rectangular area is also rectangular area.

Area of patch1 = Area of patch- Area of cavity

$$A_{patch1} = [Lp * Wp - Lc * Wc] \tag{2.13}$$

$$\frac{1}{C_{patch1}} = \frac{4d}{\varepsilon_{sub}} \frac{1}{(Lp * Wp - Lc * Wc)} \tag{2.14}$$

Here Lp = length of the patch

Wp = width of the patch

Lc = length of the cavity

Wc = width of the cavity

d = thickness or height of one layer of the dielectric

ε_{sub} =dielectric constant of material under the area of patch1

The capacitance of the patch1 area will be finally

$$C_{patch1} = \varepsilon_{sub} \frac{(Lp * Wp - Lc * Wc)}{4d} \tag{2.15}$$

And for calculating the capacitance of cavity

$$\frac{1}{C_{cavity}} = \frac{3d}{\varepsilon_{sub}} \frac{1}{(Lc * Wc)} + \frac{d}{(Lc * Wc)\varepsilon_{air}} \tag{2.16}$$

Here putting ε_{air} = 1 in eq. (3.16)

$$\frac{1}{C_{cavity}} = \frac{d}{(Lc * Wc)} \left[\frac{3}{\varepsilon_{sub}} + 1\right] \tag{2.17}$$

$$C_{cavity} = \frac{(Lc * Wc)}{d} \left[\frac{\varepsilon_{sub}}{(\varepsilon_{sub} + 3)}\right] \tag{2.18}$$

Now the equivalent capacitance will be

$$C_{eq} = C_{patch1} + C_{cavity} \tag{2.19}$$

Putting the values of C_{patch1} from eq. (2.15) and C_{cavity} from eq. (2.18) into the eq. (2.19)

$$C_{eq} = \varepsilon_{sub} \frac{(Lp * Wp - Lc * Wc)}{4d} + \frac{(Lc * Wc)}{d} \left[\frac{\varepsilon_{sub}}{\varepsilon_{sub} + 3}\right] \tag{2.20}$$

The value of C_{eq} is the total capacitance of four layers so d = 4d and area is

$(\mathrm{Lp} * \mathrm{Wp})$

$$\frac{\varepsilon_{\mathrm{eq}}(\mathrm{Lp} * \mathrm{Wp})}{4\mathrm{d}} = \varepsilon_{\mathrm{sub}} \frac{\left(\mathrm{Lp} * \mathrm{Wp} - \mathrm{Lc} * \mathrm{W}\right)}{\frac{\mathrm{c}}{4\mathrm{d}}} + \frac{(\mathrm{Lc} * \mathrm{Wc})}{\mathrm{d}} \left[\frac{\varepsilon_{\mathrm{sub}}}{\varepsilon_{\mathrm{sub}} + 3}\right] \tag{2.21}$$

Solving the eq. (2.21) for ε_{eq}

$$\varepsilon_{\mathrm{eq}} = 4\varepsilon_{\mathrm{sub}} \left[\frac{1}{4} - \frac{1}{4}\frac{\mathrm{Ac}}{\mathrm{Ap}} + \frac{1}{(\varepsilon_{\mathrm{sub}} + 3)}\frac{\mathrm{Ac}}{\mathrm{Ap}}\right] \tag{2.22}$$

Here

$$\frac{\mathrm{Ac}}{\mathrm{Ap}} = \frac{(\mathrm{Lc} * \mathrm{Wc})}{(\mathrm{Lp} * \mathrm{Wp})} \tag{2.23}$$

Ac = Area of cavity , Ap= Area of patch

$$\varepsilon_{\mathrm{eq}} = \varepsilon_{\mathrm{sub}} \left[1 - \frac{\mathrm{Ac}}{\mathrm{Ap}}\left(\frac{\varepsilon_{\mathrm{sub}} - 1}{\varepsilon_{\mathrm{sub}} + 3}\right)\right] \tag{2.24}$$

We know that if the length of patch (L) and ΔL are constant then the relation of dielectric constant and resonance frequency f_0 is as in eq. (2.25)

$$\mathrm{f}_0 = \frac{c}{2(L + \Delta L)}\sqrt{\frac{1}{\varepsilon_0}} \tag{2.25}$$

Where f_0 = resonance frequency of the structure without cavity

ε_o = dielectric constant of the structure without cavity

And from above results, the graph between resonance frequency with cavity and without cavity to area ratio of the cavity to patch is drawn. Now put the value of ε_{eq} from eq. (2.24) in the relation below

$$\frac{f_r}{f_o} = \sqrt{\frac{\varepsilon_o}{\varepsilon_{eq}}} \tag{2.26}$$

Here f_r = resonance frequency of the structure with the cavity

ε_{eq} = Effective dielectric constant of the structure with the cavity.

For the four layer structure the value of ε_{eq} can be taken from eq. (2.24) and $\varepsilon_o = \varepsilon_{sub}$ by putting these values, in eq. (2.26)

$$\frac{f_r}{f_o} = \frac{1}{\sqrt{1 - \frac{Ac}{Ap}\left(\frac{\varepsilon_{sub} - 1}{\varepsilon_{sub} + 3}\right)}} \tag{2.27}$$

Finally, it is concluded that this formula given by eq. (2.27), can be used for fine tuning the resonance frequency of the multilayered antenna, simply by cutting the material from the second layer of dielectric. From the formula the change in resonance frequency produced by fabrication error can be set back by calculating the dimension of the air-cavity (Ac) from the above formula by putting the values of designed resonance frequency(f_0) , the measured resonance frequency having the error of above $\pm 10\%$ tolerance from the designed frequency, which is abbreviated as measured resonance frequency f_r, the known area of fabricated patch A_p and dielectric constant $\varepsilon_{sub}$of the fabricated antenna. Then cutting the material of that calculated dimension of the cavity area (A_c) from the substrate below the patch will tune back the resonance frequency to its designed value.

2.5 Measured Result

The microstrip antenna having the four layers of dielectric substrate FR4 Epoxy (ε_r =4.4) has designed for frequency 2.4 GHz. The height of each substrate is 1.6 mm. The first layer having the patch of structure and the last layer has the ground of structure.The middle layers have the substrate only. The whole process is shown in Fig. 2.21 (a) and (b). The simulated result of designed antenna is already shown in Fig. 2.2. The measured result of the fabricated antenna has shown in Fig. 2.22 without the cavity and with the cavity.

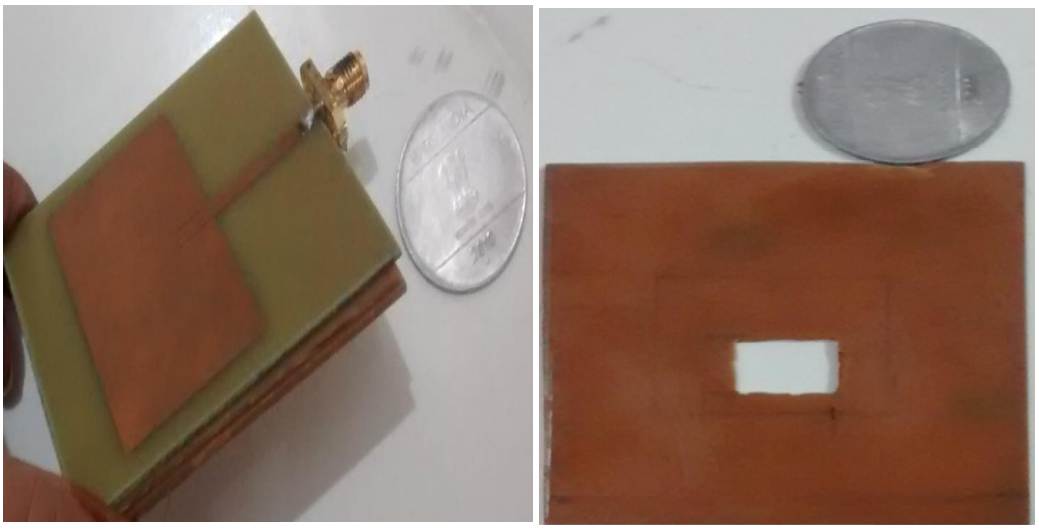

(a) (b)

Fig. 2.21(a) Four layered fabricated antenna on substrate FR4 Epoxy ($\varepsilon_r = 4.4$) (b) second layer of substrate after removing the material

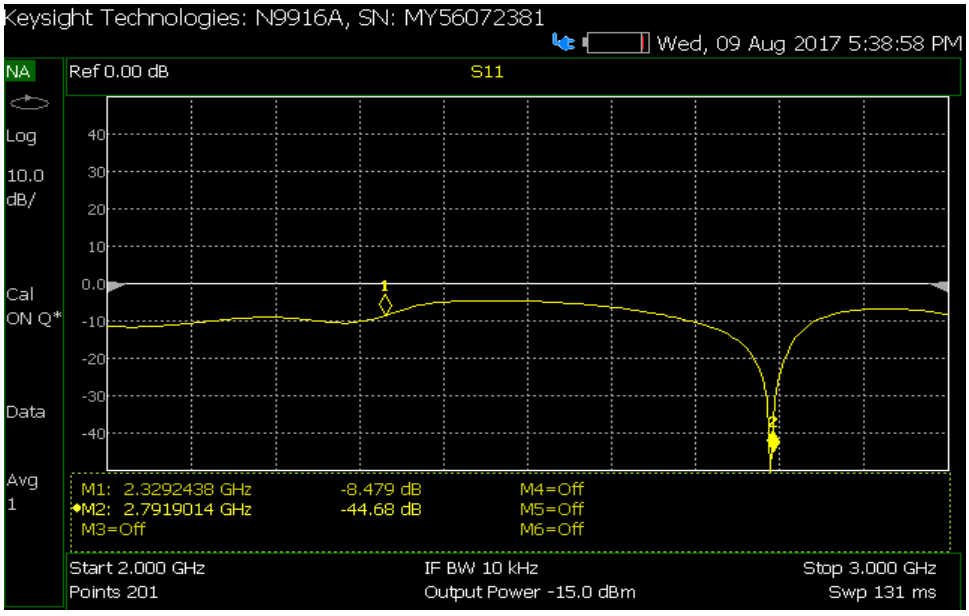

(a)

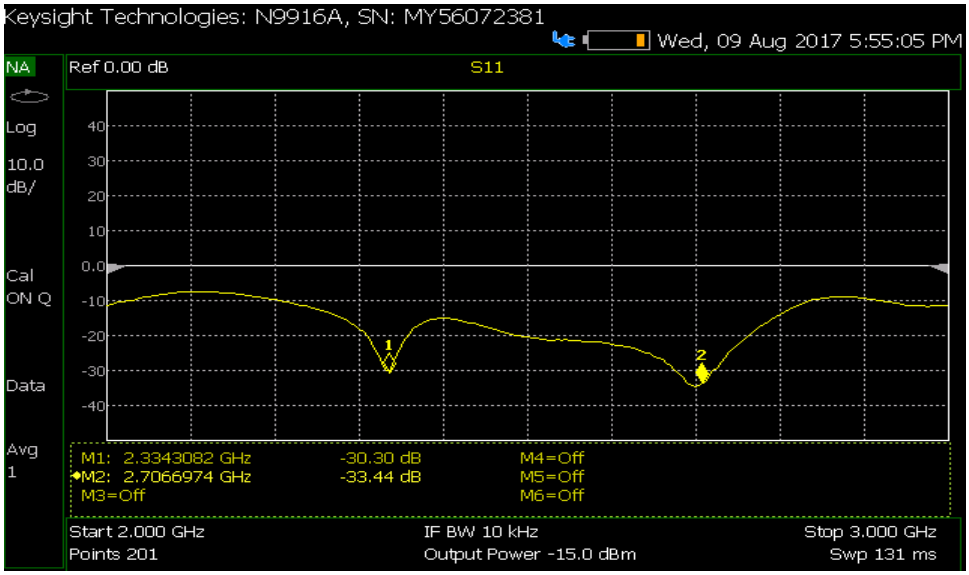

(b)

Fig. 2.22 Measured results of four layered fabricated antenna (a) without cavity (b) with cavity

The resonance frequency of four layered structure for FR4 Epoxy (ε_{sub}=4.4) is 2.79 GHz as shown in Fig. 2.22(a). This is the value of f_r in the formula.The designed frequency is 2.4 GHz which is the value of f_o. The patch area for this structure is (27× 38) mm^2. To retune this frequency f_r to its designed value, the A_c has been calculated from the formula (2.27) which is 127.52 mm^2. Now from the second layer this area (10×12.752) mm^2 has been removed by using the PCB fabricating machine. Now the resonance frequency is tuned to 2.33 GHz as shown in Fig. 2.22(b).

2.6 Conclusion

Dielectric constant engineering can be successfully used for fine tuning resonance frequency of microstrip antenna. Slight variation in effective dielectric constant can offset the effect of change in patch length. Cutting a cavity in the antenna dielectric below the patch is one way of doing so. Processes like LTCC using multilayer dielectric structure are useful in this method. The composite dielectric constant of this multilayer structure is altered in such a way that the resonance frequency is set back to the designed value. Effect of cavity size of the shift in resonant frequency has been investigated. Three different dielectric materials were investigated for several resonance frequencies. f/f_0 was plotted against Area Ratio (R) to generalize the findings. Area Ratio is the ratio of the area of the cavity to the area of the

patch, f is the resonance frequency for a given cavity area and f_0 is its value without any cavity. The depth of the cavity may be equal to either one or two dielectric layer thickness in a four- layered dielectric structure. Very interesting results have been obtained. For all ε and all f/f_0 the curve can be described by the equation of the form $f/f_0 = \alpha R^2+\beta R+ \Upsilon$ where R is the area ratio. This mathematical model is true up to R=1.27. After this saturation effects set in and the curve changes to a straight line $f/f_0 = m R+n$.

A mathematical model is suggested. If resonance frequency alters from its design value due to fabrication error, then to set its value back to designed value a cavity of dimension given by the formula below is cut. This air-cavity will tune back the resonance frequency to its designed value without disturbing other fabrication arrangements.

$$\frac{f_r}{f_o} = \frac{1}{\sqrt{1 - \frac{Ac}{Ap}\left(\frac{\varepsilon_{sub} - 1}{\varepsilon_{sub} + 3}\right)}}$$

From this formula, the dimension of the cavity will be calculated by putting the values of dielectric constant and designed resonance frequency. After that the material of calculated dimension will be removed from the dielectric. This behaves like a cavity that is filled with air.

Chapter 3:NOVEL TECHNIQUE FOR ESTIMATING FEED LINE DIMENSIONS OF RECTANGULAR AND TRIANGULAR MICROSTRIP ANTENNA

3.1 Introduction

In the designing process of microstrip patch antenna, dimensions of the patch, as well as feed line are very important. These dimensions are usually calculated by the formulae (1.13), (1.17) and (1.21) for every new design. This is very time consuming and lengthy. This method has to be repeated even if designs are made for the same frequency for different substrates having different dielectric constants. To overcome this repetitive process of designing the structures on different dielectric substrates for the same designed frequency 'equivalent design concept' was evolved [60]. It states that a well designed structure of the microstrip antenna can be transformed quickly into other design for the same frequency with another dielectric constant by using scaling factors Ψ and ϕ. It comes from Bhatnagar's Postulate theory. However, those transformation formulae were developed only for the patch dimensions. The dimensions of feed line are also very important for this designing process. So to complete the process of transforming the designs, this thesis adds on the formulae for feed line with that set of formulae . It makes a complete set of formulae for the transformation of design from one dielectric substrate to another substrate for the same designed frequency. The investigations done by me considered two conditions (i) $\frac{w}{h} \leq 1$ and (ii) $\frac{w}{h} > 1$, where $\frac{w}{h}$ is the ratio of width of trace/line to the height of substrate. This impedance matching of feedline depends upon these two parameters directly.

The proposed formulae of feedline for the transformation of design have been verified for both rectangular and triangular shape patch design transformations. This is described in the following sections of this chapter.

An attraction of this thesis is the algorithm in Matlab for these set of transformation of designs. From this MATLAB program the transformed design parameters from one substrate to another substrate is quickly found and the structure from that transformed design parameters is directly drawn on the MATLAB. This is very unique because no designing is required in any simulator for finding the characteristic of MS antenna. One has to insert the values of dielectric constants (ε_{r1} and ε_{r2}) of transforming designs, designed resonance

frequency (f_r) , and heights of those substrates (h_1 and h_2) as the input of algorithm and output is taken in terms of the transformed structure of antenna .

A modification in the formula for the patch width (w_2) by eq. (1.53) is also presented in section 3.3 by eq. (3.38). The need of this modification was to fulfill the condition $W_p > L_p$ for designing the structure of MS antenna .The novelty in this modification is that it is independent of height ratio (ϕ). The modified formula is also presented in this chapter.

3.2 Literature Review

Microstrip antennas are becoming essential and major part of wireless communication. For a good microstrip antenna, several constraints are used like the value of dielectric constant and its height, patch dimensions and its alignment, ground configuration, feeding technique, etc. This chapter is concerned with the feed line dimensions of the rectangular microstrip patch antenna. The resonance frequency, VSWR etc are considered as performance parameter in this work. Various types of feeding are used in microstrip antenna and all have a different approach to implement. The feeding used in this work is inset fed. The formulae for calculating the dimensions of feed line are complex and time- consuming. So this work gives a new approach for calculating the dimensions with the new formulae. But to find the new formulae first, a study is made that how in all these years, the innovation and improvisation in the feed line are made. The detailed literature survey is given below.

Different types of feeding are used in the designing of the microstrip antenna. In this concern [80] presented a rigorous solution by using three different kinds of strip line feed (patch fed at the radiating edge, at the non-radiating edge and proximity coupled patch). The results are better with the radiating edge and proximity couple patch, but not with the non-radiating edge. An experiment of the input resistance of the patch on the feed position differs when using microstrip line and probe feed was presented [81]. And [82] measured the various parameters of an antenna at a frequency of 1 GHz by using probe feed and shows that proper feed and impedance matching is very important in antenna design. The feed position affects the performance of the antenna. [83] gave the effect of feed position on the input impedance of a rectangular microstrip patch antenna. The Finite-Difference Time-Domain (FDTD) technique is used for the microstrip and probe feeding. [84] says that for a probe feed, the input resistance can be signalized with the shifted sine squared function and for inset feed, the notch width is shifted to get 50 Ω resistances. Another similar investigation [85]

shows that a wider notch can be used to maintain the impedance and produce less effect on cross polarization. A shifted cosine-squared function [86] can be used to explain the variation of input resistance and feed location. If the input resistance is fixed, then notch depth decreases when width increases. The cross- polarization increases if either notch width or depth increases. Another paper shows the use of corporate feed technique for excitation of the microstrip patch antenna array of X-band applications [87]. All these papers are help to understand the behavior of feed line and its characteristics. The formulae for the feed line dimensions calculations are not much discussed in the literature. As our objective is to find out the feed line dimension formulae in some easy form or design the formulae of dimensions of feedline in the form of constants of the equivalent design (i.e. ϕ and ψ) [60]. we decided to start work with the classical feed line impedance formula as shown in eq. (1.28) and eq. (1.29) and design it in the easy form with the constants ϕ and ψ.

One paper [88] shows the formula for designing this and the formula for calculating the resonant frequency for l,m,n mode. An another formula for equilateral triangle shape patch was also presented [89]. The authors of this thesis also presented a formulae for designing the equilateral triangle shape MS antenna by using Bhatnagar postulate [90] which is very easy and having good design results. But again this formula is only for the patch dimensions of equilateral shape patch, so the feed line dimensions formulae by using the equivalent design concept for triangular shape patch is also required.

Problem Statement

This part of work is devoted to developing the feedline dimensions transformation formula for rectangular and triangular shape patch microstrip antenna using "equivalent design concept".

Methodology adopted for investigations

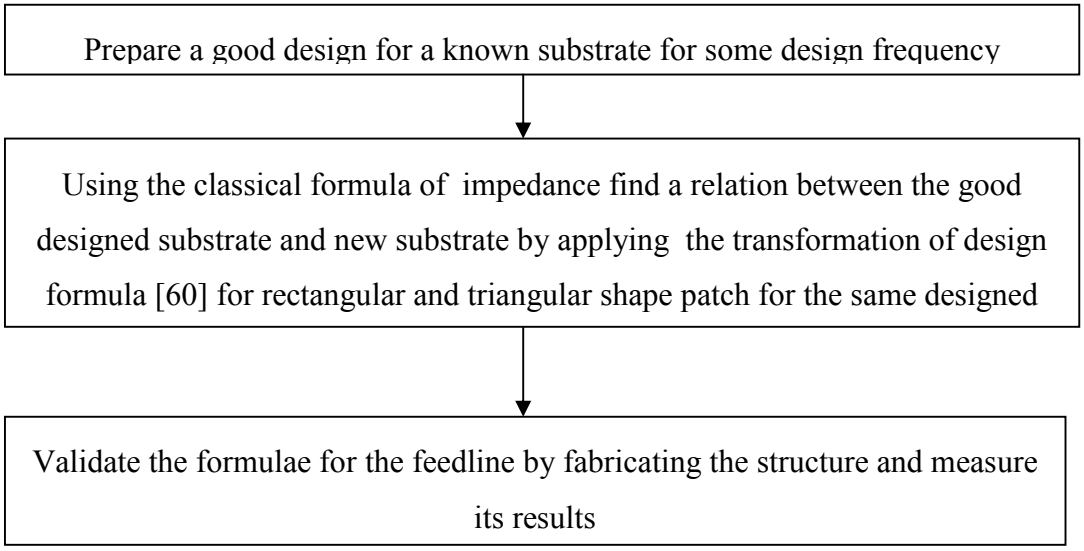

The objective of this part of work is to derive a set of formulae for feed line dimensions which should be a part of the transformation of design [60]. The work is started by taking the conventional impedance formulae of microstrip line. Then putting the value 50 Ω of characteristic impedance in this relation, solve them and after analyzing it present a suitable form of transformation of design for feedline structure.

3.3 Mathematical Expression of Feedline of MS Antenna for Transformation of Designs

The characteristic impedance Z_c of a Microstrip line is given by [10]

$$Z_C = \frac{60}{\sqrt{\varepsilon_{reff}}}\left[\ln\left(\frac{8h}{Wo}+\frac{Wo}{4h}\right)\right] \quad \text{for } \frac{W_0}{h} \leq 1 \tag{3.1}$$

$$Z_C = \frac{120\pi}{\sqrt{\varepsilon_{reff}}\left[\frac{W_0}{h}+1.393+0.667\ln\left(\frac{W_0}{h}+1.444\right)\right]} \quad \text{for } \frac{W_0}{h} > 1 \tag{3.2}$$

where, W_0 = Width of the microstrip line and h is the height of the substrate

As we know from the equivalent design constant ψ is the ratio of square root of the dielectric constants of two substrates, so considering the effective dielectric constants for two

different substrates ε_{reff1} and ε_{reff2} and putting it into the formula as in eq. (3.2). A very important result is taken into account in this work is that for resonant frequency(f_0) from 1 GHz -10 GHz and the value of the ε_{r1} and ε_{r2} from the value 1-10 the ratio of dielectric constants $\sqrt{\frac{\varepsilon_{r1}}{\varepsilon_{r2}}}$ is near about equal the ratio of the effective dielectric constant $\sqrt{\frac{\varepsilon_{eff1}}{\varepsilon_{eff2}}}$ of the substrate.So in this work we have used the approximate relation

$$\sqrt{\frac{\varepsilon_{reff1}}{\varepsilon_{reff2}}} \approx \sqrt{\frac{\varepsilon_{r1}}{\varepsilon_{r2}}} \tag{3.3}$$

For impedance matching the characteristic impedance of the microstrip feed line is taken as Z_c = 50 Ω. The characteristic impedance is calculated for two conditions (i) $\frac{W_0}{h} \leq 1$ (ii) $\frac{W_0}{h} > 1$ for developing relations for the transformation of feed line design.

CASE I

First consider the case of $\frac{W_0}{h} \leq 1$, on putting Z_c = 50 Ω in equation (3.1) and using eq. (3.3), we get a relation between dielectric constant (ε_r) and the ratio of the width of the feed line to a height of dielectric substrate (W_0/h).

$$50 = \frac{60}{\sqrt{\varepsilon_r}} \ln\left[\frac{8h}{W_0} + \frac{W_0}{4h}\right] \tag{3.4}$$

$$\sqrt{\varepsilon_r} = \frac{60}{50} \ln\left[\frac{8h}{W_0} + \frac{W_0}{4h}\right] \tag{3.5}$$

On squaring both sides, the equation (3.5) becomes

$$\varepsilon_r = \left(\frac{60}{50}\right)^2 \left(\ln\left[\frac{8h}{W_0} + \frac{W_0}{4h}\right]\right)^2 \tag{3.6}$$

$$\varepsilon_r = 1.44 \times \left(\ln\left[\frac{8h}{W_0} + \frac{W_0}{4h}\right]\right)^2 \tag{3.7}$$

On putting different values of W_0/h (W_0/h ≤ 1) in this equation , we get different values of ε_r. The values of W_0/h are taken from 0.01 to 1. But the physically available substrate found in the range 2.2 < ε_r > 10.5. So only those values of W_0/h are considered (from 0.56 to

0.65) for $W_0/h \leq 1$ condition which is able to provide the practically realizable substrate value. By putting the value of $W_0/h = 1$ the calculated value of dielectric constant is $\varepsilon_r = 6.4$ .. For the substrate of known dielectric constant in between range $6.4 < \varepsilon_r > 10.5$ and also of the known height (h), the width of the feed line (w_0) may be calculated from this eq. (3.7). It will provide the 50 Ω impedance matching .

The graphical representation of W_0/h with dielectric constant is shown in Fig. 3.1

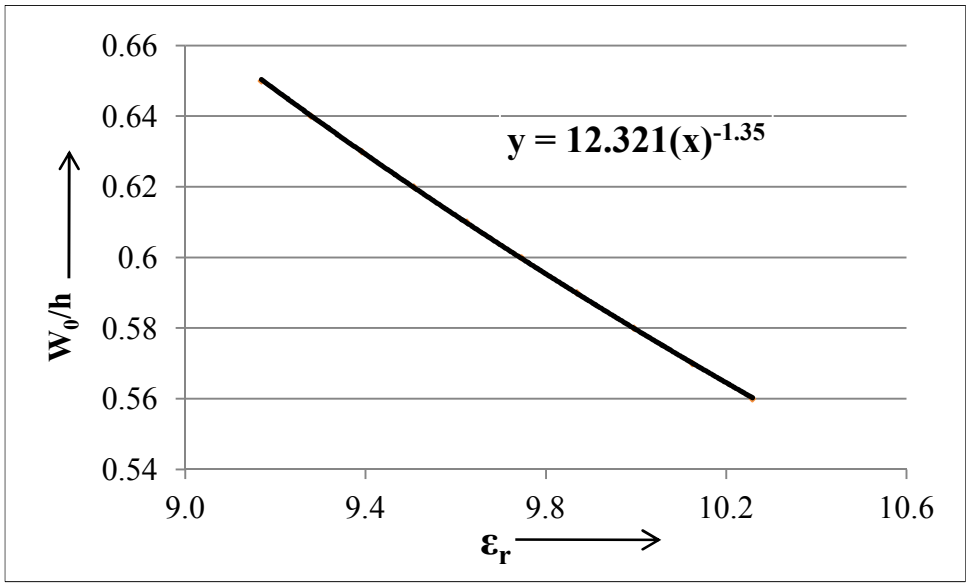

Fig. 3.1. Graphical representation of dielectric constant of substrate (ε_r) with Wo/h when Wo/h ≤ 1

From the above graph, the equation satisfying the maximum points can be wriiten as

$$\frac{W_0}{h} = 12.321 \times (\varepsilon_r)^{-1.35} \tag{3.8}$$

For transformation of designs let's assume that W_{01}, h_1 and ε_{r1} are the width of the microstrip feed line, height of dielectric substrate and effective dielectric constant respectively of a good design whose dimension parameters are known to us and abbreviated as design-I. Similarly W_{02}, h_2 and ε_{r2} are the width of the microstrip feed line, height of dielectric substrate and effective dielectric constant of another substrate on which the good design (The design I) is to be transformed for the same frequency .This is abbreviated as the parameters of design II. Then eq. (3.8) can be written for design I as

$$\frac{W_{01}}{h_1} = 12.321 \times (\varepsilon_{r1})^{-1.35} \tag{3.9}$$

And for design II as

$$\frac{W_{02}}{h_2} = 12.321 \times (\varepsilon_{r2})^{-1.35} \tag{3.10}$$

On dividing equations (3.9) and (3.10), we get

$$\frac{\frac{W_{01}}{h_1}}{\frac{W_{02}}{h_2}} = \frac{12.321 \times (\varepsilon_{r1})^{-1.35}}{12.321 \times (\varepsilon_{r2})^{-1.35}} \tag{3.11}$$

$$\frac{W_{01}}{h_1} \times \frac{h_2}{W_{02}} = \frac{(\varepsilon_{r1})^{-1.35}}{(\varepsilon_{r2})^{-1.35}} \tag{3.12}$$

Using equation (1.46) in equation (3.12),

$$\frac{W_{01}}{W_{02}} \times \Psi = \left(\frac{\varepsilon_{r1}}{\varepsilon_{r2}}\right)^{-1.35} \tag{3.13}$$

$$\frac{W_{01}}{W_{02}} \times \Psi = \left(\sqrt{\frac{\varepsilon_{r1}}{\varepsilon_{r2}}}\right)^{-2.7} \tag{3.14}$$

Now, using equation (1.47) in equation (3.14),

$$\frac{W_{01}}{W_{02}} \times \Psi = (\Psi)^{-2.7} \tag{3.15}$$

On interchanging the parameters,

$$\mathbf{W_{02} = W_{01} \times (\Psi)^{3..7}} \tag{3.16}$$

This is one of the new add-on formula with the transformation of designs series. This is used to calculate the width of feed line for the design which has to be transformed for the substrate of dielectric constant having in between the range $6.4 < \boldsymbol{\varepsilon_r} > 10.5$.

The length of feed line is directly taken using Equivalent design concept (Bhatnagar's Postulate) for this case and can be given as

$$\mathbf{L_{f2} = \Psi \times L_{f1}} \tag{3.17}$$

Where L_2 and L_1 are length of feed line of IInd and Ist design respectively.

CASE II

Repeating the whole above process for case II. Consider the case of $\frac{W_0}{h} > 1$, on putting Z_c = 50 Ω in equation (3.2) and using equation (3.3), we get a relation between dielectric constant (ε_r) and the ratio of width of feed line to a height of dielectric substrate (W_0/h).

$$50 = \frac{120\pi}{\sqrt{\varepsilon_r}\ \left[\frac{W_0}{h} + 1.393 + 0.667 \ln\left(\frac{W_0}{h} + 1.444\right)\right]} \tag{3.18}$$

$$\sqrt{\varepsilon_r} = \frac{120\pi}{50\ \left[\frac{W_0}{h} + 1.393 + 0.667 \ln\left(\frac{W_0}{h} + 1.444\right)\right]} \tag{3.19}$$

On squaring both sides, the equation (3.19) becomes

$$\varepsilon_r = \frac{(120\pi)^2}{(50)^2 \left[\frac{W_0}{h} + 1.393 + 0.667 \ln\left(\frac{W_0}{h} + 1.444\right)\right]^2} \tag{3.20}$$

$$\varepsilon_r = 56.791 \times \left[\frac{W_0}{h} + 1.393 + 0.667 \ln\left(\frac{W_0}{h} + 1.444\right)\right]^{-2} \tag{3.21}$$

On putting different values of W_0/h, considering $W_0/h > 1$, we get different values of ε_r. The same restriction of the values $W_0/h > 1$ is here also that physically available substrate are in the range from $2.2 < \varepsilon_r > 10.2$. For the range $6.4 < \varepsilon_r > 10.5$ the relation by eq. (3.7) is applied . So this case is considered for the substrate range $2.2 < \varepsilon_r > 6.4$. By putting the values of W_0/h from 1.01 to 2.73 in eq. (3.21) the values of dielectric constants results for the range $2.2 < \varepsilon_r > 6.4$. If the dielectric constant of any substrate lies in this range ($2.2 < \varepsilon_r > 6.4$) of height h the width of feedline for 50 Ω matched impedance, also calculated from this eq. (3.21).

The graphical representation of this relation is shown in Fig. 3.2.

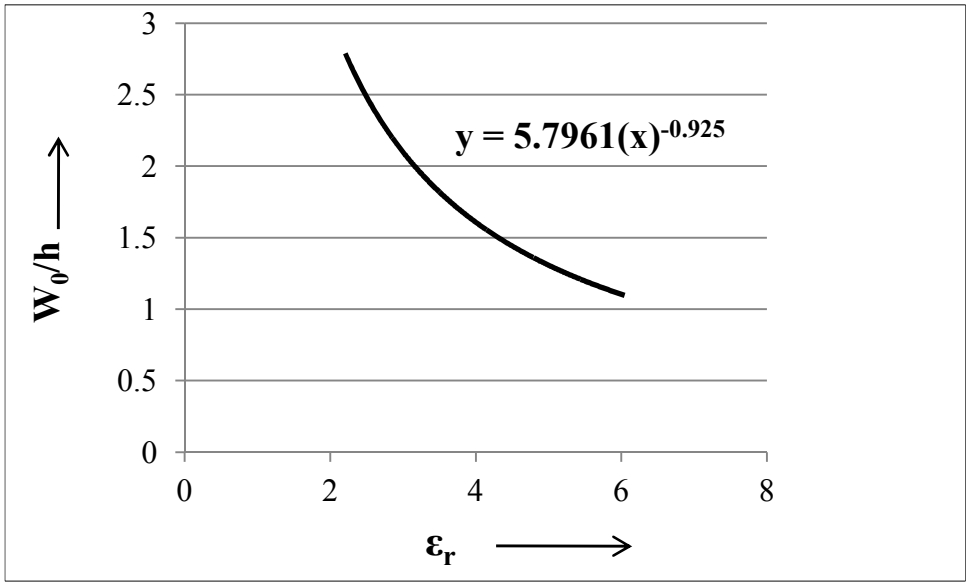

Fig. 3.2. Graphical representation of dielectric constant of substrate (ε_r) with Wo/h when Wo/h>1.

From the above graph, the equation satisfying the maximum points can be given as

$$\frac{W_0}{h} = 5.7961 \times (\varepsilon_r)^{-0.925} \tag{3.22}$$

Let's assume that W_{01}, h_1 and ε_{r1} are the widths of the microstrip feed line, height of dielectric substrate and effective dielectric constant are respectively the parameters of a known good design abbreviated as the design I parameters. Similarly W_{02}, h_2 and ε_{r2} are the width of the microstrip feed line, height of dielectric substrate and effective dielectric constant are respectively the parameters of design II on which design has to be transformed for the same designed frequency. Then eq. (3.22) can be written as

$$\frac{W_{01}}{h_1} = 5.7961 \times (\varepsilon_{r1})^{-0.925} \tag{3.23}$$

$$\frac{W_{02}}{h_2} = 5.7961 \times (\varepsilon_{r2})^{-0.925} \tag{3.24}$$

On dividing eq. (3.23) and (3.24), we get

$$\frac{\frac{W_{01}}{h_1}}{\frac{W_{02}}{h_2}} = \frac{5.7961 \times (\varepsilon_{r1})^{-0.925}}{5.7961 \times (\varepsilon_{r2})^{-0.925}} \tag{3.25}$$

$$\frac{W_{01}}{h_1} \times \frac{h_2}{W_{02}} = \frac{(\varepsilon_{r1})^{-0.925}}{(\varepsilon_{r2})^{-0.925}} \tag{3.26}$$

Put value of h_2 from equation (1.46) to eq. (3.26),

$$\frac{W_{01}}{W_{02}} \times \Psi = \left(\frac{\varepsilon_{r1}}{\varepsilon_{r2}}\right)^{-0.925} \tag{3.27}$$

$$\frac{W_{01}}{W_{02}} \times \Psi = \left(\sqrt{\frac{\varepsilon_{r1}}{\varepsilon_{r2}}}\right)^{-1.85} \tag{3.28}$$

Using equation (1.47) in eq. (3.28), we get

$$\frac{W_{01}}{W_{02}} \times \Psi = (\Psi)^{-1.85} \tag{3.29}$$

On interchanging the parameters,

$$\mathbf{W_{02} = (\Psi)^{2.85} \times W_{01}} \tag{3.30}$$

This is the second new add on formula with the transformation of designs series. This is used to calculate the width of feed line for the design which has to be transformed for the substrate of dielectric constant having in between $2.2 < \boldsymbol{\varepsilon_r} > 6.4$ range .

The formula for the length of feed line in this case is also the same as eq. (3.17).

An important thing is that the if the substrate dielectric constant lies in the range $6.4 < \varepsilon_r > 10.5$ formula of the design of feedline eq. (3.16) and eq. (3.17) is applied and substrates of known good design (design-I) and the another one on which design to be transformed (design II) should lie in this range only. Similarly for the substrate dielectric constant lies in the range $6.4 < \varepsilon_r > 10.5$ formula of design of feed line eq. (3.30) and (3.17) is applied and substrates of known good design (design-I) and the another one on which design to be transformed (design II) should lie in this range only.

Both eq. (3.16) and eq. (3.30) are considered with the condition that $h_2 = \Psi \times h_1$. But in practical consideration, the dielectric constant (ε) and the height of dielectric substrate (h) must be chosen as per physical availability in the market.

So now considering the second scaling factor $\phi = \frac{h_1}{h_2}$ where h_1 and h_2 are both user input parameters, i.e. h_2 is not dependent on h_1 by some scaling factor Ψ. Then we can change in equation (3.12) as

$$\frac{W_{01}}{W_{02}} \times \frac{h_2}{h_1} = \frac{(\varepsilon_{r1})^{-1.35}}{(\varepsilon_{r2})^{-1.35}} \tag{3.31}$$

$$\frac{W_{01}}{W_{02}} \times \frac{1}{\phi} = (\Psi)^{-2.7} \tag{3.32}$$

On rearranging the equation, we get

$$\mathbf{W_{02}} = \frac{(\boldsymbol{\Psi})^{\mathbf{2.7}}}{\boldsymbol{\phi}} \times \mathbf{W_{01}} \tag{3.33}$$

The above eq. (3.33) is for the case I for $\frac{W_0}{h} \leq 1$.

Now consider similar case for $\frac{W_0}{h} > 1$, and then eq. (3.26) can be written as

$$\frac{W_{01}}{W_{02}} \times \frac{h_2}{h_1} = \frac{(\varepsilon_{r1})^{-0.925}}{(\varepsilon_{r2})^{-0.925}} \tag{3.34}$$

$$\frac{W_{01}}{W_{02}} \times \frac{1}{\phi} = (\Psi)^{-1.85} \tag{3.35}$$

On rearranging the equation, we get

$$\mathbf{W_{02}} = \frac{(\boldsymbol{\Psi})^{\mathbf{1.85}}}{\boldsymbol{\phi}} \times \mathbf{W_{01}} \tag{3.36}$$

The formulae are given by eq. (3.33) and eq. (3.34) are the novel add-on formulae for the transformation of design series. The known set of good design on a substrate having the known parameters dielectric constant (ε_{r1}), substrate height (h_1), dimensions of patch (L_1, W_1) , dimensions of feedline (L_{01} ,W_{01}) can be transformed to another substrate, for the same

designed frequency , having known dielectric constant (ε_{r2}), substrate height (h_2) by calculating new patch dimensions by eq. (1.53), (1.56) and feed line dimensions by eq. (3.33) and (3.36).

This transformation of design formulae for feed line is applicable for any shape of patch design. In this thesis the validation of this is presented for rectangular and triangular shape patch only.

3.4 Modification in the Width Formula of Transformation of Designs Formulae Set

The formula to calculate the width of the patch from the design transformation of formulae is given by eq. (1.53)[60]

$$W_{p2} = \frac{W_{p1}}{\phi}$$

Where

$$\phi = \frac{h_1}{h_2}$$

Generally, the value of the width of the patch is greater than the length of the patch. But from this relation for width transformation if $h_1 > h_2$ then the calculated width from the above formula is less than the length of patch. So most of the transformed width (W_{p2}) has found the value $Wp_2 < L_{p2}$ which is not desirable for designing the structure of MS antenna. So modification in this width transformation formula was needed. This work presented the transformation of the width of the patch with the help of the length of the transformed design patch.

If the ratio of width to length of design I and design II is to be kept constant then

$$\frac{W_{p2}}{L_{p2}} = \frac{W_{p1}}{L_{p1}} \tag{3.37}$$

$$\mathbf{W_{p2}} = \frac{\mathbf{W_{p1}}}{\mathbf{L_{p1}}} \times \mathbf{L_{p2}} \tag{3.38}$$

where L_{p2} is calculated from the transformation design formula as per eq. (1.56). This is the modified formula for the transformation of design for the width of the patch.This formula is taken now with the whole set of the transformation of designs. Now in all the validation of new feedline transformation formulae, this formula is used.

3.5 Validation of Transformation Formulae for Feed Line and the Width of Patch for Rectangular Shape Patch

3.5.1 Case I

The above two add -on formulae of line feed and the modification in width formula was validated by taking a well designed structure . In this thesis for the range $6.4 < \boldsymbol{\varepsilon_r} > 10.5$ the good design has been taken on substrate RT/Duroid (Roger TMM10) $\boldsymbol{\varepsilon_r} = 9.2$ h = 1.5mm. This is considered as the design I for this range of dielectric constant.

Table 3.1 shows the design parameters of this known good design which is already available with us .

Table 3.1 Design Parameters of a Microstrip Antenna for $\varepsilon_r = 9.2$ and h= 1.5 mm

Designed resonance frequency is 2.4 GHz	
Patch Dimensions	
Width of the Patch (W)	27.67 mm
Length of the Patch (L)	20.4 mm
Feed dimension where line width has been calculated from new formula eq. (4.16)	
Width of feed line (W_{01})	1.13 mm
Length of feed line (L_{01})	25 mm

The Simulated designed structure of the MS antenna corresponding to the above Table 3.1 design parameter is shown in Fig. 3.3 (a) and its frequency-return loss curve is shown in Fig. 3.3 (b)

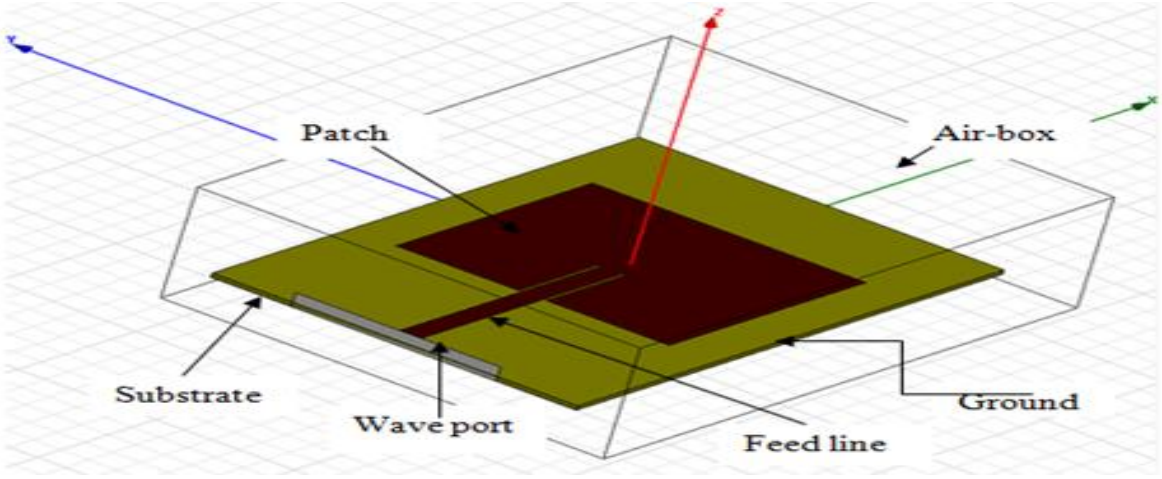

(a)

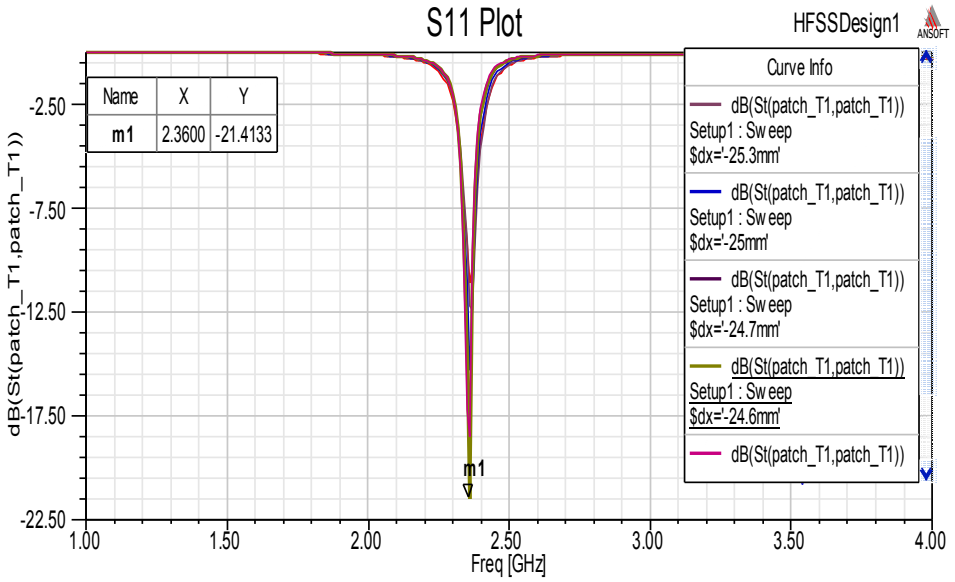

(b)

Fig. 3.3. (a) Good design structure for $\varepsilon_r = 9.2$ from the simulator (b) Simulated return loss versus frequency plot for $\varepsilon_r = 9.2$ (imported result ; already designed from classical approach)

Fig. 3.3(b) shows the return loss versus frequency plot for $\varepsilon_{r1} = 9.2$ designed at an operating frequency of 2.4 GHz. The value of the return loss at this point is -21.4133 dB at resonant frequency of 2.36 GHz. Here only the resonance frequency with the return loss is studied as the performance parameter.

Now suppose we have to design a structure for the same designed frequency 2.36 GHz on the substrate Rogers RO3210 having dielectric constant (ε_{r2} = 10.2) with thickness h_2 =1.28 mm. This is considered as design II in this case.

Table 3.3 shows the dimensions of the final design of the rectangular microstrip patch antenna for ε_{r2} = 10.2 using the transformation design formulae. The equations (1.46), (1.47), (1.56), (3.38), (3.33) and (3.17) are used for calculations. The simulation of design is as shown below. The value of return loss at this point is -23.37 dB at the resonant frequency of 2.38 GHz.

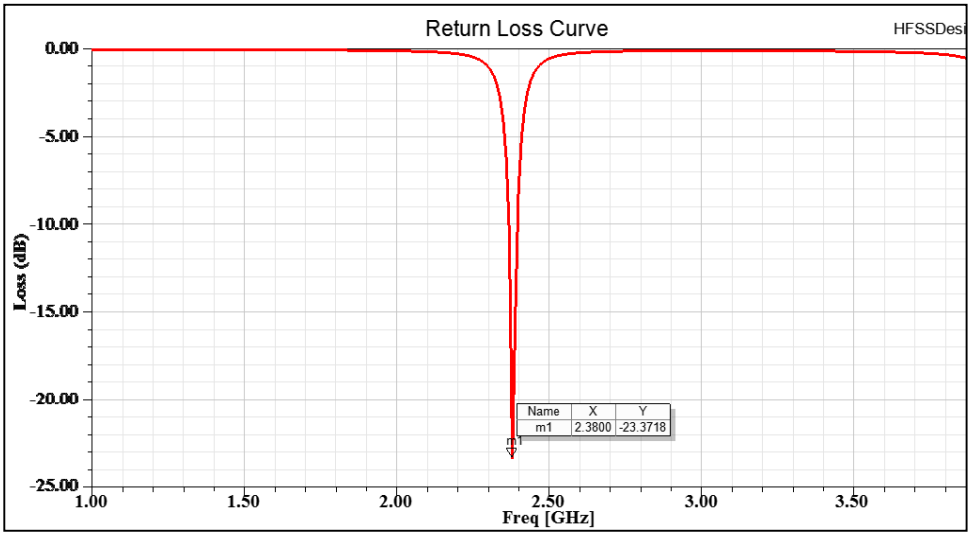

Fig. 3.4 . Simulated return loss verss frequency plot for εr2 = 10.2 .

3.5.2 Case II

Similarly, the design on the substrate having dielectric constant ranging in between 2.2 < $\boldsymbol{\varepsilon_r}$ > 6.4 can be transformed by using eq. (3.36) and eq. (3.17). For verifying these equation the known good design is considered here is on substrate RT/duroid (5880) (ε_{r1}= 2.2) with thickness h_1=1.6 mm.This design is considered as the design I for the transformation of design formulae. Table 3.2 shows the dimension parameters taken as a good design of rectangular microstrip antenna for ε_{r1} = 2.2.

Table 3.2 Design Parameters of a Microstrip Antenna for ε_r = 2.2 and h = 1.6 mm

Designed resonance frequency 2.4 GHz	
Patch Dimensions	
Width of the Patch (W)	49.41 mm
Length of the Patch (L)	41.36 mm
Feed width calculated from New Formulae from eq. (3.16)	
Width of feed line (W_{01})	4.56 mm

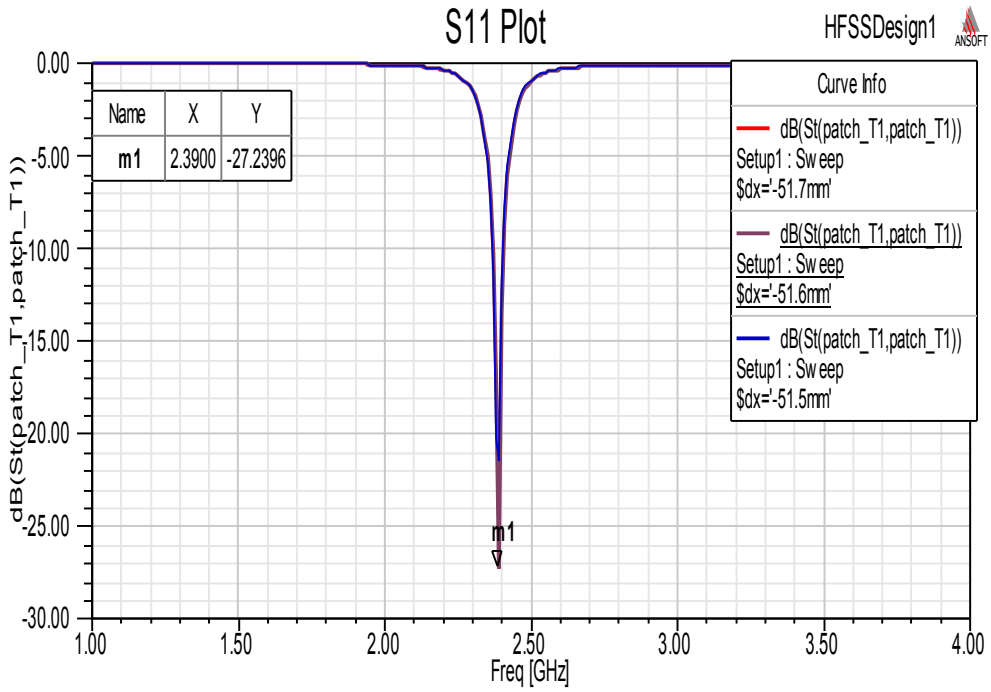

Fig. 3.5. Simulated return loss versus frequency plot for εr = 2.2 (Imported result; already designed from classical approach)

Now suppose we have to design a structure for the same designed frequency 2.39 GHz on the substrate FR4 Epoxy having dielectric constant (ε_{r2} = 4.4) with the thickness h_2 = 1.6 mm. This is considered as the design II in this case.

Table 3.3 shows the dimensions of the final design of the rectangular microstrip patch antenna for $\varepsilon_{r2} = 4.4$ using the transformation design formulae. The equations (1.46), (1.47), (3.36) and (3.17) are used for calculations.

Fig. 3.6 shows the simulated return loss versus frequency plot for $\varepsilon_{r2} = 4.4$ designed at an operating frequency of 2.39 GHz.

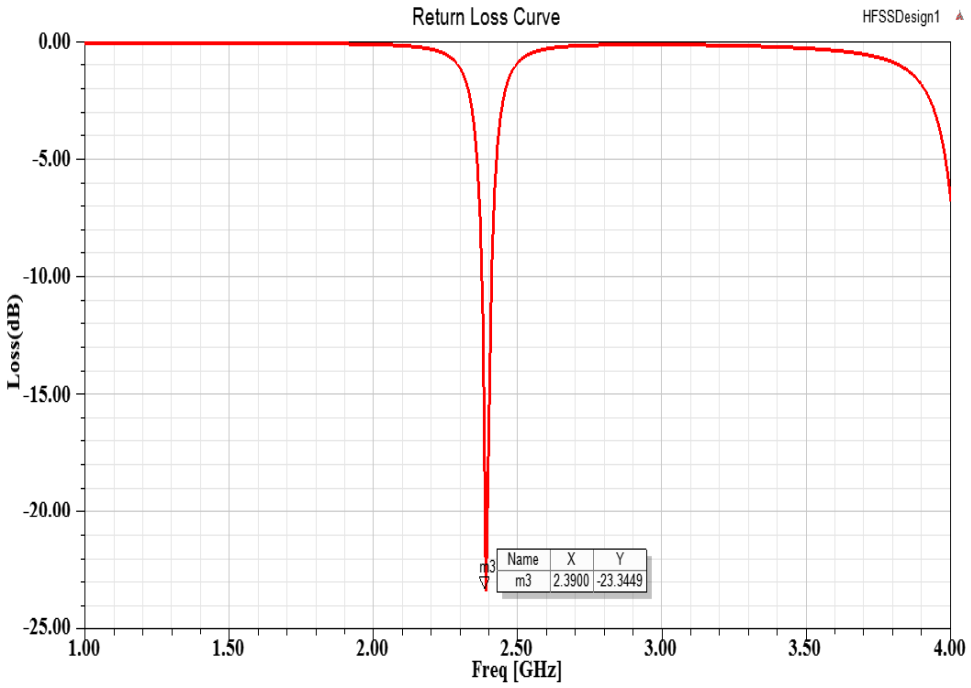

Fig. 3.6. Simulated return loss versus frequency plot for $\varepsilon_{r2} = 4.4$.

The value of return loss at this point is noticed -23.34 dB at resonant frequency of 2.39 GHz for the design on the simulator.

The transformation of designs for different substrates has been verified on HFSS version 16 . The good design for the case I is considered as Table 3.1 and for the case II as Table 3.2. The comparison of the simulated results for rectangular shape patch on some substrates (three for the case I and three for case II) whose design parameters calculated by the transformation of design and also calculated from classical formulae have been tabulated in Table 3.3. The simulation results of the work have been compared with the simulation result of design whose dimension parameters are calculated by classical formulae.

Table 3.3 Comparison of Simulation Results of Different Rectangular Microstrip Antenna Designed on Different Substrates

Dielectric constant range for two cases	Known parameters of a good design : **Design I**	New known parameters of **Design II**	Design parameters of Design II calculated from the new transformation of design formulae set	Simulated result of Design II parameters designed by **transformation of designs formulae**		Simulated result of Design II parameters designed by **classical formulae**	
			L,W=Patch length,width L_{01},W_{01}= Line feed length, width (mm)	Res. Freq. (GHz)	Return Loss (dB)	Res. Freq. (GHz)	Return Loss (dB)
$6.4 < \varepsilon_r > 10.5$	f_r= 2.4 GHz ε_{r1} =9.2 h1= 1.52mm L_1=27.67mm W_1=20.4mm L_{01}=25mm W_{01}=1.13mm	f_r= 2.4GHz ε_{r2} =**6.4** h2= **1.57mm**	L_2=24.51 W_2=33.23 L_{02}=31.20 W_{02}=2.27	2.39	-30.2	2.27	-40.1
		f_r= 2.4GHz ε_{r2} =**10.2** h2= **1.28 mm**	L_2=19.4 W_2=23.24 L_{02}=23.75 W_{02}=0.83	2.38	-23.37	2.35	-22.6
		f_r= 2.4GHz ε_{r2} =**10.2** h2= **0.64 mm**	L_2=19.818 W_2=26.06 L_{02}=24.36 W_{02}=0.586	2.29	-20.4	2.34	-25.5
$2.2< \varepsilon_r > 6.5$	f_r= 2.4 GHz ε_{r1} =2.2 h1= 1.575mm L_1=49.41mm W_1=41.36mm L_{01}=45.7mm W_{01}=4.56mm	f_r= 2.4GHz ε_{r2} = **4.4** h2= **1.6 mm**	L_2=29.13 W_2=34.80 L_{02}=31.86 W_{02}=2.64	2.39	-23.34	2.37	-31.47
		f_r= 2.4GHz ε_{r2} = **3** h2= **1.52 mm**	L_2=35.5 W_2=47.68 L_{02}=39.3 W_{02}=3.33	2.38	-30.1	2.21	-32
		f_r= 2.4GHz ε_{r2} = **6** h2= **1.52 mm**	L_2=24.76 W_2=39.84 L_{02}=27.42 W_{02}=1.44	2.41	-26.2	2.39	-26.4

3.5.3 Measured Result of Rectangular Patch Antenna with Line Feed Designed by Transformation of Designs Formulae

From the good designed structure for frequency 2.4 GHz , on Rogger TMM10 ($\boldsymbol{\varepsilon_r}$ = 9.2, h = 1.524mm) the design has been transformed on Rogers RO3210 (ε_{r2} = 10.2 , h=1.28 mm). The design was simulated on HFSS version16. The design parameters were calculated and shown in Table 3.3. An antenna was fabricated and shown in Fig. 3.7 (a) . The measured result is shown in Fig. 3.8 and marked as 2 and the resonance frequency is 1.9 GHz which is approximately equal to the simulated result which validated the formula of the case I.

(a) **(b)**

Fig. 3.7. (a) Fabricated antenna on substrate Rogers RO3210 (ε_{r2} = 10.2) (b) Fabricated antenna on substrate Rogers FR4 Epoxy (ε_{r2} = 4.4)

Similarly for the case II the good designed structure for frequency 2.4 GHz , on RT/Duriod 5880 ($\boldsymbol{\varepsilon_r}$ = 2.2, h = 1.575mm) the design has been transformed on Rogers Fr4 Epoxy (ε_{r2} = 4.4 , h=1.6 mm). The design has been simulated on HFSS@16 the design parameters have been calculated and shown in Table 3.3. The fabricated antenna is shown in Fig. 3.7 (b) and the measured result is shown in Fig. 3.8 . As shown in Fig. 3.8 marked as -1 the resonance frequency is 2.6 GHz which validated the formula for this case II.

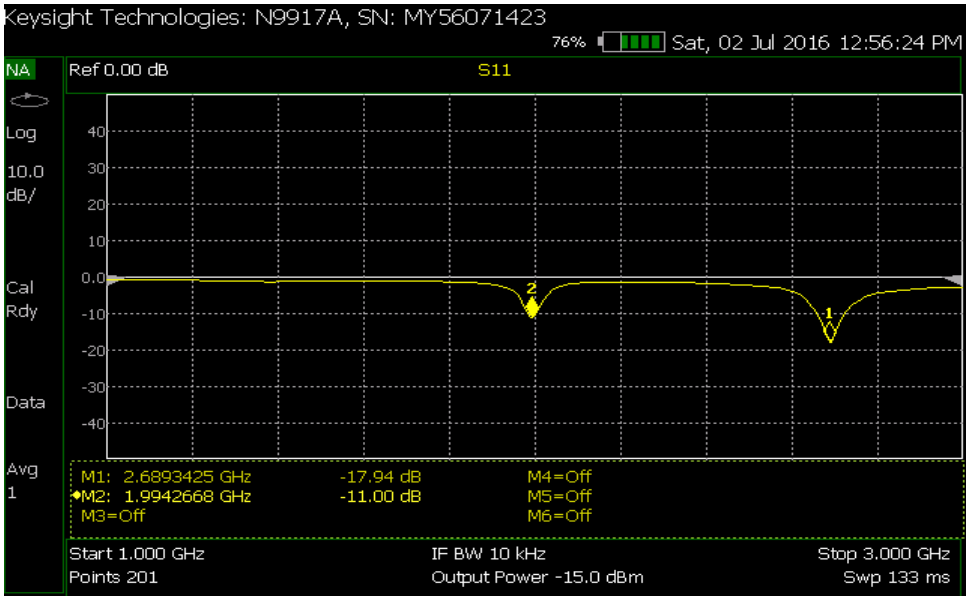

Fig. 3.8. Measured return loss curve for the case-I and II.

3.6 Transformation Design Formulae for Equilateral Triangular Shape Patch and Its Feed Line Design of MS Antenna

A new formula (by using Bhatnagar postulates) to design the equilateral triangle shape patch for MS antenna) was presented by us [90]. In this work the good design of equilateral triangle shape antenna has been considered which is designed by that formula [90].

$$\mathbf{Sp} = (\mathbf{1} - \mathbf{H\beta}) \times \mathbf{Se} \tag{3.39}$$

Here Se is calculated from [88]

$$Se = \frac{2C}{3f_r\sqrt{\varepsilon_r}} \tag{3.40}$$

β is the proportionality constant (Bhatnagar's constant) for rectangular shape patch it value is 1

H= $\frac{h}{\lambda_g}$ is the normalized height of the substrate. λ_g is the guided wavelength

Se = Electrical length of radiating sides

Sp = Physical length of radiating sides

Its transformation of design into another substrate for the same frequency has presented in this part of the chapter . The formulae of the transformation of designs for feed line of rectangular shape patch is as it is applicable for equilateral triangular shape patch too. The simulated results validated it.

The transformation of one good design of equilateral triangle shape patch on one substrate (ε_{r1}) of known side Sp_1 into the another substrate (ε_{r2}) of side Sp_2 is presented by the given formula

$$\mathbf{S_{p2} = (\psi) \times S_{p1}} \tag{3.41}$$

And the transformation of feed line for this shape is also calculated from the same as formulae of rectangle shape patch antenna given by eq. (3.7) , eq. (3.33) and eq. (3.36)

3.7 Validation of Transformation Formulae for Feed Line for Equilateral Triangle Shape Patch

For validation of transformation designs formulae for this, a triangular shape patch antenna design having good simulation result in terms of return loss has been considered as basic design1 [90]. The equilateral arm's length of this triangular patch antenna was calculated by the formulae given in eq. (3.39) and eq. (3.40). FR4 Epoxy (having dielectric constant ε_{r1} = 4.4) was taken as substrate material for this design. The design frequency of this structure was taken as 2 GHz. The structural diagram of this design from the simulator is shown in Fig. 3.9.

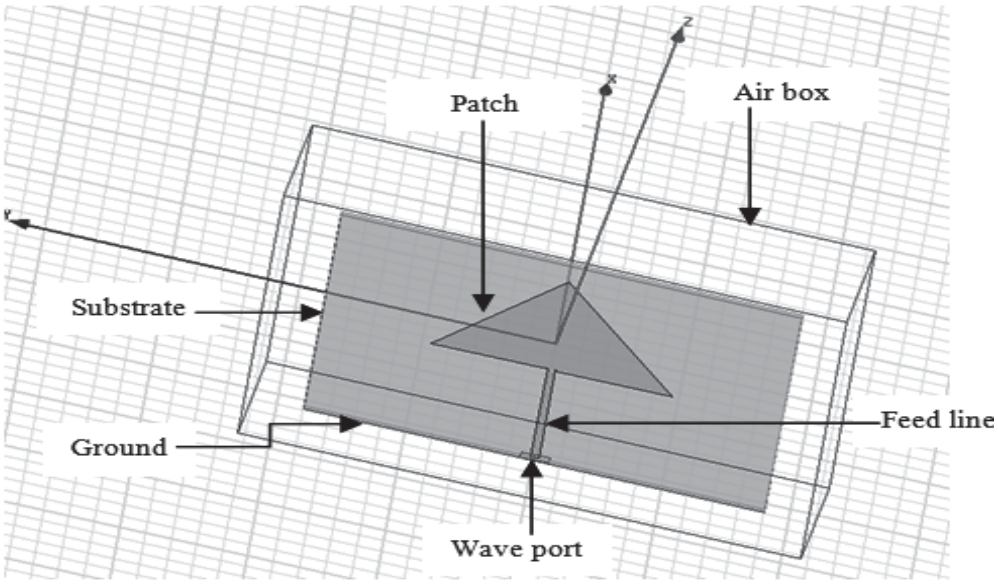

Fig. 3.9. Structural diagram of equilateral triangular shape patch antenna from the simulator [90].

Now this design1 was to be transformed into another substrate material for the same design frequency 2 GHz. First, we have to use eq. (3.41) for patch sides transformation and eq.'s (1.46), (1.47), (3.17), (3.33) and (3.36) for feed line transformation to calculate new design parameters for another substrate material.The structure has been designed on simulator HFSS version 16. The design was transformed onto three different materials (ε_{r2} = 2.2 , 3 and 9.8) and the corresponding results of return loss on simulator are shown below . The Fig. (3.10) shows the simulation result of good design on FR4 Epoxy substrate as the design I . The simulation of designs on another substrate by using transformation formulae is shown in Fig. (3.11) and Fig. (3.12) and later tabulated in Table 3.4.

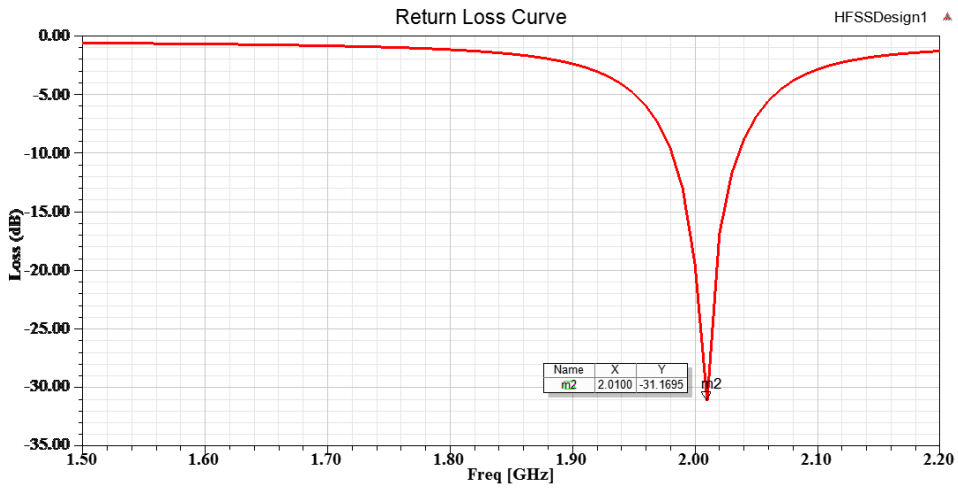

Fig. 3.10. Simulated return loss plot of the equilateral triangular patch on substrate FR4 Epoxy ($\varepsilon_r = 4.4$) for designing frequency $f_r = 2$ GHz [90].

Now the design is transformed into design 2, on another substrate material Rogers/ Duroid 5880 (tm) (having $\varepsilon_r = 2.2$) by using the formulae of transformations.

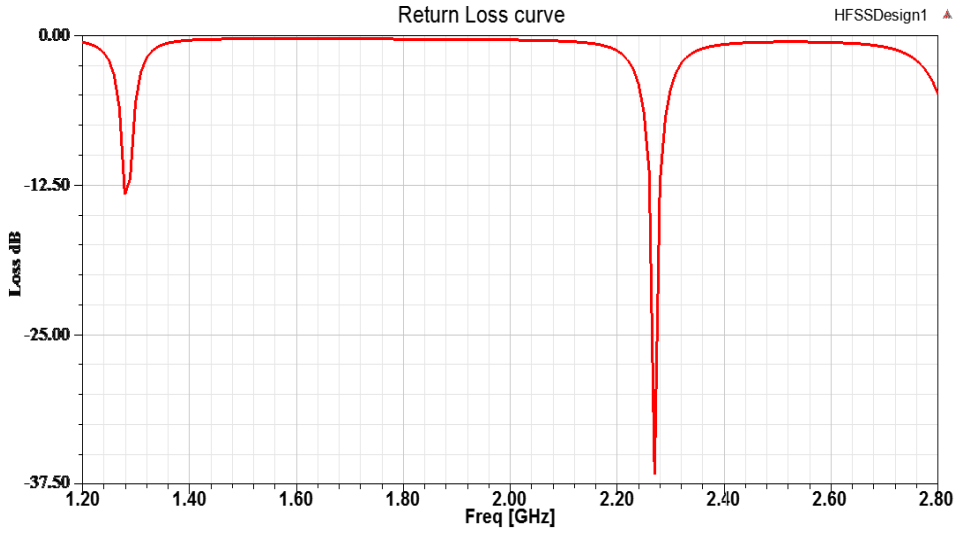

Fig. 3.11. Simulated return loss plot of structure having an equilateral triangular patch on substrate Rogers/ Duroid5880 (tm) ($\varepsilon_r = 2.2$) for designing frequency $f_r = 2.01$ GHz.

The above figure shows that the structure is resonant at the same designed frequency, i.e. 2.01 GHz after this transformation.

Again the design1 is transformed into design 3, on a different substrate material of Rogers RO 3003 (having ε_r = 3) repeating the same process and the return loss plot is as shown below in Fig. 3.12.

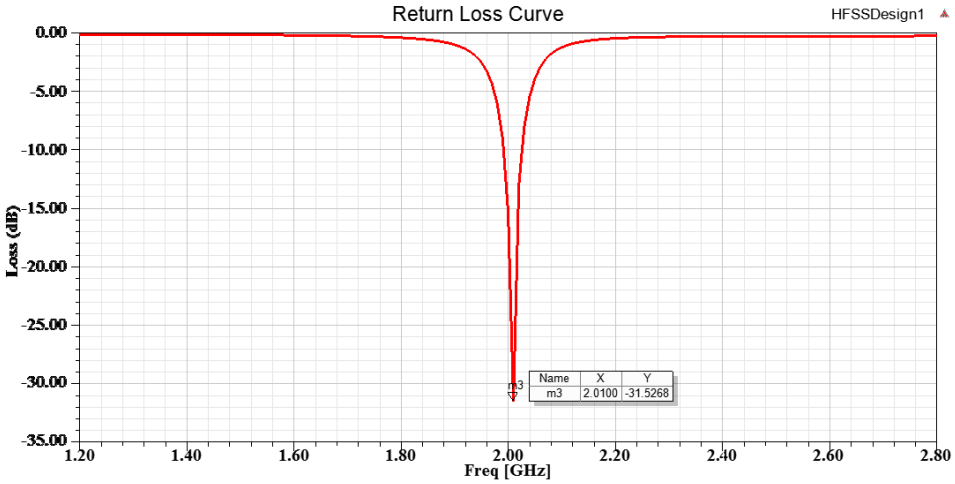

Fig. 3.12 . The Simulated return loss plot of the structure having an equilateral triangular patch on substrate Rogers RO 3003 (ε_r = 3) for designing frequency f_r = 2.01 GHz.

The above figure again shows that the structure is resonating on the same designed frequency, i.e. 2.01 GHz with the return loss -31.53 dB.

One more design was validated for transformation law on the substrate material Rogers TMM10i (having ε_r = 9.8). The return loss plot is as shown below in Fig. 3.13.

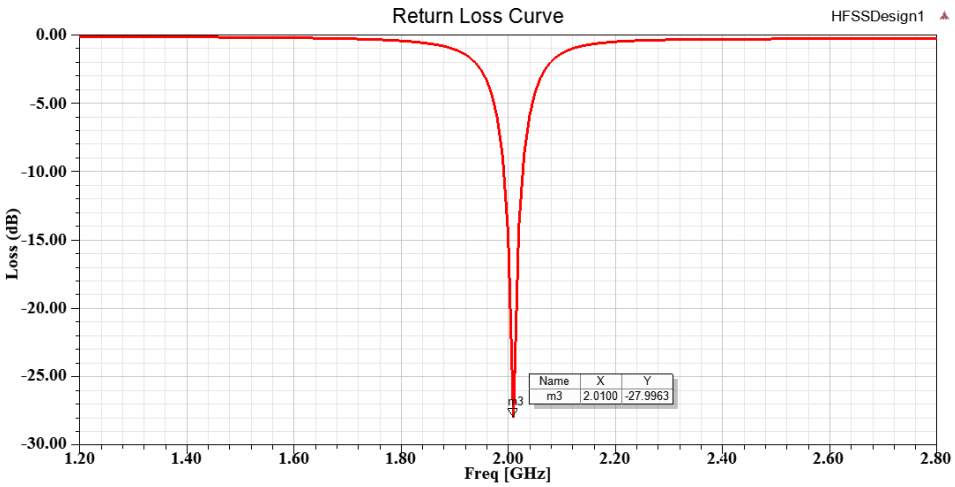

Fig. 3.13. Simulated return loss plot for structure having an equilateral triangular patch on substrate Rogers TMM10i (ε_r = 9.8) for design frequency f_r = 2.01 GHz.

Table 3.4 A Summary Table of Return Loss Results on the Simulator By Applying the Law of Transformation of Design for Equilateral Triangle Shape Patch for MS Antenna .

Substrate Material	**Dielectric Constant (ε_r)**	**Resonant Frequency (Simulated) in GHz**	**Return loss (in dB)**
FR4 Epoxy	4.4	2.01	-31.1
Rogers/Duroid 5880 (tm)	2.2	2.27	-36.6
Rogers RO 3003	3	2.01	-31.5
Rogers TMM10i	9.8	2.01	-27.9

3.8 Conclusion

This chapter presented the formulae for the transformation of feed line dimensions from one type of substrate to another type of substrate, with the condition that both have the structure designed for the same designed frequency. These formulae work for both rectangular and equilateral triangle shape patch designed structure. This is the add-on formulae to the transformation design formulae for the rectangular shape patch [60] and equilateral triangle shape patch [90] . In this work modification in the formula of transformation for width [60] has been also presented and verified . The need of this modification was to satisfy the condition $W_{p2} > L_{p2}$ for the width of patch which was not satisfied by the earlier presented formula [90]. In this modified formula, the width of the patch of the transformed design (W_{p2}) is estimated by the multiplication of the ratio of the width to length of the patch of good design $\left(\frac{W_{p1}}{L_{p2}}\right)$ to the newly calculated length of the patch of transformed design (L_{p2}).

$$\mathbf{W_{p2} = \frac{W_{p1}}{L_{p1}} \times L_{p2}}$$

The simulated and measured return loss results validated this modified formula for the transformation of the width of rectangular shape patch.

The transformation of line feed designs of MS antenna is presented in this chapter. The formulae for feed line gives good results and are also easy to use. This has been developed for two conditions

Case I for $\frac{W_{01}}{h_1} \leq 1$ ($\frac{W_0}{h}$ is the ratio of feed line width to height of substrate)

$$\mathbf{W_{02}} = \frac{(\boldsymbol{\Psi})^{\mathbf{2.7}}}{\boldsymbol{\phi}} \times \mathbf{W_{01}}$$

Case II for $\frac{W_{01}}{h_1} > 1$

$$\mathbf{W_{02}} = \frac{(\boldsymbol{\Psi})^{\mathbf{1.85}}}{\boldsymbol{\phi}} \times \mathbf{W_{01}}$$

Where

$$\phi = \frac{h_1}{h_2}$$

and

$$\Psi = \sqrt{\frac{\varepsilon_{r1}}{\varepsilon_{r2}}}$$

Simulated and measured results of this chapter verified the developed formulae. The designed are verified only by taking the performance parameter resonance frequency. Other parameters are not in the scope of this chapter s.

Further, the transformation of sides of equilateral triangle shape patch and its line feed has also presented in this chapter. The transformation of side S_{p1} of a good designed equilateral triangle shape patch from one type of substrate to another type of substrate for the same designed frequency is presented as

$$\mathbf{S_{p2}} = (\boldsymbol{\psi}) \times \mathbf{S_{p1}}$$

The line feed design transformation of triangular patch has the same formulae as for rectangular shape patch with two conditions as given earlier .

An algorithm for the design transformation of rectangle shape patch and its feed line has been presented as in appendix A. By implementing this in Matlab @16 all the parameters i.e. return loss, radiation pattern, VSWR can be found by inserting the values of parameters for which we want to design a new structure for the same frequency.

Chapter 4: INVESTIGATIONS OF COPLANAR MONOPOLE WIDEBAND ANTENNA AND IT'S ARRAY ARRANGMENTS

4.1 Introduction

In Present era, electronic systems frequently use sensors, sensor networks and communication devices. Some of these sub-systems may be remotely situated (physically) and may be difficult to power by physical wires. The Wireless energy transfer is then the only means to supply energy to such sub-systems. If the energy is to be harvested from the ambient then Rectennas are preferred. Antenna is a major functionary part of any Rectenna. This motivated me to develop an antenna structure for application in Rectennas.

This chapter presents inveastigations into antennas that work for almost all useful ranges of GSM (900 MHz-1.6GHz) , ISM (2.1-2.6 GHz) and UWB (5.6-10GHz) for RF energy harvesting module. This has resulted in a compact coplanar monopole antenna. Its single structure rejects the range of WLAN (3.1-5.6 GHz).

Particularly the wideband operation is not only the important factor for the antenna section of the RF energy harvesting module. The gain and radiation efficiency are the dominating factors for the antenna because the DC output is directly proportional to the AC input of the converter circuit. So to increase these parameters, array of possible arrangements are also studied in this chapter. With the array structure, these parameters increase their values but the antenna loses the reject band property and is unable to show wideband operation. Investigation shows that by the array arrangements the antenna works as a multifrequency coplanar monopole antenna.

The comparative study of these arrangements is tabulated at the end of this chapter.

4.2 Literature Review

In the field of wireless communication, the emerging technologies need compact and miniature devices. Such devices have small batteries that need to be charged well in time. Day by day increase in the usage of data demands that the batteries are charged frequently. A possible solution is that the batteries are charged automatically by any technique (for example by energy harvesting technique). RF energy harvesting is the related and interesting topic for this. For RF energy harvesting, a compact combined structure of microstrip antenna (receiving energy) with a suitable converter (rectifier and voltage multiplier circuits) may be

designed. The Antenna should be able to receive the energy of the ambient spectrum. Converter circuit and appropriate arrangements should be able to provide the energy to activate the batteries of the devices at all times. It may remove the need for the charger of the batteries. Such a combined structure has been named as RECTENNA by the researchers [91-94].

The key parameter of the Rectenna circuit is to design a microstrip/monopole/slot antenna that would be able to receive the energy from almost all useful bands, e.g. Radio, GSM, ISM, UWB, so that the device remains activated in all the places where the RF spectrum is in use. Ranges of RF spectrum widely used are 900 MHz - 2MHz (Band for radio & television applications, GSM), 2.1GHz - 2.6GHz (ISM band for various applications) and 3.1GHz -10.6 GHz (ultra wideband for satellite applications) [95]. Narrow band systems such as WLAN (3.1GHz - 4.4GHz), HIPERLAN (5.1GHz - 5.3GHz), C-BAND (4.4GHz - 5GHz) may provide interference. So band rejection for these bands is also required for Rectennas under consideration. A band stop filter is one of the solutions for rejecting any band, but this will make the device bulky. A parasitic element along with the antenna patch may be a good candidate for this purpose [96-98] .The band notch characteristics may be produced by cutting the slots in patch [99-102] Microstrip antenna structures for the above mentioned particular ranges are available [103-106]. Planar antennas for UWB applications have also been reported [107-111]. It has been observed from the literature studies that the coplanar structure is the easiest way to design UWB range antenna. All these techniques have been used in developing a coplanar monopole antenna structure for the band from 900 MHz - 9.9 GHz with band rejection from 3.1GHz - 5.6 GHz. Although the antenna is designed for RF energy harvesting application, it may also be used for mobile, satellite and military communication applications. The new design of the antenna has been simulated and optimized with the simulation software ANSYS HFSS ™16. In the next section, the antenna design and the simulated and measured results of the reflection coefficient (S_{11}) and radiation patterns are given.

Further, it is studied that the array arrangements are used for the RF energy harvesting purposes [112-114]. The stacking of antenna structure was also studied for this purpose [115]. This chapter also presents the comparative analysis of the possible array arrangements of this designed coplanar monopole antenna. Three array arrangements have been designed and compared to find the enhancement in any characteristic of the single structure. The main

motive to make the array is to increase the capturing area of received energy for the energy harvesting purpose particularly. The power combiners have also been used to add the powers of two or four antennas serially to increase the input power of RF-DC converter circuit of energy harvesting module. Stacking of two antennas has also been investigated.

4.3 A New Coplanar Monopole Antenna Design

Problem statement

Development of a single structure for the antenna that will capture energy from 900 MHz to 3.1 GHz and 5.6 GHz to 9.9 GHz bands and simultaneously reject energy from 3.1GHz to 5.6GHz. This means a wideband antenna (0.9 GHz to 9.9GHz) with a band rejection from 3.1 GHz to 5.6 GHZ. It should also maximize the utilized area for capturing the radiation energy falling on the structure.

Design Methodology

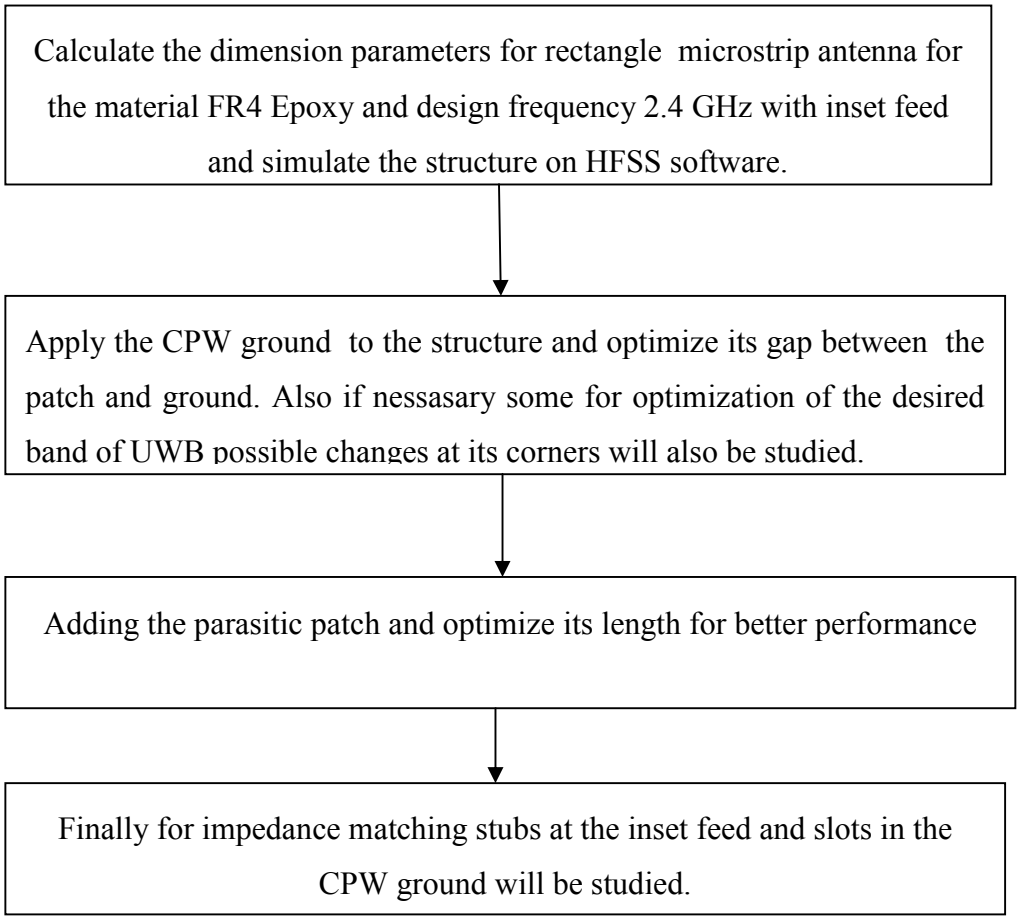

Methodical investigations have led to a new design (shown in Fig. 4.1). The proposed antenna structure consists of a coplanar ground with chamfered corners and the

unsymmetrical gap between patch and ground edges. A parasitic patch has been added for tuning the band rejection range. The structure has two unsymmetrical slots in the ground for enhancing the bandwidth as well as two unsymmetrical stubs along the feed line for impedance matching. FR4 has been selected as the substrate material. It has permittivity 4.4, loss tangent 0.001 and thickness 1.6 mm. Substrate size is 50×40 (L×W) mm^2. The width of the feed line, W_l, is 3 mm and the gap between the line and the CPW ground plane (g) is 0.5 mm.

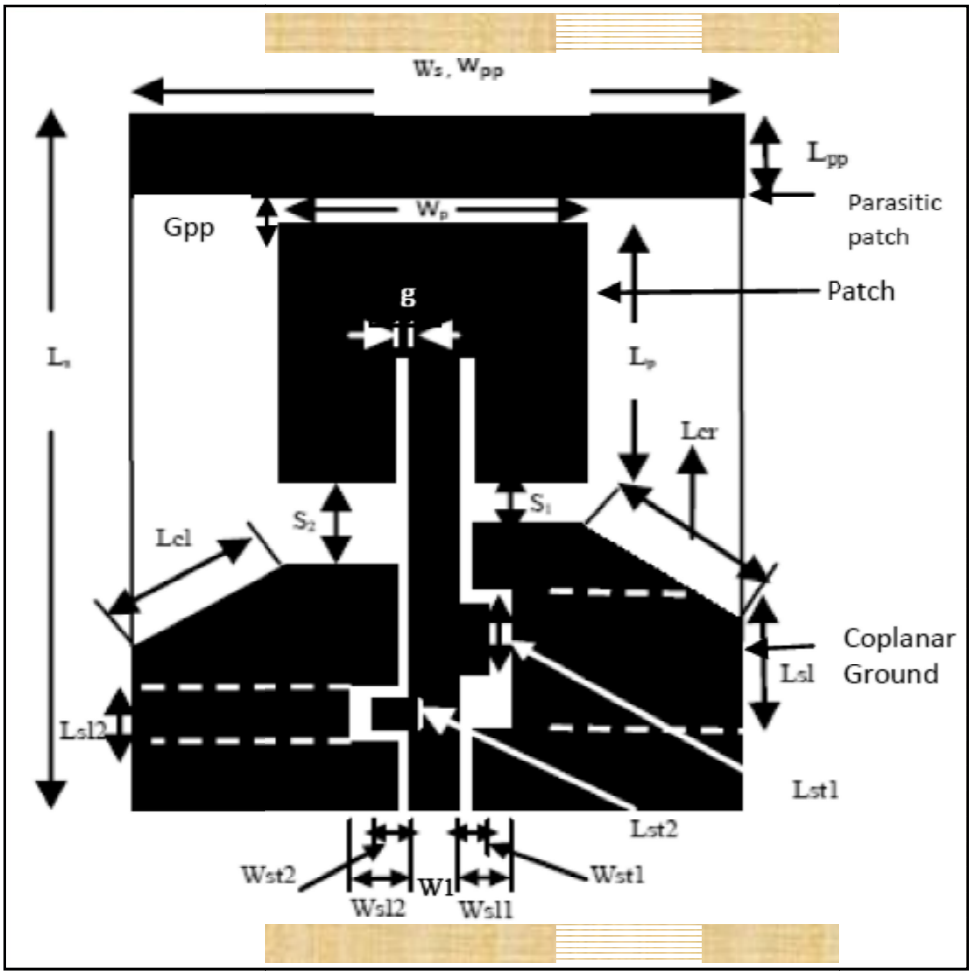

Fig. 4.1. Proposed coplanar waveguide fed monopole antenna structure.

The optimized parameters of the proposed antenna are: Lp=27 mm,Wp=38 mm, Ls=50 mm, Ws=40 mm, Wpp=40 mm, Lpp=5.4 mm,Gpp = 0.4 mm, S_1=3.2 mm, S_2=6.2 mm, Lcl=8.2 mm, Lcr=7.1mm, Lsl1=10 mm, Wsl1=3.3 mm, Lsl2=4 mm, Wsl2=4.3 mm, Lst1=5.4 mm,Wst1=1.5mm, Lst2=2.6 mm, Wst2=1.5 mm.

The design started with a rectangular patch with simple ground at the back side.The calculation of the dimensions of the patch is as shown below

The length of the patch is given by [10]

$$L_{eff} = L + 2\,\Delta L \tag{4.1}$$

where, L_{eff} = Effective length of the patch

and L = Length of the patch

The formula for Δ L is given by [10]

$$\frac{\Delta L}{h} = 0.412\frac{(\varepsilon_{reff} + 0.3)\left(\frac{W}{h} + 0.264\right)}{(\varepsilon_{reff} - 0.258)\left(\frac{W}{h} + 0.8\right)} \tag{4.2}$$

Where ε_{reff} is given by[10]

$$\varepsilon_{reff} = \frac{\varepsilon_r + 1}{2} + \frac{\varepsilon_r - 1}{2}\left(1 + 10\frac{h}{W}\right)^{-½} \tag{4.3}$$

The Width of the patch is given by [10]

$$W = \frac{\lambda_0}{2}\sqrt{\frac{2}{\varepsilon_r + 1}} \tag{4.4}$$

where, λ_0 = free space wavelength, if c = velocity of light in free space, 3×10^8 m/s and f = resonance frequency then put the value of λ_0 from the relation

$$\lambda_0 = \frac{c}{f} \tag{4.5}$$

From the equations from (4.1) – (4.5) for ε_r = 4.4 , f = 2.4 GHz, h = 1.6 mm patch dimensions are

L = 27mm , W= 38 mm

The simulation result for this dimension structure is shown in Fig. 4.2 with blue colored characteristics.

By studying the literature it is concluded that the CPW ground is the direct and easy solution to work on the UWB range frequencies. As our objective is to design an microstrip/monopole/slot antenna for the ranges GSM , ISM, UWB first we convert the design into the antenna with the CPW ground structure. And then optimize it for the UWB range with the coplanar ground. The dimensions of the CPW ground have been optimized . The width of ground plane has been varied from corner of dielectric to the feed line and length has been considered for the value which is adjusted to fulfill the condition of the gap between the patch and CPW ground (i.e. minimum $\lambda_0/2$). It has been observed that as we vary the width of CPW from the corner towards feedline the design starts showing wide band operation in UWB, GSM and ISM ranges with band rejection. The optimized dimensions result is shown in Fig. 4.2 in red colored characteristics.

Due to it's monopole structure simulation results showed a pass band from 0.94 GHz to 8.22 GHz with a band rejection from 2.82 GHz to 6.96 GHz as shown in Fig. 4.2.

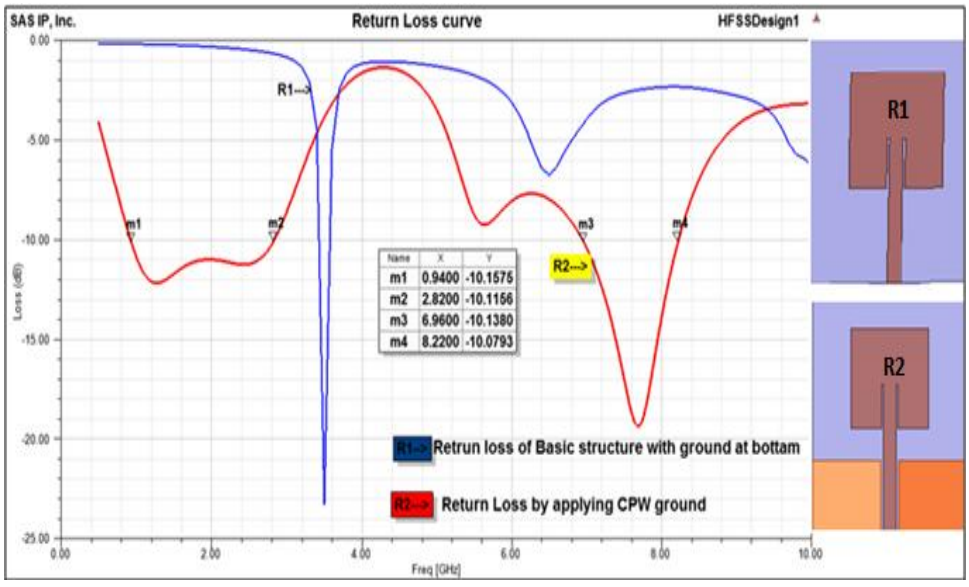

Fig. 4.2. Simulated return loss curves of basic structure with conventional ground and effect of applying CPW ground.

To improve the results, the gap between the patch and ground has been optimized and the corners of the ground plane have been chamfered. Cutting slots in the ground plane (on both the sides of the feed line) and optimization of various dimensions further improved the

results. A parasitic patch has been added in the design and optimized to tune the band of frequencies to be rejected [96]. This also increased the area for collecting the RFenergy.

4.4 Parametric Analysis

ANSYS HFSS version16 software has been used for analyzing the 3D structure. Initially a monopole structure with coplanar ground has been constructed for the resonant frequency (2.4 GHz). After that the parametric study has been applied at the four parts of the structure as mentioned in the next parts in 4.4.1, 4.4.2, 4.4.3 and 4.4.4.

4.4.1 Effect of the Gap Between the Patch and CPW Ground (S1, S2):

By keeping other parameters constant, S_1 and S_2 have been varied from 1 to 10 mm. The asymmetrical gap between the patch and the ground at the right and left side of line feed have shown a remarkable effect on the resonance characteristics of the antenna for Ultra wide band range.

It is well known that the gap between the patch and coplanar ground will be minimum $\lambda_0/2$ for good performance. So taking the gap between the CPW ground and Patch > $\lambda_0/2$ and then observed the variation in result by minimizing this gap approximately equal to $\lambda_0/2$ by parametric analysis. The observation is taken by keeping both sides of gap at the value > $\lambda_0/2$. Now keeping one side gap constant other is varied. by decreasing that gap will produce the widening of the band in UWB range with shifting of resonance frequency of UWB range from 6GHz -8 GHz towards 5.6 GHz- 8GHz and no considerable effect noticed on lower range of frequencies. Similarly keeping that side constant and varied first side will provide the same effect. The observation by variying the both gap simultaneously concluded that the gap between the patch and the CPW ground is important parameter to define the resonanace frequencies of UWB range and also helpful to widend the band in this range.To work on the UWB range the wideband operation may be optimized for the design frequency range with this type of operation i.e. controlling the gap between the patch and CPW ground.

The optimized curve for S_1 = 3.2 mm and S_2 = 6.2 mm has been marked as R3 in Fig. 4.3.

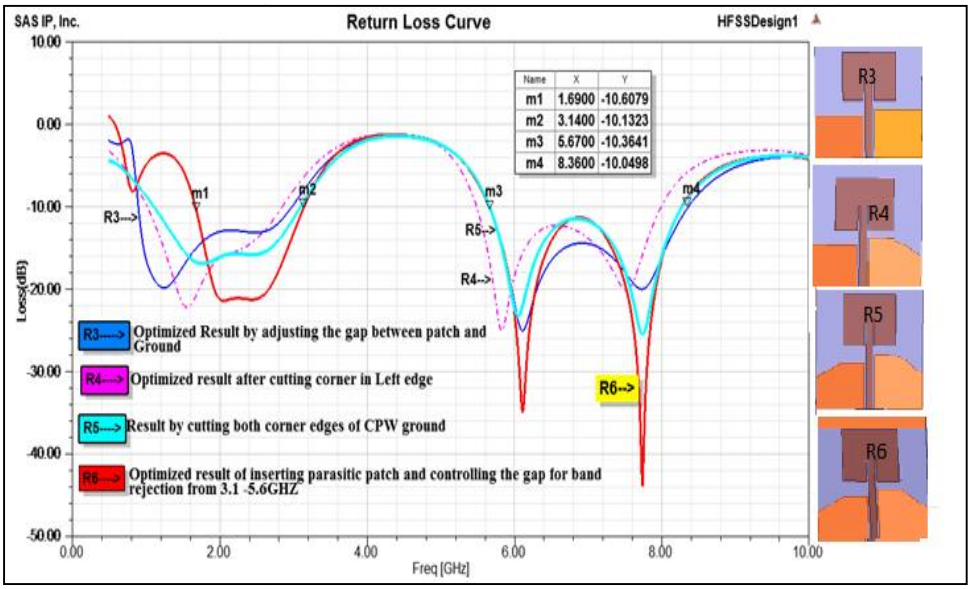

Fig. 4.3. Optimized simulated return loss curve for the CPW ground structure after chamfering and adding optimized parasitic patch structure.

4.4.2 Effect of Chamfering of the Corners of Ground (Lcl And Lcr) As Well As the Gap Between the Parasitic Patch and Resonant Patch:

The corners of the CPW ground have been chamfered .The cutting length (diagonal length) is Lcl = 8.2 mm and Lcr= 7.1 mm at which the maximum enhancement in the ISM band has been noticed (Fig. 4.3).

The chamfering at the corner of the optimized dimension of CPW ground is consider as the defected ground structure (DGS) of microstrip antenna. As we champher the corener by applying the parametric on the cutting length at corners of both side from 1 mm -10 mm the return loss increases for the band 900 MHz-3 GHz (GSM and ISM band)but after a certain value it has no effect on the characteristic. Because the gap between the patch and two sided CPW is asymmetrical so the value of the cutting length of the corner are also unequal. It has been concluded that by producing the defect at the corners of CPW ground the wide band operation with good return loss in GSM and ISM band may be produced.

The parasitic patch of optimized dimension is added to tune the required rejection band. According to the theory two resonant frequencies are separated according to the coupling between the two patches [96].

So controlling the gap between these two patches will control the range of frequencies which need to be rejected. In this section a parasitic patch above the resonating patch has been investigated. The demand of the structure is to maximize the capturing area for RF energy so the width of patch has been taken equal to the substrate width and the length of this parasitic patch has been varied from 1mm to 5mm. It is observed that as we increases the length of parasitic patch the rejected band shifted from left to right. At the length of parasitic patch Lpp = 5.4 mm the rejected band from 3.1 -5.6 GHz has been achieved.This is due to the change in the coupling ratio of these two patches.

The effect of varying Length (L_{pp}) of the Parasitic patch has been shown in Fig. 4.3. The variation in this parameter will change the gap between parasitic patch and resonant patch and will result in change in the band frequencies. By adjusting this gap (Gpp) between the resonant patch and this parasitic patch the desired range of rejection has been acheived. The parasitic patch is added for tunning the band reject range from 3.1 GHz-5.6 GHz.

4.4.3 Effect of Cutting Slots in the CPW Ground:

The effect of cutting slots of the dimensions (Lsl_1, Lsl_2, Wsl_1, and Wsl_2) in CPW ground edges is shown in Fig. 4.4.

These slots will change the path of current and will consequently enhance the bandwidth in ultra wide band range and lower range of frequencies. Observations concluded that the slot in left part of coplanar ground will effect the characteristic of the lower range of frequencies and slot in the right side of coplanar ground will effect the characteristic of ultra range of frequencies.The dimension and position of the slot is also important for the desired performance. As we move the slot in the coplanar far from the patch return loss increases. Parametric analysis has been applied for the slot dimensions and positions at both side of coplanar and optimized results has been noticed.

The optimized values Lsl_1=10 mm, Wsl_1=3.3 mm, Lsl_2=4 mm, Wsl_2=4.3 mm show the maximum enhancement in the ultra wideband range from 5.6 -8.3 GHz to 6.2 -10 GHz at the cost of some impedance mismatching.

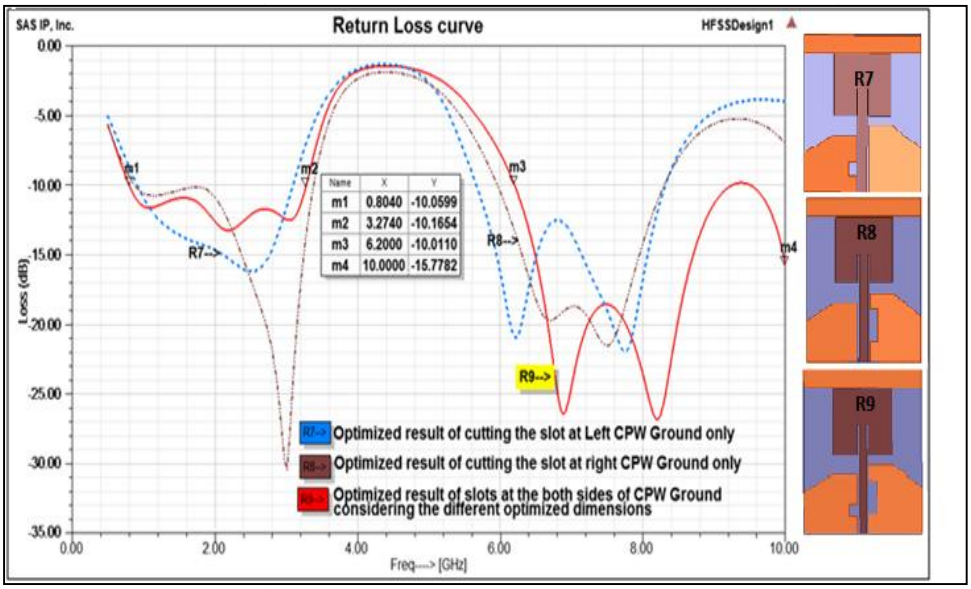

Fig. 4.4. Simulated return loss curve for optimized results by introducing slots in the CPW ground for enhancing the range of UWB.

4.4.4 Effect of Stubs in the Feedline for Impedance Matching:

Effect of adding stubs of the dimensions (Ls_{t1}, Ls_{t2}, Ws_{t1} and Ws_{t2}) to the Feed Line is shown in Fig. 4.5. ***To improve the impedance mismatching produced by the above optimized slots the stubs has added. As slots introduced the capacitive effect we can introduce the stubs with the feeding line to increase the inductive part to counter balance the impedance. The dimention and postion of stubs are optimized by applying the parametric.***

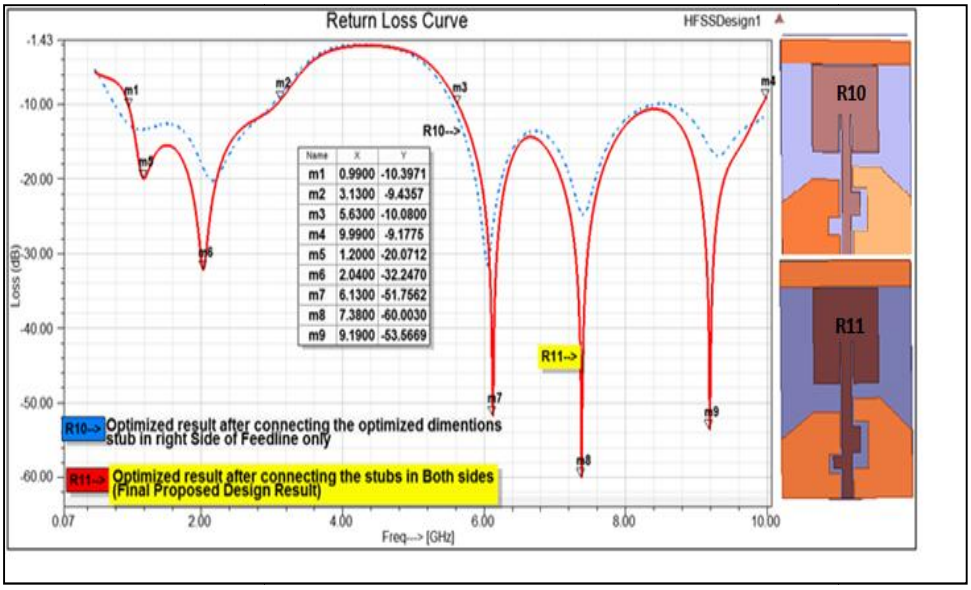

Fig. 4.5. Simulated return loss curve for the optimized result of connecting the stubs in the feed line.

The optimized dimensions of stubs Ls_{t1}=5.4 mm, Ws_{t1}=1.5mm, Ls_{t2}=2.6 mm, Ws_{t2}=1.5 mm show the desired result in the ultra wide band range i.e. from 5.6 - 9.9 GHz with good return loss values.The return loss curve and VSWR curve for the optimized final new design is shown in Fig. 4.6(a) and 4.6(b).

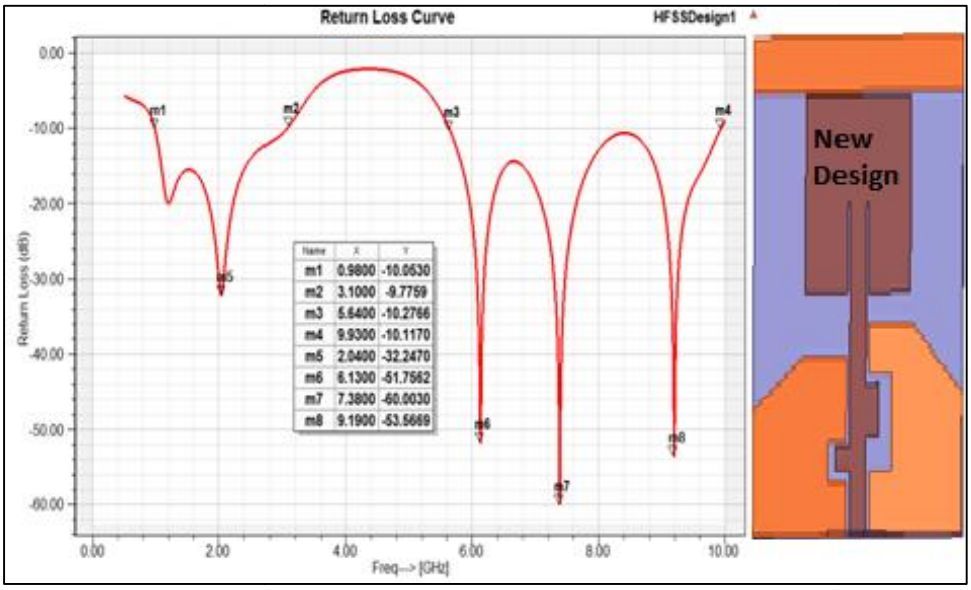

(a)

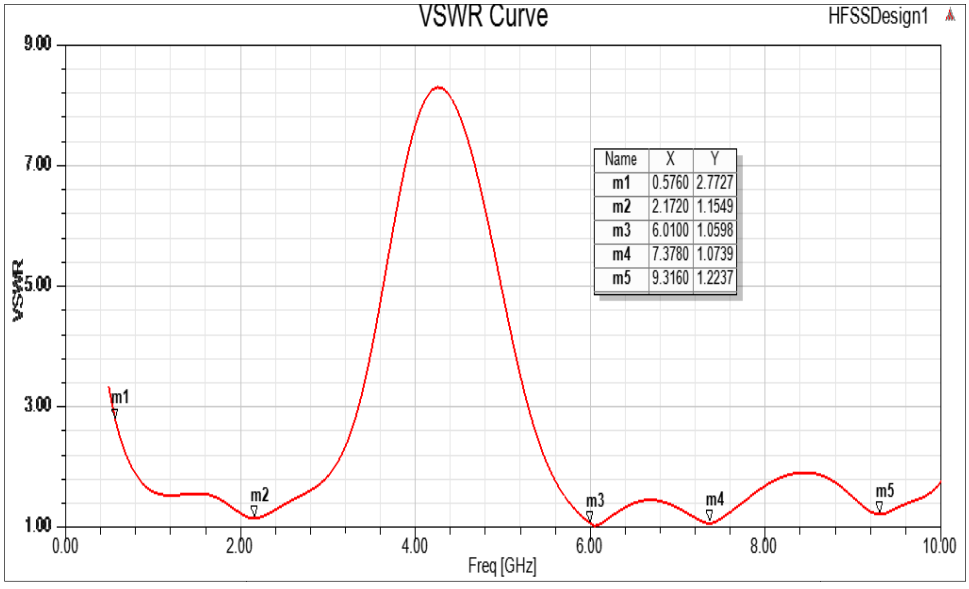

(a)

(b)

Fig. 4.6. (a) Simulation result for S_{11} of the new design (b) Simulation result of VSWR for the new design.

As shown in the Fig. 4.6(a) the new proposed design is resonant from 900 MHz-9.9 GHz with the band reject form 3.1 GHz-5.6 GHz (WLAN & HIPER LAN). This band has been rejected because this provides only interference for the RF energy harvesting application.

4.5 Experimental Verification

For experimental verification of the results, the new design structure has been fabricated. It is shown in Fig. 4.7. Simulation of the proposed design showed maximum gain of 7 dBi at resonant frequency 7.2 GHz, impedance matching of the desirable frequencies and rejection of the unwanted band. Measurements of fabricated antenna have proven the predictions.

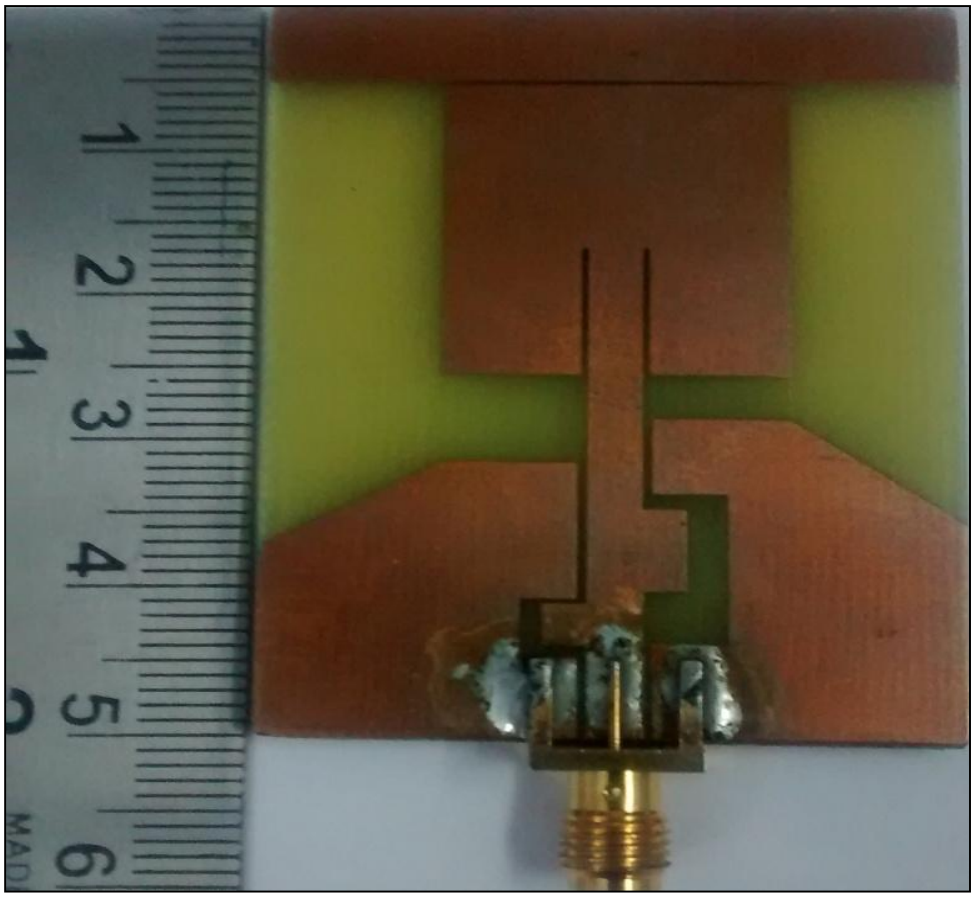

Fig. 4.7. Photograph of fabricated antenna.

4.5.1 Measurement of Return Loss

As shown in Fig. 4.6 (simulated results) and Fig. 4.8 (measured results) the measured results match the simulated results. These results indicate that the proposed monopole antenna works

on multiple bands of frequencies from 900 MHz-9.9 GHz and also rejects band from 3.1 GHz to 5.6 GHz.

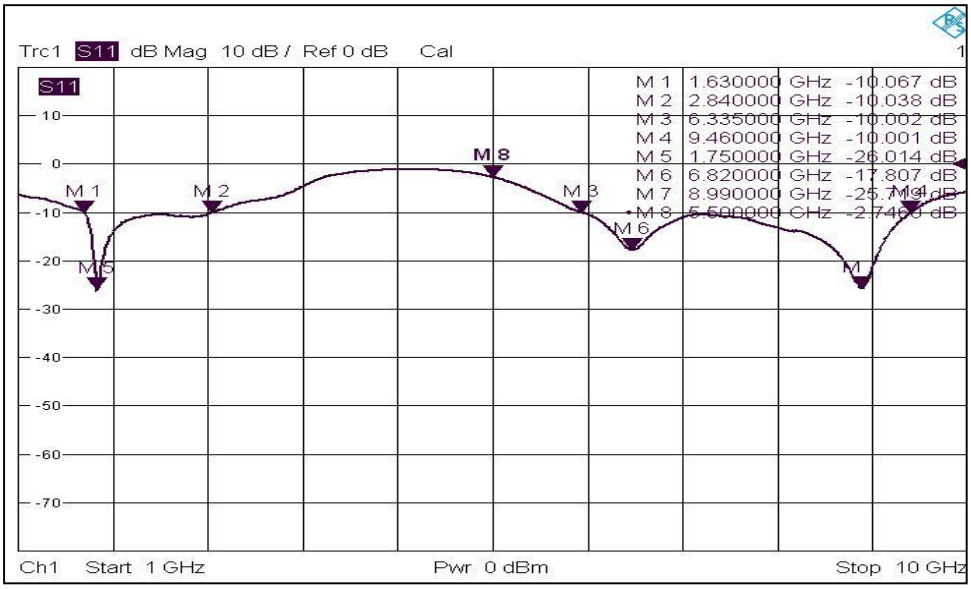

(a)

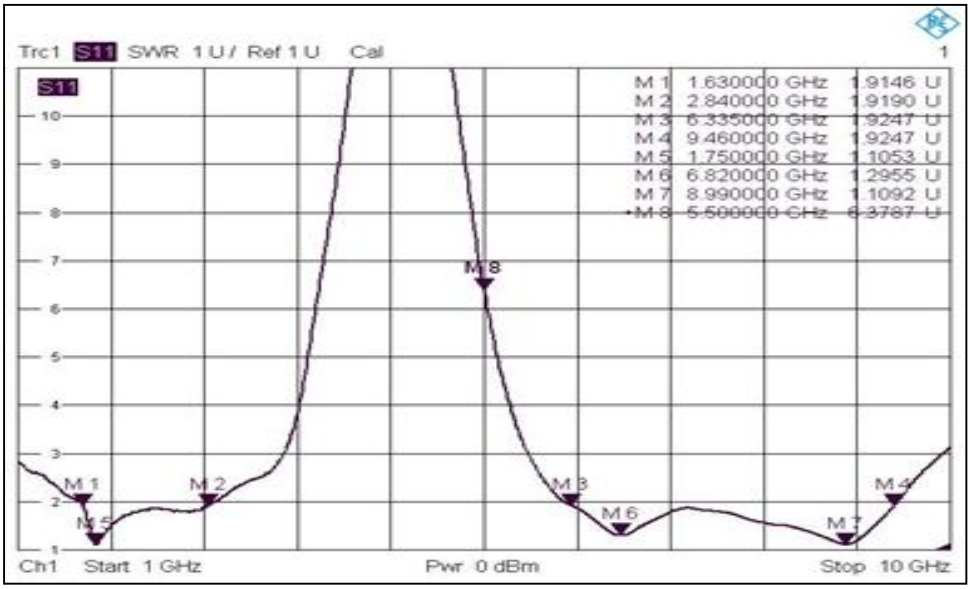

(b)

Fig. 4.8. (a) Measured results of S_{11} parameter of the proposed design. (b) Measured results of VSWR parameter of the proposed design

4.5.2 Measured Radiation Patterns (E-plane & H-plane)

For the fabricated antenna, measured radiation patterns E- Plane & H- Plane have been shown in Fig. 4.9 {(a) –(e)} for resonant frequencies 900 MHz, 2.4 GHz, 6.1 GHz ,7.03GHz and 9.1 GHz. One result of rejected band frequency has also shown in Fig. 4.9 (f) for comparison .The measurement were possible only at the International centre for radio science (ICRS) lab at Jodhpur , Rajasthan, INDIA under the guidance of Dr. O. P. Calla sir.

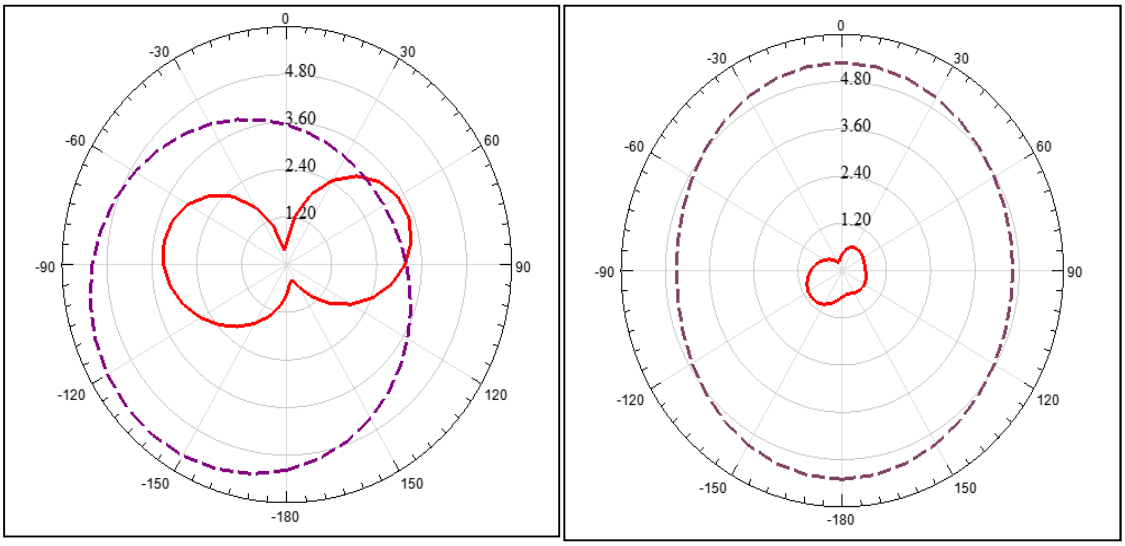

(a) (b)

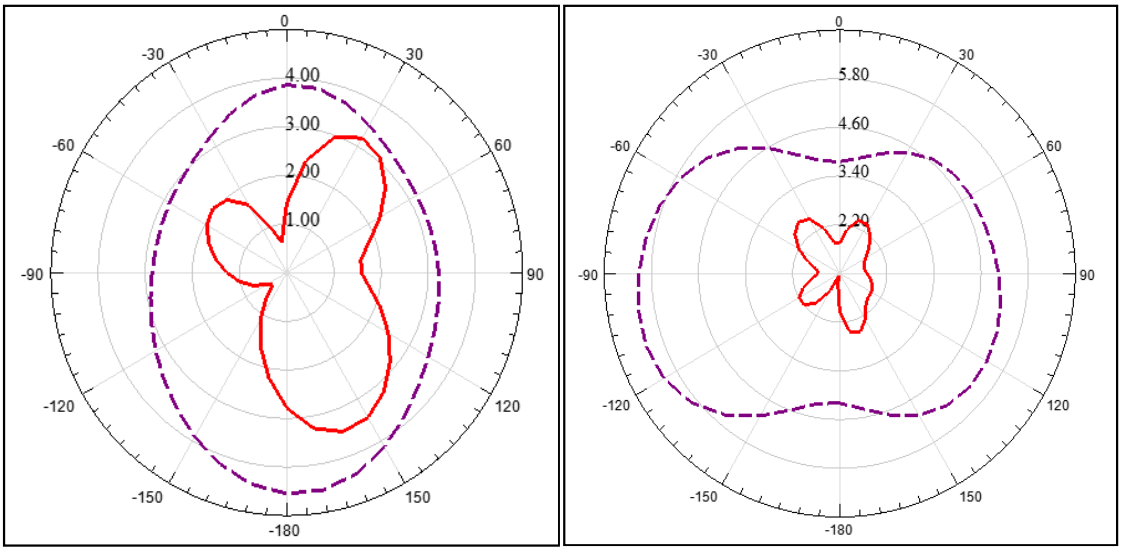

(c) (d)

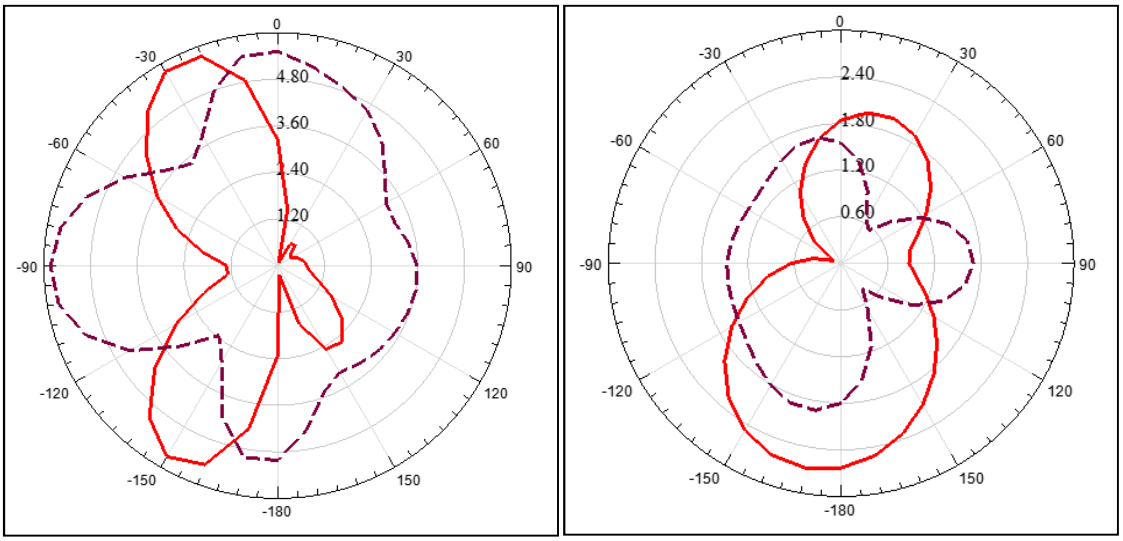

Fig. 4.9. Measured radiation pattern (H-plane & E plane) at Φ= 90o for frequencies (a) 900 MHz (b) 2.4 GHz, (c) 6.1GHz (d) 7.03 GHz (e) 9.1 GHz (f) 5 GHz (one of the rejected band frequency)

These patterns are shown as sample measured patterns for the proposed design because it is not possible to show all the results. The sample patterns indicate that the antenna has omni directional characteristics.

4.5.3 Current Distribution

The current distribution for only one resonant frequency (2.4 GHz) is shown here in Fig. 4.10. It indicates that at the resonant frequency surface current flows at the radiators edges only.

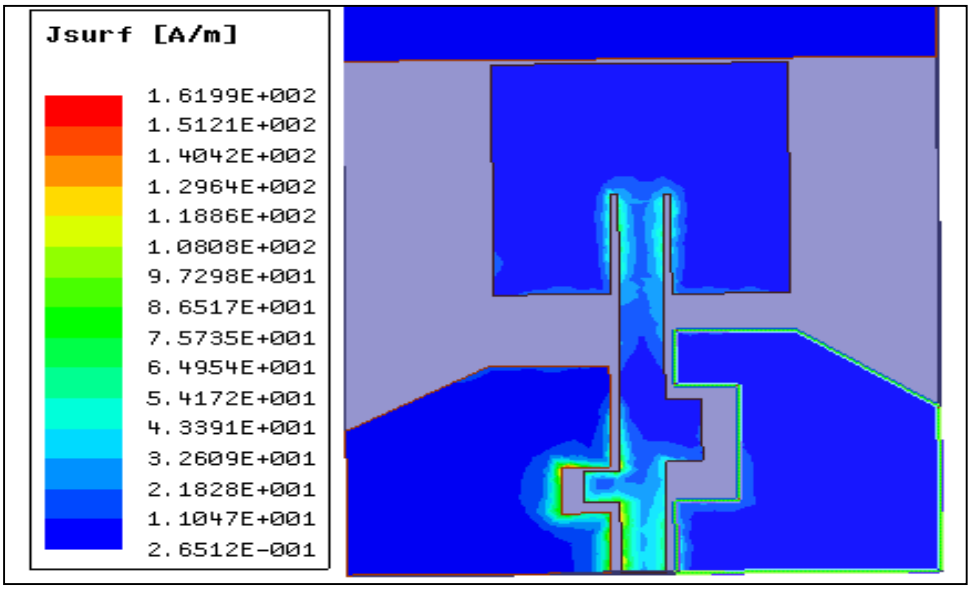

Fig. 4.10. Simulation result of new design for current distribution at one of the resonant frequency 2.4GHz.

4.5.4 Gain and Radiation Efficiency

The result of total gain has been plotted.The proposed antenna has shown the maximum gain of 7 dBi at 7.2 GHz and from 2dBi to 4 dBi for other resonant frequencies. Radiation efficiency of the structure is 70.2 % maximum.

4.6 Some Possible Array Arrangements of the Proposed Coplanar Monopole Antenna

The above presented monopole antenna is good for the energy harvesting purposes as it works for wide range of band from 900 MHz – 9.9GHz with good radiation characteristics . It also rejects the WLAN band from 3.1 GHz – 5.6 GHz. It is known that for RF-DC converter circuit the DC output value is propotional to the available magnitude of AC at the input port of this circuit. And this AC voltage is dependent on the capturing RF power from the receiving antenna . As the input AC power increases DC voltage at output increases.

Different array arrangements of the design have been studied for this purpose.The spectrum range for the operation of array structure considered here is from 900 MHz -10 GHz. The rejection of WLAN band (3.1 -5.6 GHz) is not considered here. The only arrangements having the gap of $\lambda_0/2$ between the two or four antenna structure (horizontally and vertically) have been reported in this thesis. For this particular gap the structures show

the resonance for multi frequencies (not the wide band) in this range. With these array arrangements, the gain and radiation efficiency increase at the cost of its wide band operation.

Four types of array struectures have been designed and their characteristics has compared and discussed in next section of this chapter.

To combine the power of more than one antenna Wilkinson power combiner has been used in this work . The advantages of using this combiner are listed below:

1. The impedance matching of two or more antennas are easy . Any value of impedance may be matched eaisly by inserting the resistor at the combining branch of the combiner.
2. The Line feed is directly connected to the ports of the combiner without disturbing the design of antenna.
3. The losses are comparatively less than other types of combiners.

4.6.1 An Array Structure of 2×1 (Vertically Connected) Compact Coplanar Monopole Antenna with Wilkinson Power Combiner

The array of two single coplanar monopole antenna connected front to front (2×1) is shown in Fig. 4.11. The simulated return loss characteristics (S_{11}) is shown in Fig. 4.12. As shown in Fig. 4.12 the structure has been resonant at the frequencies 900 MHz, 1.6 GHz, 2.4 GHz, 3.8 GHz, 5 GHz and 7.8 GHz. These resonance frequencies have covered the GSM, ISM, WLAN and UWB ranges.The fabricated antenna is shown in Fig. 4.13 (a) and its measured result of return loss characteristic is shown in Fig. 4.13(b) . The measurement was taken by the VNA of the range 10MHz- 14 GHz of keysight technologies .

The VSWR curve has been shown in Fig. 4.14. As shown in Fig. 4.14 the refelction coefficient is less than 2 for these particular frequencies. In study of array arrangement of the design we have shown the characteristics of simulated results in all respect but the measurement of return loss was taken only for validation purpose.

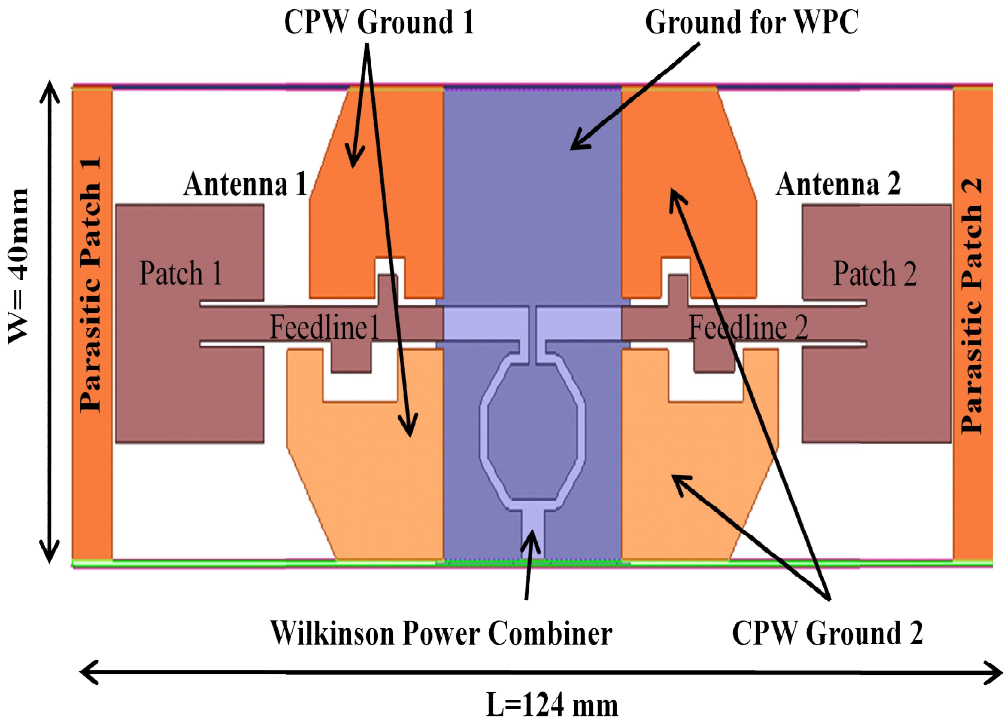

Fig. 4.11. Simulated structure of 2×1 array of design (vertically connected)

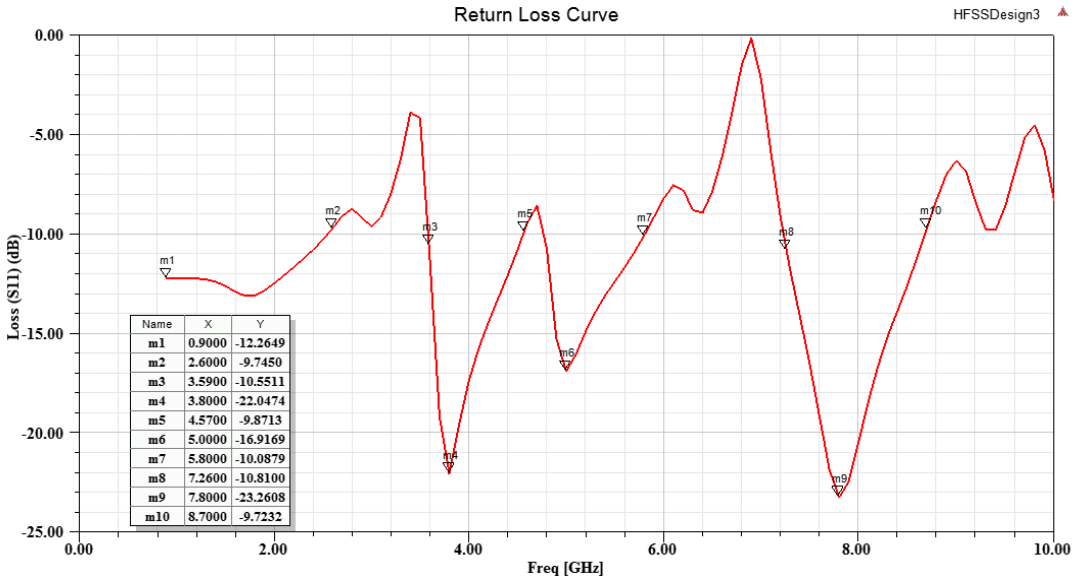

Fig. 4.12. Simulated return loss (S11) curve for 2×1 array of design (vertically connected).

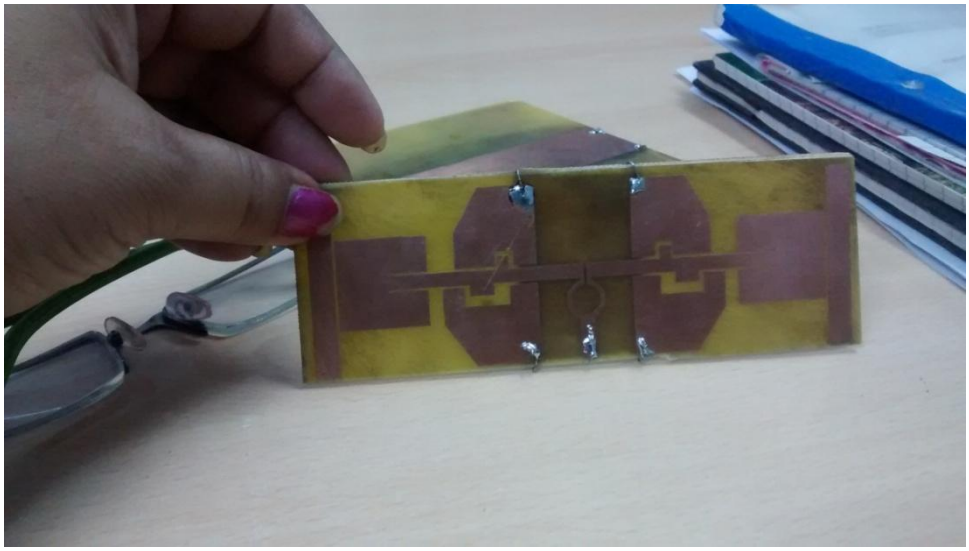

(a)

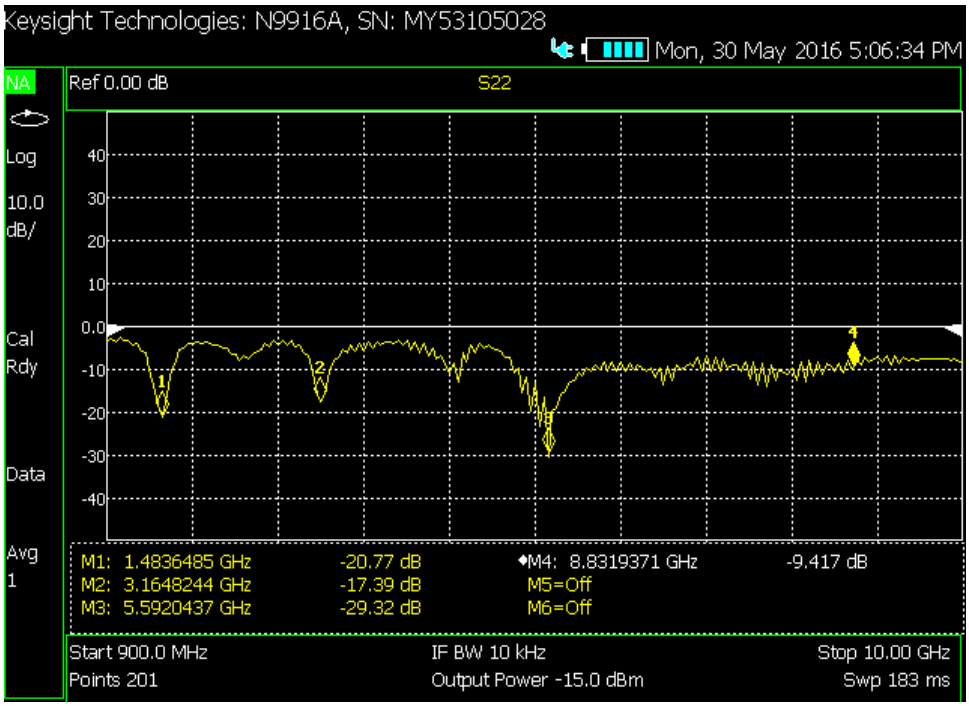

(b)

Fig. 4.13. (a) Fabricated design (b) Measured return loss (S_{11}) curve for 2×1 array of design (vertically connected)

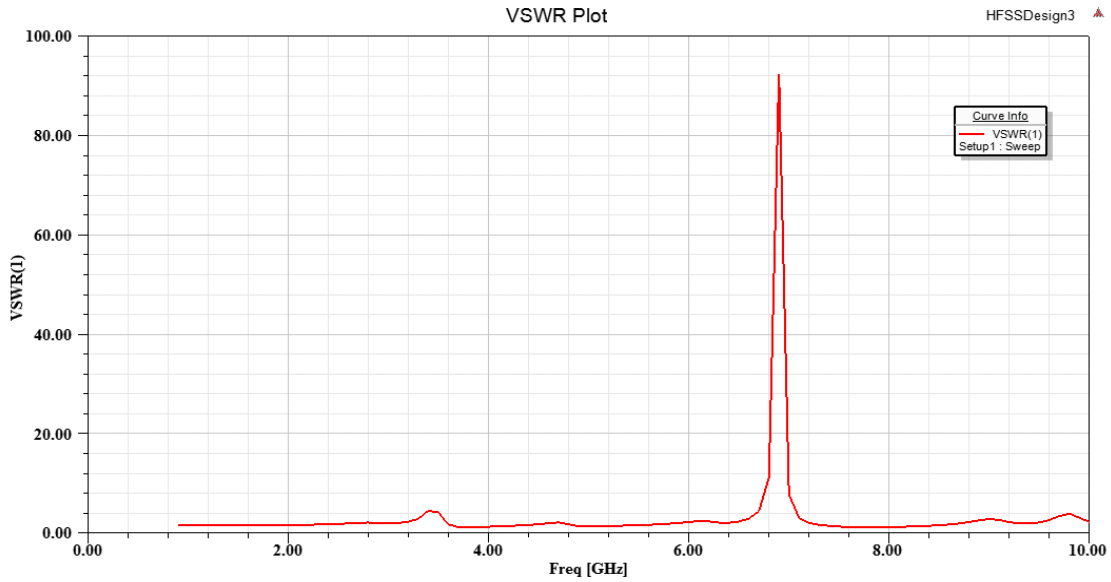

Fig. 4.14. Simulated VSWR curve of 2×1 array of design (vertically connected)

The gain –frequency curve has been shown in Fig. 4.15. As shown in the figure the gain has increased maximum 24.6 dB for the frequency 900 MHz. The structure did not provide the gain for the range WLAN and UWB. So this arrangement is very useful for the operation in GSM and ISM ranges.

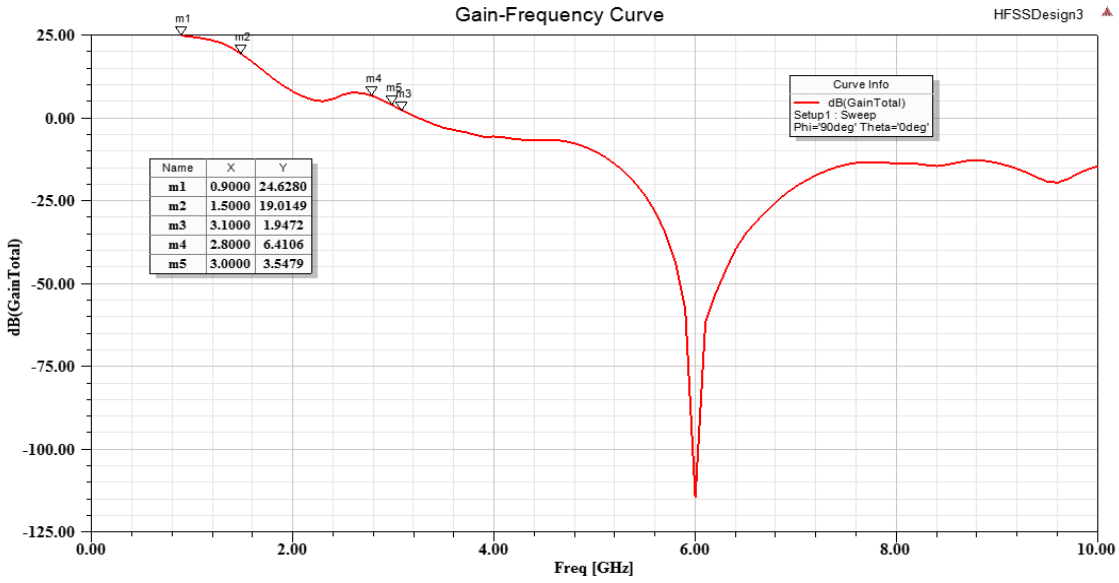

Fig. 4.15 Simulated Gain of the structure of 2×1 array of design (vertically connected)

The peak realized gain for this array arrangement is shown in Fig. 4.16(a). It shows that for all the frequencies the structure has 51.7 magnitude of realized gain. In Fig. 4.16(b) the radiation efficiency for $\phi = 90^{o}$ and $\theta = 0^{o}$ is 71.4.

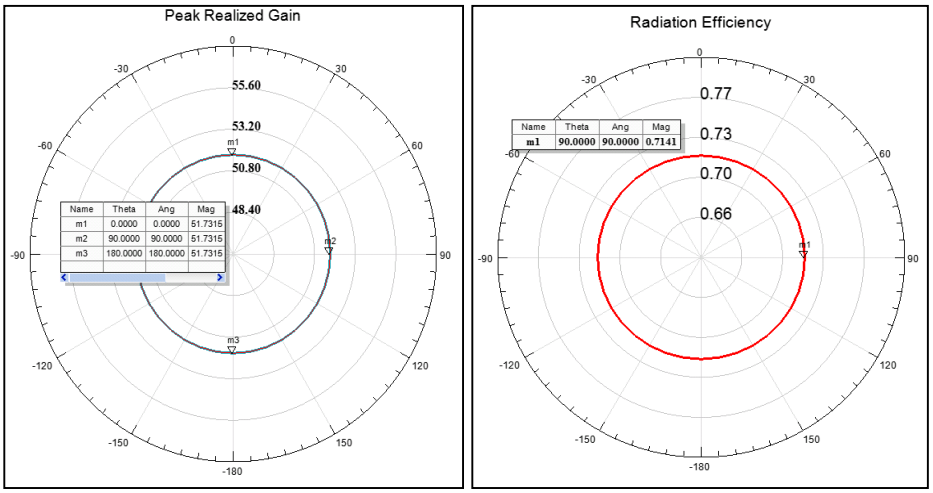

(a) **(b)**

Fig. 4.16. (a) Simulated realized peak gain and (b) radiation efficiency of the structure of 2×1 array of design (vertically connected)

The radiation efficiency is surprisingly high for the GSM and ISM ranges. It is satisfactory for all other ranges.The radiation efficiency is 71.4 for $\Phi=90^{o}$ and $\theta=0^{o}$.The H-field and E-Field patterns are shown in Fig. 4.17 (a) and (b). As shown in fig. (a) the array arrangement is circularly polarized and Fig. 4.17 (b) indicated that the array of the antenna has the magnitude of electric field intensity of maximum 64 mV/m^2.

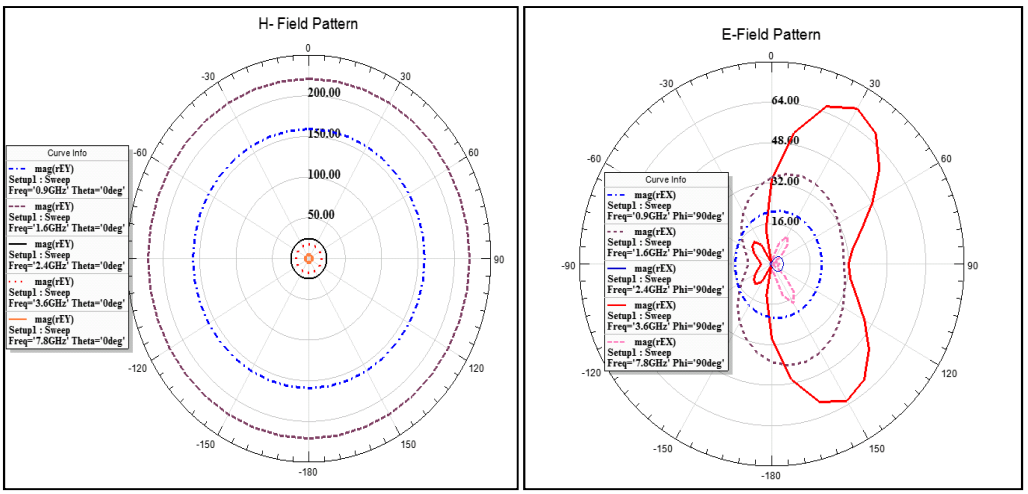

(a) (b)

Fig. 4.17. Field patterns of the structure of 2×1 array of design (vertically connected) (a) H-field (b) E- field

The current distribution is shown in Fig. 4.18. As shown in the figure the current flows maximum at the corners of surfaces.

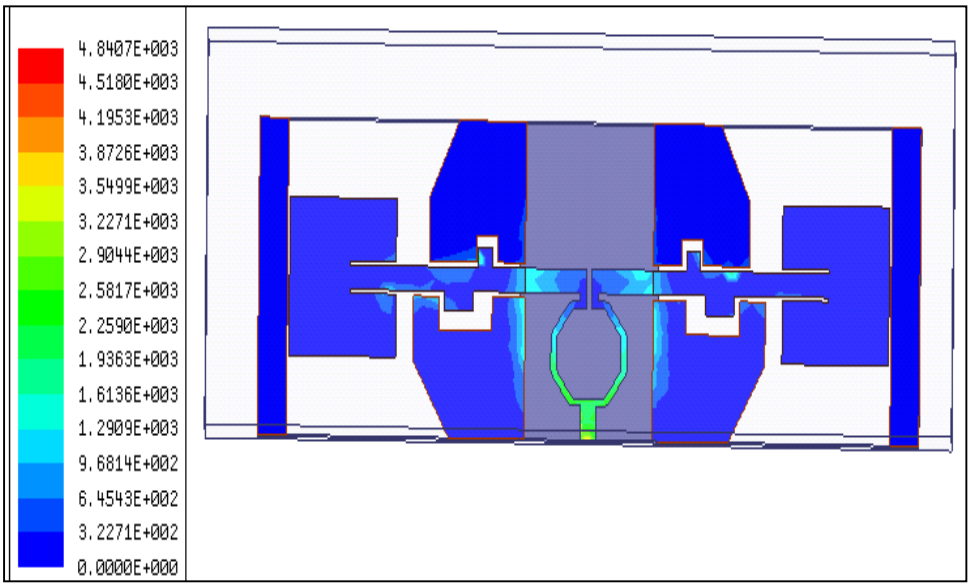

Fig. 4.18. Current distribution of the structure of 2×1 array of design (vertically connected)

4.6.2 An Array Structure of 2×1 (Horizontally Connected) Compact Coplanar Monopole Antenna with Wilkinson Power Combiner

The array of 2×1 horizontally connected coplanar antenna is shown in Fig. 4.19. The gap between the antenna is the same λg/2. The power is combined by same Wilkinson power combiner. The simulated result is shown in Fig. 4.20. As shown in Fig. 4.20 the range of resonance frequencies is the same as with vertically connected array , the only addition of one extra resonant frequency range from 9.1- 9.6 GHz. The measured return loss graph is shown in Fig. 4.21.

The VSWR curve is shown in Fig. 4.22. As shown in Fig. 4.22 the value of the VSWR is less than 2 for the range of resonant frequencies.

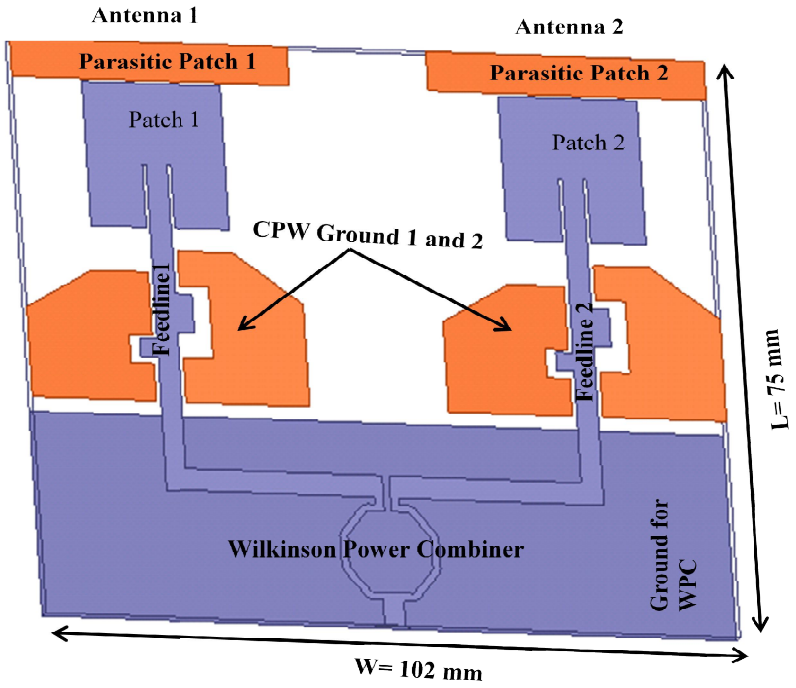

Fig. 4.19. Simulated structure of 2×1 array of design (Horizontally connected)

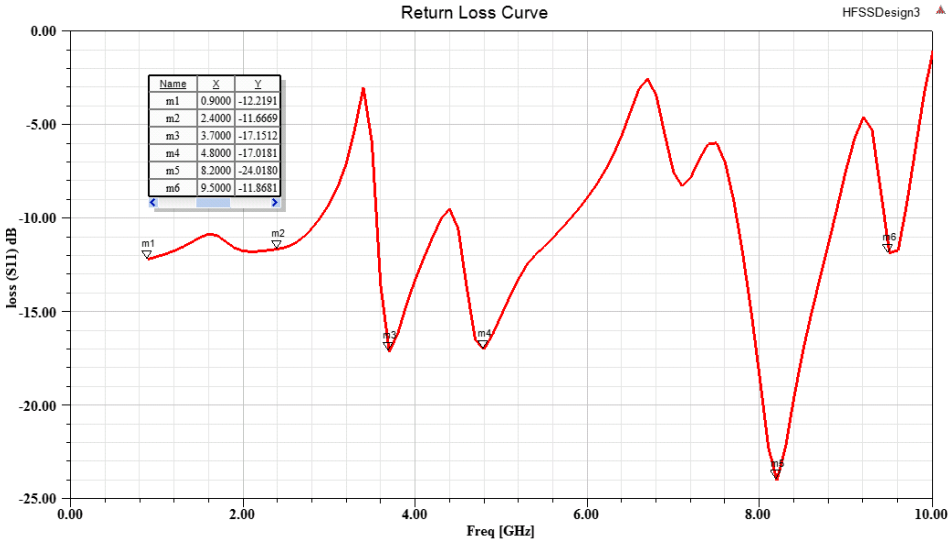

Fig. 4.20. Simulated result of return loss of the structure of 2×1 array of design (Horizontally connected)

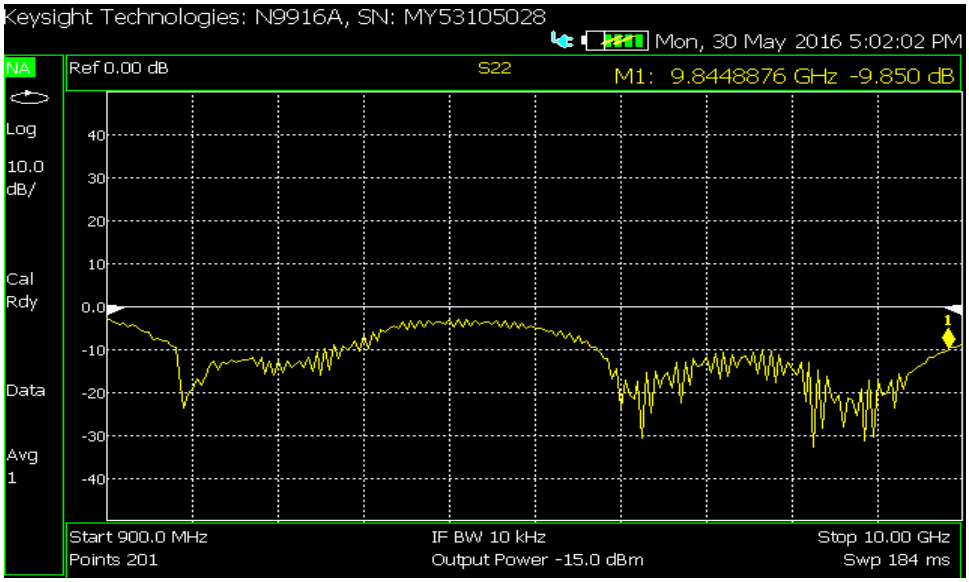

Fig. 4.21. Measured result of return loss of the structure of 2×1 array of design (Horizontally connected)

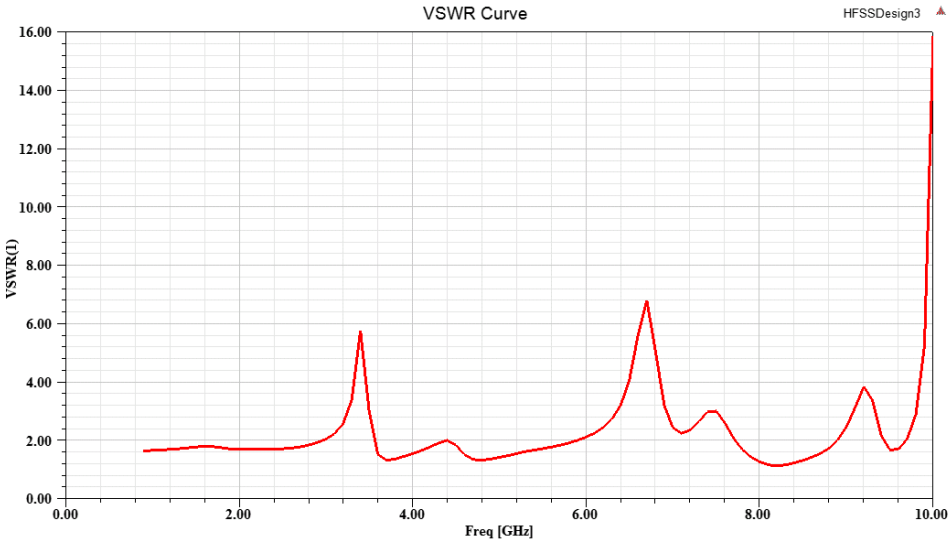

Fig. 4.22. VSWR curve of the structure of 2×1 array of design (Horizontally connected)

The gain-frequency curve of the structure is shown in Fig. 4.23. As shown in the figure the gain is positive with the maximum range of 22.6 dB in the lower range of frequencies. The gain is negative for the UWB range of frequencies.

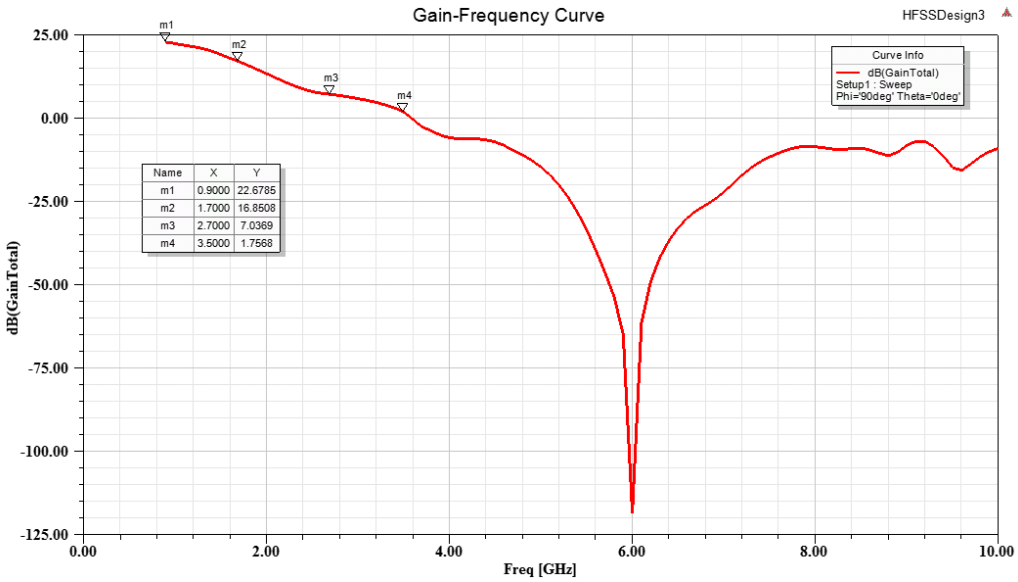

Fig. 4.23. Gain- frequency curve of the structure of 2×1 array of design (Horizontally connected)

The peak realized gain and radiation efficiency for far field region is shown in Fig. 4.24 (a) and (b) respectively. As shown in the figure the peak realized gain has decreased from 51.7 to 38.53 for this arrangement but the radiation efficiency is increased from 71% to 82.1%.

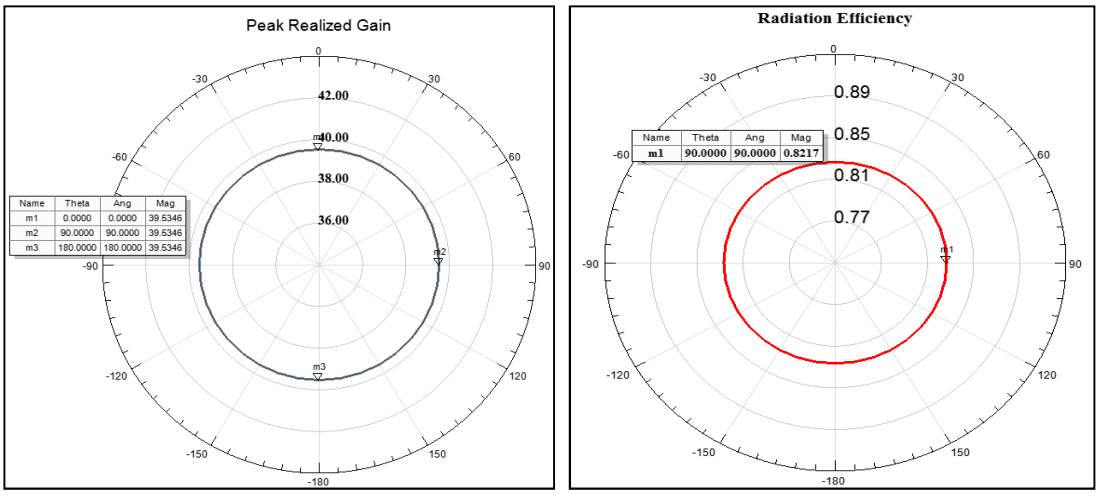

(a) (b)

Fig. 4.24. (a) Peak Realized gain and (b) Radiation efficiency of the structure of 2×1 array of design (Horizontally connected)

The H- field and E-field pattern for the structure for the same resonance frequency is as shown in Fig. 4.25 (a) and (b). As shown in figure the sturucture is circularly polarized for the frequency 900 MHz. The E-field pattern shows that the radiation intensity is maximum 40 mV/m^2.

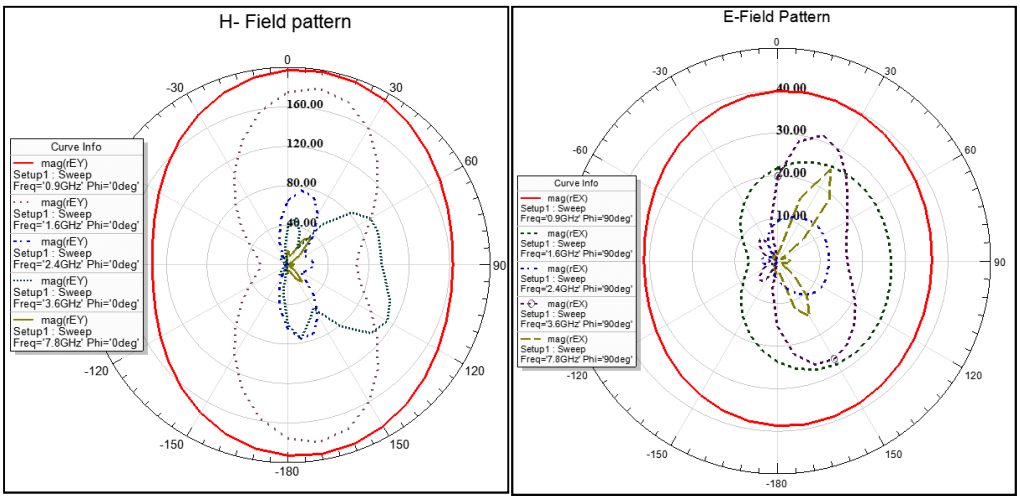

(a) (b)

Fig. 4.25. (a) H- Field and (b) E-Field pattern of the structure of 2×1 array of design (Horizontally connected)

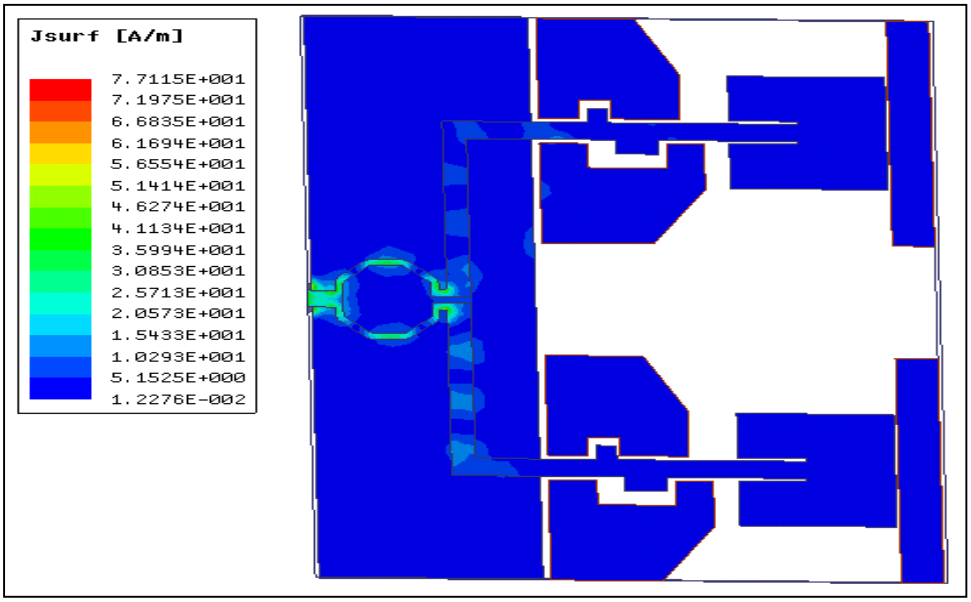

Fig. 4.26. Current Distribution of the structure of the 2×1 array of design (Horizontally connected).

The current distribution of the structure is as shown in above Fig. 4.26. the current is circulate to the whole structure's outer surface.

4.6.3 An Array Structure of 2×2 Compact Coplanar Monopole Antenna with Wilkinson Power Combiner

The 2×2 array arrangement of the coplanar monopole antenna is shown as in Fig. 4.27 . This arrangement is the combination of vertically and horizontally 2×1 array arrangement. The simulated return loss curve of the structure is shown in Fig. 4.28. As shown in figure the structure is resonant at multiple frequencies (but does not shows the wideband operation) from 900 MHz-10 GHz.

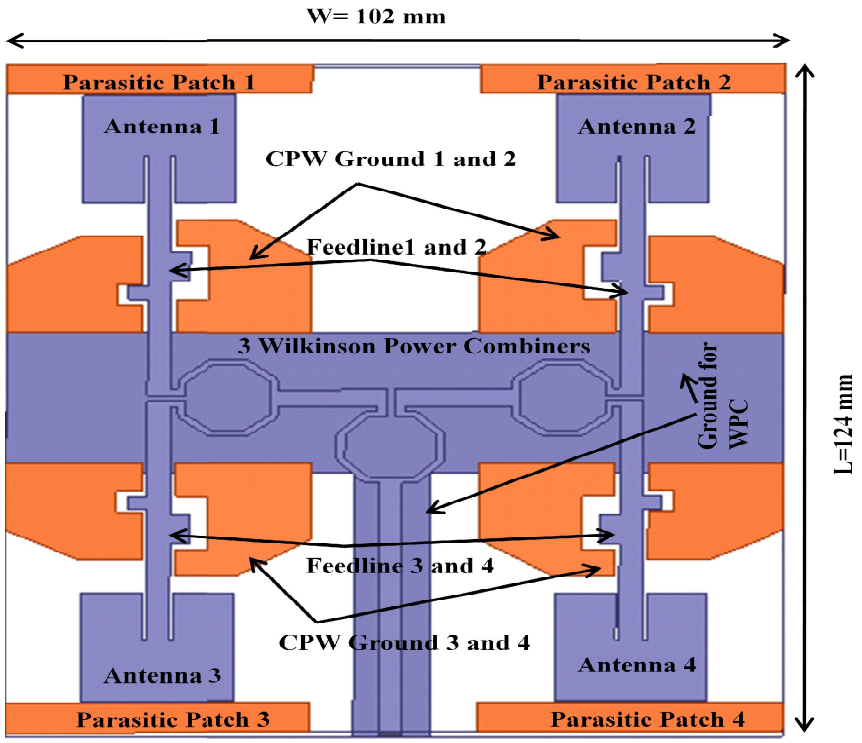

Fig. 4.27. Structure of 2×2 array of the design of the coplanar monopole antenna from the Simulator.

The fabricated structure of this design is shown in Fig. 4.29 (a) and its measured result of return loss is shown in Fig. 4.29 (b).

As shown in Fig (4.29)(b) the measured results are nearly equal to the simulation results, this validates the array arrangement of the structure.

The VSWR curve is shown in Fig. 4.30 . It is noticed in the curve that the value of VSWR is less than 2 for all the resonant frequencies and it is more than 2 for all other frequencies.

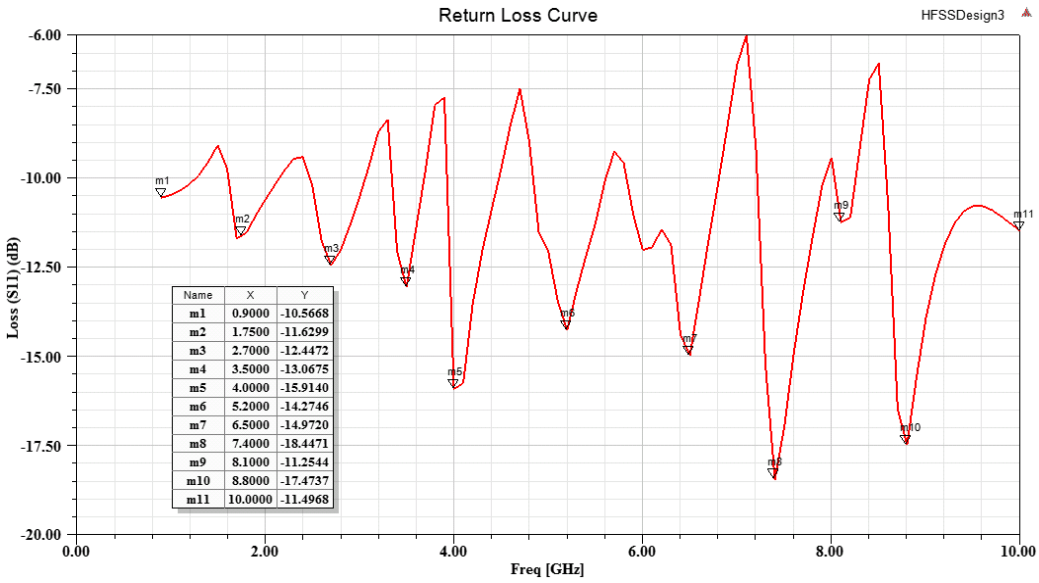

Fig. 4.28. Simulation result of the 2×2 array of the design of the coplanar monopole antenna.

Later on we will discuss that this structure has comparatively high efficiency and gain. It also have the capturing area of receiving the EM waves that is why this design is most suitable for RF energy harvesting purposes.

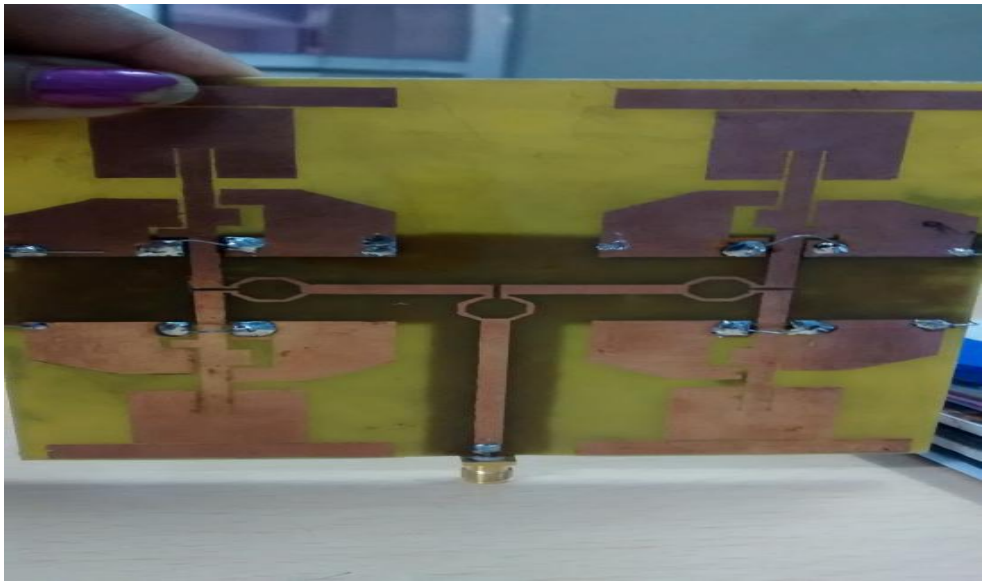

(a)

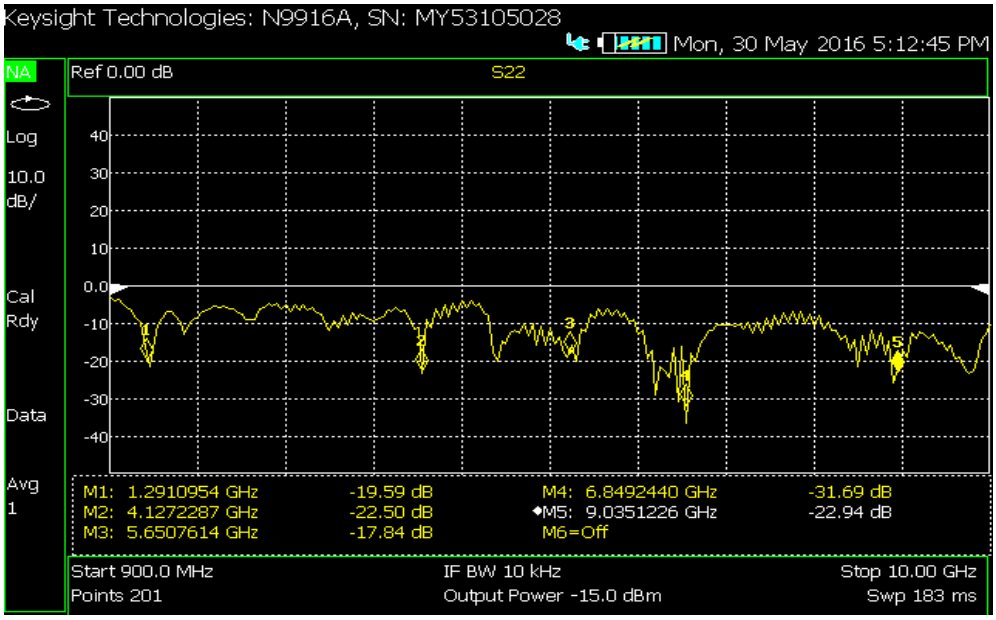

(b)

Fig. 4.29. (a) Fabicated design and (b) measured result of the 2×2 array of the design of the coplanar monopole antenna.

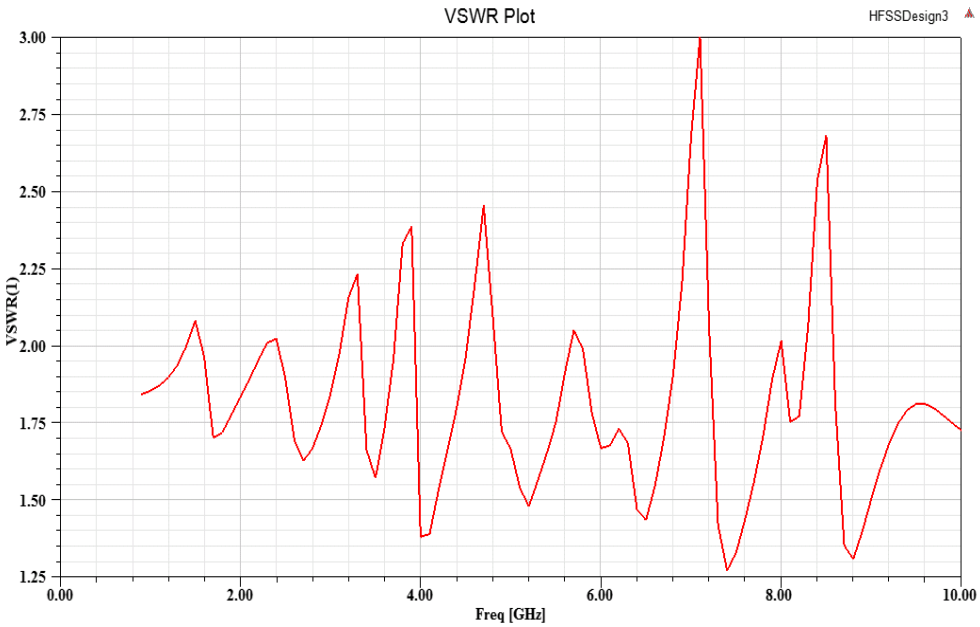

Fig. 4.30. VSWR curve of the 2×2 array of the design of the coplanar monopole antenna.

The gain -frequency curve for the 2×2 array of structure is shown in Fig. 4.31. As shown in fig. the gain is positive for the lower range of frequencies with the maximum value 13.3dB.

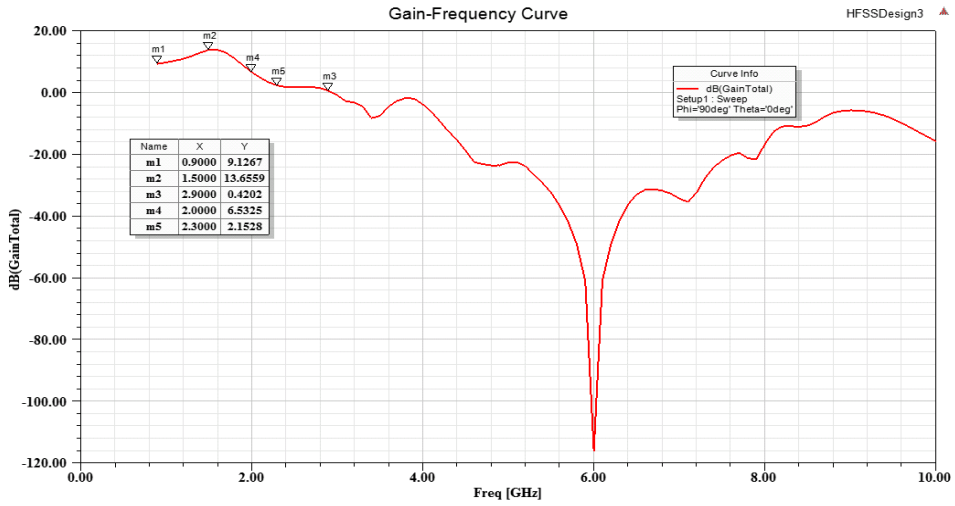

Fig. 4.31. Gain – frequency curve of the 2×2 array of the design of the coplanar monopole antenna.

The peak realized gain for this structure is 53.8 as shown in Fig. 4.32 (a) which is greater than that for both the reported structures 2×1 vertically and horizontally connected array. The radiation efficiency of the structure is 80.7%.

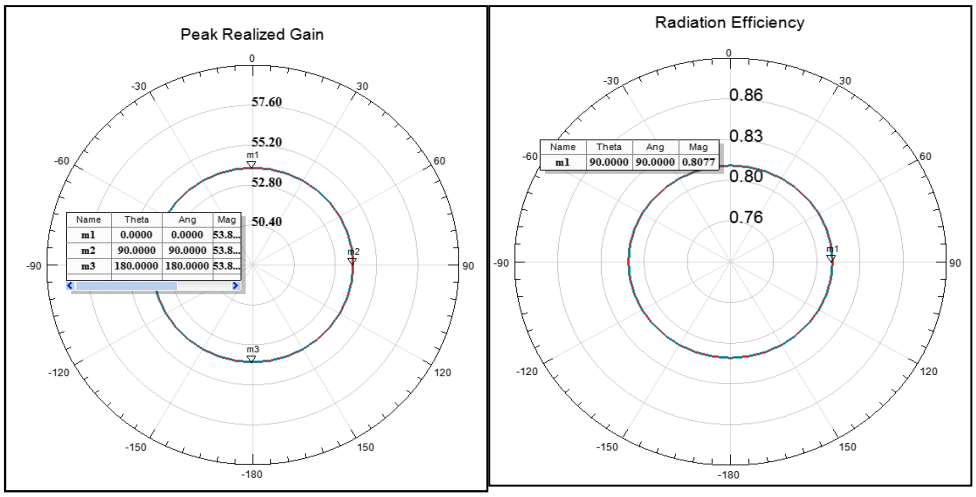

(a) (b)

Fig. 4.32 (a) Peak Realized gain and (b) Radiation efficiency of the 2×2 array of the design of the coplanar monopole antenna.

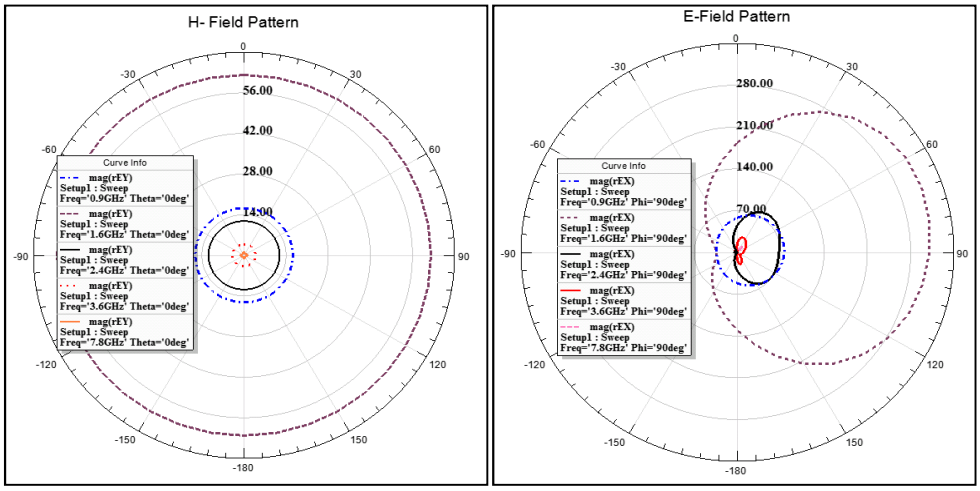

(a) (b)

Fig. 4.33. (a) H- Field Pattern (b) E- field pattern of the 2 ×2 array of the design of the coplanar monopole antenna.

In above Fig. 4.33(a) the H- field pattern shows that the antenna is circularly polarized and in Fig. 4.33(b) the radiation intensity is maximum 210 mv/m^2 for 900 MHz frequency. The current distribution of the structure is shown in Fig. 4.34.

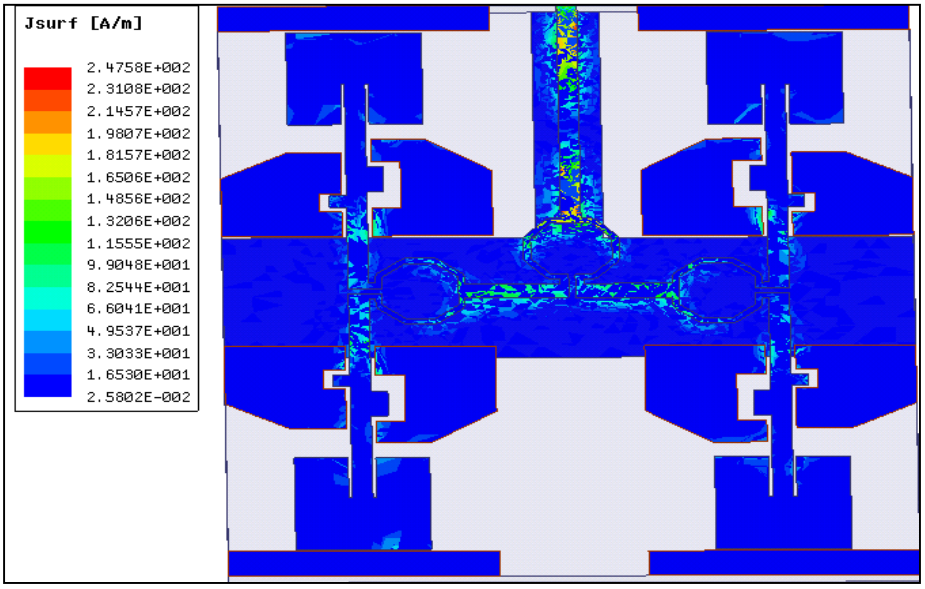

Fig. 4.34. Current distribution of the 2×2 array of the design of the coplanar monopole antenna.

4.6.4 The Stacking of Two Single Structure (Back To Back) of Compact Coplanar Monopole Antenna

The Stacking of the two single antenna connected back to back is also studied in this concern. The results were surprisingly very good as shown in figures later on . The one more important application of this stacking arrangement is that we can connect these module in parallel and after that connect the RF-DC converter circuit at its output. We could find the increased value of DC output. The satcking arrangement on the simulator is as shown in Fig. 4.35.

Due to stacking of the antennas the S_{11}, S_{22}, S_{12} and S_{21} parameters are studied .The simulation results for these parameters are as shown in Fig.'s 4.36, 4.37, 4.38, 4.39 correspondingly.

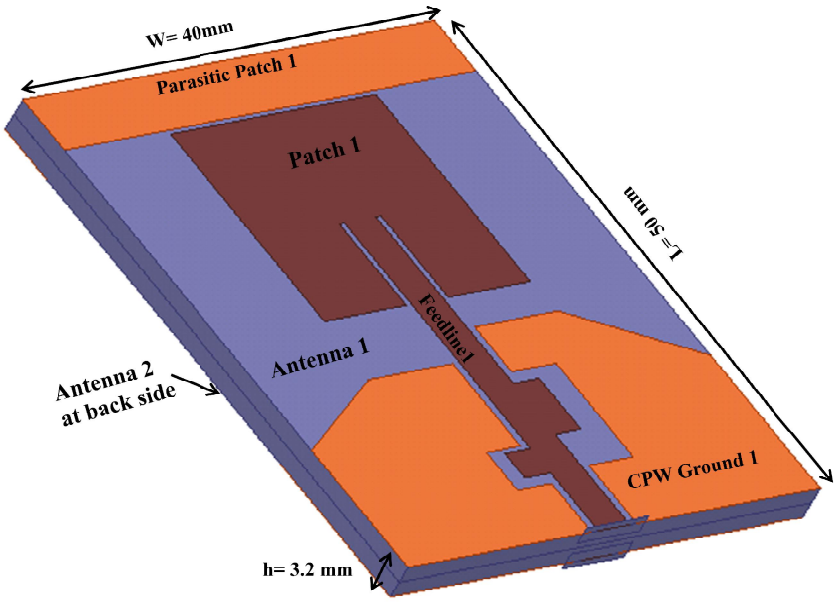

Fig. 4.35. Simulator structure of two back to back stacked coplanar monopole antenna

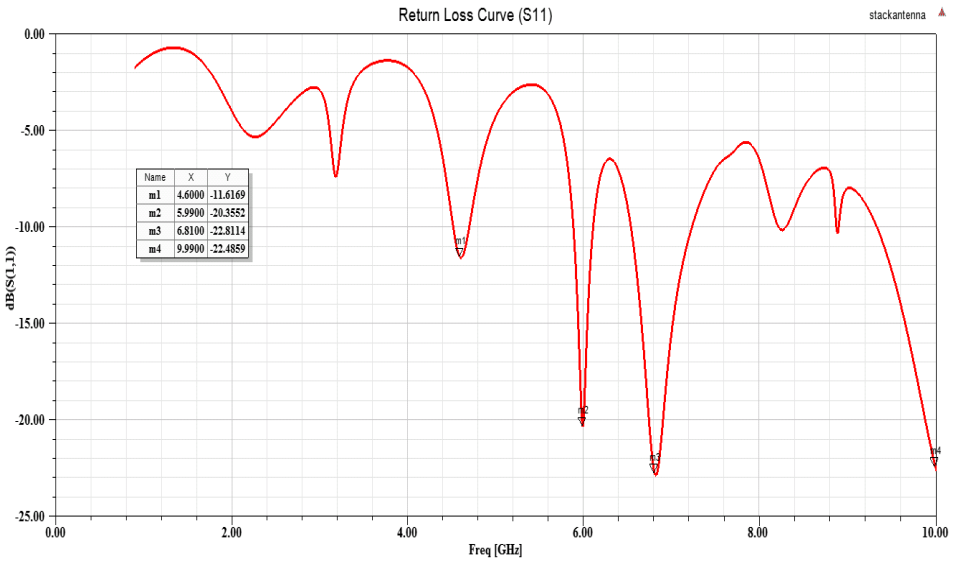

Fig. 4.36. Simulated return loss (S_{11}) result of two back to back stacked coplanar monopole antenna.

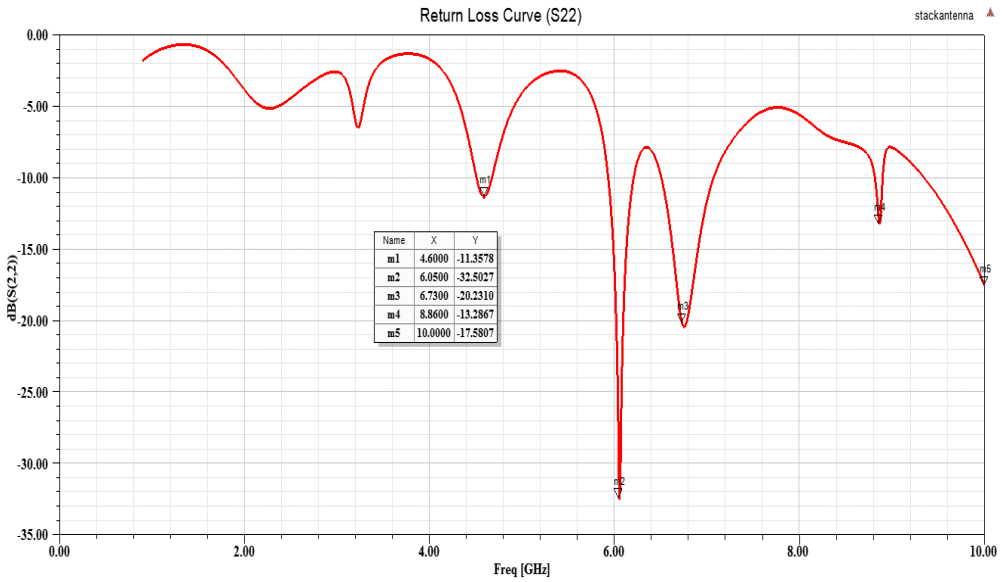

Fig. 4.37. Simulated return loss (S_{22}) result of two stacked coplanar monopole antenna.

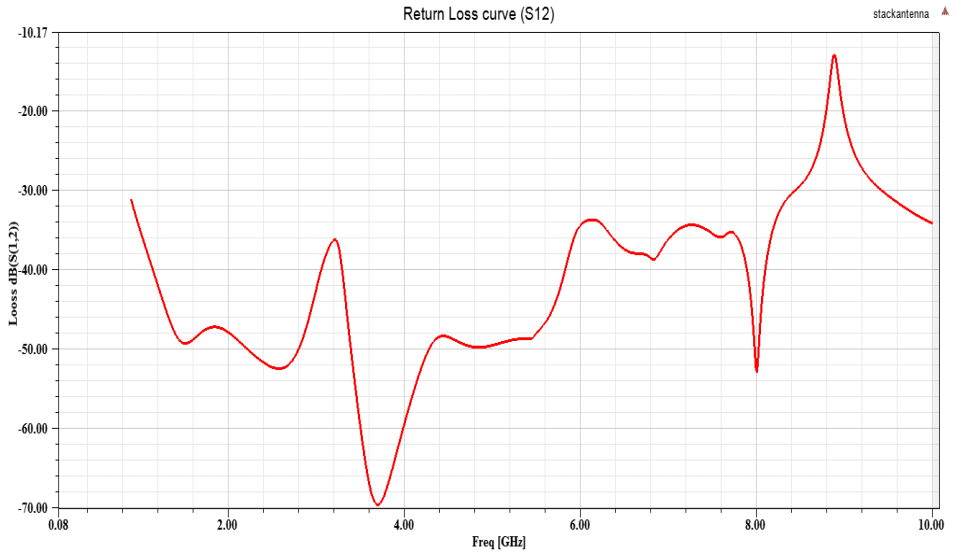

Fig. 4.38. Simulated return loss (S_{12}) result of two back to back stacked coplanar monopole antenna

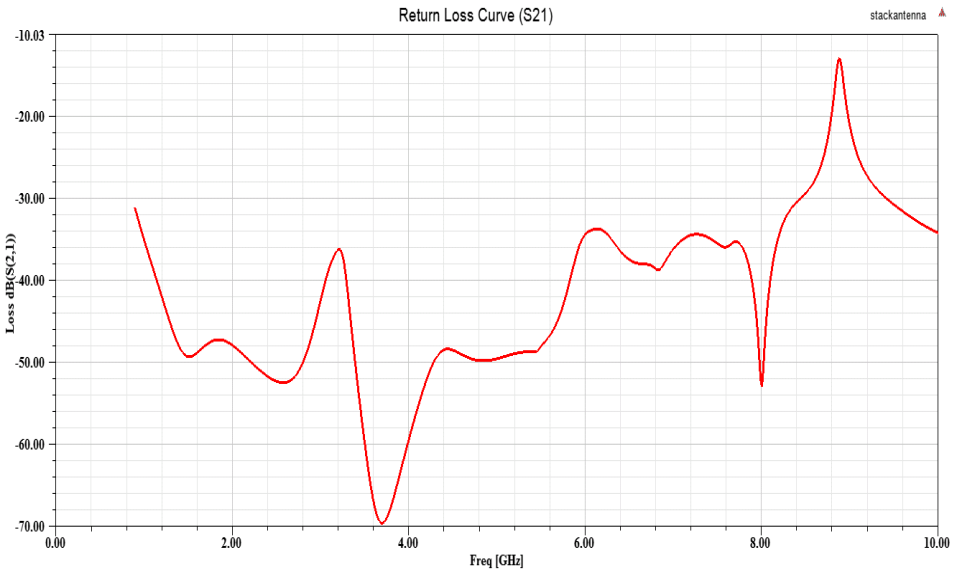

Fig. 4.39. Simulated return loss (S_{21}) result of two stacked coplanar monopole antenna

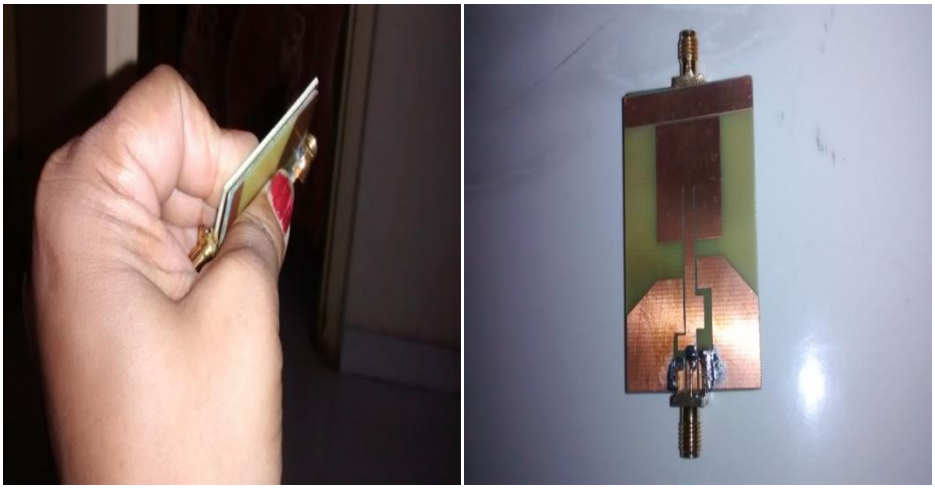

Fig. 4.40. Fabricated structure of two back to back stacked coplanar monopole antenna

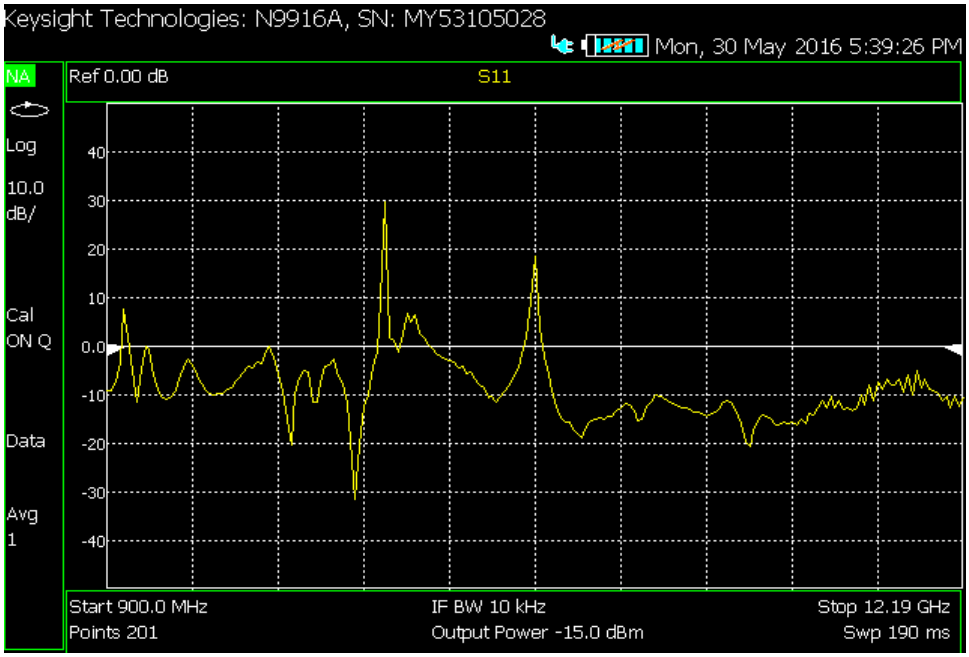
Keysight Technologies: N9916A, SN: MY53105028
Mon, 30 May 2016 5:39:26 PM
NA
Ref 0.00 dB
S11
Log
10.0
dB/
Cal
ON Q
Data
Avg
1
40
30
20
10
0.0
-10
-20
-30
-40
Start 900.0 MHz
Points 201
IF BW 10 kHz
Output Power -15.0 dBm
Stop 12.19 GHz
Swp 190 ms

(a)

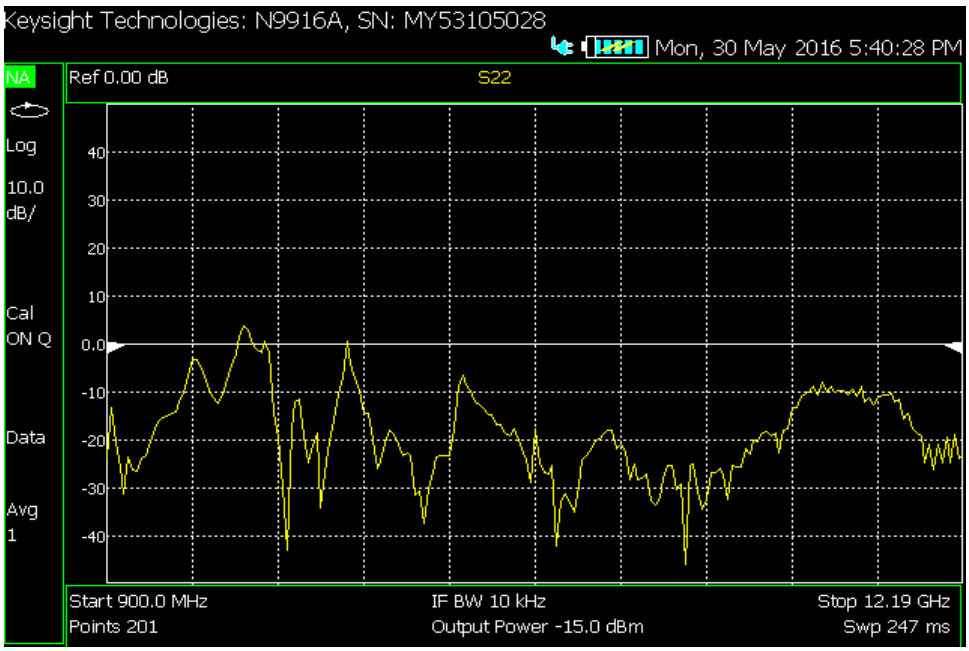
Keysight Technologies: N9916A, SN: MY53105028
Mon, 30 May 2016 5:40:28 PM
NA
Ref 0.00 dB
S22
Log
10.0
dB/
Cal
ON Q
Data
Avg
1
40
30
20
10
0.0
-10
-20
-30
-40
Start 900.0 MHz
Points 201
IF BW 10 kHz
Output Power -15.0 dBm
Stop 12.19 GHz
Swp 247 ms

(b)

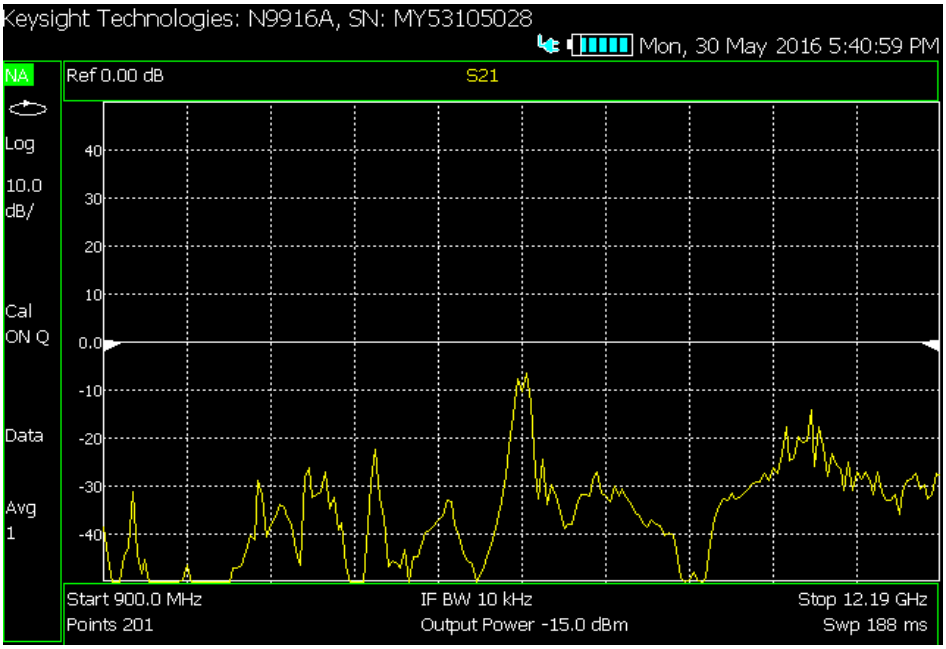

(c)

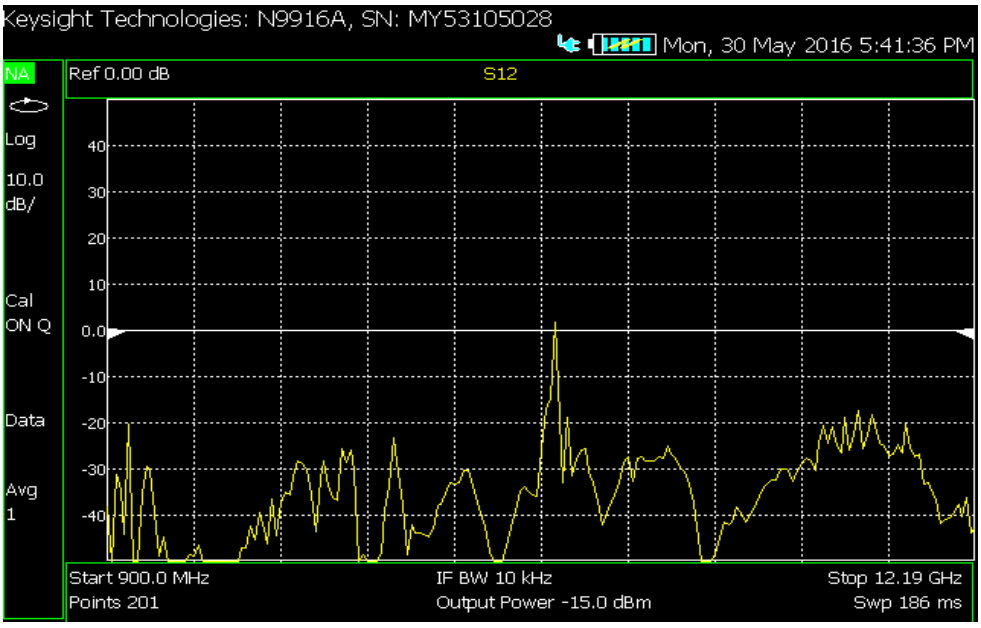

(d)

Fig. 4.41. Measured return loss (a) S_{11} (b) S_{22} (c) S_{21} and (d) S_{12} results of two back to back stacked coplanar monopole antenna

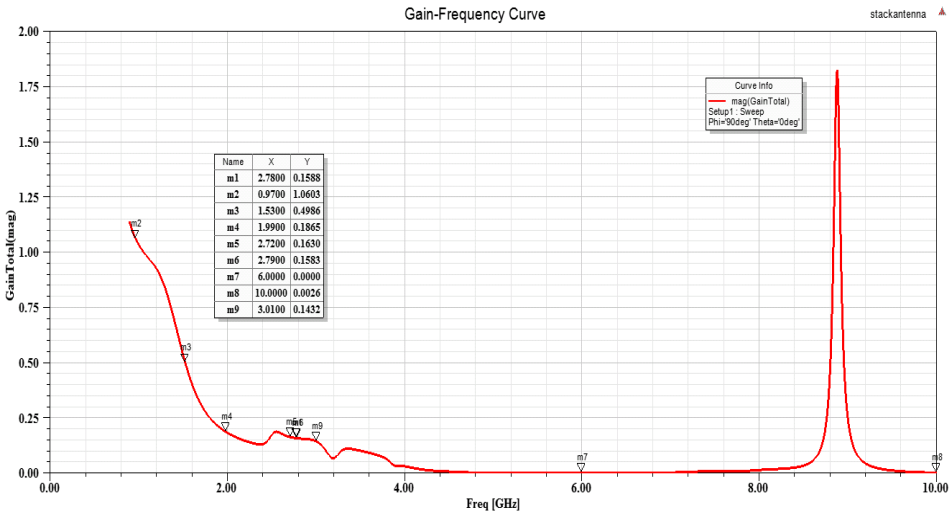

Fig. 4.42. Gain-frequency curve of two back to back stacked coplanar monopole antenna

The gain frequency curve as shown in Fig. 4.42 indicated that the gain for UWB ranges is high and for lower range it is positive only.The peak realized gain for this arrangement is 0.76 and the radiation efficiency is 83.1% as shown in Fig. 4.43(a) and (b).

The stacking of antenna is also important in the RF energy harvesting concern because the DC output voltage may be increased if we connect the output of many module in that mode in series combination. It also consumes the less space when integrated on a whole circuit. With stacking of two back to back coplanar antenna the received RF energy is combined at the input port.

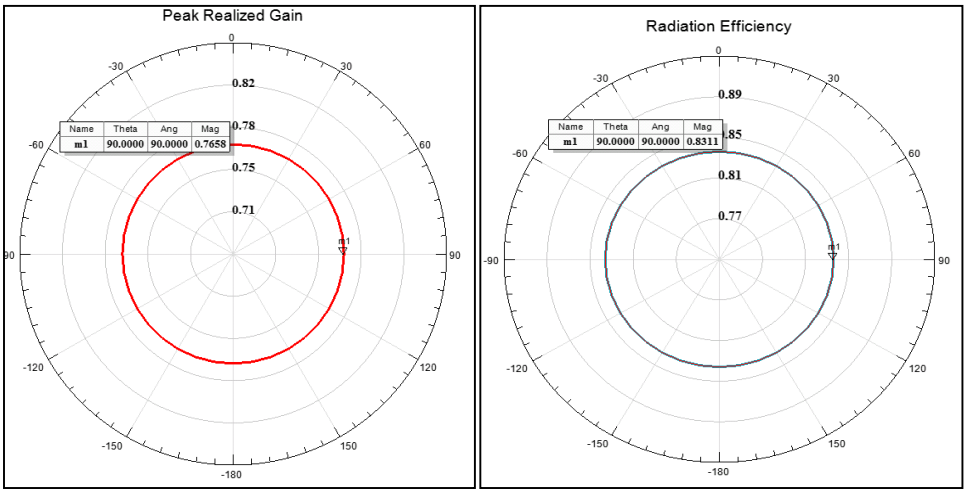

Fig. 4.43. (a) Peak realized gain (b) radiation efficiency of two back to back stacked coplanar monopole antenna

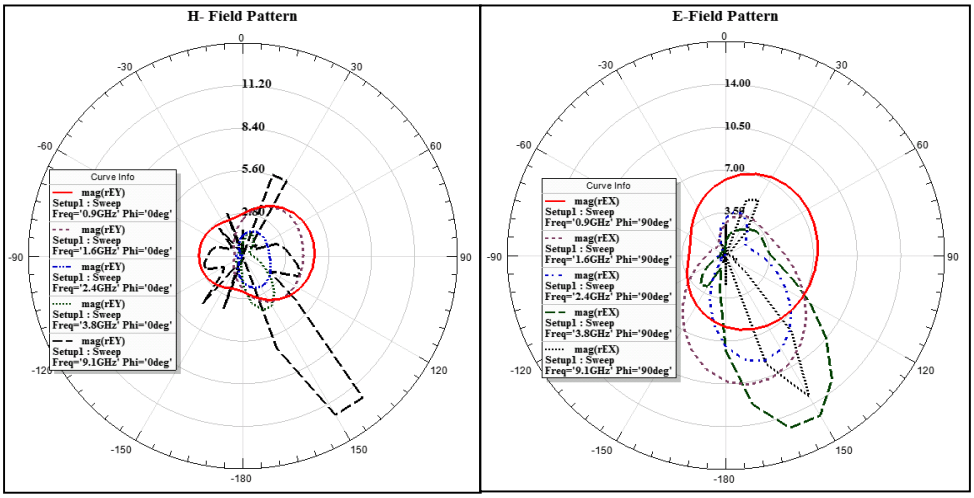

Fig. 4.44. (a) H- field Pattern (b) E-field pattern of two back to back stacked coplanar monopole antenna

The H-field and E-field pattern are shown in Fig. 4.44(a) and (b). It indicates the current and electric field magnitudes of the resonant frequencies.

The results have been summarized in Table 4.1.

Table 4.1 Comparative Results for Different Possible Array Arrangements of the Coplanar Monopole Antenna

Design	**Resonant on the frequencies**	**Gain**	**Peak Realized Gain**	**Radiation Efficiency**
2×1 array (Vertically Connected)	900 MHz-2.5 GHz (GSM & ISM band) 3.5 GHz-5.8 GHz (WLAN Band) 7.2 GHz-8.4 GHz (UWB band)	Max. 24 dB Positive only for GSM & ISM band . Negative for other ranges	51.7	71.4
2×1 array (Horizontally Connected)	900 MHz-2.5 GHz (GSM & ISM band) 3.5 GHz-5.8 GHz (WLAN Band) 7.2 GHz-8.4 GHz and 9.1 GHz-9.3 GHz (UWB bands)	Max. 22 dB Positive only for GSM & ISM band . Negative for other ranges	39.5	82.17
2×2 array	Multifrequency resonance for almost all useful ranges (i.e. GSM, WLAN, ISM, UWB)	Max. 13.6 dB Positive only for GSM & ISM band Negative for other ranges	52.80	80.77
Stacking of 2 single antennae (1×2 array)	Resonant for 6 GHz-9GHz (UWB ranges)	Max 1.85 dB for UWB ranges and 1 for lower ranges	76.58	83.11

Investigations of different array arrangement describe the behavior of each particular design .The peak realized gain and radiation efficiency are important parameters to study for particular RF energy harvesting applications, that is why only related parameters are compared here. The above studied arrays are connected with our RF-DC conveter circuit .

4.7 State of Art of the Designed Antenna (Single Coplanar Monopole Antenna)

In this section we have compared the designs which has been recently developed in this field for the UWB ranges with notch bands. The Table 4.2 shows that although our antenna is not too compact but showing more gain and efficiency as compared to others which make it more suitable for RF energy harvesting purposes.

Table 4.2 State of Art of the Designed Antenna

Properties	Designed Antenna	[4]	[7]	[9]	[10]
Frequency of operation	900 MHz-9.9 GHz with the band rejection of 3.1-5.6 GHz	2.4 GHz	3.1-10.6 GHz with the band rejection of 5 - 6 GHz	3.1-10.6 GHz with notched band of 5.1-5.9 GHz	3.1-10.6 GHz with two band rejection WiMAX (3.3-3.8 GHz) and WLAN (5-6 GHz) band
Area of structure	50×40 mm^2	40×40 mm^2	39×35 mm^2	29×31 mm^2	26×30 mm^2
Radiation Efficiency	70.2%	69%	77%	Not available	Not available
Gain	2 - 7 dBi	Not available	3 dBi	2.1 - 5.8 dBi	2-4 dBi
Application	RF energy harvesting	RF energy harvesting	Not available	Portable UWB systems	UWB communication

4.8 Conclusion

In this chapter a compact coplanar waveguide fed wideband monopole antenna for RF energy harvesting applications has been proposed. The proposed antenna is suitable for RF energy harvesting applications due to two reasons, firstly because the area of capturing radiation energy through receiving antenna is larger due to parasitic patch, resonant patch & the coplanar ground above the substrate. Secondly it is resonant on almost all the bands available in the RF spectrum. The proposed antenna is compact in size ($50\times40\times1.6$ mm^3) and may be used for the wide range from 900MHz to 9.9GHz with band reject (3.1-5.6 GHz) characteristic. For RF energy harvesting purposes WLAN & HIPERLAN (3.1-5.6 GHz) band is less useful because it provides interference due to weak strength of signals.

The tuning slots in the coplanar ground are responsible for the bandwidth enhancement of UWB range and the stubs in feed line are responsible for impedance matching. The designed UWB monopole antenna shows omnidirectional radiation patterns and good radiation efficiency of 70.2% and gain (2-7dBi for different frequencies). The proposed antenna has perfect impedance matching for the GSM, ISM, and UWB ranges and rejects interference from HIPERLAN and WLAN range.

A study of different array arrangements has also been presented in this chapter. The array has been designed in such a way that the gap between the two radiating patches is $\lambda_0/2$ fixed .Then I have compared the results of all the arrangements. It is concluded that the 2×2 array provides the modearate gain and efficiency and works for five resonant frequencies. So this arrangement is considered here as most suitable for RF energy harvesting purposes.

Chapter-5 : DEVELOPMENT OF A NOVEL RF ENERGY HARVESTING MODULE

5.1 Introduction

For charging the low power electronic devices RF energy harvesting system is the best approach. This chapter presents one more bargain of RF energy harvesting for powering low power devices with specially designed antenna. It is very compact in size because the receiving antenna is a coplanar monopole antenna of size 50 ×40 mm^2 and the seven stage converter circuit is also of size 20×30 mm^2. The uniqueness of this system is the coplanar monopole antenna that is specially designed by us for RF energy harvesting application particularly. The antenna resonates from 900MHz -9.9 GHz as explained in the chapter 4. This covers all the useful ranges of the spectrum. The importantce of the work is that the antenna captures the energy from the RF spectrum from the multibands i.e. the antenna works as receiving port for GSM, ISM, UWB ranges. Also the area of conductor at the antenna for capturing the RF energy from ambient is more in this structure due to parasitic patch, Resonating patch and coplanar design. The measurements were taken from a set up of horn antenna having maximum transmitting power of + 40 dBm. The output of this module having single coplanar monopole antenna, is 289 mV. Next as we connect the array of antenna to this seven stage converter the DC voltage increases. This study is reported in this chapter.

The DC voltage may be boosted by connecting a booster circuit or we may use a super capacitor at the output of module for increasing this DC and charging low power devices.

The work reported here presents the comparative study with simulation and measured results of single coplanar antenna and its different arrays connected with RF- DC converter circuit with connectors. And finally presents a module of RF energy harvesting having 2×2 array as receiving antenna and seven stage RF- DC converter circuit on a single substrate .The novelty in this design is that the whole module including 2×2 array of antenna , RF-DC converter and load circuit are on a single substrate with a small area of 124× 120 mm^2. Also the impedance matching has been acheived by simply adding the SMD component (resistors with capacitor/inductor) in the wilkinson's combining branches and at the input of converter circuit. The 2×2 array of designed antenna with seven stage RF-DC converter circuit on the

single substrate and its characterstics are shown in this chapter. The stacking of the module is also possible . This is also a uniqueness of this module.

The experimental work has been performed in two phases.

(i) In first phase the microwave power source of the range 500 MHz- 14 GHz was directly connected to the antenna (single coplanar antenna and its arrays) with the RF-DC converter circuit and DC output is measured by the digital multimeter. From the measurement results the design which provides the maximum DC output has selected as the final receiving antenna structure for new RF energy harvesting module.

(ii) Then in second phase prepare the new RF energy harvesting module with connecting the final selected receiving antenna to the RF-DC converter with appropriate impedance matching between antenna and converter. The Horn transmitting antenna set up of the varying power from ± 10 dBm to ± 40 dBm was placed at a distance of 1 m from this module. The receiving power and the DC output is measured on the power meter and digital multimeter.

The DC output voltage versus input power and conversion efficiency versus input power (dBm) have been investigated.

5.2 Literature Review

RF Energy harvesting from the ambient is playing an active role in the present era of microelectronics devices. The researchers named it as RECTENNA. Two important design parts of this rectenna are an efficient receiving antenna and a good RF-DC converter circuit. Many antennas especially for this RF energy harvesting purpose were designed for single resonant frequency operation in GSM, ISM, C and X band [116-119]. Dual resonant frequency operated antennas were also reported [120-121] for the same purpose. To enhance the receiving power of these antenna array arrangements were also studied [122-123]. After designing the efficient receiving antenna circuit, RF-DC converters having single stage were designed [124-125] . To improve the conversion, 2 to 7 stages of RF-DC converter circuits with multiband and dual band receiving antenna were reported [126-128]. Matching circuit in between antenna and converter circuit for impedance matching is also important to deliver maximum power.

I have proposed a novel RF Harvester module. The novelty in this work is in the design of antenna. In the previous chapter 5 the antenna and its arrays for RF energy harvesting purposes have been presented. The antenna is a coplanar monopole antenna with wideband operation on multiple frequencies of useful bands. From the comparison of the measured results of first phase suitable selected design of the antenna array (i.e. which shows the maximum DC output voltage) is working here as receiving antenna for RF-DC converter circuit. A seven stage RF- DC converter circuit has specially designed for this purpose and results of the experimental setup are reported in this chapter. The value of DC output from this novel module is 1.823 V with respect to the input power +40dBm .

Problem statement

An RF energy harvesting module is needed whose receiving antenna would resonates over multifrequencies and covers almost all usefull band of spectrum. The DC output of that module would be more than 0.8 V to powering the low power devices. Also needed an better idea of impedance matching between the antenna and converter circuit to remove the need of impedance matching at 50 ohms value paticularly.

Methodology adopted

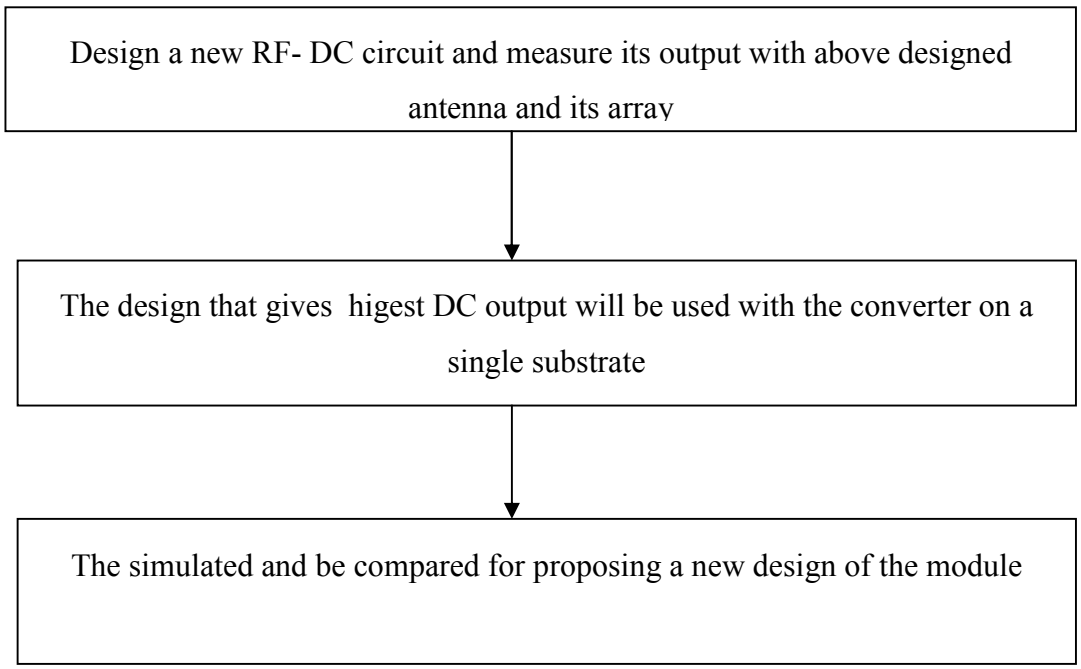

5.3 Design of RF Energy Harvesting Module

The block diagram of RF energy harvesting is shown in Fig. 5.1. Basically, it is comprised of three sections a) antenna (As a RF Receiver) b) matching network (for impedance matching) c) RF–DC converter and voltage multiplier module and load circuit. The next section describes the system blocks one by one.

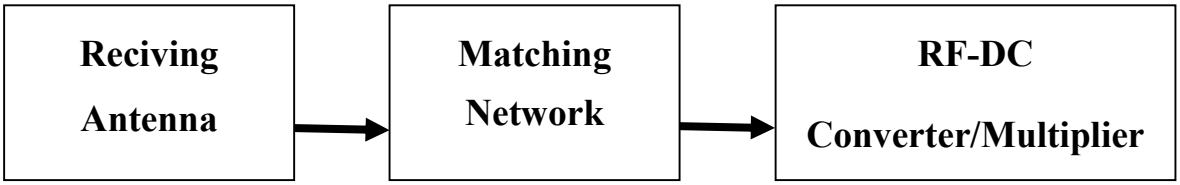

Fig. 5.1 General block diagram for the energy harvesting system.

5.3.1 Receiving Antenna

The receiving antenna for this thesis is the specially designed coplanar monopole antenna. The characteristics of this antenna have been already described in the chapter 4. This antenna is designed to operate on multi frequencies so it works on all important RF ambient regions i.e. GSM, ISM, UWB.

The array structures of this antenna have been explored. These array shows enhancement in gain as well as radiation efficiency. So they also provide the increased input power to the module and cosequently increase the DC voltages.

5.3.2 Matching Network

For minimum return loss and maximum conversion efficiency, the impedance should be matched. The matching network is placed between the antenna and RF-DC Converter to match the impedance. In our design a Wilkinson power combiner has been used to combine the power from the array of coplanar monopole antenna and this combined power is delivered to the RF-DC converter circuit. The big advantage of this Wilkinson is that in between the combining legs of it the SMD resistor can be easily mounted. This resistor will change the resistance of the output leg of Wilkinson [126].

The novel idea of impedance matching is that , consider the complex input impedance of RF-DC converter circuit as the value of load resistance (R_L) of the output of Wilkinson power divider . This impedance is measured by vector network analyzer. It is the

value of resistor (R) inserted at the combining leg of output Wilkinson power divider as explained below. The SMD resistor of the above measured value are soldered in between the combining leg of wilkinsin power divider. In this way we can match the impedance of antenna and converter circuit this will fulfill the condition of maximum power transfer.

The procedure of matching the impedance of Wilkinson output leg to the two input leg with the help of resistor is described below. The Wilkinson power divider/combiner is as shown in Fig. 5.2.

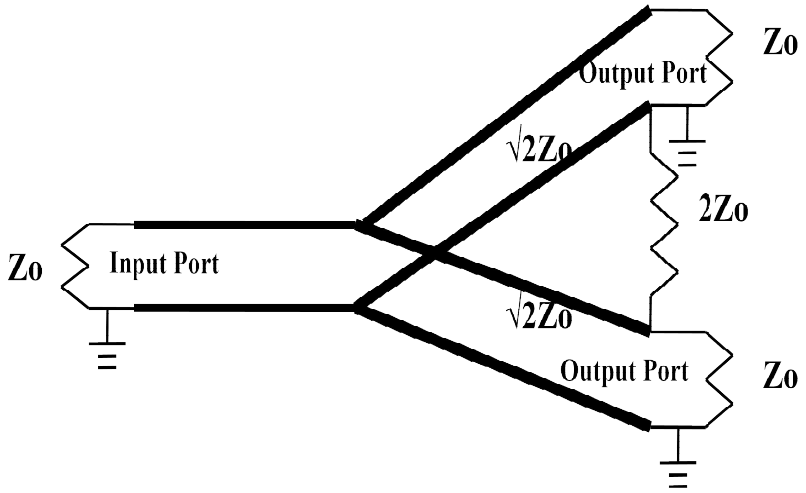

Fig. 5.2 Wilkinson power divider/combiner

In Fig. 5.2 an equal divide Wilkinson has been shown i.e. at the two output port two signals of equal phase and amplitude are applied. The sum of these two signals is observed at the input port. The resistor will have the same potential at input and output port due to equal amplitude and phase of the signal. The power divider acts as a power combiner when the signals meet at the intersection they will usefully interfere. On the other part if the unequal power division is considered by using the Wilkinson power divider, we have to apply a particular set of design equations to determine the impedances of these quarter-wave sections and also the value of the connecting resistor. These impedances are indicated by the value of *M*, given by eq. (5.1)

$$M = \frac{P_3}{P_2} \tag{5.1}$$

where P_2 and P_3 are the desired powers at output ports two and three respectively. At the quarter-wave transmission line connected to port 3 as shown in Fig. 5.2 , the impedance is then given by

$$Z_{03} = Z_0\sqrt{\frac{1+M^2}{M^3}} \tag{5.2}$$

Similarly, the impedance of the transmission line connected to port 2 as shown in Fig. 5.2 is given by

$$Z_{02} = Z_0 M^3 = Z_0\sqrt{M(1+M^2)} \tag{5.3}$$

and the value of the connecting resistor is

$$R = Z_0\sqrt{(M+\frac{1}{M^2})} \tag{5.4}$$

If the ratio of the output powers at the output ports is equal to 1 (equal power division), the impedances shrink. For a given number of output ports N, an input impedance R_S and output load impedance R_L, and the characteristic impedance of each quarter-wave section, $Z_{\lambda/4}$, is given by

$$Z_{\lambda/_4} = \sqrt{(N\,R_L\,R_S)} \tag{5.5}$$

Additionally,

$$R = R_L \tag{5.6}$$

It shows that the resistor (R) that connect between the common junction and the output ports are simply equal to the load impedances (R_L) at each output.

In this thesis, a new RF energy harvesting module has been presented. For impedance matching of the 2×2 array structure as receiving antenna of this module to the input impedance of the seven stage RF-DC converter circuit, the equation (5.6) has been

considered. The surface mount device (SMD) resistor ($\tilde{R} + jX$) of the measured value of resistance at the input of converter circuit has been mounted at the combining port of the Wilkinson. So that the load resistance (R_L) of the same value has found at the input of the RF- DC converter circuit.This is the novel approach of the impedance matching of antenna and converter circuit from this thesis. This impedance changes according the change in frequencies. The impedance has measured only for those frequencies which shows the resonance for the 2 X 2 array structure of coplanar antenna as previously shown in Fig. 4.29 .

The real and imaginary measured impedance at the input port of RF-DC converter circuit is as shown in Fig. 5.3.

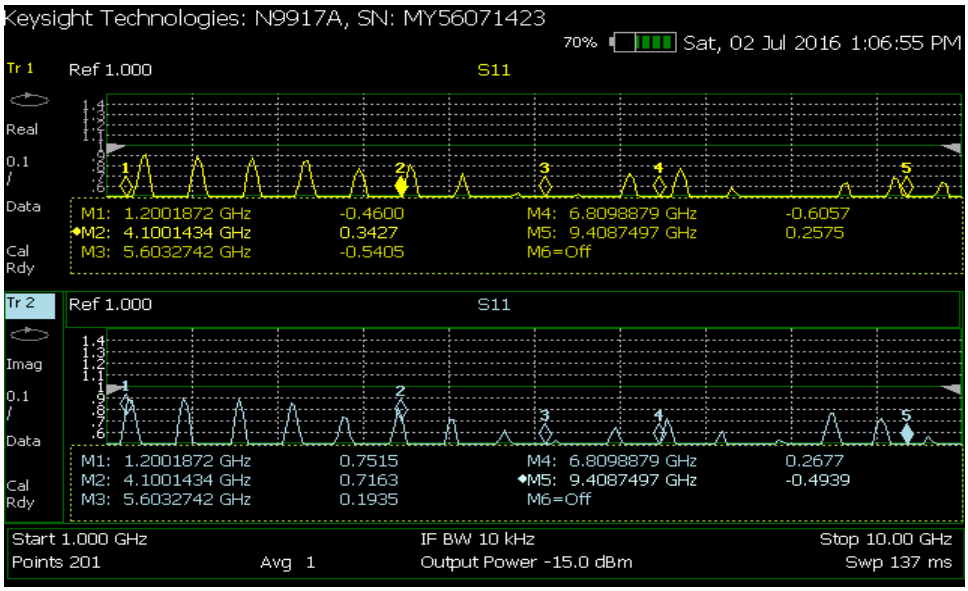

Fig. 5.3. Measured real and imaginary parts of impedance at the input port of RF-DC converter circuit of the module.

By adding this value of resistor at the combining leg of Wilkinson power combiner the impedance matching has been achieved. Further measurements have been taken by inserting the SMD component at the combining leg of output Wilkinson combiner.

The fabricated module is shown in Fig. 5.13. and the characteristics of the module is discussed later in this chapter.

5.3.3 RF- DC Converter (Energy Conversion) Circuit

The output of harvester circuit is the DC voltage. The input of this module is the AC voltage at the antenna port. This AC voltage is propotinal to the captuered power on the antenna from the RFspectrum. In this work a voltage doubler circuit has been used. The conversion design contains seven stages of Villard voltage doubler circuit. Main function of this conversion circuit is to convert the RF harvested energy from the ambient into the direct current (DC) voltage. This seven stage Schottky diode voltage doubler circuit is first designed, modelled and simulated on ANSYS RF designer circuit and then fabricated and tested. Simulation and measurement for various input power levels and the specified frequency spectrum were carried out. The converter circuit in this design uses zero bias schottkey diode (SMS7621-001-SOT23) from Skyworks. The SPICE model parameters of this diode are as shown in Table 5.1

Table 5.1 Spice Model of Schottkey Diode (SMS 7621-001-SOT23)

Parameter	Units	SMS7621 Series
I_S	A	4E-8
R_S	Ω	12
N	–	1.05
TT	Sec	1E-11
C_{JO}	pF	0.1
M	–	0.35
E_G	eV	0.69
X_{TI}	–	2
F_C	–	0.5
B_V	V	3
I_{BV}	A	1E-5
V_J	V	0.51

Each independent stage with its devoted voltage doubler circuit can be considered a single battery with open circuit output voltage V_0 (with internal resistance R_0). With load resistance R_L the overall output voltage is calculated as

$$V_{output} = \frac{V_0}{R_0 + R_L} R_L \tag{5.8}$$

When m number of stage are connected in series

$$V_{output} = \frac{mV_0}{mR_0 + R_L} R_L \tag{5.9}$$

From the above eq. (5.9) the output voltage is determined by the addition of $\frac{1}{m}$ and $\frac{R_L}{R_0}$ if the value of V_0 is fixed.We see that with the values of V_0, R_L and R_0 constant at some point by increasing the m stage their is negligible change in V_{output}.

Modeling and simulation of the seven stage converter circuit were performed on ANSYS RF designer circuit simulator. The circuit diagram of the software is as shown in Fig. 5.4.

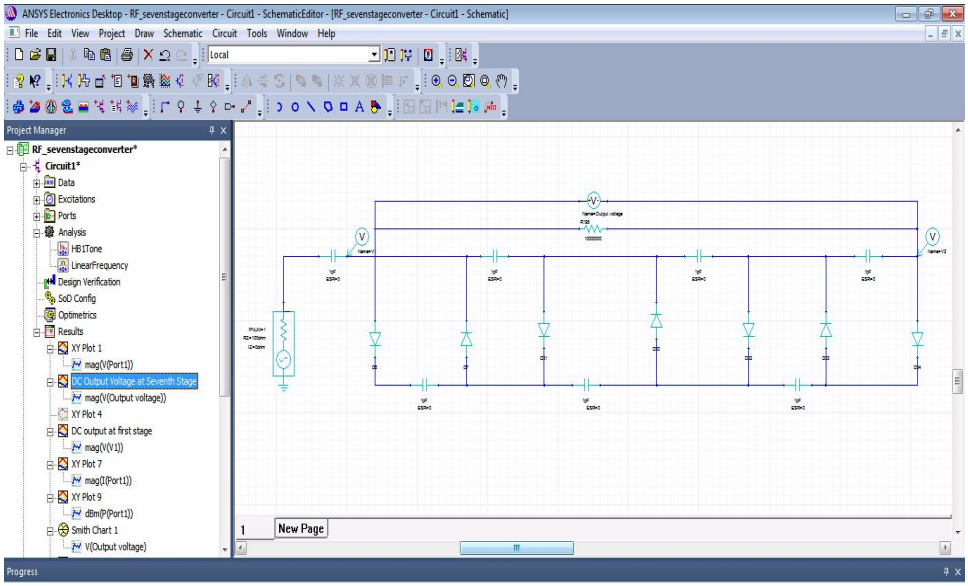

Fig. 5.4. Seven stage RF-DC converter circuit on the RF designer circuit simulator.

The DC output voltage of this seven stage converter circuit is 288.3 mV with respect to the input power of -10dBm from the microwave sourse. The characteristic curve of DC voltage at the first stage is shown in Fig. 5.5. And the DC voltage at the output load resistace of the value 10 kΩ is shown in Fig. 5.6. The power sourse value has been varied from -40 dBm to + 40 dBm and the DC

output voltage with respect to all frequency ranges has been observed. The simulated graph of power input verses DC outpur is shown in Fig. 5.7.

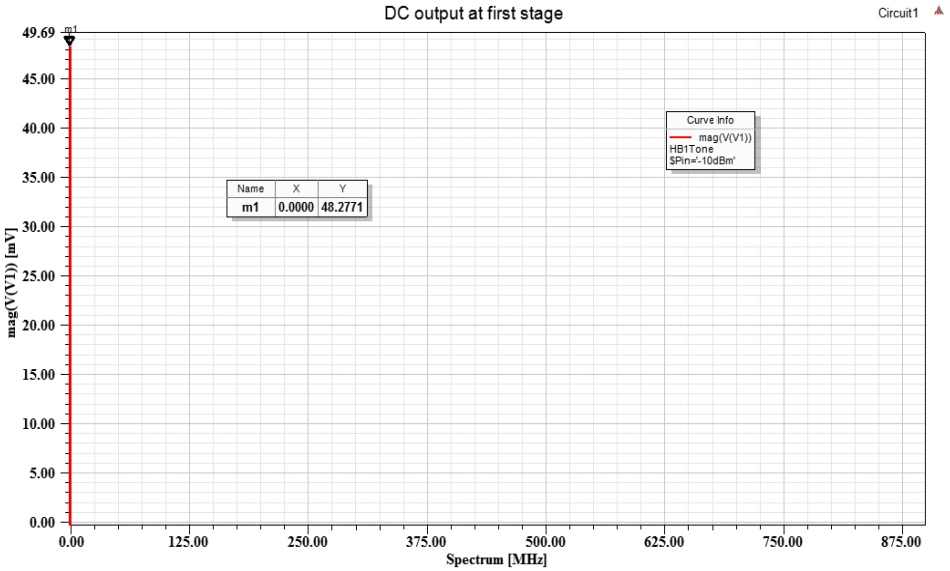

Fig. 5.5. DC voltage at the first stage

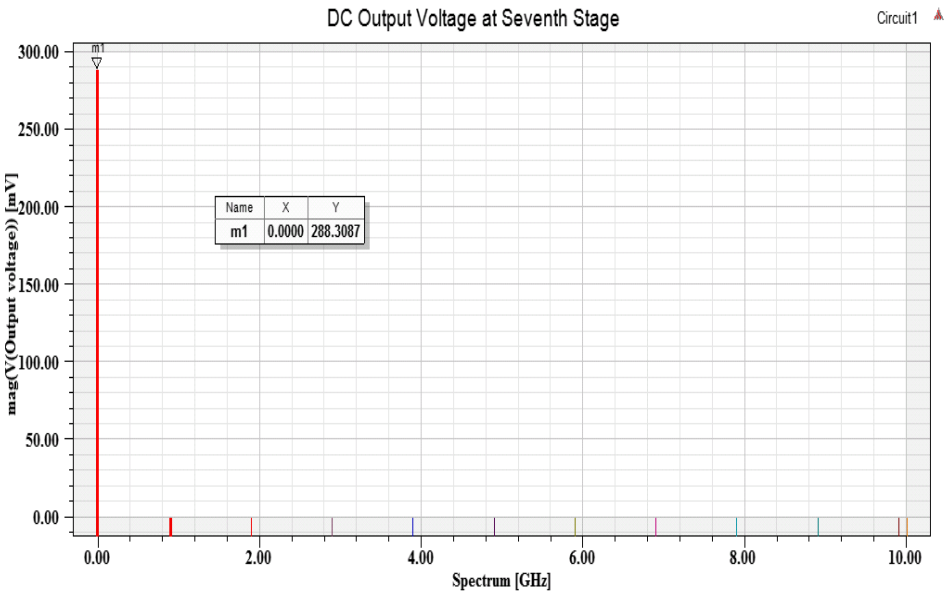

Fig. 5.6. Simulated DC output voltage

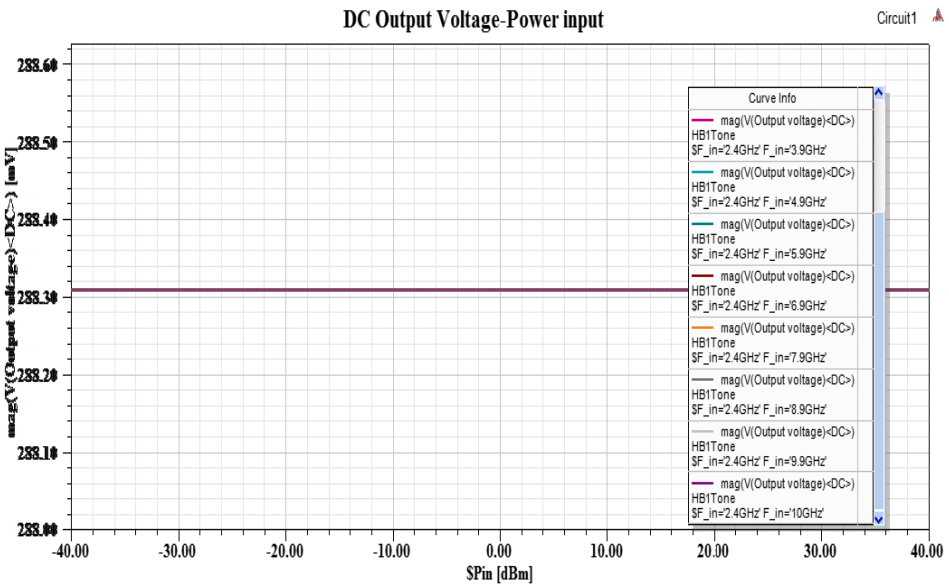

Fig. 5.7. Simulated power input verses - DC output voltage curve for the frequency 900 MHz-10 GHz.

The fabricated structure of this RF-DC converter circuit is shown in Fig. 5.8. The Schottkey diodes are the SMS 7621-001-SOT23 from skyworks and SMD capacitors are of the value 1µF. The load resistance is of the value 10 kΩ.The input resistance is of the value 100 Ω.

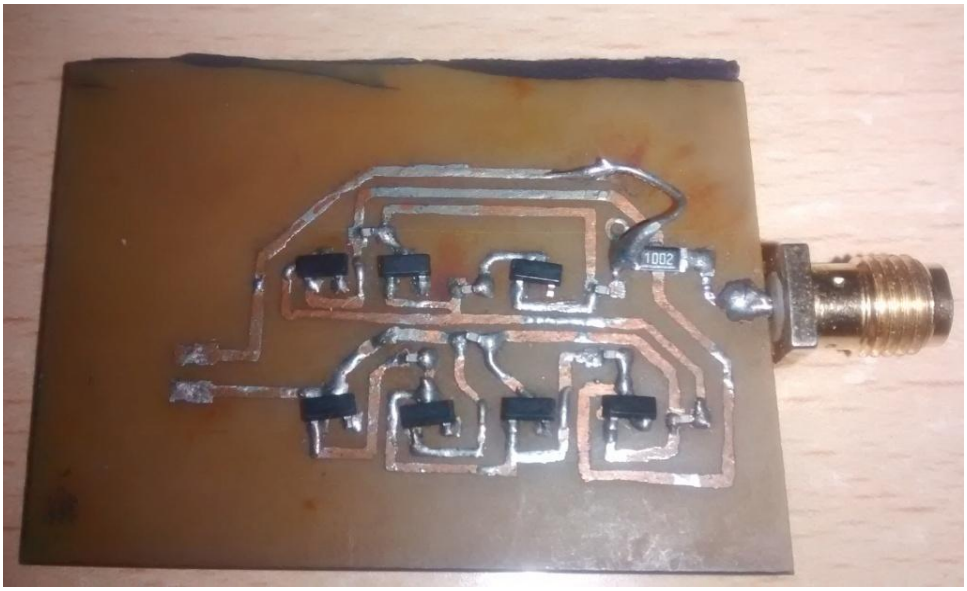

Fig. 5.8. Fabricated structure of the seven stage RF-DC converter circuit.

The DC output voltage of the circuit shown has been measured by directly connecting the circuit to the microwave source as shown in Fig. 5.9.The DC of the value 256 mV has been observed on the digital multimeter which is close to the simulated value.

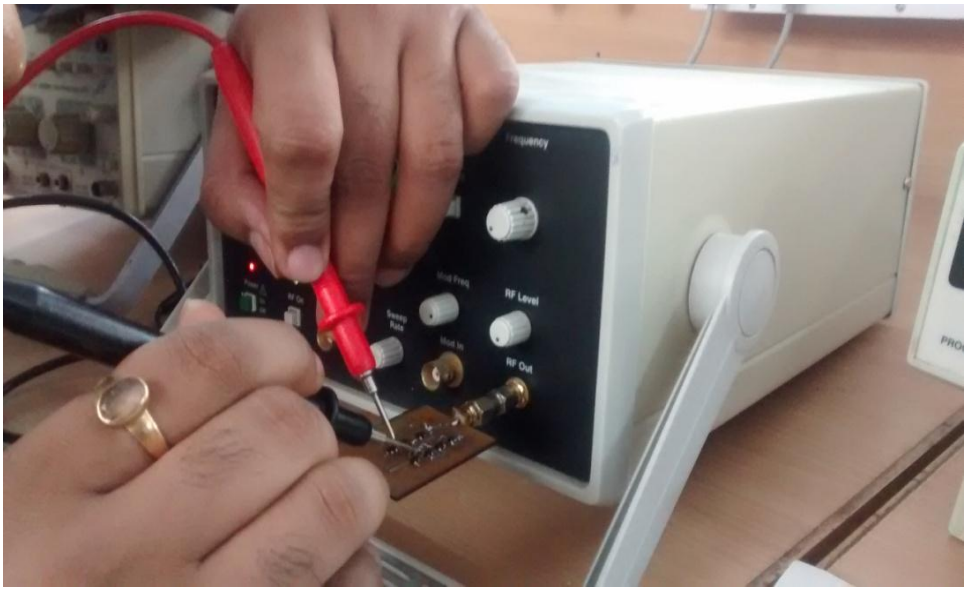

Fig. 5.9. Fabricated structure of the seven stage RF-DC converter circuit connected to the microwave source .

5.3.4 Lab Measurement of Different Array Structures As Receiving Antenna for Energy Harvesting Module

As discussed above the energy harvesting module is the combined structure of the antenna , impedance matching circuit and the converter circuit. The antenna and its arrays are discussed already in the chapter 4. The matching is also discussed in this chapter in part 5.3.2 and the RF- DC converter circuit is discussed in this chapter in section 5.3.3. Now the harvesting module is the combination of antenna , RF-DC converter, load resistance and impedance matching between antenna and converter circuit.

For this we have done the study of connecting the antenna and its arrays to the converter circuit and compare their results. These results were noted with the lab set up i.e. by connecting the module to the microwave power source and observing the results in digital multimeter. The captured input power at the antenna port has also been noted from the

microwave power meter, for the resonant frequencies of the respective antenna arrangements and it is shown in Table 5.2.

Table 5.2 Measurement of Received Power At the Port for Coplanar Monopole Antenna Structures With the Microwave Power Source of 10 MHz-14 GHz with 10 dBm Power

S. No.	Type of designed structure	Power measured at the input port of antenna at resonant frequencies	
		Frequency	Power in dBm
1	Single coplanar monopole antenna	914 MHz 1.6GHz 2.4 GHz 3.8 GHz 6.1 GHz 7.8 GHz 9.1 GHz	-35.2 -30.5 -31.6 -45.8 -32.5 -31.2 -35.6
2	2*1 Array of two coplanar monopole antennas (Power combined by Wilkinson power combiner)	914 MHz 1.48GHz 3.14 GHz 5.6 GHz 8.4 GHz	-34.6 -30.5 -36.5 -36.4 -38.4
3	2*2 Array of two coplanar monopole antennas (Power combined by Wilkinson power combiner)	914 MHz 1.2 GHz 4.1 GHz 5.6 GHz 6.8 GHz 9 GHz	-34.5 -32.6 -37.5 -32.5 -32.5 -30.5
4	Stacking of two pair of single coplanar monopole Antenna connected back to back	914 MHz 1.6GHz 2.4 GHz 3.8 GHz 6.1 GHz 7.8 GHz 9.1 GHz	-32.4 -35.4 -33.4 -36.8 -32.6 -37.4 -32.1

Further measuring the DC output on digital multimeter by connecting the seven stage RF-DC converter circuit to the designed antenna and its different array structure with connectors (one by one). The RF energy is transmitted to the arrangement by the antenna (transmitting mode) connected to the microwave power source of the same range. The arrangements are as shown

in Fig. 5.10 , Fig. 5.11 and Fig. 5.12. The DC output from the converter with antenna and its different array structures with this type of lab set up is tabulated in Table 5.3.

Table 5.3 Measurement of DC Output Voltage with the Microwave Power Source (with +10 dBm input power)

S. No.	Type of designed structure	DC output voltage	Area of the structure
1	Single coplanar monopole antenna	0.256 V	50 x 40 mm^2
2	2*1 Array of two coplanar monopole antennas (Horizontally connected and Power combined by Wilkinson power combiner)	1.09 V	102 x 40 mm^2
3	2*2 Array of two coplanar monopole antennas (Power combined by Wilkinson power combiner)	1.35 V	102 x 124mm^2
4	Stacking of two pair of single coplanar monopole Antenna connected back to back	0.886 V	50 x 40 mm^2

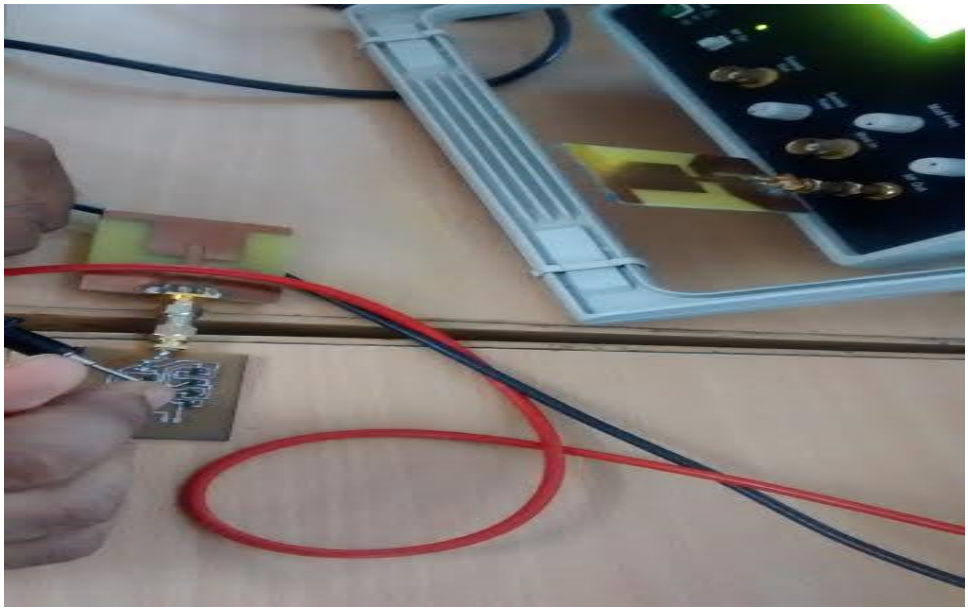

Fig. 5.10. RF-DC converter circuit with single coplanar monopole antenna.

Fig. 5.11. RF-DC converter circuit with 2×1 array coplanar monopole antenna.

Fig. 5.12. RF-DC converter circuit with 2× 2 array coplanar monopole antenna.

It is observed from Table 5.3 that the 2×2 array shows maximum DC output voltage. A module for RF energy harvesting (on a single substrate by using 2×2 array of coplanar structure as receiving antenna) has been designed and measured for DC output. It is explained

seperately in the following section 5.4. This is called a novel module due to its specially designed antenna and also due to elimination of connectors.There is no connector between antenna and the matching network or between the RF-DC converter and the matching network. Impedance matching is also a novelty of this module. The performance of the antenna array is already studied and the design is optimized. As explained above in our design Wilkinson power combiner has been applied and we have used it for maximum power transfer. According to maximum power transfer theorem if the source impedance is equal to the load impedance then maximum power will be transferred to the output from input. The impedance at the RF-DC converter circuit and at the antenna output are measured by VNA. By soldering the SMD passive component (of appropriate value) at the combiner's combining legs, the circuit will fulfill the condition of maximum power transfer. In this sense the impedance matching of antenna and RF-DC circuit has been achieved this has never been used before.

5.4 A Novel RF Energy Harvesting Module With 2×2 Antenna Array of Coplanar Structure on a Single Substrate

The novel RF- DC converter circuit is as shown in Fig. 5.13. The substrate is FR4 Epoxy (dielectric constant 4.4) with 1.6 mm thickness. The size of the overall module is 124 mm × 102 mm.

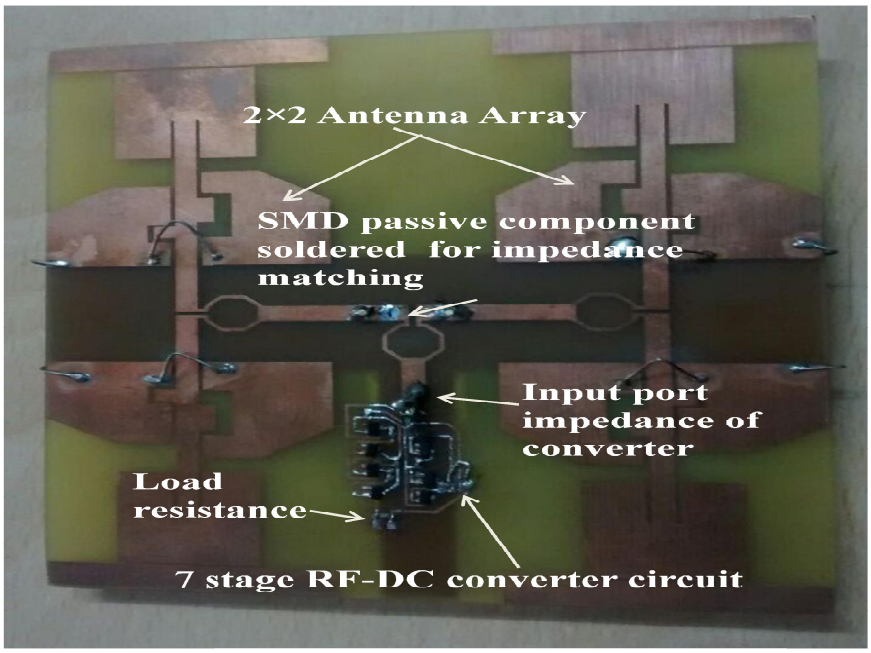

Fig. 5.13. Fabricated RF energy harvesting module .

The experimental set up is as shown in Fig. 5.14. The observation has been taken with the help of horn antenna set up. In this experimental set up the RF source of range 500 MHz- 40 GHz has been used with the transmitting power range -40 dBm to + 40 dBm . The distance between the transmitting antenna and the module has been calculated by the formula

$$Minimum\ Distance\ (D) = \frac{2d^2}{\lambda} \tag{5.10}$$

Wher d = diameter of transmitting horn antenna and λ is the wavelength at which the measurement is being taken. By this calculation the distance is 1m between the antenna and the fabricated module (receiving antenna). The received power at the output port of Wilkinson combiner is measured by powermeter and the output DC voltage is measured by multimeter respectively. The observations are taken at those frequencies only on which the 2× 2 array coplanar monopole antenna shows resonance. These values are observed from the measured result of the designed structure by the Fig. 5.14.

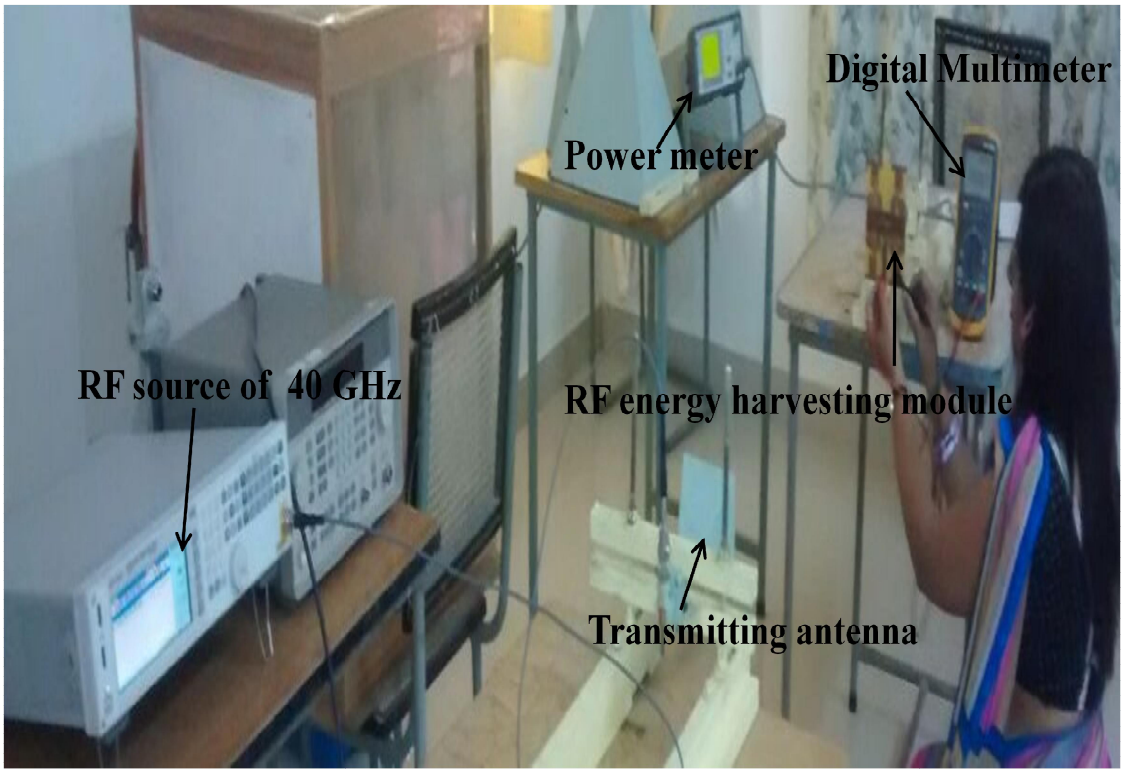

Fig. 5.14. Experimental horn transmitting antenna set up for RF energy harvesting module.

The observations with +10 dBm inpur from the RF power source are as tabulated in the Table 5.4.

Table 5.4 Measurement of DC Output Voltage of RF Energy Harvesting Module with the Transmitting Horn Antenna Set Up

S. No.	RF energy harvesting module with 2*2 Array of coplanar monopole antennas (Power combined by Wilkinson power combiner)			
	The transmitting frequency	Horn transmitting antenna of the band for this range	Received power by the antenna of the module	DC output voltage of the module
1	900 MHz	L band	-32.2 dBm	0.987 V
2	1.2 GHz	EL band	-36.5 dBm	0.765 V
3	4.1GHz	SC band	-37.6 dBm	0.750 V
4	5.6 GHz	CJ band	-35.5 dBm	0.789 V
5	6.8 GHz	CJ band	-40.5 dBm	0.484 V
6	9.4 GHz	X band	-35.7 dBm	0.897 V

The data by changing the input power of the source is as shown in fig. 5.14. The data are collected from the measurement set up as shown in Fig. 5.14. It has been shown in the Fig. 5.15 that if we increase the input power to + 40 dBm this value increases up to 1.823 V DC.

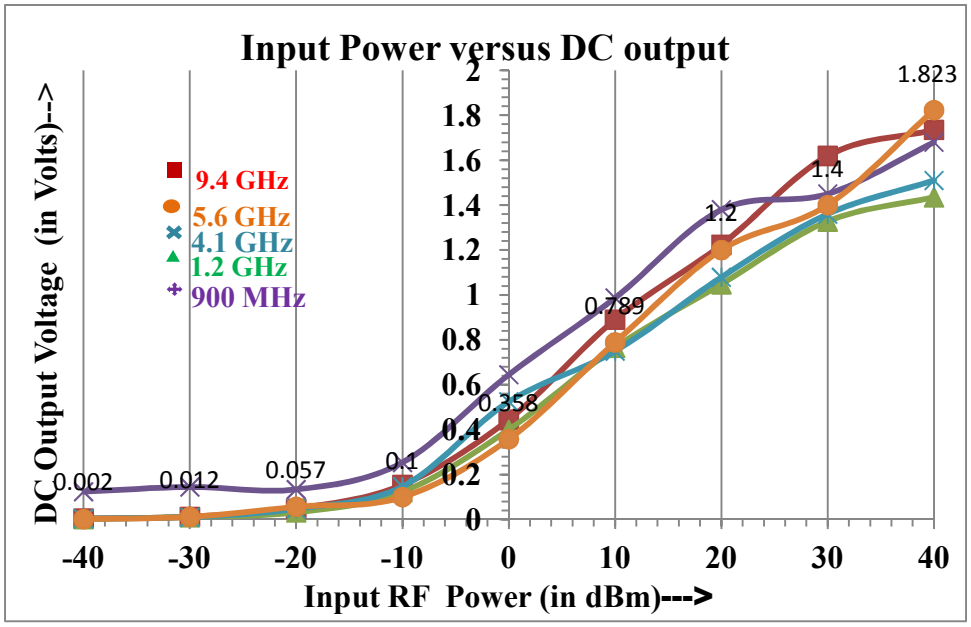

Fig. 5.15. Input RF power versus DC output graph for the five resonance frequencies of the antenna of the RF energy module.

The rectifier efficiency of the given substrate and with the circuit design, is complex to calculate. As we know the efficiency of any RF circuit is a function of input power, operational frequencies range and the output load. Hence, three parameters are studied here.

Initially, the efficiency was calculated for change in power (Pin) from -40 dBm to +40 dBm by using formula

$$\text{Efficiency} = \frac{P_{output}}{P_{in}} \tag{5.11}$$

$$P_{output} = \frac{V^2{}_{DC\ output}}{R^2} \tag{5.12}$$

While the frequency and the load fixed for 9.4 GHz and 20 kohms respectively . The input power versus efficiency graph is as shown in Fig. 5.16.

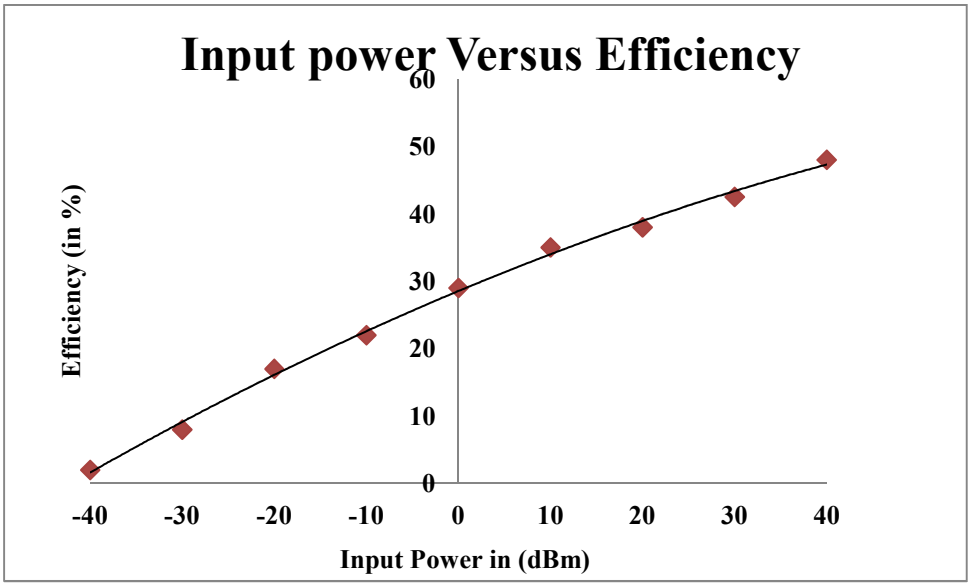

Fig. 5.16. Input power versus efficiency curve for f_0 = 9.4GHz and R = 20 kohms.

As depicted in Fig. 5.16 efficiency reaches 48 % for 40 dBm power and 32% for 0dBm . Next the effect on efficiency of change in load resistance was plotted. For this frequency is set at 9.4 GHz with P_{in} is set at -10dBm , 0dBm and +10dBm. The plot between efficiency and load resistance (R_L) is shown in Fig. 5.17. As observed from figure, for 10 dBm power input efficiency reaches 43% and 57% when load is equal to 16 kohms and 20 kohms respectively. Higher effieciency can be achieved by suitable load.

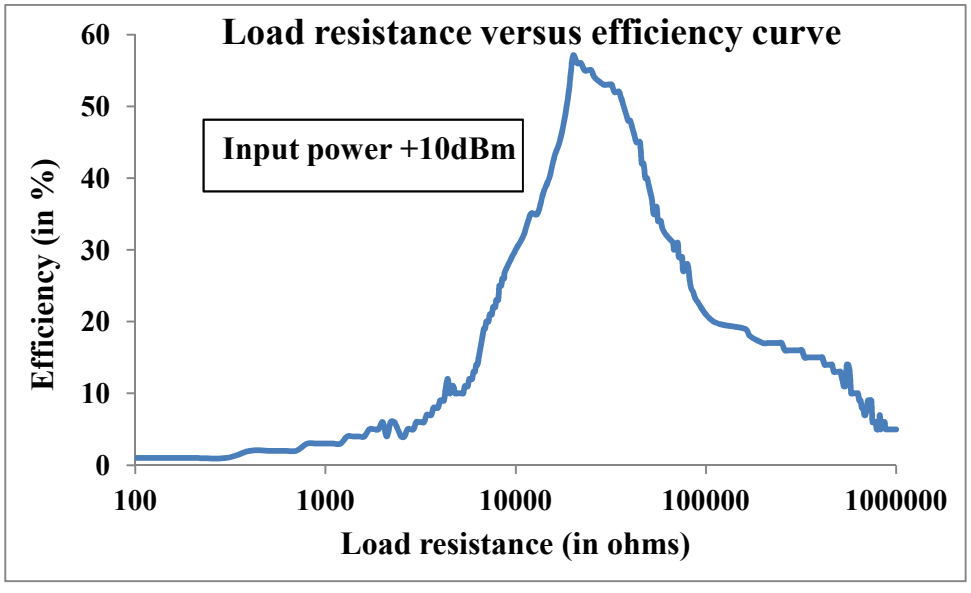

Fig. 5.17. Load resistance versus efficiency curve for f_0 = 9.4GHz at input power = 10 dBm.

5.5 Conclusion

This chapter presents a novel module for RF energy harvesting purposes. A seven stage RF-DC converter circuit has been designed and simulated in ANSYS HFSS – RF circuit Designer software. This circuit is able to provide maximum 1.823 V with our designed coplanar antenna array. A study of all the designed coplanar antenna and its array connected to the RF-DC converter and their DC outputs was presented. Two types of measurements were performed and discussed in this chapter . One is with the microwave source in the lab and other is with the transmitting horn antenna set up.

The novelty in this circuit is it's antenna of 2×2 coplanar monopole structure. The converter circuit is also of specially designed in this concern. The process of impedance matching between the antenna and converter circuit is also novel. In this process maximum power transfer concept at the Wilkinson power combiner leg has been applied and this will provide the impedance matching easily. Fo this process antenna and seven stage converter circuit are fabricated on the same substrate. The combined output arrangement of the antenna array is at the output port of wilkinson power combiner . The impedance at the input port of the RF-DC converter circuit has been measured after connecting its input with the antenna feed port. This impedance is dependent upon the frequency. As we change the frequency the impedance varies . The resonance frequencies of the antenna are known so the impeadnce of the input port of RF-DC converter circuit for these resonance frequencies may be noted down. The impedance at the combining leg of output wilkinson power combiner has been measured . Simply solder the SMD components of the value measured at the input port of converter. This will provide the impedance matching and maximum power will be transferred to the converter. No connector is used here for transfering the RF power to RF-DC converter circuit. This is the uniqueness of the presented module. For five resonace frequencies the observations were taken by changing the SMD components (values measured at the converter input port) at the combinig leg of output wilkinson combiner of the antenna array. In future this step of soldring -desoldering of different passive components may be avoided by using the variable resistors and inductors/capacitors at that place and work to do this impedance matching automatically while the range of frequeny of resonance changes .

This module is able to deliver 1.823 V with respect to +40 dBm input RF power and the efficiency of the module is 48% for it.

Chapter 6 : CONCLUSION AND FUTURE ASPECTS

The microstrip antenna is a very popular antenna in wireless communication. Due to its wide applications, the research on microstrip antenna is continuously carried out. The designing of the microstrip antenna is the most important part. The development of microstrip antenna is combination of three parts : First is the design dimension calculations, second is the simulation of the designed structure and third is the fabrication of antenna. The design may then be validated by comparing the simulation and measurement.

Every design process has its own problems. This thesis is a step towards making the design calculation simple and easy . Also, it provides a solution for tuning the frequency deviation due to fabrication tolerances. This also saves time of re-designing the structure. In other words as discussed in chapter 2 and 3 this thesis presented two solutions for making the process easy in designing and fabrication part of the antenna.

This thesis presented two sets of formulae , one for designing the antenna and other is for tunning the frequency of antenna if there is deviation occurs due to fabrication tolerances.This is named as 'Dielectric Constant Engineering'. Resonance frequency of the microstrip antenna is inversely proportional to the square root of dielectric constant. So the designed resonance frequency can be tunned by changing the effective dielectric constant of the antenna substrate. By using the presented formula, altered resonance frequency is retuned by cutting the material from one of the layer of the multilayered substrate. Top layer having the patch and bottom layer having the ground structure, so in between these two layers we can cut the material and this will alter the resonance frequency. In chapter 2 the discussion about the effect of the dimension of cutting material on the resonance frequency has been discussed and the generalized formula for finding the dimension of cutting the material (Area of cavity A_c) with respect to the ratio of designed frequency and altered frequency has been presented as below

$$\frac{\mathbf{f_r}}{\mathbf{f_0}} = \frac{\mathbf{1}}{\sqrt{\mathbf{1} - \frac{\mathbf{Ac}}{\mathbf{Ap}}\left(\frac{\boldsymbol{\varepsilon}_{\mathbf{sub}} - \mathbf{1}}{\boldsymbol{\varepsilon}_{\mathbf{sub}} + \mathbf{3}}\right)}}$$

The unknown parameter Ac is the area of the cavity. All other parameters are known. f_r is the resonance frequency, f_0 is the designed frequency and Ap is the patch area and ε_{sub} is the substrate dielectric constant. The area of the cavity is calculated by putting the known

parameters and this material will be cut from the second or third layer and again reorganize the structure will automatically retune the resonance frequency to the designed value. Verification of the process has been discussed into the chapter 2.

The application of these formulae is in the production antenna where LTCC techniques are used.

Next formula from this thesis is for designing process. This part of work is the extension of the transformation of designs formulae discussed in the chapter 1. According to that, If one antenna dimension parameters are available and someone has to design the antenna for another type of substrate with the same resonance frequency then theknown design may be able transformed into a design on another substrate simply by using scaling factors. This makes the calculation of new design parameters comparatively easier than using the classical formulae. This thesis presented the transformation design formulae for feedline transformation from one substrate to another type of substrate. The patch dimension design transformation from one substrate to another substrate is already described [60]. This thesis presented a minor correction in the transformation of design formula for width of patch presented earlier. The problem in that earlier defined formula was that in some cases the calculated width is less than the length of patch which is not favorable in designing the antenna. So the modified formula for this has been presented in this thesis along with the feedline transformation formulae.

In the presented formulae, ψ is the ratio of the square root of the dielectric constants of the substrate of a known antenna and the substrate over which design has to be transformed. A new parameter has been defined earlier , this is 'H' parameter. It is the ratio of the height of the substrate to guided wavelength . The wavelength is proportional to frequency and frequency is inversely proportional to the square root of the dielectric constant. This 'H' parameter may remain constant for all designs if the designed frequency is same. We can vary one parameter and alter the value of another parameter to make the 'H' parameter constant. That's why in this part of work the necessary condition for transforming the designs is that the resonance frequency for all the transformed designs should be same. For transforming one design parameters of feedline for another substrate the work was started with the impedance formulae of classical theory and it is developed into the easier form and relates it to the term ψ in simple and easy form.

The new simplified formulae for the feed line dimensions of the rectangular shape patch design antenna have been presented in this thesis.

Case I for $\frac{W_{01}}{h_1} \leq 1$ ($\frac{W_0}{h}$ is the ratio of trace line width to height of substrate)

$$W_{02} = \frac{(\Psi)^{2.7}}{\phi} \times W_{01}$$

Case II for $\frac{W_{01}}{h_1} > 1$

$$W_{02} = \frac{(\Psi)^{1.85}}{\phi} \times W_{01}$$

Where

$$\phi = \frac{h_1}{h_2}$$

and

$$\Psi = \sqrt{\frac{\varepsilon_{r1}}{\varepsilon_{r2}}}$$

And for the equilateral triangular shape antenna this formula for radiating side is presented as

$$S_{p2} = (\psi) \times S_{p1}$$

These new formulae can be used as an alternate easy formula for calculating the width or the feed line. It gives a simple relation between effective dielectric constant of the substrate material (ε_{reff}) and the ratio of the width of the feed line to the thickness of substrate material (W_0/h). For the validation of these formulae, various antennas have been designed and their S_{11} plots have also been studied. The S_{11} plot results validated the new formulae for feed line dimensions successfully.

The simulations of antennas has been carried out with the help of ANSYS HFSS Version 16 Licenced software. For the validation of these formulae, six types of antennas

have been designed and the S_{11} plots studied. The antennas have been designed for the frequency of 2.4 GHz. The characteristic impedance of the feed line was taken as 50 Ω.

In chapter 3, in addition to the new transformation design formulae for feed line the modification in the formula of transformation for width [60] has also been presented and verified . In previous formula the width of patch of transformed design (W_{p2}) was given by

$$W_{p2} = \frac{W_{p1}}{\phi}$$

Where

$$\phi = \frac{h_1}{h_2}$$

And the modified formula presented by this thesis is

$$W_{p2} = \frac{W_{p1}}{L_{p1}} \times L_{p2}$$

At last, an algorithm for design transformation of rectangular shape patch and its feed line has been presented. By implementing this in Matlab all the parameter i.e. returns loss , radiation pattern , VSWR can be found by inserting the values of parameters for which we want to design a new structure for the same frequency.

This transformation of design has been applied to design the antenna for RF energy harvesting. The good design was available with us for dielectric substrate RT Duroid ($\boldsymbol{\varepsilon_r}$ =2.2). The design has been transformed onto the dielectric substrate FR4 epoxy ($\boldsymbol{\varepsilon_r}$ =4.4) as discussed in chapter 3. And that design has been modified RF energy harvesting purpose as discussed in chapter 4. This antenna works for the 900 MHz -3.1 GHz (GSM and ISM band) and 5.6 GHz- 10GHz (UWB) and reject the band from 3.1 GHz-5.6GHz (WLAN band) because this band is not so beneficial for this purpose.

The geometry of antenna has been prepared from the transformation of design formula this antenna is designed for 2.4 GHz. The simulation result of this design validated the result. Then as our objective is to design an antenna for the range 900MHz-10 GHz with a band rejection of 3.1GHz-5.6 GHz. So modification on antenna has been performed .

Different techniques have been analyzed for it (i.e. gap between the patch and CPW ground, champhering the corners, inserting parasitic patch, cutting slots and inserting the stubs at the feedline). The gain of this modified antenna has been obtained in the range 2-7dB and the radiation efficiency has been noted as 70.2%. This antenna is a good candidate for energy harvesting purpose because the receiving area is maximum due to its coplanar structure and the parasitic patch. Also the antenna is working for a wide range .

To enhance its gain and radiation efficiency different configuration of its possible array arrangements has been reported in the chapter 4. As shown in chapter 4 the gain and radiation efficiency increases if the number of element of array increases. In this thesis the 2×1 and 2× 2 array and the two back to back stacking of antenna has been presented. And a module for RF energy harvesting was reported in next chapter by using one of the array (2× 2) structure of theses designs as a receiving antenna . The peak gain of this 2× 2 array structure has been reported on 52.8 and the radiation efficiency has been 80.7%.

Finally, in chapter 5 a novel RF energy harvesting module has been presented . The antenna for this module has been taken the 2× 2 array of the designed antenna and a seven stage converter circuit for this purpose has been designed. A study of the combination with the different designs of antenna reported in chapter 4 and this seven-stage converter has also been presented in this chapter. The novelty in this module is that whole module is on a single substrate and impedance between the antenna and the converter circuit is matched by using the maximum power transfer concept. A Wilkinson power divider has been used to combine the power of antenna arrays . The input impedance has been measured at the converter circuit input port and the components of the value of this measured value impedance has been soldered at the Wilkinson combining port. After matching the ports the output of the circuit has been measured . The DC output has been shown with respect to spectrum , RF input power and the output load .The maximum DC output is 1.823 V with respect to +40dBm RF input power , and with the load resistance 22 kohms for the frequency 9.4 GHz.

6.1 Future Aspects

As the presented work of this thesis contains two parts: one is the formulation part and the second is the designing part, so the future aspects is also discussed in two parts. For transformation of design formulae, we considered the rectangular and triangular shape of patch only, there are many other shapes of patch i.e. circular, circular ring and disc , for

which these formulae may find out. Further in this thesis, we have been presented the Matlab programme of the set of the transformation of design formulae. The output of this programme provide the dimension parameter for transform the design on new substrate from the another type of substrate , where the resonant frequency of these two designs are same. Anyone can draw the structure directly fron these parameters without any calculations. Matlab@16 version has the module of designing the antenna and also show its performance/ characterstic i.e. return loss, gain, radiation patterns and efficiency. The furtre work suggestion for this is to link the given programme to that module of the antenna in Matlab @16 version so that by inputting the good design parameter of one type of substrate and new parameters of substrate the design is directly drawn in the matlab. This will make the designing process of microstrip antenna very easy and simple without any manual calculations and manual designing of the structure on the software. This will be the great finding in the microstrip antenna designing field.

The new coplanar monopole antenna has been presented in this thesis. The future aspects for this design are that to find out the generalized formula for this structure. The array in this thesis has designed for keeping the distance between the two antenna $\lambda/2$. The range of working frequencies of the array arrangements is different for different arrangements due to the fixed distance. The suggestion for this work is that analyze and synthesise the design of all array structure for the same wide band operation i.e. from 900 MHz - 10 GHz with the band rejection of 3.1 GHz - 5.6 GHz.

The module of RF energy harvesting has been presented in this thesis . This module produces the DC voltage 1.8 V with respect to + 40 dBm RF input power. There is a need of increase this DC voltage upto 5 V, so that all the low power devices can be charged directly. There is also a need of miniaturization of the presented harvesting module. It may be done by using the dielectric of having higher dielectric constant.The module is investigated only for the array of 2×2 design more combination may be used for increase the DC output. There is always have a limit of the number of elements of the array and above which there will no change in the DC output. This thesis has also been investigated the stacking arrangements of the single antenna. That arrangement has also observed results in fruitful form. So the stacking of antenna or its arrays may be used for enhancing the DC output voltage . This may also be useful for miniaturization of the structure. Stacking of two or more module may also be used for it.

REFERENCES

[1] T. Rappaport, "*Wireless Communications: Principles and Practice*", ISBN 978-8-13173-186-4, 2nd ed. Pearson India, 2010.

[2] K. D. Prasad, "*Antenna and Wave Propagation*", *ISBN 81-7684-025-4*, 3rd ed. Satya Prakashan, New Delhi, 2005.

[3] G. A. Deschamps and W. Sichak, "Microstrip Microwave Antennas", *Proceeding of the Third USAF Symposium on Antenna Research and Development Program,* pp. 18-20, Oct. 1953.

[4] R. E. Munson, "Conformal Microstrip Antennas and Microstrip Phased Arrays", *IEEE Trans. on Antennas Propagation,* vol. AP-22, no.-1, pp. 74-78, Jan. 1974.

[5] J. Q. Howell, "Microstrip antennas", *IEEE Trans. Antennas and Propagation*, vol. AP-23, no.-1, pp. 90-93, Jan. 1975.

[6] K. R. Carver and J. W. Mink, "Microstrip Antenna Technology", *IEEE Trans. Antennas and Propagation*, vol. AP-29, no. 1, pp. 2-24, January 1981.

[7] D. M. Pozar, "Microstrip Antennas", *IEEE Proc.*, vol.-80, pp. 79-91, Jan 1992.

[8] R. Garg, P. Bhartia, I. J. Bahl, and A. E. Ittipiboon, "*Microstrip Antenna Design Handbook*", ISBN 978-0-89006-513-6, Boston, MA: Artech House, 2001.

[9] G. Kumar, K. Ray, "*Broadband Microstrip Antennas*", ISBN: 978-1-58053-244-0, Artech House, 2003.

[10] C. A. Balanis, "*Antenna Theory: Analysis and Design*", ISBN 978-8-12651-393-2, 3rd ed. New York: Wiley, pp. 727–752, 2005.

[11] R. A. R. Ibrahim, M. C. E. Yagoub and R. W. Y. Habash, "Microstrip Patch Antenna for RFID Applications", *Canadian Conference on Electrical and Computer Engineering (CCECE)*, St. John's, NL, U.S. Virgin Island, pp. 940-943, May 2009.

[12] F. Kuang, D. Shen, J. Xu, X. Shuai and W. Ren, "A Triple-Band Microstrip Antenna for WLAN Applications", *International Conference on Communications and Mobile Computing (CMC)*, Shenzhen, China, vol.-2, pp. 68-71, April 2010.

[13] R. Sharma and M. Kumar, "Dual Band Microstrip Antenna for C And X Band Wireless Applications", *International Conference on Multimedia, Signal Processing and Communication Technologies* , Aligarh, India, pp. 154-158, Nov. 2013.

[14] M. Fallah-Rad and L. Shafai, "Gain Enhancement in Linear and Circularly Polarised Microstrip Patch Antennas Using Shorted Metallic Patches", *IEE Proc. on Microwaves, Antennas and Propagation*, vol.-152, no.-3, pp. 138-148, June 2005.

[15] Jia-Yi Sze and Kin-Lu Wong, "Slotted Rectangular Microstrip Antenna for Bandwidth Enhancement", *IEEE Trans. Antennas and Propagation*, vol. AP-48, no.-8, pp. 1149-1152, August 2000.

[16] Sang-Hyuk Wi, Yong-Shik Lee and Jong-Gwan Yook, "Wideband Microstrip Patch Antenna With U-Shaped Parasitic Elements", *IEEE Trans. Antennas and Propagation*, vol. AP-55, no. 4, pp. 1196-1199, April 2007.

[17] S. Satthamsakul, N. Anantrasirichai, C. Benjangkaprasert and T. Wakabayashi, "Rectangular Patch Antenna with Inset Feed and Modified Ground-Plane for Wideband Antenna", *SICE Annual Conference*, Tokyo, Japan, pp. 3400-3403, Aug. 2008.

[18] N. Tahir and G. Brooker, "A Novel Approach of Feeding, Impedance Matching and Frequency Tuning of Microstrip Patch Antenna by Single Microstrip Line", *IEEE Symposium on Industrial Electronics and Applications (ISIEA)*, Langkawi,Malaysia, pp. 593-597, Sept. 2011.

[19] M. Elsdon, A. Sambell and S. C. Gao, "Inset Microstrip-Line Fed Dual Frequency Microstrip Patch Antenna", *International Conference on Antennas and Propagation (ICAP)*, Exeter, UK, vol.-1, pp. 28-30, March 2003.

[20] R. G. Halappa, C. N. Anoop, M. M. Naik, S. P. Archana, R. Nandini, B. K. Pushpitha and R. Kumar, "The Microstrip Fed Rectangular Microstrip Patch Antenna (RMPA) with Defected Ground Plane for HIPERLAN/1", *International Journal of Electronics & Communication Technology*, vol.-2, no.-3, pp. 172-175, Sept. 2011.

[21] J. Venkataraman, D. Chang and K. R. Carver, "Input Impedance to Probe Fed Microstrip Antenna", *International Symposium Antennas and Propagation Society, Albuquerque*, NM, USA, vol.-20, pp. 89, May 1982.

[22] B. M. Alarjani and J. S. Dahele, "Feed Reactance of Rectangular Microstrip Patch Antenna with Probe Feed", *IET Electronics Letters*, vol.-36, pp. 388-390, March 2000.

[23] A. Kundu, B. Roy, S. Batabyal and U. Chakraborty, "A Coaxial Fed Compact Rectangular Microstrip Antenna with Multi-Layer Configuration for WLAN 2.4/5.2/5.8 GHz Band Applications", *International Conference on Industrial and Information Systems (ICIIS)*, Gwalior,India, pp. 1-4, Dec. 2014.

[24] L. I. Basilio, M. A. Khayat, J. T. Williams and S. A. Long, "The Dependence of the Input Impedance on Feed Position of Probe and Microstrip Line-fed Patch Antennas", *IEEE Trans. Antennas and Propagation*, vol. AP-49, no.1, pp. 45-47, Jan. 2001.

[25] T. Samaras, A. Kouloglou, and J. N. Sahalos, "A Note on the Impedance Variation with Feed Position of A Rectangular Microstrip Antenna", *IEEE Antennas and Propagation Magazine*, Malaysia, vol. AP-46, pp. 90-92, April 2004.

[26] P. Ikmo, C. J. Bum and R. Mittra, "An Aperture-Coupled Small Microstrip Antenna With Enhanced Bandwidth", *IEEE International Symposium Antennas and Propagation Society*, Orlando, FL, USA, vol.-2, pp. 1212-1215, July 1999.

[27] M. K. A. Rahim, Z. W. Low, P. J. Soh, A. Asrokin, M.H. Jamaluddin and T. Masri, "Aperture Coupled Microstrip Antenna with Different Feed Sizes and Aperture Positions", *International RF and Microwave Conference*, Putra Jaya, Malaysia, pp. 31-35, Sept. 2006.

[28] S. K. Tripathi and A. Sharma, "Dual Resonant Aperture Coupled Microstrip Antenna", *International Conference on Electronics Computer Technology (ICECT)*, Kanyakumari,India, vol.-5, pp. 320-323, April 2011.

[29] S. Dan and Y. Lizhi, "A Broadband Impedance Matching Method for Proximity-Coupled Microstrip Antenna", *IEEE Transactions on Antennas and Propagation*, vol. AP-58, pp. 1392-1397, Jan. 2010.

[30] P. S. Bakariya, S. Dwari, M. Sarkar and M. K. Mandal, "Proximity-Coupled Microstrip Antenna for Bluetooth, WiMAX, and WLAN Applications", *IEEE Antennas and Wireless Propagation Letters*, vol. AP-14, pp. 755-758, Dec. 2014.

[31] P. S. Bakariya, S. Dwari, M. Sarkar and M. K. Mandal, "Proximity-Coupled Multiband Microstrip Antenna for Wireless Applications", *IEEE Antennas and Wireless Propagation Letters*, vol. AP-14, pp. 646-649, Dec. 2014.

[32] H. K. Varshney, M. Kumar, A. K. Jaiswal, R. Saxena and K. Jaiswal, "A Survey on Different Feeding Techniques Of Rectangular Microstrip Patch Antenna", *International Journal of Current Engineering and Technology*, vol.-4, no. 3, pp.1418-1423, June 2014.

[33] K. F. Lee and K. F. Tong, "Microstrip Patch Antennas—Basic Characteristics and Some Recent Advances", *IEEE Proceedings*, vol. 100, pp. 2169-2180, Feb. 2012.

[34] R. C. Johnson and H. Jasik, "*Antenna Engineering Handbook*'', ISBN 978-0-07032-291-92, pp 7-1 and 7-14, McGraw Hill, Inc. NY, USA2, Second Edition, 1984..

[35] S. Babu, I. Singh and G. Kumar, "Improved Linear Transmission Line Model for Rectangular, Circular and Triangular Microstrip Antennas", *IEEE International Symposium on Antennas and Propagation Society*, Canada, vol.-2, pp. 614-617, July 1997.

[36] H. An, F. Demuynck and A. Van de Capelle, "Simple Transmission Line Feed Model for Microstrip Antennas in Two-Sided Structure with Coaxial Probe Coupling", *IET Electronics Letters,* vol.-28, no.-18, pp. 1722-1724, August 1992.

[37] Y. T. Lo, D. Solomon and W. F. Richards, "Theory and Experiment on Microstrip Antennas", *IEEE Trans. on Antennas Propagation*, vol. AP-27, no.-2, pp. 137–145, March 1979.

[38] W. F. Richards, Y. T. Lo and D. D. Harrison, "An Improved Theory of Microstrip Antennas with Applications", *IEEE Trans. on Antennas Propagation*, vol. AP-29, no.-1, pp. 38–46, January 1981.

[39] A. Benalla and K. C. Gupta, "Multiport Network Model and Transmission Characteristics of Two-Port Rectangular Microstrip Patch Antennas", *IEEE Trans. on Antennas Propagation,* vol. AP -36, no.-10, pp. 1337-1342, Oct. 1988.

[40] A. Benalla and K. C. Gupta, "Multiport Network Approach for Modeling the Mutual Coupling Effects in Microstrip Patch Antennas and Arrays", *IEEE Trans. on Antennas Propagation,* vol. AP -37, no.-2, pp. 148-152, Feb. 1989.

[41] A. Reineix and B. Jecko, "Analysis of Microstrip Patch Antennas using Finite Difference Time Domain Method", *IEEE Trans. on Antennas Propagation,* vol. AP -37, no.-11, pp. 1361-1369, Nov. 1989.

[42] R. J. Luebbers and H. S. Langdon, "A Simple Feed Model That Reduces Time Steps Needed for FDTD Antenna and Microstrip Calculations", *IEEE Trans. on Antennas Propagation,* vol. AP -44, no.-7, pp. 1000-1005, July 1996.

[43] B. El Jaafari, M. A. G. de Aza and J. Zapata, "An Approach Based on Finite Element Method for CAD of Printed Antennas", *IEEE Trans. on Antennas and Wireless Propagation Letters,* vol.-11, pp. 1238-1241, Oct. 2012.

[44] D. T. McGrath and V. P. Pyati, "Phased Array Antenna Analysis with the Hybrid Finite Element Method", *IEEE Trans. on Antennas Propagation,* vol. AP-42, no.-12, pp. 1625-1630, Dec. 1994.

[45] R. A. Abd-Alhameed, N. J. McEwan, P. S. Excell, M. M. Ibrahim and B. A. W. Ibrahim, "Procedure for Analysis of Microstrip Patch Antennas using the Method of Moments", *IEEE Proc. on Microwaves, Antennas and Propagation,* vol.-145, no.-6,

pp. 455-459, Dec. 1998.

[46] E. H. Newman and P. Tulyathan, “Analysis of Microstrip Antennas using Moment Methods”, *IEEE Trans. on Antennas Propagation*, vol. AP-29, no.-1, pp. 47–53, January 1981.

[47] I. Park, R. Mittra and M. I. Aksun, “Numerically Efficient Analysis of Planar Microstrip Configurations using Closed-Form Green's Functions”, *IEEE Trans. on Microwave Theory and Techniques,* vol.-43, no.-2, pp. 394-400, Feb. 1995.

[48] G. Bianconi, C. Pelletti, R. Mittra, K. Du, S. Genovesi and A. Monorchio, “Spectral Domain Characteristic Basis Function Method for Efficient Simulation of Microstrip Devices in Layered Media”, *IET Microwaves, Antennas and Propagation,* vol.-6, no.-4, pp. 411-417, March 2012.

[49] E. Van Lil and A. Van De Capelle, “Transmission Line Model for Mutual Coupling Between Microstrip Antennas”, *IEEE Transactions on Antennas and Propagation*, vol. AP-32, pp. 816-821, Aug. 1984.

[50] H. Pues and A. Van De Capelle, “Accurate Transmission-Line Model for the Rectangular Microstrip Antenna”, *IEEE Proceedings Microwaves, Optics and Antennas*, vol.-131, no.-6, pp. 334-340, Dec. 1984.

[51] R. W. Dearnley and A. R. F. Barel, “A Broad-Band Transmission Line Model for a Rectangular Microstrip Antenna”, *IEEE Transactions on Antennas and Propagation*, vol. AP-37, pp. 6-15, Jan. 1989.

[52] D. M. Pozar and D. H. Schaubert, “*Microstrip Antennas: The Analysis and Design of Microstrip Antennas and Arrays*”, ISBN 978-0-7803-1078-0, IEEE Press, New York, May 1995.

[53] Y. T. Lo and S. W. Lee, “*Antenna Handbook Theory, Applications & Design’’*, ISBN 978-1-46156-461-4, Springer, US, 1988.

[54] L. W. Stutzman and G. A. Thiele, “*Antenna Theory & Design*”, ISBN 978-0-47057-664-9, John Wiley & Sons Inc., NY, 2002.

[55] A. Mandal, A. Ghosal, A. Majumdar, A. Ghosh, A. Das and S. K. Das, "Analysis of Feeding Techniques of Rectangular Microstrip Antenna", *IEEE International Conference on Signal Processing, Communication and Computing (ICSPCC)*, Hong Kong, pp. 26-31, Aug. 2012.

[56] Y. Hu, D. R. Jackson, J. T. Williams, and S. A. Long, "A Design Approach for Inset-Fed Rectangular Microstrip Antennas", *AP-S International Symposium*, Albuquerque, New Maxico, pp. 1491-1494, July 2006.

[57] J. Volakis, "*Antenna Engineering Handbook*", ISBN 978-0—07147-574-7*,* 4th ed. McGraw-Hill Professional, 2009.

[58] E. Chang, S. A. Long, and W. F. Richards, "An Experimental Investigations of Electrically Thick Microstrip Antenna" , *IEEE Trans. Antennas and Propoga*. , vol. AP-34, pp. 767-772, June 1986

[59] A. Elrashidi , K. Elleithy, H. Bajwa, "Input Impedance, VSWR and Return Loss of a Conformal Microstrip Printed Antenna for TM_{01} Mode using Two Different Substrates" *, International Journal of Networks and Communications,* vol. 2(2), pp. 13-19, 2012.

[60] D. Mathur, S. K. Bhatnagar and V. Sahula, "Quick Estimation of Rectangular Patch Antenna Dimensions Based on Equivalent Design Concept", *IEEE Antennas and Wireless Propagation Letter*, vol. AP-13, pp. 1469-1472, July 2014.

[61] S. K. Bhatnagar, "A New Approach for Designing Rectangular Microstrip Antenna", In Proc. of *National Conference on Recent Trends in Microwave Techniques and Applications,*University of Rajasthan, 30 July-1 Aug. 2012.

[62] Ansoft Corporation, "*An Introduction to HFSS: Fundamental Principles, Concepts, and Use*", Ansoft Corporation, Pennsylvania, USA.

[63] K. K. A. Devi, N. M. Din and C. K. Chakrabarty, " Optimization of the doubler stages in an RF- DC convertor module for energy harvesting" , *Science Research- Circuit and System*, vol. 3, pp. 216-222, 2012.

[64] F. Zhang, Xin Liu, F.-Yi Meng, Qun Wu, J. C. Lee, J.-F. Xu, C. Wang and N.-Y. Kim, " Design of a Compact Planar Rectenna for Wireless Power Transfer in the ISM Band" , *Hindwai Publishing Corp.- International Journal of Antennas and Propagation ,* vol. 2014, article ID 298127- 9 pages, Feb 2014.

[65] H. Takhedmit, L. Cirio, O. Picon, C. Vollaire, B. Allard and F. Costa, "Design and Characterization of an Efficient Dual Patch Rectenna for Microwave Energy Recycling in the ISM Band" , *Progress In Electromagnetic Research,* vol. 43, pp. 93-108, 2013.

[66] Fu-J. Huang, C. M. Lee, C. L. Change, L.K. Chen, T. C. Yo and C. H. Luo, " Rectenna Application of Miniaturized Implantable Antenna Design for Triple –Band Biometry Communication" , *IEEE Tranction on Antenna and Propagation*, vol. 59, no. 7, pp. 2646-53 July 2011.

[67] G. Monti, L. Tarricone and M. Spartano, " X- Band Planar Antenna" , *IEEE Antenna and Wireless Propagation Letter*, vol. 10, pp. 1116-19, Oct. 2011.

[68] D. M. Pozar and D. H. Schaubert, "*Microstrip Antennas: The Analysis and Design of Microstrip Antennas and Arrays*", *ISBN 978-0-7803-1078-0*, IEEE Press, New York, May 1995.

[69] M.Olyphant, Jr. and J.H. Ball, "Strip Line Method For Dielectric Measurements at Microwave Frequency", *IEEE Trans. Elec. Insul*., vol.EI-5, pp.26-32, March,1970.

[70] L.S. Napoli and J.J. Hughes, "A Simple Technique for the Accurate Determination of the Microwave Dielectric Constant for Microwave Integrated Circuit Substrates", *IEEE Trans. Microwave Theory Tech.*, vol. MTT-19, pp.664-665, July 1971.

[71] T. Itoh, "A New Method for Measuring Properties of Dielectric Materials Using A Micro Strip Cavity", *IEEE Trans. Microwave Theory Tech.*, vol-MTT-22, pp. 572-576, May 1974.

[72] D. Shimin, "A New Method for Measuring Dielectric Constant Using the Resonant Frequency of A Patch Antenna", *IEEE Trans. Microwave Theory Tech*., vol. MTT-34, pp.923-931, Sept. 1986.

[73] Ranjit Singh, Ashok De, R.S. Yadav, "A Simple Method For Measuring Dieledtric Constant At Microwave Frequency", *IEEE Trans. Microwave Theory Tech*., vol.MTT-22, pp.1-5, Jan. 1990.

[74] Jiri Svacina, "Analysis of Multilayer Microstrip Lines by a Conformal Mapping Method", *IEEE Trans. Microwave Theory Tech*., vol. 40,no.4, pp. 769-72., 1992.

[75] A.K. Verma, et al., "Unified Dispersion Model for Multilayer Microstrip Line", *IEEE Trans. Microwave Theory Tech.*, vol. 40. no.7, pp. 1587-92, 1992.

[76] R.H. Jansen, " A Novel CAD Tool Ad Concept Compatible with the Requirement of Multilayer Gaas MMIC Technology", *IEEE MTT-S Microwave Symp. Dig*., pp. 711-14, 1980.

[77] M. Y. Frankel, " Coplanar Transmission Lines on Thin Substrate for High Speed Low Loss Propagation", *IEEE Trans. Microwave Theory Tech.,* vol. 42, no. 3, pp. 396-400, 1994.

[78] C. Veyers, et al., "Extension of the Application of Conformal Mapping Techniques to Coplanar line with Finite Dimension", *Int'l J. Electronics*, vol. 48, no.1, pp. 47-52,1980.

[79] Yeong J. Yoon, Bruce Kim, "A New Formula for Effective Dielectric Constant in Multilayer Dielectric Microstrip Structure", *IEEE Trans. Microwave Theory Tech.* vol.55. no.9, pp. 1587-90, 2000.

[80] D. M. Pozar and S. M. Voda, "A Rigorous Analysis of a Microstrip Line Fed Patch Antenna*," IEEE Trans. Antennas Propagat*., vol. 35, pp. 1343-1350. Dec. 1987.

[81] L. I. Basilio, M. A. Khayat, J. T. Williams and S. A. Long, "The Dependence of the Input Impedance on Feed Position of Probe and Microstrip Line-fed Patch Antennas," *IEEE Trans. Antennas and Propagation*, vol. AP-49, pp. 45-47, Jan. 2001.

[82] Z. I. Dafalla, W. T. Y. Kuan, A. M. A. Rahman, S. C. Shudakar, "Design of a Rectangular Microstrip Patch Antenna At 1 GHz", *Proceedings IEEE Explore, RF and Microwave Conference (RFM 2004)* ,Malaysia , pp. 145-149, Feb. 2004.

[83] T. Samaras, A. Kouloglou, and J. N. Sahalos, "A Note on the Impedance Variation with Feed Position of a Rectangular Microstrip Antenna," *IEEE Antennas and Propagation Magazine*, vol. 46, pp. 90-92, April 2004.

[84] Y. Hu, E. Lundgren, D. R. Jackson, J. T. Williams, and S. A. Long, "A Study of the Input Impedance of the Inset-Fed Rectangular Microstrip Antenna as a Function of Notch Depth and Width," *IEEE Antennas and Propagation Society International Symposium*, Washington DC, vol 4A, pp. 330-333 , July 2005.

[85] Y. Hu, D. R. Jackson, J. T. Williams, and S. A. Long," A Design Approach For Inset-Fed Rectangular Microstrip Antennas" *IEEE Antennas and Propagation Society International Symposium*, Albuquerque, NM USA, vol.1, pp. 1491-1494, July 2006.

[86] Y. Hu, D. R. Jackson, J. T. Williams, and S. A. Long, and V R Komanduri "Characterization of the Input Impedance of the Inset-Fed Rectangular Microstrip Antenna" *IEEE Trans. Antennas and Propagation*, vol. 56, no. 10, pp. 3314-3318, October 2008.

[87] P.Subbulakshmi, R. Rajkumar, "Design and Characterization of Corporate Feed Rect-Angular Microstrip Patch Array Antenna", *IEEE International conference on Emerging Trends in Computing, Comm-unication and Nanotechnology (ICECCN) India*, vo. 1, pp. 547-552, Jan. 2013.

[88] Swati, T. Kumar, A. K. Aggarwal, "Dual Band Equilateral Triangular Patch Antenna," *International Journal of Computational Engineering and Management*, vol.15, pp. 77-79, Sept. 2012.

[89] S. H. Al-Charchafchi, W .K. Wan Ali, M. R. Ibrahim, S. R. Barnes,"Design of a Dual Patch Triangular Microstrip Antenna," *Applied Microwave & Wireless*, pp. 60-67, March 1998.

[90] Swati Swami, S. K. Bhatnagar, Abhijat vats, Monika Mathur, "Equilateral Triangular Microstrip Antenna- A New Design Formula Based on Bhatnagar's Postulate", *SKIT Research Journal,* vol. 5 Issue 1, pp. 40-42 , April 2015.

[91] X.X. Yang, J.S. Xu, D.-M. Xu, and C.L. Xu, "X-Band Circularly Polarized Rectennas for Microwave Power Transmission Applications," *J. Electron*. , vol. 25 , no. 3 , pp. 389-93, 2008.

[92] Y.Y. Gao, X.X. Yang, C. Jiang, and J.Y. Zhou, "A Circularly Polarized Rectenna With Low Profile for Wireless Power Transmission," *Prog. Electromagn. Res. Lett.* , vol. 13, pp. 41-49, 2010.

[93] F.J. Huang, C.-M. Lee, C.-L. Chang, L.-K. Chen, T.-C. Yo, and C.-H. Luo, "Rectenna Application of Miniaturized Implantable Antenna Design for Triple-Band Biotelemetry Communication," *IEEE Trans. Antennas Propag*. **,** vol. 59, no. 7, pp. 2646-53, 2011**.**

[94] H. Takhedmit, L. Cirio, S. Bellal, D. Delcroix, and O. Picon, "Compact and Efficient 2.45 GHz Circularly Polarised Shorted Ring-Slot Rectenna," *Electron. Letter* , vol. 48 , no. 5 , pp. 253-54, 2012.

[95] Federal Communications Commission, First report and Order, (Revision of part 15 of commission's rule regarding UWB transmission system FCC, Washington, DC, pp. 02-48, 2002.

[96] J. Jung, H. Lee and Y. Lim, "Compact Band-Notched Ultra-Wideband Antenna with Parasitic Elements." *Electron Letter*, vol. 44 , no. 19 , pp. 1104-06, 2008.

[97] M. Yazdi and N. Komjani,"A Compact Band-Notched UWB Planar Monopole Antenna with Parasitic Elements" , *Prog. Electromagn. Res. Lett* , vol. 24, pp. 129-138, June 2011.

[98] A. M. Abbosh and M. E. Bialkowski "Design of UWB Planar Band-Notched Antenna using Parasitic Elements ", *IEEE Trans. on Antenna and Prop.* , vol. 57 , no. 3, pp. 796-799, March 2009.

[99] A. Subbarao, S. Raghavan , “Coplanar Waveguide-fed Ultra-wideband Planar Antenna with WLAN-band Rejection” , *Jour. of Micr., Optoel. and Electromag. Appli.* , vol. 12, No. 1, pp. 50-59, June 2013.

[100] D. Trhiripurasundari and D. S. Emmanuel, “ Compact Dual Band-Reject UWB Antenna with Sharp Band-Edge Frequency” , *Prog. Electromagn. Res. Lett* , vol. 36, pp. 41-55, Jan 2013.

[101] A. M. Abbosh and M. E. Bialkowski “A Planar UWB Antenna with Signal Rejection Capability in the 4-6 GHz Band *”, IEEE Microwave and Wireless Compo. letters*, vol. 16 , no. 5, pp. 278-280, May 2006.

[102] M. Jahanbakht and A. Ali L. Neyestanak, “ A Survey on Approaches in the Design of Band Notching UWB Antennas” , *Journ. of Electromag. Analy. And Applications*, vol. 4 , pp. 77-84, Feb. 2012.

[103] Choi, S. T., Hamaguchi, K., and Kohno, R., "Small Printed CPW-Fed Triangular Monopole Antenna for Ultra-Wideband Applications", *Microw. Opt. Technol. Lett*., vol. 51, no.1, 1180-82, 2009.

[104] Zha, F. T., Gong S. X., Liu G., Yang H. Y., and Lin S. G., "Compact Slot Antenna for 2.4GHz/UWB with Dual Band-Notched Characteristic", *Microw. Opt. Technol. Lett*., vol. 48, no.1 , pp. 1859-62, 2009.

[105] Ali Foudazi, Hamid Reza Hassani and Sajad Mohammad Ali Nezhad,”Small UWB Planar Monopole with Added GPS/GSM/WLAN Bands”, *IEEE Trans. Antennas Propag***. ,** vol. 60 , no. 6 , pp. 66-69, 2012 .

[106] A.M. Abbosh and M.E. Bialkowski, “ Dseign of Ultrawideband Planar Monopole Antennas of Circular and Elliptical Shape” , *IEEE Trans. Antennas Propag.* **,** vol. 56, no.1, pp. 17-23, Jan 2008.

[107] Lin, C.-C., Y.-C. Kan, L.-C. Kuo, and H.-R. Chuang,“A Planar Triangular Monopole Antenna for UWB Communication,” *IEEE Microw. Wireless Compon. Lett*. , vol. 15, no. 10, pp. 624-26, 2005.

[108] Y. Li, W. Li, Q. Ye and Raj Mittra, "A Survey of Planar Ultra-Wideband Antenna Designs and their Applications , *Forum for Electromagnetic Research Methods and Application Technologies (FERMAT)*, 2016.

www.e-fermat.org/files/articles/153371b85cc609.pdf

[109] X. Qing and Z. N. Chen, "Compact Coplanar Waveguide-Fed Ultra-Wideband Monopole-Like Slot Antenna*," Microwaves, Antennas & Propagation*, vol. 3, no. 5 , pp. 889-98, 2009.

[110] W.-T. Li, X.-W. Shi, T.-L. Zhang, and Y. Song, "Novel UWB Planar Monopole Antenna with Dual Band Notched characteristics," *Microwave and Optical Technology Letters* , vol. 52, no. 1 , pp. 48-51, 2010.

[111] M.J. Ammann and L.E. Doyle, "Small Panar Monopole Covers Multiband BRAN's," *Proc. of 30th European Microwave Conference*, Paris, France ,vol. 2, pp. 242-246, 2000.

[112] U. Olgun, C. C. Chen, J. L. Volakis, " Invesigation of Rectenna Array Configurations For Enhanced RF Power Harvesting", *IEEE Antenna and Wirel. Prop. Letters*, vol. 10, pp. 262-265, 2011.

[113] T. Sakamoto, Y. Ushijima, E. Nishiyama, M. Aikawa and I. Toyoda, " 5.8 GHz Series/Parallel Connected Rectenna Array using Expandable Differential Rectenna Units" , *IEEE Trans. on Antenna and Prop*. , vol. 61, no. 9, 2013.

[114] N. Hasan and S. K. Giri, "Design of Low Power RF to DC Generator for Energy Harvesting Applications", *Int. Journal of Applied Scien.and Engg. Research*, vol.1 , Issue 4, pp. 562-569, 2012.

[115] H. Tiwari and M. V. Kartikeyan, "A Stacked Microstrip Patch Antenna Loaded With U-Shaped Slots", *Frequenz.* vol. 65, Issue 5-6, pp 167–172, Aug. 2011.

[116] S. Ladan, N. Ghassemi, Anthony Ghitto and Ke Wu "Highly Efficient Compact Ractenna for Wireless Energy Harvesting Application", *IEEE microwave magazine*,

pp 117-122, Jan 2013.

[117] F. Zang, X. Liu, F.Y. Meng , Q. Wu, J. C. Lee, T. F. Xu, C. Wang and N.Y. Kim, " Design of a Compact Planar Rectenna for Wireless Power Transfer in the ISM Band", *International Jou. of Anten. and Propa., Hindwai Pub. Cor.* , vol. 2014, pp 1-9, 2014.

[118] G. Monti, L. Tarricon and M. Spartano, " X- Band Planar Rectenna", *IEEE Antenna and Wirel. Prop. Lett.* , vol. 10, pp 1116-1119, 2011.

[119] G. Monti and F. Congedo, "UHF Rectenna using a Bowtie Antenna", *Progress in Elec. Rese*., vol. 26, pp 181-192, 2012.

[120] Y. H. Suh and K. Chang, " A highly Efficient dual Frequency Rectenna for 2.45 and 5.8 GHz Wireless Power Transmission", *IEEE Trans. Microwave Theory Tech*. , vol 50 , no. 7 , pp 1784-1789, July 2002.

[121] J. Herkkinen and M. Kuvikoski, "A Novel Dual Frequency Circularly Polarized Rectenna", *IEEE Antenna and Wirel. Prop. Lett*. , vol. 2, pp 330-333, 2003.

[122] B. strassner and K. chang, " Higly Efficient C- band Circularly Polarized Rectifying Antenna Array for Wireless Microwave Power Transmission ", *IEEE Antenna and Wirel. Prop*. , vol. 51, no 6, pp 1347-1356, Jan. 2003.

[123] N. Shinohara and H. matsumoto, "Experimental Study of Large Rectenna Array for Microwave Energy Transmission", *IEEE Trans. Microwave Theory Tech*. ,vol. 51, no. 5 , pp 1548-1553, may 2003.

[124] J. A. G. Akkermans, M. C. Van Beurden. G. J. N. Doodeman and H. J. visser, "Analytical Models for Low Power Rectenna Design", *IEEE Antenna and Wirel. Prop. Lett*. , vol. 4 , pp 187-190 , 2005.

[125] N. M. Din , C. K. Chakarabararty, a. Bin Ismail, K. K. Devi and w. Y. Chen, " Design of RF Energy Harvesting System for Energizing Low Power Devices" , *Progress in Elec. Rese*., vol. 132, pp 49-69, July 2012.

[126] L. M. Borges, N. Barroca, H. M. Saraiva, et al., “Design and evaluation of multi-band RF energy harvesting circuits and antennas for WSNs,” in Proceedings of the 21st *IEEE International Conference on Telecommunications*, pp. 308–312, Lisbon, Portugal, May 2014.

[127] A. Bakkali, J. Pelegri-Sebastia, T. Sogorb, V. Llario and A. Bou-Escriva, “A Dual-Band Antenna for RF Energy Harvesting Systems in Wireless Sensor Networks” , *Hindawi Publishing Corporation- Journal of Sensors* , vol. 2016, Article ID 5725836, pp 1-8, 2016.

http://dx.doi.org/10.1155/2016/5725836.

[128] M. A. M. Said, Z. Zakaria, M. N. Husain, M. Abu, N. Mohd Salleh and M. H. Misran, “Dual Band Rectifying Circuit for RF Energy Scavenging” , *ARPN Journal of Engineering and Applied Sciences*, vol. 11, no. 5, pp 3286-3289, March 2016.

PUBLICATION DETAILS

1. Monika Mathur, Ankit Agrawal , Ghanshyam Singh, S. K. Bhatnagar "The Array Structure of 2 x 2 Coplanar Monopole Antenna with Wilkinson Power Combiner for RF Energy Harvesting Application" *IEEE Xplorer 2016 , ISBN 978-1-5090-2807-8 pp. 1-4 DOI: : 10.1109/ICRAI.2016.7939563.*

2. Monika Mathur, Ankit Agarwal, Ghanshyam Singh, S. K. Bhatnagar "A Novel Design Module of RF Energy Harvesting for Powering the Low Power Electronics Circuits" *© 2016 ACM. ISBN 978-1-4503-4213-1/16/08, article no. 68, pp. 1-6, DOI: http://dx.doi.org/10.1145/2979779.2979847 (2016).*

3. Monika Mathur, Ghanshyam Singh, S. K. Bhatnagar, Swati Swami, Abhijat Vats "Transformation of Design Formulae for Feed Line of Triangular Microstrip Antenna", *American Institute of physics (AIP) Conf. Proc. 1715, 020035 (1-5); http://dx.doi.org/10.1063/1.4942717, (2016).*

4. Monika Mathur, Ghanshyam Singh, S. K. Bhatnagar "An Analytical Approach for Fine Tuning of Resonant Frequency of MSPA using Dielectric Constant Engineering (DCE)" *Proc. of ICRCWIP 2015 ISBN e-Book/hardcover: 978-81-322-2638-3/978-81-322-2636-9, pp. 107-114, DOI 10.1007/978-81-322-2638-3_12, Springer Publication, December (2015).*

5. Monika Mathur, Abhijat Vats, Ankit Agrawal, " A New Design Formula for Feed line Dimensions of the Rectangular Microstrip Patch Antenna by using Equivalent Design Concept" *IEEE Xplorer, 2015 ISBN 978-1-4799-6761-2/15, pp. 105-110, DOI: 10.1109/ICSPCom.2015.7150629, (2015).*

6. Swati Swami, S. K. Bhatnagar, Abhijat vats, Monika Mathur, "Equilateral Triangular Microstrip Antenna-A New formula based on Bhatnagar Postulates" *SKIT Research Journal, vol.5 Issue-1,pp. 40-45, ISSN-2278-2508 (2014).*

7. Monika Mathur, Ghanshyam Singh, S. K. Bhatnagar "A novel approach for fine tuning of resonance frequency of patch antenna" *Proc. of SPIE Vol. 8760, 87601T (1–6), DOI: 10.1117/12.2012335, (2013).*

<u>(Communicated/Under review):</u>

1. Monika Mathur, Ghanshyam Singh, S. K. Bhatnagar "A Compact Coplanar Waveguide Fed Wideband Monopole Antenna for RF Energy Harvesting Applications", communicated in *Elsevier Journal: AEU–International Journal of Electronics and Communications.*

Appendix-A

Algorithm for the Process of Transformation of Rectangle Shape Patch and Its Feed Line Designs on Matlab

```
clear
clc
close all
er1=input('enter old dielectric ')
h1=input('enter old height ')
f=input('enter frequency in Hz')
 c=3*10^2;
Z0=50
W1=(c/(2*f))*sqrt(2/(er1+1))
z1=W1/h1;
lamda=c/f
erff1=((er1+1)/2)+((er1-1)/2)*(1+12*(h1/W1))^(-0.5)
dl1=(0.412*h1*((erff1+0.3)/(erff1-
0.258))*((z1+0.264)/(z1+0.813)))
L1=(lamda/(2*sqrt(erff1)))-2*dl1

if W1<(lamda)
    G1=(1/90)*(W1/lamda)^2
else
    G1=(1/120)*(W1/lamda)
end
r1=1/(2*G1)
lf1=(L1/pi)*acos((50/r1)^0.5)
A=(Z0/60)*sqrt((er1+1)/2)+((er1-1)/(er1+1))*(0.23+(0.11/er1));
B=(377*pi)/(2*Z0*sqrt(er1));
Wf1=h1*((8*exp(A))/(exp(2*A)-2))
if Wf1<= h1
   Wf1=h1*10.83*(er1)^(-1.27)
else
    Wf1=h1*5.752*(er1)^(-0.92)
end
```

```
chi=sqrt(er1/er2)
phi=h1/h3
W2=(W1)/phi
if h1-h3>0
L2=(chi*L1)+((chi*h1-h3)/er2)
else
L2=(chi*L1)+((chi*h2-h3)/er2)
end
lf2=phi*lf1
if (Wf1/h1<1 & er1>6.4)
  Wf2=Wf1*phi^(3.7)
 else
     Wf2=Wf1*phi^(2.85)
 end
lx=L1/1000
wx=W1/1000
t                                                                    =
dielectric('Name','FR4','EpsilonR',4.4,'LossTangent',0.02);
p = pifa('Height',0.0008,'Substrate',t)
ant=patchMicrostrip('Length',lx,
'Width',wx,'Height',0.0016,'Substrate',t,
'GroundPlaneLength',.06,        'GroundPlaneWidth',        0.04,
'PatchCenterOffset', [0 0], 'FeedOffset',[0 0])
figure(1)
show(ant);
freq = linspace(0.9e9, 10e9, 10);
figure(2);
impedance(ant, freq);
figure(3);
returnLoss(ant, freq);
S = sparameters(ant, freq);
figure(4);
rfplot(S);
figure(5);
vswr(ant, freq);
S = sparameters(ant, freq, 20);
```

```
Figure(6);
rfplot(S);
figure(7);
polarpattern(ant);
```

BRIEF CV

I received the M. tech. degree from Rajasthan Technical University, Kota, Rajasthan with Ist divison. I did B.E. from Rajasthan University, Jaipur with Honors and was secured 9th rank in University. I did Diploma from Board of Technical Education, Jodhpur, Rajasthan with Honors. I won Gargi Award for secondry board examinations. I have 10 years of teaching experience and 2 years of industrial experience. I have been attended more than 20 workshops, natonal and international conferences and presented papers in the conferences. I am the life member of important professional societies such as IETE, IEI, and ISTE etc. My field of interest are “Microwave Engineering” and “Microstrip Antenna Designing” . I authored and co-authored more than 12 publications in Microstrip Antenna Engineering field.